Jean-Louis **Migeot** Jean-Pierre **Coyette** Grégory **Lielens**

ACOUSTICS

Essential concepts, theory and models of linear acoustics for engineers

Published by:
IJK Numerics
15 rue du repos
B-1180 Bruxelles
BELGIUM
For information, please contact:
jean-louis.migeot@ijknumerics.com

ISBN 978-1-329-90391-3

What is taught is either evident or obscure. What is evident to all needs no teaching. The obscure will not be teachable.
— **Sextus Empiricus** (c.160-210), Against the Grammarians.
English translation by David L. Bank.

We can say that Muad'Dib learned rapidly because his first training was in how to learn. And the first lesson of all was the basic trust that he could learn.
— **Frank Herbert** (1920-1986), Dune (1965).

The power of instruction is seldom of much efficacy except in those happy dispositions where it is almost superfluous.
— **Edward Gibbon** (1737-1794), The Decline and Fall of The Roman Empire (1788).
quoted by Richard Feynman (1918-1988) in *Lectures on Physics*, Basic Books, 1963.

He is an honest, conscientious man, whose science I trust as much as he distrusts it.
— **Michel Tournier** (1924-2016), The four wise men (1980).
English translation by Ralph Manheim (1982).

He who seeks to understand everything risks dying of anger.
— Arab proverb.
quoted by Jean-Claude Guillebaud (1944-), La trahison des lumières (1995).

Our deepest gratitude and love goes to:

Coline, Gaspard and Aline.
J-L.M.

Brigitte, Olivier and Julie.
J-P.C.

Jacques, Odette and Yannick.
G.L.

This book has immensely benefited from the friendly, fun and intellectually challenging collaboration we have enjoyed with the entire staff of Free Field Technologies since the company was founded in 1998. They all deserve our sincere thanks and appreciation:

Raphaël, Rami, Chris, Thibaut, Nagisa, Clément, Zbigniew, Benoît, Bernard, Isabelle, Mickaël, Fabien, Yoshiyuki, Thomas, Danisa, Alexis, Gai, Yves, Joël, Thaïssa, Mehdi, Erwan, Prateek, Joe, Alain, Claire, Aurélien, Julie, Ken, Jonathan, Vincent, Lou, Benjamin, Laurent, Barthélémy, Fayçal, Olivier, Romain, Xavier, Marie-Laure, Valérie, Boris, Dave, Alexandra, Marie, Nicolas, Eberhard, Elias, Maxime, Steve, Mathieu, Masatake, Morgan, Toon, Shriram, Bastien, Julien, Jean-David, Paul, Pierre-Charles, César, François, Eveline, Markus, Debbie, Dimitri, Stéphane, Christophe, Françoise, Yuru Bai, Nancy, Eloi, Karl, Cécile, Karthik, Karim and Diego.

In addition, we gratefully acknowledge the important contribution of the following proofreaders who made countless and invaluable suggestions for improvements:

Lisa Hornsey (Thoughtful), César Legendre, Karthik Balachandran, Debbie Reeves and Pierre-Charles Dubé (Free Field Technologies), Cecilia Dagg (Ford Motor Company), Eric Pesheck, Doug Malcolm, Martin McNamee, Konrad Juethner, Sanjay Patel and David Seidensticker (MSC Software).

Contents

Table of Contents V

1 Introduction 1

2 Definition and scope of acoustics 3
2.1 Definitions . . . 4
2.2 Fields of acoustics . . . 6
2.3 Spectral range of sounds . . . 12
2.4 Relevance of acoustics . . . 14

I Governing equations and fundamental concepts 17

3 Continuum Mechanics 19
3.1 Continuity equation . . . 20
3.2 Index notation . . . 22
3.3 Momentum equation . . . 25
3.4 Equation of state . . . 31

4 The wave equation 33
4.1 The wave equation . . . 34
4.2 Linearity and non-linearity in acoustics . . . 40
4.3 General one-dimensional solution . . . 41
4.4 Mechanics of propagation . . . 43
4.5 Dispersive and non-dispersive propagation . . . 46
4.5.1 General wave equations . . . 46
4.5.2 Non-dispersive propagation . . . 48
4.5.3 Dispersive propagation . . . 48
4.5.4 Wave packet and group velocity . . . 49
4.6 Speed of sound . . . 50
4.6.1 Perfect gas . . . 50
4.6.2 Liquids . . . 51
4.6.3 Solids . . . 53

5 Fourier analysis **55**
5.1 Combination of simple signals . . . 57
5.1.1 Signals with identical frequencies . . . 57
5.1.2 Signals with different frequencies . . . 62
5.2 Fourier series . . . 67
5.2.1 Square wave and Gibbs phenomenon . . . 69
5.2.2 Spectra and complex amplitudes . . . 71
5.3 Fourier transform . . . 76
5.3.1 Hermitian character of the spectrum . . . 76
5.3.2 One-sided spectrum . . . 77
5.4 Convolution product . . . 79
5.4.1 Definition . . . 79
5.4.2 Windowing of a signal . . . 80
5.4.3 Filtering of a signal . . . 81
5.5 Properties of the Fourier transform . . . 81
5.5.1 Time shift . . . 81
5.5.2 Time and frequency scaling . . . 83
5.5.3 Time derivatives . . . 83
5.5.4 Signal and spectrum width . . . 85
5.6 Summary of the chapter . . . 87

6 Equations in harmonic regime **89**
6.1 Helmholtz equation . . . 90
6.2 Pressure-velocity relationship . . . 90
6.3 Acoustic impedance . . . 91
6.4 Sound intensity . . . 92
6.4.1 Monochromatic signal . . . 92
6.4.2 General periodic signal . . . 94
6.4.3 General signal . . . 95
6.5 Plane waves . . . 97
6.5.1 General solution in one-dimension . . . 97
6.5.2 Characteristic impedance . . . 97
6.5.3 Intensity . . . 98
6.5.4 Attenuation . . . 98
6.5.5 Plane wave with arbitrary incidence . . . 100
6.6 Spherical waves . . . 101
6.6.1 Monopoles . . . 101

6.6.2 Volume flow of a source . . . 104

7 Sound levels 107

7.1 The decibel scale . . . 108
7.1.1 Definition . . . 108
7.1.2 Weber and Fechner laws . . . 112
7.2 Adding levels . . . 114
7.2.1 General principle . . . 114
7.2.2 Masking . . . 116
7.3 Octaves and third-octaves . . . 117
7.3.1 Band level . . . 117
7.3.2 White, pink and brown noise . . . 120
7.4 Corrected and cumulative levels . . . 123
7.4.1 Fletcher and Munson curves . . . 123
7.4.2 Filters . . . 125
7.4.3 Equivalent and statistical levels . . . 128
7.4.4 L_{den} . . . 128
7.4.5 EPNdB . . . 130
7.4.6 Noise Rating (NR) . . . 130

II Fundamental phenomena of linear acoustics 131

8 Reflection and absorption 133

8.1 Reflection under normal incidence . . . 134
8.1.1 Rigid surface (zero velocity) . . . 134
8.1.2 Free surface (zero pressure) . . . 138
8.1.3 Absorbing surface . . . 140
8.2 Reflection under oblique incidence . . . 143
8.2.1 Rigid surface and Descartes law . . . 143
8.2.2 Absorbing surface . . . 144
8.3 Reflection of a monopole source . . . 147
8.3.1 Image source . . . 147
8.3.2 Reflectogram . . . 150
8.3.3 Ray tracing method . . . 156
8.4 Notes on the concept of impedance . . . 162
8.4.1 Sign of the impedance coefficient . . . 162
8.4.2 Frequency dependency of the impedance . . . 163

8.4.3 Vibrating and absorbing panel . . . 164
8.4.4 Locally and non-locally reacting material . . . 165
8.4.5 Impedance measurement with a Kundt tube . . . 166
8.5 Reverberation time . . . 172
8.5.1 Sound build-up . . . 172
8.5.2 Sound extinction . . . 174
8.5.3 Sabine law . . . 176
8.5.4 Anechoic and reverberant chambers . . . 179
8.5.5 Eyring and Millington formulas . . . 179
8.5.6 Absorption coefficient measurement . . . 182

9 Resonance 185
9.1 Resonance of a closed tube . . . 186
9.1.1 Velocity source . . . 186
9.1.2 Pressure source . . . 188
9.1.3 Comparison of the pressure and velocity sources . . . 189
9.2 Eigenmodes and eigenfrequencies . . . 190
9.3 Modal superposition . . . 194
9.4 Box-shaped cavity . . . 197
9.5 Resonance of an arbitrary cavity . . . 199

10 Guided propagation 201
10.1 Cutoff frequency . . . 202
10.2 Transfer matrices . . . 204
10.2.1 Constant cross section . . . 204
10.2.2 Transfer matrix of three connected ducts . . . 206
10.2.3 T-connection . . . 208
10.2.4 Quarter-wavelength resonator . . . 210
10.2.5 Helmholtz resonator . . . 211
10.2.6 Alternative definitions of transfer matrices . . . 214
10.2.7 Transfer matrix measurement . . . 216
10.3 Transmission Loss (TL) . . . 218
10.3.1 Definition . . . 218
10.3.2 Transmission Loss of an expansion chamber . . . 219
10.3.3 TL of a tube fitted with a resonator . . . 221
10.4 Insertion Loss (IL) . . . 222
10.4.1 Source impedance . . . 222

10.4.2 Impedance matching . . . 222
10.4.3 Generalised source connected to a silencer . . . 223
10.4.4 Insertion loss (IL) . . . 224
10.4.5 Comparing Insertion Loss and Transmission Loss . . . 224
10.5 Circular ducts . . . 226
10.5.1 Bessel equation and functions . . . 226
10.5.2 Cutoff frequency . . . 227
10.6 Role of evanescent modes . . . 230
10.7 Reactive and dissipative silencers . . . 238

11 Sound radiation 239
11.1 Dipoles and quadrupoles . . . 240
11.1.1 Dipoles . . . 240
11.1.2 Longitudinal quadrupole . . . 243
11.1.3 Lateral quadrupole . . . 245
11.2 Multipole expansion . . . 249
11.3 Helmholtz integral equation . . . 258
11.3.1 Bounded domain . . . 258
11.3.2 Unbounded domains . . . 263
11.3.3 Indirect form of the integral equation . . . 264
11.3.4 Sound radiation by a vibrating plate . . . 266
11.4 Power, efficiency and impedance . . . 270
11.4.1 Radiated power . . . 270
11.4.2 Radiation efficiency . . . 270
11.4.3 Radiation impedance . . . 271

12 Diffraction 273

13 Refraction 275

14 Propagation in dissipative media 281
14.1 Introduction . . . 282
14.2 Equivalent fluid for a porous material . . . 284
14.2.1 Delany-Bazley model . . . 284
14.2.2 Miki model . . . 285
14.3 Biot theory . . . 286
14.3.1 General assumptions . . . 286
14.3.2 Biot parameters . . . 287

14.3.3 Equilibrium equations . . . 296
14.3.4 Constitutive equations . . . 297
14.3.5 *u-p* model for poro-elastic materials . . . 300
14.3.6 Waves in a poro-elastic media . . . 301
14.3.7 Micro-models . . . 308
14.4 Practical use of poro-elastic materials . . . 309
14.4.1 Limited impact of open porous layers . . . 309
14.4.2 Qualitative analysis of poro-elastic sandwich . . . 311

15 Convected propagation 315
15.1 Constant flow . . . 316
15.1.1 Convected wave equation . . . 316
15.1.2 Acoustical resonances in a tyre . . . 318
15.1.3 Prandtl-Glauert transformation . . . 320
15.1.4 Monopole source in a constant mean flow . . . 322
15.1.5 Doppler effect . . . 323
15.2 Potential flow . . . 327
15.2.1 Velocity potential . . . 328
15.2.2 Continuity equation . . . 328
15.2.3 Euler equation . . . 329
15.2.4 Non-linear potential equation . . . 331
15.2.5 Acoustic decomposition . . . 331
15.3 Arbitrary flow . . . 333
15.3.1 Continuity equation . . . 333
15.3.2 Momentum equation . . . 334
15.3.3 Entropy and perfect gas . . . 334
15.3.4 Energy equation . . . 336
15.3.5 Linearised Euler equations . . . 337
15.4 Application to a turbo-engine . . . 338

16 Atmospheric propagation 341
16.1 Main phenomena . . . 343
16.1.1 Geometric attenuation . . . 343
16.1.2 Atmospheric absorption . . . 343
16.1.3 Atmospheric refraction . . . 345
16.1.4 Turbulence . . . 345
16.2 Axisymmetric formulation . . . 347

16.3 Parabolic approximation . . . 348
16.3.1 Far field approximation . . . 348
16.3.2 Outgoing waves . . . 349
16.3.3 *Narrow-angle* approximation . . . 350
16.4 Finite difference solution . . . 351
16.4.1 Discrete form . . . 351
16.4.2 Discrete boundary conditions . . . 353
16.4.3 System of algebraic equations . . . 355
16.5 Evaluating Ψ at $r = 0$ . . . 356
16.6 Numerical performances . . . 359
16.7 Conclusions . . . 367

17 Fluid-structure interaction 369
17.1 One-dimensional model . . . 370
17.1.1 General case . . . 370
17.1.2 Tube of infinite length . . . 372
17.1.3 Tube of finite length . . . 373
17.2 Matrix theory of fluid-structure interaction . . . 379
17.2.1 Weak and strong coupling . . . 380
17.2.2 Modal approaches . . . 381
17.2.3 Radiation impedance . . . 382

18 Transmission and insulation 383
18.1 Rigid plate on elastic mounts . . . 386
18.2 Infinite flexible wall . . . 390
18.2.1 Attenuation evaluation . . . 390
18.2.2 Coincidence frequency . . . 392
18.2.3 Diffuse attenuation . . . 396
18.3 Double walls . . . 397
18.3.1 Mass-air-mass resonance . . . 397
18.3.2 Transmission Loss of double walls . . . 398
18.4 TL of finite plates . . . 401
18.5 Transmission Loss measurement . . . 403
18.5.1 Overview of the measurement methodology . . . 403
18.5.2 Transmission Loss of realistic partitions . . . 404

List of Figures 409

Index **417**

List of symbols **421**

1

Introduction

I quite realise that I do not know; but I foresee that I am going to have known.
— **Henri Bergson** (1859-1941), Works.
quoted by Vladimir Jankélévitch (1903-1985) *in* Henri Bergson (1930).

This book introduces the basic concepts of acoustics and vibro-acoustics. **Part one** develops the linear equations of acoustics. Taking the fundamental equations of continuum mechanics (Chapter 3) as a starting point, different assumptions are successively made in order to arrive at a wave equation for the acoustic pressure fluctuation (Chapter 4). The review of some key results of the Fourier analysis (Chapter 5) allows us to introduce the Helmholtz equation and associated canonical solutions (plane waves, spherical waves) in Chapter 6 as well as the concept of noise level in Chapter 7.

Part two presents the fundamental physical mechanisms of linear acoustics. The phenomena of reflection and absorption (Chapter 8) and the study of resonances (Chapter 9) are first addressed. Guided propagation theory and its application to intake and exhaust systems are presented in Chapter 10. Chapter 11 covers sound radiation, while Chapters 12 and 13 introduce, very briefly, diffraction and refraction. Sound propagation in dissipative media and in moving fluids is presented in Chapters 14 and 15. The problem of atmospheric propagation is then introduced in Chapter 16. The concepts associated with fluid-structure interaction are discussed in Chapter 17 and then applied in Chapter 18, where the transmission of sound through elastic walls is discussed.

This work proposes a mathematical approach to acoustics which reflects the professional experience of the authors in the field of acoustic modeling. It is

also based on the idea that engineers must be able to quantify the phenomena they study and this cannot be achieved without models, whether simple or complex.

2

Definition and scope of acoustics

You must attend to the commencement of this story, for when we get to the end, we shall know more than we do now [...]
— **Hans Christian Andersen** (1805-1875), The Snow Queen (1845).

Contents

2.1 Definitions **4**
2.2 Fields of acoustics **6**
2.3 Spectral range of sounds **12**
2.4 Relevance of acoustics **14**

2.1 Definitions

Acoustics is the science of sound and noise:

- A **sound** is an *oscillation in pressure, stress, particle displacement, particle velocity, etc., propagated in a medium with internal forces (e.g. elastic or viscous), or the superposition of such propagated oscillations.* A sound is also the *auditory sensation evoked by the oscillation described above*[1].
- ***Noise*** *is an acoustic phenomenon producing an auditory sensation considered unpleasant or annoying. This feeling is not only related to the loudness, but also to cultural and psychological factors.*[2]

A sound is a *small* temporal variation of pressure around a mean reference value (e.g., atmospheric pressure in air or hydrostatic pressure in water):

$$p_{tot}(t) = p_{atm} + p_{ac}(t) \tag{2.1}$$

where:

$$p_{atm} \gg p_{ac}(t) \tag{2.2}$$

and:

$$p_{atm} = \frac{1}{T}\int_{t_0}^{t_0+T} p_{tot}(t)dt \tag{2.3}$$

where the time T is assumed to be large compared to the time scale of the fluctuations of $p_{ac}(t)$. To simplify notations in subsequent chapters, we will often write $p(t)$ for $p_{ac}(t)$ to designate the difference between the total pressure and the local reference pressure. Pressures (total, reference or acoustic) are measured in Pascal (Pa).[3]

Acoustics, initially the science of audible sounds, has broadly become the science that studies the propagation of pressure waves in any elastic continuum. For example, underwater acoustics and P-waves in geodynamics are

[1] ANSI/ASA S1.1-2013.
[2] NASA Space Flight Human-system Standard, Volume 1: Crew Health (NASA-STD-3001).
[3] Reminder: 1 atm = 101325 Pa.

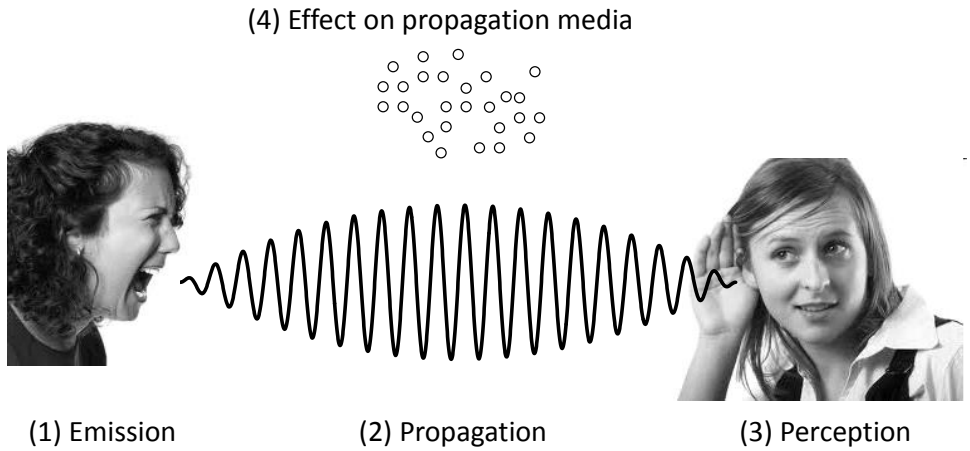

Figure 2.1: The four dimensions of acoustics: generation, transmission, perception and effects on the environment.

considered parts of acoustics. Furthermore, acoustics considers four different aspects of sound (Figure 2.1):

1. sound generation (emission);
2. sound propagation from its source to one or more receivers;
3. sound measurement, recording or perception by the receiver (microphone or ear);
4. sound effects on its propagation environment (these effects are not observed in linear acoustics and will not be discussed here).

Etymology

- **Sound**: from the latin word *sonum* (sound, noise) perhaps of the same origin as the Sanskrit word *svanáh*.[4]
- **Noise**: *early 13th century, "loud outcry, clamor, shouting" from Old French* noise *"din, disturbance, uproar, brawl" also "rumor, report, news",*

[4] **Alain Rey**, *Dictionnaire historique de la langue française* (Historical Dictionary of the French Language, 1992).

apparently from Latin nausea "disgust, annoyance, discomfort" literally "seasickness".[5]

- **Acoustics**: from the ancient Greek word $\alpha\kappa o\upsilon\varepsilon\iota\nu$ (hear), followed by the ending *-tics* found in the name of many disciplines such as numismatics, propædeutics, æsthetics, hermeneutics and casuistics. The word was proposed in 1700 by the French scholar Joseph Sauveur[6] and was then adopted in many other languages (acoustique in French, acoustiek in Dutch, akustik in German, Danish and Swedish, acustica in Italian).

2.2 Fields of acoustics

Figure 2.2 shows how the different branches of acoustics (underwater sound, electro-acoustics, shocks and vibrations, etc.) revolve around fundamental physical acoustics and are linked to various arts and sciences. A useful classification of acoustics is proposed by the Acoustical Society of America:

- **General linear acoustics**: see Section 4.2 for a discussion of linearity and non-linearity in acoustics.
- **Aeroacoustics and atmospheric sound**: aeroacoustics studies noise produced by flows and the propagation of noise in moving fluids (convected propagation, see Chapter 15) including the atmosphere (Chapter 16). More generally, any phenomena where an acoustic field interacts with a fluid flow can be categorised as aeroacoustics.
- **Structural acoustics, vibration** or *vibro-acoustics* studies noise generation by vibrating structures or the vibration of structures induced by acoustic fields.
- **Architectural acoustics**: building and room acoustics (the latter is discussed in Chapter 8).

[5] Online etymology dictionary, January 2015.

[6] **Joseph Sauveur**, a French physicist, member of the Academy of Sciences and professor of mathematics at the Collège de France, was born in La Flèche in 1653 and died in Paris in 1716. Sauveur is known as the founder of musical acoustics, in the tradition of René Descartes and Marin Mersenne.

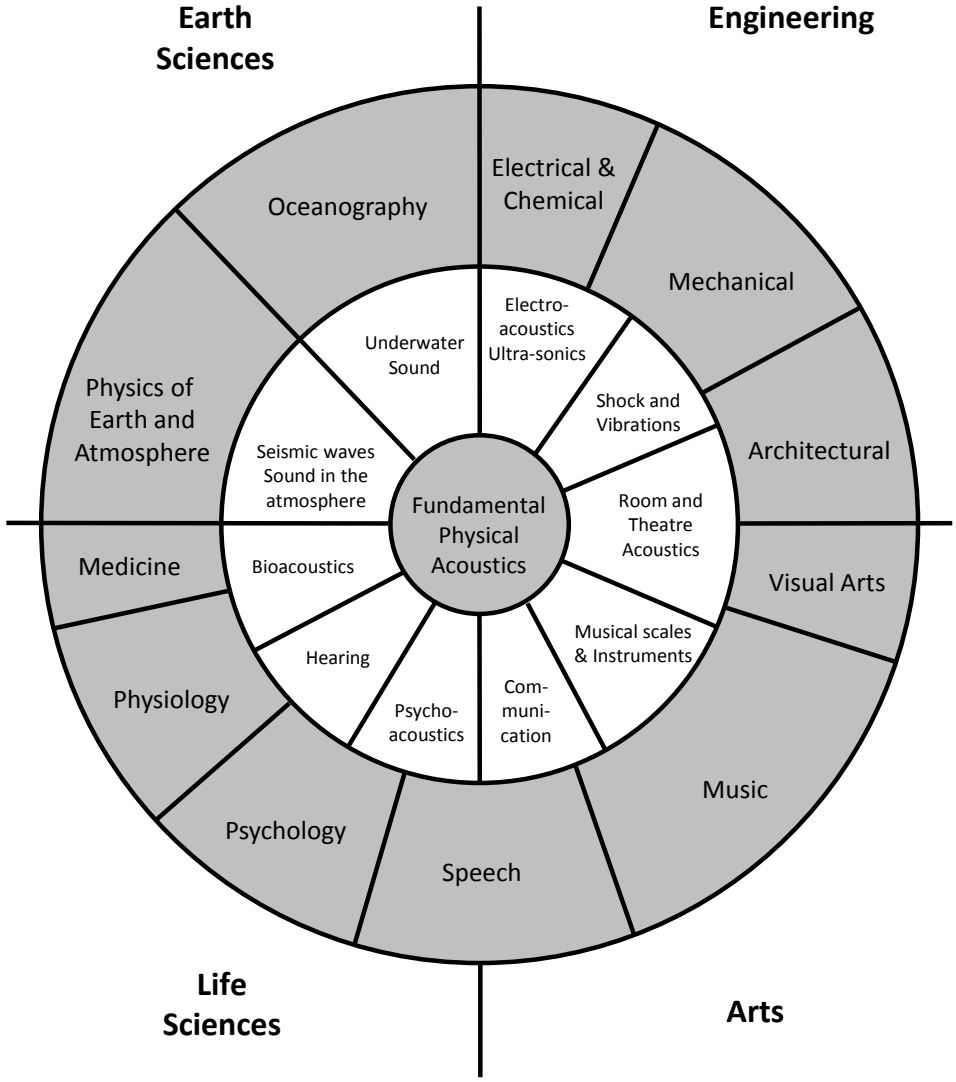

R.B. Lindsay, JASA 36:2242 (1964)
Adapted by A.D. Pierce, Acoustics, ASA and AIP (1994).

Figure 2.2: Lindsay's Wheel of Acoustics.

- **Ultrasonics, quantum acoustics and physical effects of sound**: ultrasounds have frequencies between 20 kHz and 1 GHz, while quantum acoustics or *hypersonics* are concerned with frequencies higher than 1 GhZ (see Section 2.3).

- **Physiological acoustics** studies the human ear and, more generally, the response of the human body to sounds.

- **Speech production** and **speech perception** investigate the mechanisms involved in the generation of the spoken and sung voice as well as the mechanisms by which the ear (or an artificial system) perceives or records the transmitted signal. The analysis of the pathologies of speech production (phonation) also falls into this framework. *Auralisation* technology belongs to the same topic; auralisation is a neologism designating the auditory equivalent of visualisation, that is to say the techniques used to let synthetic sound signal (for example, the results of a numerical simulation) be heard in a realistic way.

- **Bioacoustics** is the study of the physiological mechanisms by which animals generate sounds or communicate by sounds (and ultrasounds). This research may seem exotic and lacking applications; however the article of Löhse et al., published in Nature in 2001[7], describing noise generation by *snapping shrimps* shows:

  - that the living world displays extremely remarkable physical phenomena;[8]
  - that the metrological ingenuity of researchers is without limit;
  - that nature displays amazing inventiveness, as far as weapons of attack or defense are concerned.

  What is so special about snapping shrimps (Figure 2.3)? It is their ability to generate a very high noise level by brutally closing their claw. The noise is not generated by the shock of the two claws, but by the fact that, when closing, a protrusion of the movable claw fits into a

[7] **Löhse, D. Schmitz, B. and Versluis, M.**, *Snapping shrimp make flashing bubbles*, Nature 413 (6855), 477-478, 2001. See also their YouTube video (keyword snapping shrimp).

[8] *If it's amazement you want, the real world has it all* as **Richard Dawkins** so aptly wrote in *The ancestor's tale: a pilgrimage to the dawn of life* (2004).

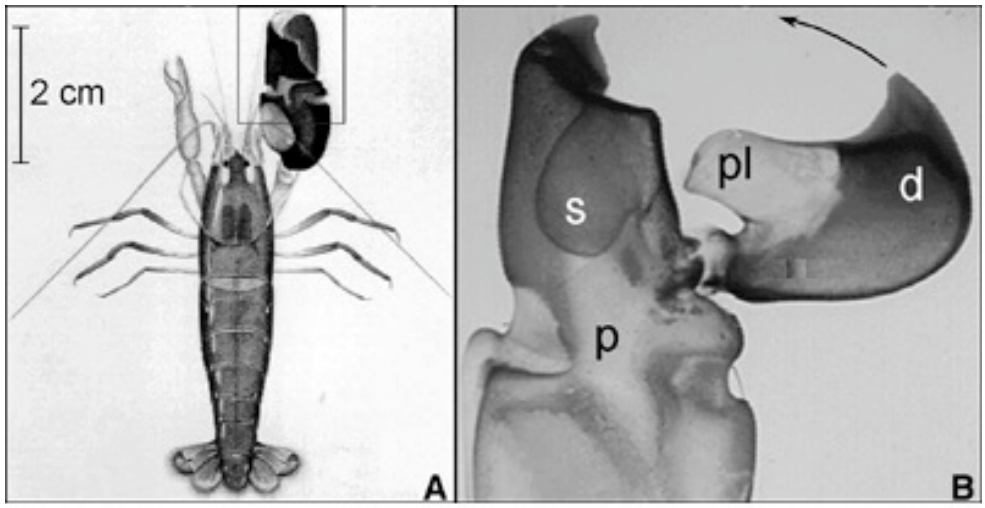

Versluis, Schmitz, von der Heydt, Löhse, *How Snapping Shrimp Snap: Through Cavitating Bubbles*, Science, Vol. 289 no. 5487 pp. 2114-2117. Reprinted with permission from AAAS.

Figure 2.3: The famous *snapping shrimp*.

hole located in the fixed claw and ejects the water contained in the tiny cavity at a speed of over 100 km/h. The depression at the back of the water jet induces an unstable cavitation bubble which implodes and generates the high noise. This violent implosion, and the accompanying high pressure and temperature peaks, are capable of killing small prey. Löhse and colleagues also identified the production of a flash of light by a mechanism similar to sono-luminescence which they humorously named *shrimpoluminescence*!

- **Non-linear acoustics**: Section 4.2 analyses linearity and non-linearity in acoustics.

- The study of **underwater sound** is a distinct field due to the nature of its applications. In many respects, however, the phenomena involved are similar to those observed in airborne acoustics.[9] Underwater acoustics is an important research topic for the military such as:

[9] Among important specific phenomena, we can mention the waveguide effect arising from the finite vertical extension of the acoustic domain and the variation of the speed of sound with depth due to temperature, salinity and hydrostatic pressure gradients (see Mackenzie formula in Section 4.6.2).

  - design of powerful ultrasonic transmitters and sensitive receivers for the detection of potential targets by sonars;
  - analysis of faint underwater sound signals to identify enemy vessels (ship, submarine).

  Oceanography, marine science, climatology and meteorology also make use of sonars:

  - bathymetry and analysis of sedimentary layers;
  - imaging of the seabed, search of wrecks, mines or submerged archæological sites;
  - controlling fish stocks;
  - analysis of underwater flora.

- **Transduction and acoustical measurements**: in the context of acoustics, transduction is the study of the production of sound by various energy sources (electric, magnetic, mechanical) and, conversely, the conversion of sound waves into different energy forms, primarily for metrological purpose. Well known transducers (emitters) include speakers and active materials.

  - Speakers consist of a permanent magnet mounted on the base of a cone and surrounded by a fixed coil through which a varying electric current circulates. Current circulation induces an electromagnetic force that causes the cone to vibrate, therefore creating pressure waves in the air.
  - Active materials (piezoelectric, magnetostrictive) feature a coupling between elastic ($\bar{\bar{\sigma}}$ and $\bar{\bar{\varepsilon}}$) and electric ($\vec{E}$ and $\vec{D}$) or magnetic ($\vec{B}$ and $\vec{H}$) fields. A piezoelectric material, for example, vibrates when traversed by an alternating electric current and these vibrations are transmitted to the surrounding fluid as sound.

  Sound measurement and recording devices use the same mechanisms, but cause and effect are exchanged:

  - the vibrations of a piezoelectric crystal induce an electric current that can be measured;

  - vibrations of the diaphragm of a microphone lead to a variation of the electrical impedance of the circuit and a change of the amplitude and phase of the current flowing through it.

- **Noise, its effects and control**: this category covers the *regulatory* aspects of acoustics:
  - definition of noise measurement procedures adapted to different situations: road noise, noise in the workplace, noise mapping around an airport or factory;
  - interpretation of measurements, correlation between objective measurements and people's subjective perception of the related nuisances;
  - norms and standards;
  - practical solutions to noise problems in a given environment: optimal placement of machines and operators in a workshop, choice of materials for floors, ceilings, partitions.
- **Acoustic signal processing** looks at specific techniques of signal processing used in acoustics (an introduction is given in Chapter 5 devoted to Fourier analysis).
- **Psychological acoustics**: it is often difficult to correlate the classical objective indicators of sound level (dB for example, see Chapter 7) with the perception of this sound by a listener. Psychological acoustics attempts to:
  - define various indicators to assess perceptions;
  - explain the difference in perception by the sensory, psychological, sociological, cultural and physiological state of the listener and his/her prior history of noise exposure.
- **Music and musical instruments**: this is the mathematical and physical study of music in all its dimensions.

In addition to these topics, **electro-acoustics** should be included in the list. It is primarily documented and discussed in the Journal of the Audio Engineering Society (AES).

2.3 Spectral range of sounds

A sound is characterised by its frequency or its constituent frequencies which are expressed in Hertz[10] (Hz, s^{-1}). Acoustics can be divided into four areas (Figure 2.4) according to the frequency of the sound signal:

- infrasounds have frequencies between 0 and 20 Hz;
- the human ear is sensitive to frequencies between 20 Hz and 20,000 Hz;[11] this range, in fact, changes from one subject to another and the maximum sensitivity is limited to a smaller range extending from 100 to 4,000 Hz (Figure 2.5);
- the spectral range of ultrasounds begins at 20 kHz and conventionally stops at 1 GHz (10^9 Hz); the very broad ultrasound frequency range is divided in two regions: power ultrasounds (20 kHz - 1 MHz) and diagnostic ultrasound (1 - 10 MHz);
- hypersounds occupy the rest of the spectrum above 1 GHz.

This work focuses on audible sounds. However, most of the theoretical concepts and developments also apply to ultrasounds and, to a lesser extent, infrasound.

[10] **Heinrich Hertz**, a German physicist and pupil of Helmholtz, was born in 1857 in Berlin and died in 1894 in Bonn. Hertz was the first to confirm experimentally, in 1887, the existence of electromagnetic waves predicted by the theory proposed by James Clerk Maxwell (1831-1879).

[11] 16 Hz and 16 kHz are also often the boundary between infrasounds and sounds and between sounds and ultrasounds.

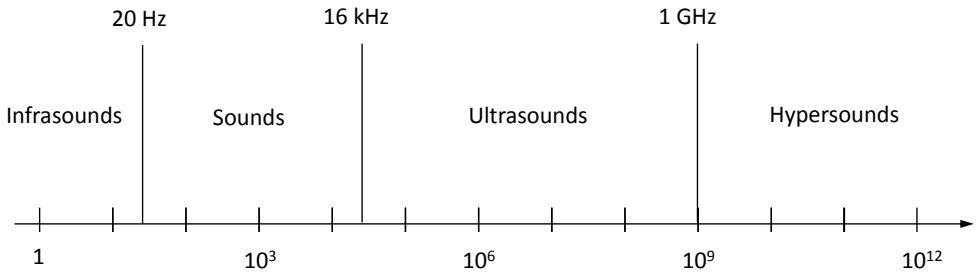

Figure 2.4: Spectral range of sounds.

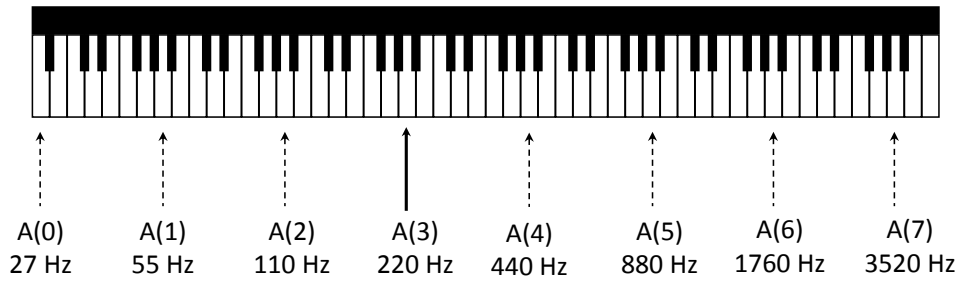

Figure 2.5: The frequency range of a piano matches the zone of maximum auditory sensitivity of the human ear.

2.4 Relevance of acoustics

> *Noise is the most impertinent of all forms of interruption. It is not only an interruption, but also a disruption of thought.*
> — **Arthur Schopenauer** (1788-1860), On noise.

The field of acoustics has seen remarkable growth in recent decades as a result of several interrelated developments:

- the perception of noise as a major nuisance to be abated;
- the introduction of increasingly stringent noise standards;
- the desire of manufacturers to supply acoustically satisfactory products and to leverage acoustic characteristics as a sales argument.

Increasing awareness of noise has driven recent developments and progress in acoustics. Many studies have been devoted to the harmful effects of noise on human activities:

- verbal communication: noise interferes with and degrades the content in messages we exchange;
- focus and task performance: noise reduces attention, increases the number of interruptions in the execution of a task and reduces the quality of the work performed;
- hearing disorders: repeated exposure to a sufficiently high level of noise induces temporary or permanent disorders ranging from limited and selective loss of hearing to complete deafness;
- other physiological disorders: the impact of noise on preterm births, cardiovascular accidents and psychiatric problems is well documented;
- sleep is clearly affected by noise, in each of its phases.

In many countries, protest movements by citizens living near airports, show the concern of populations about noise pollution.

States and supra-national entities, such as the European Commission, have imposed maximum sound levels through standards and recommendations. Regulations setting limits for admissible noise levels for airplanes, cars, trains and machinery have flourished in the last decades. This normative approach has been another important driver of acoustics research.

Producers of noisy goods and equipment have been forced to adapt to applicable standards. They have also recognised the growing importance of acoustic quality as a purchase criterion for prospective clients. The example of the automotive market is striking. Until 1973, the essential criteria were design, engine power, maximum acceleration and driving pleasure. The subsequent oil crisis put the focus on consumption and durability. More recently, safety (crashworthiness) and comfort (seats, suspension, air conditioning) have become essential buying criteria. Nowadays, acoustic comfort is of vital importance and consumers often prefer the quietest cars within a range.

Electric and hybrid vehicles are facing the opposite challenge, as the lack of noise fails to alert pedestrians and must be artificially increased. In addition, the audible feedback is not consistent with the manœuvers of the driver and so the signal must be filtered and modified in order not to be misinterpreted.

Electrical home appliances provide another example of this trend. The noise level produced by a dishwasher, vacuum cleaner or washing machine is now displayed in stores in many countries. At comparable prices, the buyer will give priority to the quietest product. Recent advertising campaigns are very revealing of this change in consumer attitude.

Figure 2.6: New York, May 2008, an expensive honk!

Part I

Governing equations and
fundamental concepts of linear acoustics

3

Fundamental equations of continuum mechanics

All the effects of Nature are only the mathematical consequences of a small number of immutable laws.
— **Pierre-Simon de Laplace** (1749-1827), Analytic theory of probabilities (1812).

Contents

3.1 Continuity equation 20
3.2 Index notation 22
3.3 Momentum equation 25
3.4 Equation of state 31

Navier-Stokes[1] equations express two fundamental principles of mechanics: the mass conservation on the one hand and Newton's[2] second law ($\vec{F} = m\vec{a}$) on the other. The state variables used to describe the fluid are pressure p, density[3] ρ and velocity $\vec{v}$.

3.1 Continuity equation

Conservation of mass can be expressed locally by considering an infinitesimal fluid volume of dimensions dx, dy and dz (Figure 3.1) and by expressing that the mass increase of the volume during a time interval dt results in a corresponding increase of the fluid density in the volume.

Mass flow

Consider, for example, the $dx.dz$ side, perpendicular to the y axis. The flow of matter entering the volume from this side during time dt is written as:

$$\rho v_y dx dz dt \tag{3.1}$$

Taking into account the variation of density and velocity between two parallel sides of the control volume, the flow of matter coming out through the opposite

[1] **Claude Louis Marie Henri Navier** was born in 1785 in Dijon and died in 1836 in Paris. A student of Joseph Fourier, he worked on several topics of applied mathematics, including elasticity and fluid dynamics. In the latter domain he formulated equations for incompressible fluids in 1821 and for viscous fluids in 1822. **Sir George Gabriel Stokes** (1819-1903) is known for his study of viscosity and fluid mechanics and for his vector calculus theorem.

[2] **Isaac Newton**, English mathematician, physicist, and astronomer, was born in Woolsthorpe in 1642 and died in Kensington in 1727. His treatise *PhilosophiæNaturalis Principia Mathematica*, published in 1687, and considered as the most influential physics book of all time, describes universal gravitation and the laws of motion that form the foundations of classical mechanics. Newton is, along with Leibniz, the founder of differential and integral calculus.

[3] Also, and more appropriately, called specific weight or volumetric mass.

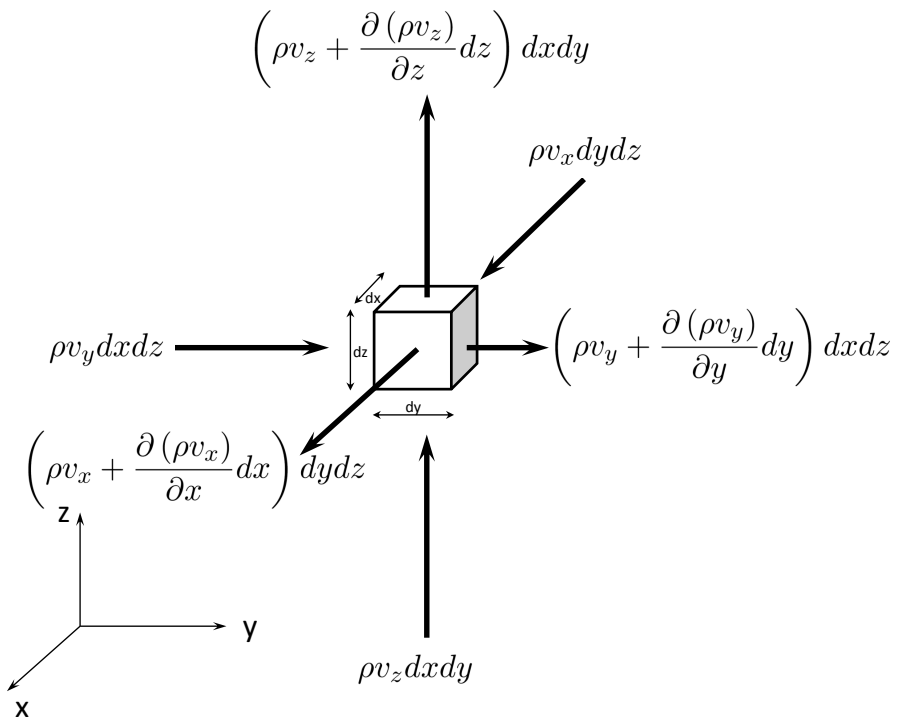

Figure 3.1: Continuity equation.

side during the same time interval is given by:

$$\left(\rho + \frac{\partial \rho}{\partial y} dy\right) \left(v_y + \frac{\partial v_y}{\partial y} dy\right) dxdzdt \tag{3.2}$$

Limiting the development to the first order, the net flow of matter across the two sides takes the form:

$$-\frac{\partial(\rho v_y)}{\partial y} dxdydzdt \tag{3.3}$$

If the same calculation is done for the other two pairs of sides, we obtain the following expression for the net flow of matter through the control volume during the time dt:

$$-\left(\frac{\partial(\rho v_x)}{\partial x} + \frac{\partial(\rho v_y)}{\partial y} + \frac{\partial(\rho v_z)}{\partial z}\right) dxdydzdt \tag{3.4}$$

Sources of mass

Consider a distributed source of mass $q(x, y, z, t)$ $[kg/(m^3.s)]$. The total mass produced by this source in the elementary volume during time dt is:

$$qdxdydzdt \tag{3.5}$$

Increase in specific mass

We can also evaluate the increase of mass in the volume by considering the variation of density:

$$\left(\rho + \frac{\partial \rho}{\partial t} dt\right) dxdydz - \rho dxdydz = \frac{\partial \rho}{\partial t} dxdydzdt \tag{3.6}$$

Continuity equation

Conservation of mass requires that the sum of (3.4) and (3.5) must be equal to (3.6). This relationship is called the *continuity equation*:

$$\frac{\partial \rho}{\partial t} = q - \left(\frac{\partial (\rho v_x)}{\partial x} + \frac{\partial (\rho v_y)}{\partial y} + \frac{\partial (\rho v_z)}{\partial z}\right) \tag{3.7}$$

or:

$$\frac{\partial \rho}{\partial t} + \left(\frac{\partial (\rho v_x)}{\partial x} + \frac{\partial (\rho v_y)}{\partial y} + \frac{\partial (\rho v_z)}{\partial z}\right) = q \tag{3.8}$$

3.2 Index notation

Index notation will be systematically used in the remainder of this chapter and in some of the following chapters. This notation is very compact and consistent. Equation 3.8 is used to present index notation.

Coordinates and components

The letters x, y and z for the three spatial coordinates of a Cartesian reference frame are first replaced by x_1, x_2 and x_3. More generally, any vector $\vec{u}$ is characterised by its three components (u_1, u_2, u_3). Equation 3.8 can then be rewritten as:

$$\frac{\partial \rho}{\partial t} + \sum_{i=1,3} \frac{\partial \left(\rho v_i\right)}{\partial x_i} = q \tag{3.9}$$

Derivatives

The derivative of a function f with respect to time is written $\partial_t f$. The derivatives with respect to x_i are written $\partial_i f$. The continuity equation can now be written:

$$\partial_t \rho + \sum_{i=1,3} \partial_i \left(\rho v_i\right) = q \tag{3.10}$$

Implicit summation

The notation can be further simplified using Einstein's[4] convention which specifies that summation is implicit on indices that are repeated twice in the same term. The second term on the left side of the continuity equation sees a repetition of the index i. There is therefore no need to keep the summation symbol and the equation becomes very compact indeed:

$$\partial_t \rho + \partial_i \left(\rho v_i\right) = q \tag{3.11}$$

A repeated index is called a mute index. Einstein's convention requires that two important rules are fulfilled:

[4] **Albert Einstein**, a German physicist, was born in Ulm in 1879 and died in Princeton (USA) in 1955. In 1905, while working at the Swiss Patent Office in Bern, he published three papers that are landmarks of twentieth century physics. In the first paper, he elucidates the photoelectric effect and introduces a new particle: the photon. In the second paper he establishes the statistical theory of Brownian motion and, in the third, he questions the foundations of mechanics by proposing his special theory of relativity. He then spent many years working on the general theory of relativity (1916). It is while developing the latter, which makes intensive use of tensor calculus and index notation, that he introduced his convention of implicit summation over repeated indices.

1. An index may not appear more than twice in the same term.

2. Different terms of an equation must contain the same non-mute indices (indices homogeneity). From this point of view the following statements are consistent:

$$c_{ik} = a_{ij} b_{jk} \tag{3.12}$$

$$e_{ikl}\delta_{kl} = a_i + b_{ij}c_j + d_{ik}c_k \tag{3.13}$$

whereas the following are not:

$$c_{ij} = a_{ij} b_{ij} \tag{3.14}$$

$$a_i + b_k + c_{ik} \tag{3.15}$$

Other examples

$$\left(\vec{\nabla} f\right)_i = \partial_i f \tag{3.16}$$

$$\vec{\nabla} \cdot \vec{u} = \partial_i u_i \tag{3.17}$$

$$\Delta f = \partial_{ii} f \tag{3.18}$$

Kronecker and Levi-Civita symbols

Many expressions using the index notation make use of the Kronecker and Levi-Civita symbols. The Kronecker[5] symbol, δ_{ij}, is defined as follows:

$$\begin{aligned} \delta_{ij} &= 1 \quad if \quad i = j \\ \delta_{ij} &= 0 \quad if \quad i \neq j \end{aligned} \tag{3.19}$$

Here are some examples of expressions using this symbol:

$$u_i \delta_{ij} = u_j \tag{3.20}$$

$$\sigma_{ij}\delta_{ij} = \sigma_{ii} \tag{3.21}$$

[5] **Leopold Kronecker**, a German mathematician, father of the theory of algebraic numbers, was born in Liegnitz in 1823 and died in 1891.

$$\begin{pmatrix} a_{11} & a_{12} & a_{13} \\ a_{21} & a_{22} & a_{23} \\ a_{31} & a_{32} & a_{33} \end{pmatrix} + \begin{pmatrix} b & 0 & 0 \\ 0 & b & 0 \\ 0 & 0 & b \end{pmatrix} = a_{ij} + b\delta_{ij} \tag{3.22}$$

The Levi-Civita[6] symbol, δ_{ijk}, is equal to:

- 1 if $i - j - k$ define an even permutation of $1 - 2 - 3$;
- -1 if the three indices define an odd permutation of $1 - 2 - 3$;
- 0 if $i - j - k$ are not a permutation of $1 - 2 - 3$.

For example:

$$\delta_{123} = 1,\ \delta_{113} = 0,\ \delta_{222} = 0,\ \delta_{132} = -1,\ \delta_{231} = 1,\ \delta_{321} = -1 \tag{3.23}$$

This symbol is especially useful in the expression of the vector product:

$$(\vec{u} \times \vec{v})_i = \delta_{ijk} u_j v_k \tag{3.24}$$

and in writing the *curl* operator:

$$\left(\vec{\nabla} \times \vec{u}\right)_i = \delta_{ijk} \partial_j u_k \tag{3.25}$$

3.3 Momentum equation

In its most familiar form, Newton's second law relates the force $\vec{F}$ acting on a body to the mass m and acceleration $\vec{a}$ of that body:

$$\vec{F} = m\vec{a} \tag{3.26}$$

[6] **Tullio Levi-Civita**, an Italian mathematician, was born in 1873 in Padua and died in 1941 in Rome. He is known primarily for his work on tensor calculus and its applications to the general theory of relativity. δ_{ijk} is sometimes inappropriately called the *second Kronecker symbol*.

In this form, it is implicitly assumed that mass does not vary over time. In a more general context, Newton's law can be written as:

$$\vec{F} = \frac{d\left(m\vec{v}\right)}{dt} \tag{3.27}$$

where $\vec{v}$ is the velocity of the body and where the quantity $m\vec{v}$ is called the momentum. This principle is applied to the same infinitesimal control volume used to derive the continuity equation. The change in momentum of the elementary volume during time dt is given by:

$$\left(\rho\vec{v} + \frac{\partial\left(\rho\vec{v}\right)}{\partial t}dt\right)dxdydz - \rho\vec{v}dxdydz = \frac{\partial\left(\rho\vec{v}\right)}{\partial t}dxdydzdt \tag{3.28}$$

The change in momentum is due to the net flow of momentum through the sides of the volume and to the action of external forces on the volume.

Forces acting on volume

If we exclude gravity, the forces acting on the volume are the resultant of the different components of the stress tensor acting on the sides of the volume (Figure 3.2). If we choose again to study the y component, the resulting force is given by:

$$\begin{aligned} F_y &= \left(\sigma_y + \frac{\partial\sigma_y}{\partial y}dy\right)dxdz - \sigma_y dxdz \\ &+ \left(\tau_{xy} + \frac{\partial\tau_{xy}}{\partial x}dx\right)dydz - \tau_{xy}dydz \\ &+ \left(\tau_{zy} + \frac{\partial\tau_{zy}}{\partial z}dz\right)dxdy - \tau_{xy}dxdy \\ &= \left(\frac{\partial\tau_{xy}}{\partial x} + \frac{\partial\sigma_y}{\partial y} + \frac{\partial\tau_{zy}}{\partial z}\right)dxdydz \end{aligned} \tag{3.29}$$

Similarly, for other directions we obtain:

$$F_x = \left(\frac{\partial\sigma_x}{\partial x} + \frac{\partial\tau_{yx}}{\partial y} + \frac{\partial\tau_{zx}}{\partial z}\right)dxdydz \tag{3.30}$$

$$F_z = \left(\frac{\partial\tau_{xz}}{\partial x} + \frac{\partial\tau_{yz}}{\partial y} + \frac{\partial\sigma_z}{\partial z}\right)dxdydz \tag{3.31}$$

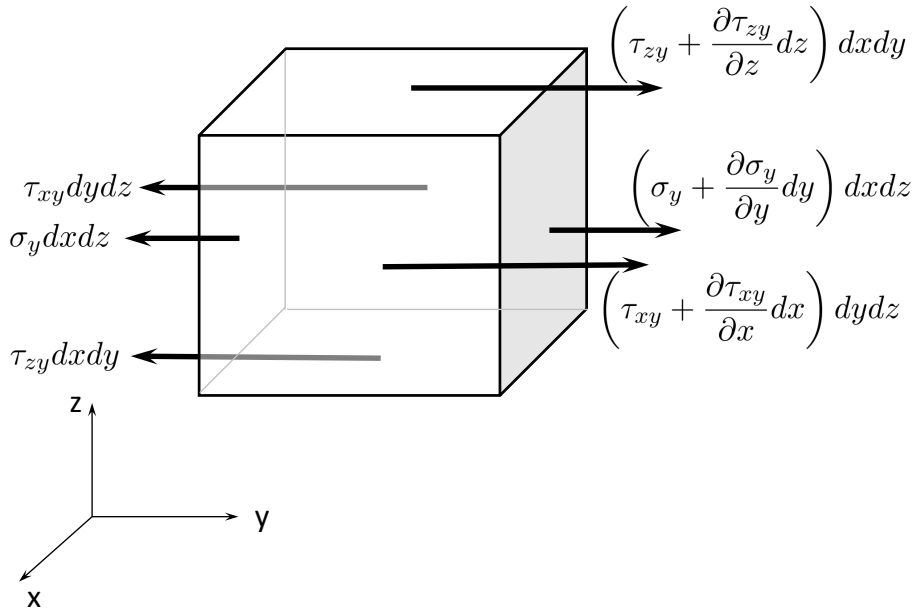

Figure 3.2: Forces acting on the volume (viscous fluid).

These three relationships can be written in a particularly compact form using index notation (taking into account the symmetry of the stress tensor: $\tau_{ij} = \tau_{ji}$):

$$F_i = \partial_j \tau_{ij} dxdydz \tag{3.32}$$

In a Newtonian fluid, the stress tensor is linked to pressure and velocity through the following equation:

$$\tau_{ij} = -p\delta_{ij} + \lambda \delta_{ij} \partial_k u_k + \mu \left(\partial_i u_j + \partial_j u_i\right) \tag{3.33}$$

where λ is the kinematic and μ the dynamic viscosity of the fluid. For an inviscid fluid, this relationship becomes:

$$\tau_{ij} = -p\delta_{ij} \tag{3.34}$$

and the only forces acting on the elementary volume are pressure forces (Figure 3.3).

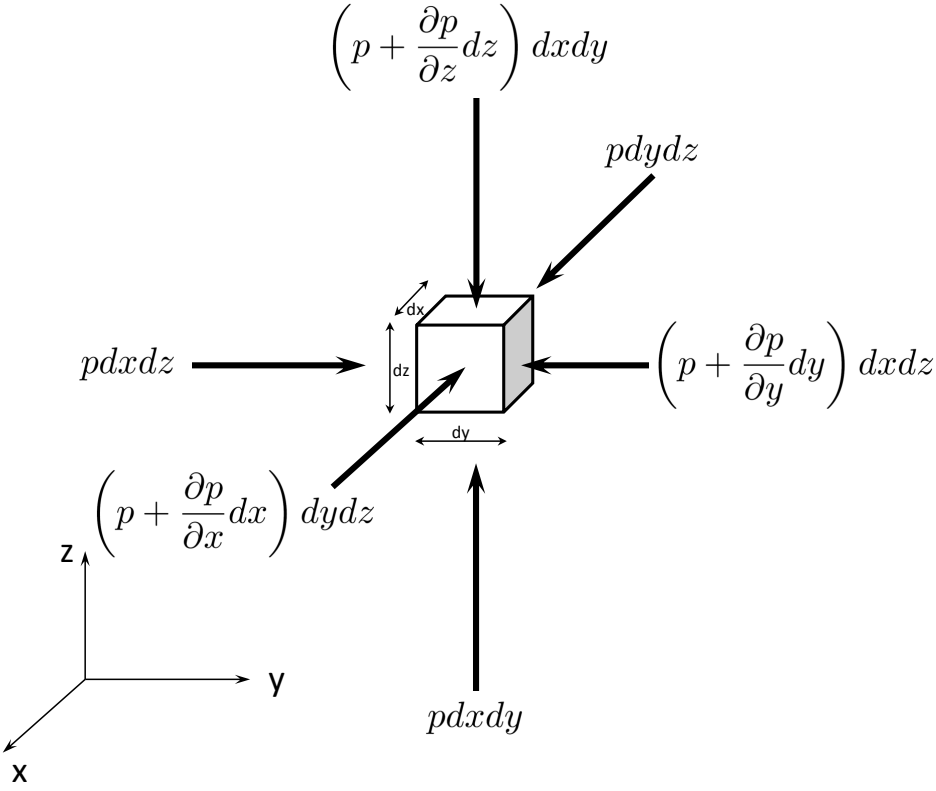

Figure 3.3: Forces acting on the volume (inviscid fluid).

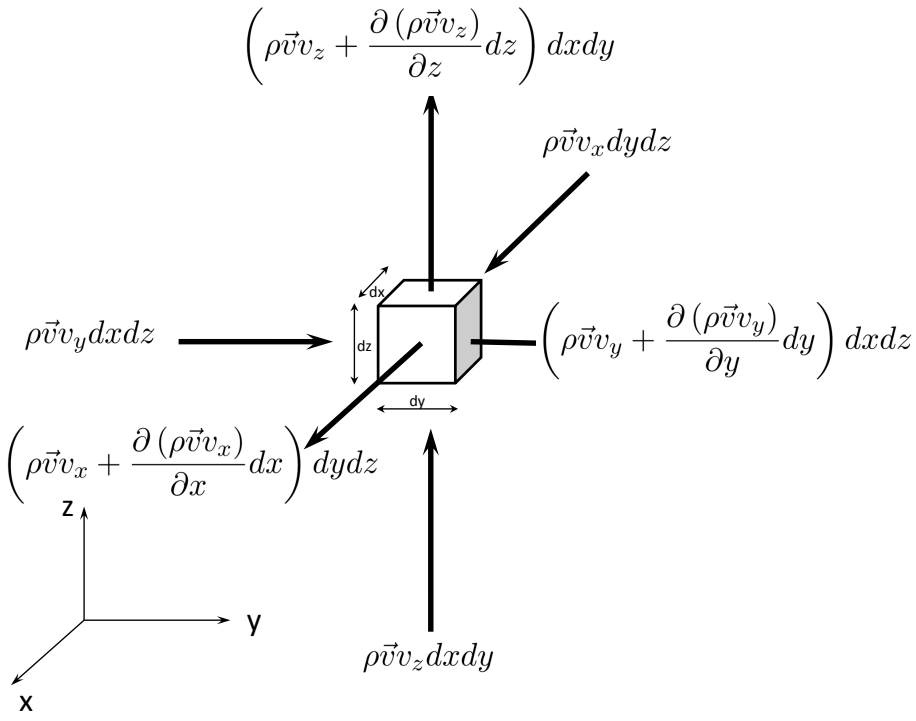

Figure 3.4: Net flow of momentum in elementary volume.

Flow of momentum

The net flow of momentum, per unit of time, through side $dx.dz$ is (Figure 3.4):

$$\rho\vec{v}v_y dxdz - \left(\rho\vec{v} + \frac{\partial(\rho\vec{v})}{\partial_y}dy\right)\left(v_y + \frac{\partial v_y}{\partial_y}dy\right)dxdz \tag{3.35}$$

Keeping only first order terms we obtain:

$$-\frac{\partial(\rho\vec{v}v_y)}{\partial_y}dxdydz \tag{3.36}$$

Adding the flow of momentum through the other two pairs of sides, we get:

$$-\left(\frac{\partial(\rho\vec{v}v_x)}{\partial_x} + \frac{\partial(\rho\vec{v}v_y)}{\partial_y} + \frac{\partial(\rho\vec{v}v_z)}{\partial_z}\right)dxdydz \tag{3.37}$$

or, using index notation:

$$-\partial_j \left(\rho v_i v_j\right) dxdydz \tag{3.38}$$

Momentum equation

Matching Equation 3.28 with the sum of Equations 3.32 and 3.38 yields the *momentum equation*:

$$\partial_t \left(\rho v_i\right) = \partial_i \tau_{ij} - \partial_j \left(\rho v_i v_j\right) \tag{3.39}$$

or:

$$\partial_t \left(\rho v_i\right) + \partial_j \left(\rho v_i v_j\right) - \partial_i \tau_{ij} = 0 \tag{3.40}$$

The first two terms can be further developed:

$$v_i \partial_t \rho + \rho \partial_t v_i + v_i \partial_j \left(\rho v_j\right) + \rho v_j \partial_j v_i - \partial_i \tau_{ij} = 0 \tag{3.41}$$

or:

$$v_i \left(\partial_t \rho + \partial_j \left(\rho v_j\right)\right) + \rho \left(\partial_t v_i + v_j \partial_j v_i\right) - \partial_i \tau_{ij} = 0 \tag{3.42}$$

Continuity (3.8) lets us replace the first bracket with the source of mass q, yielding:

$$\rho \left(\partial_t v_i + v_j \partial_j v_i\right) - \partial_i \tau_{ij} = -q v_i \tag{3.43}$$

Equations 3.40 and 3.43 are fully equivalent. Equation 3.40 will usually be preferred when $q \neq 0$ while Equation 3.43 will be preferred when $q = 0$, in which case it is simply written as:

$$\rho \left(\partial_t v_i + v_j \partial_j v_i\right) - \partial_i \tau_{ij} = 0 \tag{3.44}$$

3.4 Equation of state

Equations of continuity (Equation 3.11) and momentum (Equation 3.43) form a system of four partial differential equations involving five unknowns: density ρ, pressure p and the three components of the velocity vector v_i. The equation of state applicable to air is the ideal gas law ($p = n\rho RT$) which provides a fifth equation, but also adds a sixth unknown (absolute temperature T). Temperature can be eliminated by assuming that the acoustic compression-depression cycle involves no heat transfer (adiabatic transformation). The adiabatic transformation of an ideal gas from a state (p_1, ρ_1) to a state (p_2, ρ_2) is such that:

$$\frac{p_1}{\rho_1^{\gamma}} = \frac{p_2}{\rho_2^{\gamma}} \tag{3.45}$$

where $\gamma = \frac{c_p}{c_v}$ is the ratio of specific heat at constant pressure (c_p) and constant volume (c_v). γ is equal to $\frac{7}{5}$ for diatomic gases (O_2, N_2). Equation 3.45 closes the system of equations formed by the continuity and momentum equations: we now have five equations with 5 unknowns.

4

The wave equation

. . . and what do not the first steps in any branch of knowledge cost? One is excused from making larger steps by the merit of taking any at all.

— **Jean le Rond d'Alembert** (1717-1783), Preliminary Discourse to the Encyclopedia (1763).

Contents

4.1 The wave equation 34
4.2 Linearity and non-linearity in acoustics 40
4.3 General one-dimensional solution 41
4.4 Mechanics of propagation 43
4.5 Dispersive and non-dispersive propagation 46
4.6 Speed of sound 50

Noise has been defined in Chapter 2 as a small variation of pressure around its mean value. In this chapter, we will see the equation which rules the amplitude of this pressure fluctuation.

4.1 The wave equation

Navier-Stokes equations (Chapter 3) express the conservation of mass (continuity equation):

$$\partial_t \rho + \partial_i (\rho v_i) = q \tag{4.1}$$

and Newton's second law (momentum equation):

$$\rho (\partial_t v_i + v_j \partial_j v_i) - \partial_i \tau_{ij} = -q v_i \tag{4.2}$$

In order to arrive at an equation for the acoustic pressure fluctuation, five hypotheses will be successively applied to the continuity and momentum equations:

1. non-viscous fluid;
2. small perturbations;
3. linearised constitutive law;
4. fluid globally at rest;
5. linearisation of the resulting equations.

Non-viscous fluid

The first assumption is that the fluid in which the sound wave propagates is non-viscous; the stress tensor is then given by:

$$\tau_{ij} = -p \delta_{ij} \tag{4.3}$$

which, inserted into the momentum equation, gives Euler[1] equations:

$$\rho\left(\partial_t v_i + v_j \partial_j v_i\right) + \partial_i p = -q v_i \tag{4.4}$$

A fluid is never completely devoid of viscosity but the viscosity of air or water is very low. If necessary, viscous dissipation effect can be reintroduced *a posteriori* in an *ad hoc* way (Section 6.5.4).

Small perturbations

The second hypothesis separates the pressure and density fields into two components: a reference value, constant in time and space, and a fluctuating value assumed to be much smaller than the reference value:

$$\begin{aligned} p &= p_0 + p_a \quad with \quad p_a \ll p_0 \\ \rho &= \rho_0 + \rho_a \quad with \quad \rho_a \ll \rho_0 \end{aligned} \tag{4.5}$$

Linearised constitutive law

The four partial differential equations are coupling five quantities: three velocity components v_i, pressure p and density ρ. To close the system of equations, we have to introduce an equation of state linking pressure to density:

$$p = f(\rho) \tag{4.6}$$

A fluid described by such a relationship is said to be *barotropic*. The general relation above can be developed around the reference state (p_0, ρ_0) using a Taylor[2] expansion (Figure 4.1):

$$p = p_0 + (\rho - \rho_0)\left(\frac{df}{d\rho}\right)_{\rho=\rho_0} + \mathcal{O}\left((\rho - \rho_0)^2\right) \tag{4.7}$$

[1] **Leonhard Euler**, a Swiss mathematician and physicist, was born in 1707 in Basel, Switzerland, and died in 1783 in Saint Petersburg, Russia. Euler is one of the most prolific and influential mathematicians of the 18^{th} century. His contributions to calculus, classical mechanics, fluid mechanics, optics and astronomy are innumerable.

[2] **Brook Taylor** (1685-1731) was an English mathematician.

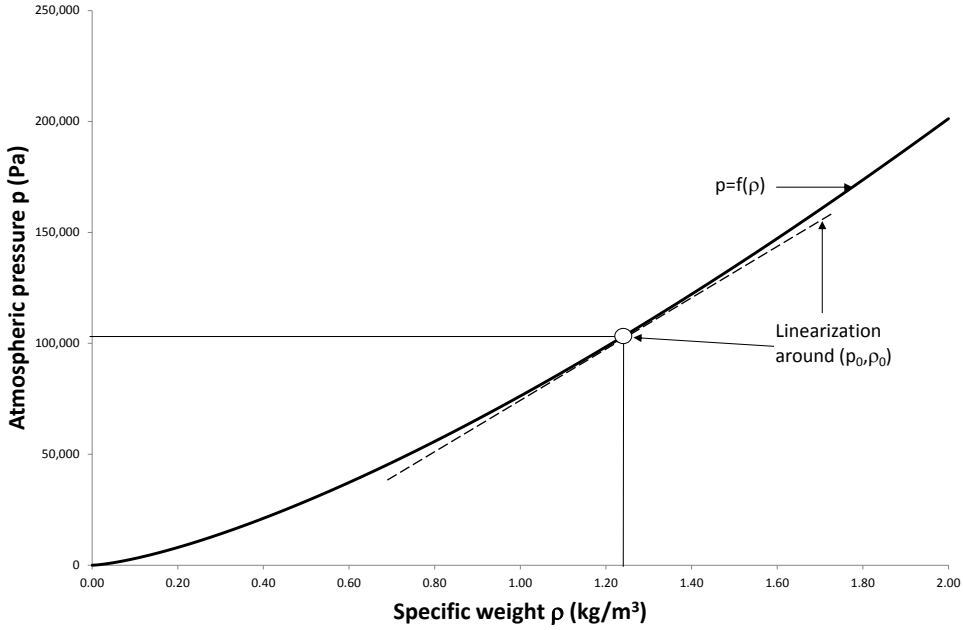

Figure 4.1: Pressure-density relationship for an ideal gas and its linearisation around a reference state.

If we limit ourselves to the first order, which is consistent with the fact that the pressure and density vary only slightly around the reference value, we find the following linearised constitutive relationship:

$$p_a = c^2 \rho_a \tag{4.8}$$

where the constant c^2 is defined as follows:

$$c^2 = \left(\frac{df}{d\rho} \right)_{\rho=\rho_0} \tag{4.9}$$

We will see later that c is the speed at which the pressure disturbance propagates in the fluid.

Fluid *globally* at rest

In the fourth hypothesis, we assume that **the fluid is globally at rest**, i.e. that movement of the fluid is restricted to small oscillations caused by the pressure fluctuation. In other words, there is no mean velocity v_{i0} and the acoustic velocity v_{ia} is assumed to be much smaller than the speed of sound c. The *no background flow* hypothesis is acceptable for a large range of problems[3]. Propagation over a background flow ($v_0 \neq 0$) will be addressed in Chapter 15.

Linearisation

Introducing Equation 4.5 into the continuity and Euler equations, we obtain:

$$\partial_t (\rho_0 + \rho_a) + \partial_i ((\rho_0 + \rho_a) v_{ia}) = q \tag{4.10}$$

$$(\rho_0 + \rho_a) (\partial_t v_{ia} + v_{ja} \partial_j v_{ia}) + \partial_i (p_0 + p_a) = -q v_{ia} \tag{4.11}$$

Taking into account the fact that $\rho_a \ll \rho_0$ and knowing that p_0 and ρ_0 are constant, we may rewrite these equations as:

$$\partial_t \rho_a + \rho_0 \partial_i v_{ia} + \partial_i (\rho_a v_{ia}) = q \tag{4.12}$$

$$\rho_0 (\partial_t v_{ia} + v_{ja} \partial_j v_{ia}) + \partial_i p_a = -q v_{ia} \tag{4.13}$$

We will linearise the equations by making the following assumptions:

- In the continuity equation, we neglect the term:

$$\partial_i (\rho_a v_{ia}) = \frac{p_0}{c} \partial_i \left(\frac{p_a}{p_0} \frac{v_{ia}}{c} \right) \tag{4.14}$$

  It is clear that the term $\rho_a v_{ia}$ is small, as it is the product of two quantities that are themselves small ($p_a \ll p_0$ and $v_{ia} < c$). However, it

[3] But there are notable exceptions where it cannot be retained, for example:

- far field propagation of sound sources is influenced by wind;
- propagation of engine noise from the valve train to the exhaust tailpipe is locally influenced by the flow in the exhaust system;
- acoustic radiation of an aircraft engine depends on the airflow through the reactor.

is less obvious that:

$$\partial_i \left(\frac{p_a}{p_0} \frac{v_{ia}}{c} \right) \ll \partial_i \left(\frac{v_{ia}}{c} \right) \tag{4.15}$$

We nevertheless use this hypothesis, considering that the quantities involved vary slowly and regularly (typically sinusoidally). We will see later that the product $p_a v_{ia}$ defines a quantity called acoustic intensity (Section 6.4). We therefore assume that intensity varies more slowly than velocity.

- In Euler equations, we neglect the second order term and assume that:

$$v_{ja} \partial_j v_{ia} \ll \partial_t v_{ia} \tag{4.16}$$

or, dividing both sides by c^2:

$$\frac{v_{ja}}{c} \partial_j \left(\frac{v_{ia}}{c} \right) \ll \frac{\partial \frac{v_{ia}}{c}}{\partial (ct)} \tag{4.17}$$

This condition is acceptable if:

$$\frac{\partial \frac{v_{ia}}{c}}{\partial (ct)} \sim \partial_j \left(\frac{v_{ia}}{c} \right) \sim \frac{v_{ja}}{c} \tag{4.18}$$

This hypothesis should also be validated *a posteriori*.

- Finally, we retain only first order terms to obtain:

$$\frac{1}{c^2} \partial_t p_a + \rho_0 \partial_i v_{ia} = q \tag{4.19}$$

$$\rho_0 \partial_t v_{ia} + \partial_i p_a = -q v_{ia} \tag{4.20}$$

Eliminating velocity

Velocity can be eliminated from the equations by differentiating the first equation with respect to time and by taking the divergence of the second equation:

$$\frac{1}{c^2} \partial_{tt} p_a + \rho_0 \partial_{ti} v_{ia} = \partial_t q \tag{4.21}$$

$$\rho_0 \partial_{it} v_{ia} + \partial_{ii} p_a = -\partial_i \left(q v_{ia} \right) \tag{4.22}$$

then by subtracting one equation from the other:

$$\frac{1}{c^2}\partial_{tt}p_a - \partial_{ii}p_a = \partial_t q + \partial_i \left(q v_{ia}\right) \tag{4.23}$$

This last equation describes the spatial and temporal variation of the sound pressure fluctuation.

Pressure-velocity relationship

The linearised Euler equation must also be retained:

$$\partial_t v_{ia} = \frac{1}{\rho_0}\left(-\partial_i p_a - q v_{ia}\right) \tag{4.24}$$

which relates the velocity of the fluid (v_{ia}) to the pressure gradient ($\partial_i p_a$) and volume source (q).

Homogeneous form of the two equations

If there are no distributed sources of mass ($q = 0$), the two previous equations may be written:

$$\frac{1}{c^2}\partial_{tt}p_a - \partial_{ii}p_a = 0 \tag{4.25}$$

$$\partial_t v_{ia} = -\frac{1}{\rho_0}\partial_i p_a \tag{4.26}$$

or, using a more familiar notation:

$$\frac{1}{c^2}\frac{\partial^2 p_a}{\partial t^2} - \Delta p_a = 0 \tag{4.27}$$

$$\frac{\partial \vec{v}_a}{\partial t} = -\frac{1}{\rho_0}\vec{\nabla} p_a \tag{4.28}$$

The first equation is called the wave equation or d'Alembert's equation[4]. The second equation shows that, in the absence of distributed sources, the

[4] **Jean le Rond d'Alembert**, a French mathematician and philosopher, was born on 16 November 1717 and died on 29 October 1783 in Paris. D'Alembert, together with Denis Diderot, was the editor of the French Encyclopedia. He introduced the concept of partial differential equations while developing his theory of vibrating strings.

acceleration of the fluid is proportional to the pressure gradient. An additional form of this equation is:

$$\rho_0 \vec{a}_a = -\vec{\nabla} p_a \tag{4.29}$$

which simply expresses Newton's second law: the net force per unit area acting on the fluid (the negative of the pressure gradient) is equal to the product of density by acceleration.

4.2 Linearity and non-linearity in acoustics

We have seen that the linearisation of the Navier-Stokes equations yields a d'Alembert equation for the acoustic disturbance. Most acoustic phenomena are indeed linear. Linearity in acoustics implies that effects are proportional to their causes and that the superposition principle applies.

However, there are phenomena where sound fields exhibit a **non-linear** behaviour. A few examples are given below.

1. If the amplitude of the pressure variation is significantly greater than the reference pressure, the second order terms can no longer be neglected and the propagation operator is non-linear, such as:

   - the sound field surrounding a space rocket taking off is so intense that non-linear effects are observed;
   - power ultrasounds are used in many industrial processes and at levels so high that non-linear effects come into play[5];
   - shock waves are the superposition of acoustic disturbances in such quantity that the phenomenon becomes altogether non-linear;
   - ultrasounds used in medicine to destroy blood clots or kidney and bladder stones (*lithotripsy*) obviously rely on non-linear effects.

[5] This is notably the case when ultrasounds are used to induce cavitation in a fluid (sonochemistry, cauterization).

2. When the properties of the propagation medium change with pressure, sound speed c becomes a function of acoustic pressure p; this renders the equation non-linear. This, for example, happens when the fluid cavitates under the effect of ultrasounds. Density of fluid and speed of sound then depend on the cavitation rate, i.e. on the local gas fraction, which itself depends on the intensity of the sound field.

3. When the amplitude of the source itself depends on the generated sound field (*feedback*) as in combustion noise.

4.3 General one-dimensional solution

The wave equation in one-dimension is written as:

$$\frac{\partial^2 p\left(x,t\right)}{\partial x^2} - \frac{1}{c^2}\frac{\partial^2 p\left(x,t\right)}{\partial t^2} = 0 \tag{4.30}$$

It is easy to demonstrate that any function of the form:

$$p\left(x,t\right) = p^+\left(t - \frac{x}{c}\right) + p^-\left(t + \frac{x}{c}\right) \tag{4.31}$$

is a solution of this equation. This general solution is the sum of two terms (Figures 4.2 and 4.3). The first term represents a pressure distribution propagating, without any deformation, from left to right, at velocity c. We indeed see that the function $p^+\left(t - \frac{x}{c}\right)$ takes the same value at points x and $x + \Delta$, but with a delay Δ/c:

$$p^+\left(t - \frac{x}{c}\right) = p^+\left(\left(t + \frac{\Delta}{c}\right) - \frac{x+\Delta}{c}\right) \tag{4.32}$$

The second term represents another pressure distribution travelling without deformation at speed c, but, this time, from right to left:

$$p^-\left(t + \frac{x}{c}\right) = p^-\left(\left(t + \frac{\Delta}{c}\right) + \frac{x-\Delta}{c}\right) \tag{4.33}$$

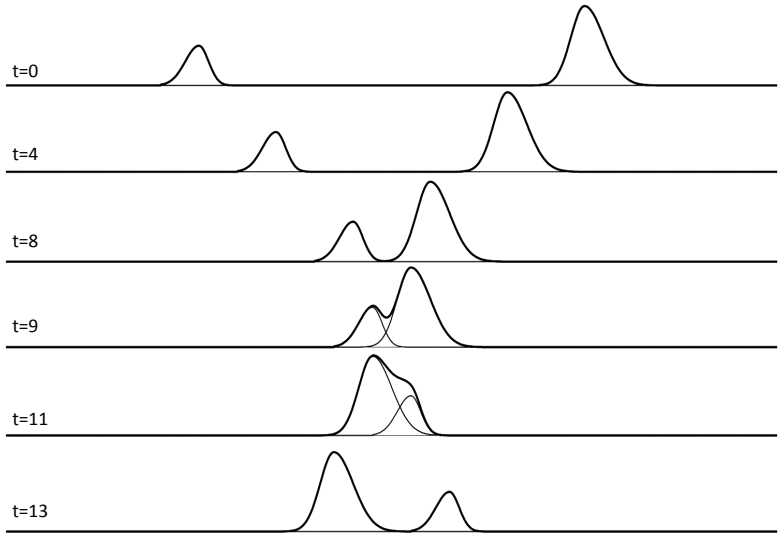

Figure 4.2: The general solution of the wave equation is the sum of two terms representing two perturbations travelling in opposite directions at speed c.

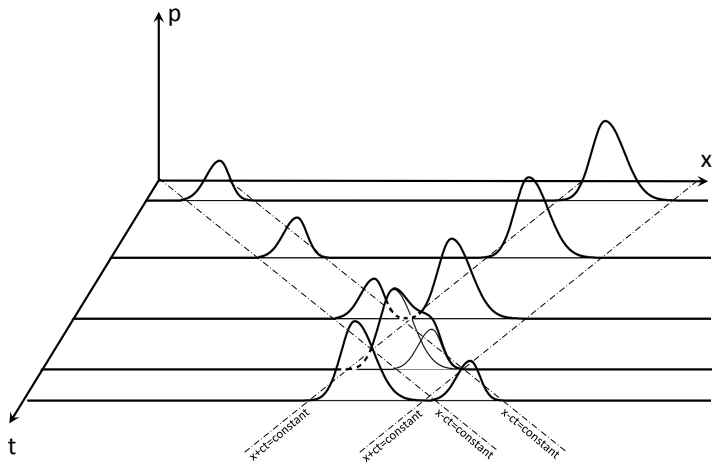

Figure 4.3: Another representation of the general solution of the wave equation showing that it is the sum of two terms representing two perturbations travelling in opposite directions at speed c.

4.4 Mechanics of propagation

Figure 4.4 shows a set of air particles located along the axis of a tube that extends to infinity on the right side and that is closed by a piston on the left side. The piston undergoes a sinusoidal horizontal movement. Each **line** represents the position of the particles at a given time while each **column** shows the position of a given particle at the different times. One can consider that each circle represents a small mass connected to its neighbours by springs. The stiffness of the spring represents the compressibility of the air. In this analogy, pressure is the net force exerted by the springs on each mass. Let's now look at the lines one by one.

1. Line (a) shows the initial position of the particles before the piston starts to move.

2. When the piston starts to move in (b), it drags the first mass along and the spring between masses 1 and 2 is compressed. However, the second mass does not yet move: its movement is prevented by its inertia and by the spring's ability to store the energy transmitted by the first mass.

3. In (c), the piston and mass 1 have reached their maximum displacement and the second mass has overcome its inertia and started moving. Movement is not yet transmitted to the third mass as the energy of the second mass is stored in the second spring.

4. In (d), the piston has started turning back and the first mass follows. The second mass, under the effect of its inertia, continues to move to the right. The spring between masses 1 and 2 is now stretched. Mass 3 starts to move. Mass 4 is still at rest.

5. Each mass reacts to the movement of the previous mass with a delay. The perturbation created by the piston moves from left to right at a finite speed determined by the compressibility (spring stiffness) and density (mass) of the medium.

If we consider the movement of each mass over time (Figure 4.5), we see that the first mass follows the movement of the piston. The other masses follow

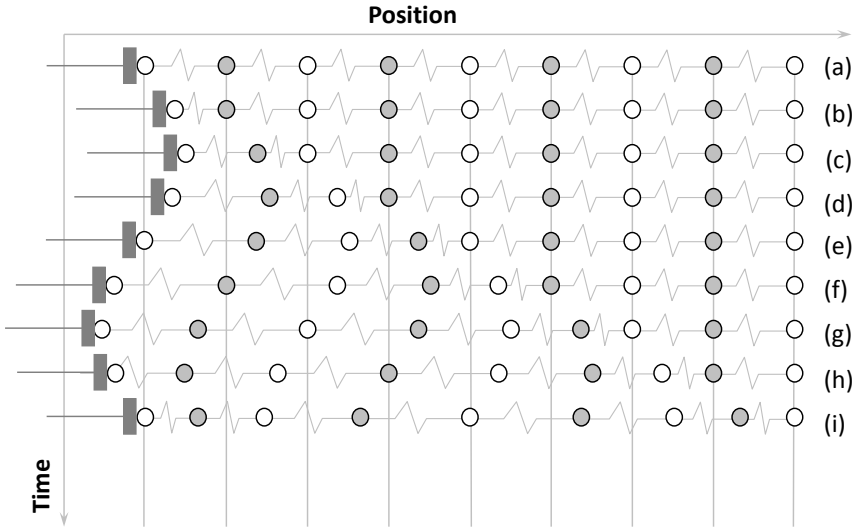

Figure 4.4: Evolution of the position of air particles in a tube excited by a vibrating piston.

the same movement, but with a time delay. If the masses are separated by a distance Δx and the second mass is set in motion after a time Δt, we can say that the piston produces a disturbance that propagates along the tube at a speed:

$$c = \frac{\Delta x}{\Delta t} \tag{4.34}$$

It must be stressed that c is the speed at which the *disturbance* propagates and **not** the speed at which each mass oscillates around its equilibrium position. The movement of the piston is assumed to be sinusoidal and has a period T. If we look at the positions of the masses at a given time, we see that their movement also follows a sinusoidal variation. To highlight this effect the horizontal movement of each mass is plotted on a vertical scale (Figure 4.6). We see that the sound propagation phenomenon exhibits a dual periodicity: the temporal periodicity imposed by the piston cycle (period T) and a spatial periodicity characterised by the wavelength λ. Wavelength, period and propagation speed are related by:

$$T = \frac{1}{f} = \frac{\lambda}{c} \tag{4.35}$$

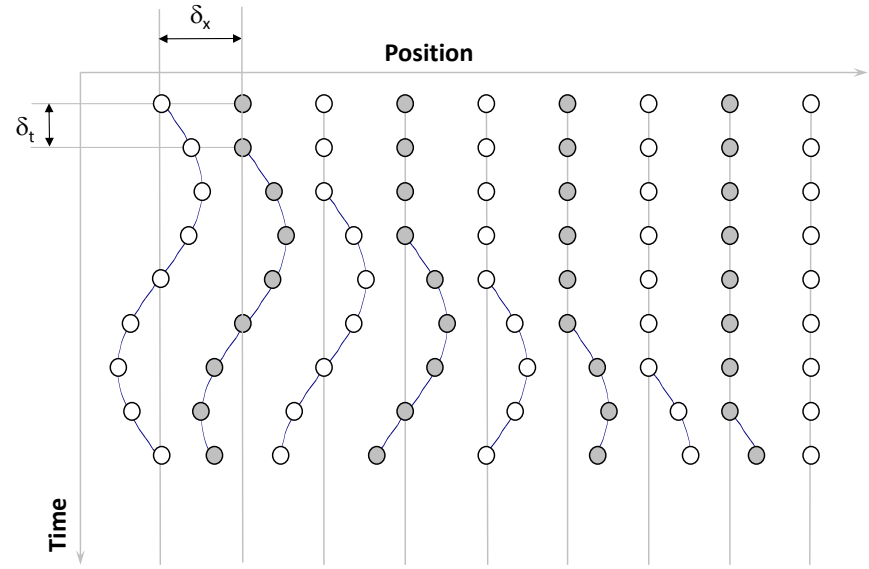

Figure 4.5: Period and phase shift.

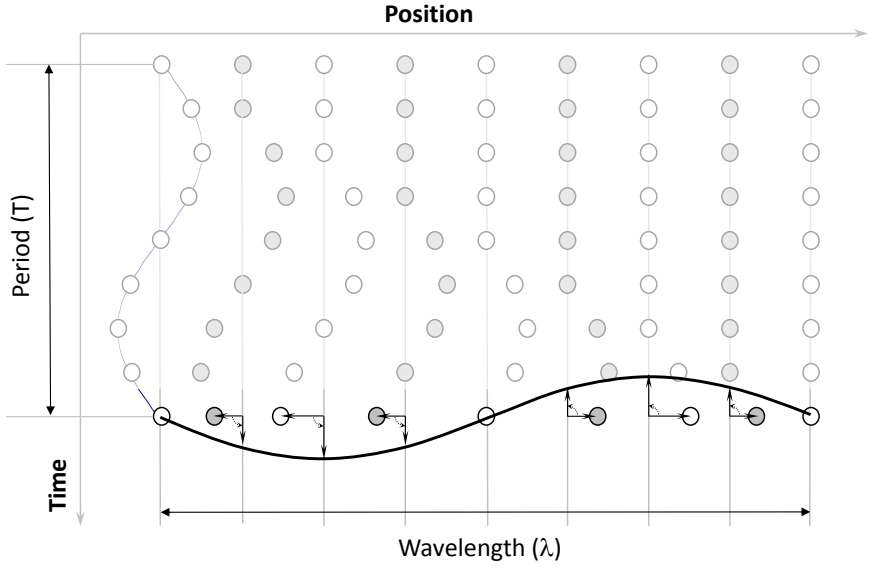

Figure 4.6: Wavelength.

4.5 Dispersive and non-dispersive propagation

4.5.1 General wave equations

The d'Alembert equation is a special case of wave equation. The general case is:

$$\alpha \frac{\partial^n f}{\partial t^n} + \beta \nabla^m f = 0 \tag{4.36}$$

or, considering a single space dimension x:

$$\alpha \frac{\partial^n f}{\partial t^n} + \beta \frac{\partial^m f}{\partial x^m} = 0 \tag{4.37}$$

Several interesting wave equations appear in physics, for example:

- the d'Alembert equation governing the vibration of strings or the propagation of sound waves ($n = 2$, $m = 2$, $\alpha = 1$, $\beta = -\gamma^2$):

$$\frac{\partial^2 p}{\partial t^2} - \gamma^2 \frac{\partial^2 p}{\partial x^2} = 0 \tag{4.38}$$

- the equation governing bending vibrations of beams with bending stiffness D and mass per unit length M ($n = 2$, $m = 4$, $\alpha = M$, $\beta = D$):

$$M \frac{\partial^2 u}{\partial t^2} + D \frac{\partial^4 u}{\partial x^2} = 0 \tag{4.39}$$

- Schrödinger's equation governing the evolution of the wave function ψ in quantum mechanics ($n = 1$, $m = 2$, $\alpha = i\hbar$, $\beta = \frac{\hbar^2}{2m}$):

$$i\hbar \frac{\partial \psi}{\partial t} + \frac{\hbar^2}{2m} \frac{\partial^2 \psi}{\partial x^2} = 0 \tag{4.40}$$

The function:

$$w\left(x, t\right) = e^{i(kx - \omega t)} \tag{4.41}$$

where k is called the *wave number* and ω the *pulsation* or *angular frequency*, is a solution of this generalised wave equation *provided* that the following condition, called the *dispersion relation*, holds:

$$\alpha\left(-i\omega\right)^n + \beta\left(ik\right)^m = 0 \tag{4.42}$$

w presents a spacial and temporal periodicity. Indeed, at any given time t_0:

$$w\left(x, t_0\right) = w\left(x + \frac{2\pi}{k}, t_0\right) \tag{4.43}$$

showing that the value of w is the same at two points separated by a distance λ called the wavelength:

$$\lambda = \frac{2\pi}{k} \leftrightarrow k\lambda = 2\pi \tag{4.44}$$

Similarly, at any given position x_0:

$$w\left(x_0, t\right) = w\left(x_0, t + \frac{2\pi}{\omega}\right) \tag{4.45}$$

showing that the value of w is the same at two instants separated by a time T called the period:

$$T = \frac{2\pi}{\omega} \leftrightarrow \omega T = 2\pi \tag{4.46}$$

Frequency f is, by definition, the inverse of the period:

$$f = \frac{1}{T} = \frac{\omega}{2\pi} \tag{4.47}$$

Finally, we observe that:

$$w\left(x + \frac{\omega}{k}\Delta t, t + \Delta t\right) = w\left(x, t\right) \tag{4.48}$$

which shows that w propagates at a speed c defined by:

$$c = \frac{\omega}{k} = \frac{\lambda}{T} \tag{4.49}$$

4.5.2 Non-dispersive propagation

Consider again d'Alembert's equation:

$$\frac{\partial^2 p}{\partial t^2} - \gamma^2 \frac{\partial^2 p}{\partial x^2} = 0 \tag{4.50}$$

The dispersion relation takes the form:

$$-\omega^2 + k^2\gamma^2 = 0 \leftrightarrow k = \frac{\omega}{\gamma} \tag{4.51}$$

The propagation speed is therefore constant and equal to γ:

$$c = \frac{\omega}{k} = \gamma \tag{4.52}$$

When the wave propagation speed is independent of k, it is said to be *non-dispersive*.

4.5.3 Dispersive propagation

By contrast, the equation describing bending waves in a beam:

$$M\frac{\partial^2 u}{\partial t^2} + D\frac{\partial^4 u}{\partial x^2} = 0 \tag{4.53}$$

leads to another dispersion relation:

$$-M\omega^2 + Dk^4 = 0 \leftrightarrow k = \sqrt{\omega\sqrt{\frac{M}{D}}} \tag{4.54}$$

showing that the wave speed is:

$$c = \frac{\omega}{k} = \sqrt{\omega\sqrt{\frac{D}{M}}} \tag{4.55}$$

When the wave propagation speed depends on k (or ω or f), it is said to be *dispersive*.

4.5.4 Wave packet and group velocity

A wave packet is a linear combination of waves whose wave numbers belong to a limited interval centered on a value k_0:

$$\psi(x,t) = \int_{k_0-\Delta k}^{k_0+\Delta k} A(k)\, e^{i(kx-\omega(k)t)} dk \tag{4.56}$$

This wave packet has a significant amplitude within an interval whose width Δx is inversely proportional to Δk. One can therefore associate a spatial localisation to a wave packet. This explains its importance, for example, in quantum mechanics. If the phase $(kx - \omega t)$ changes rapidly, the different constituent waves interfere destructively and the resulting amplitude is low. If, on the contrary, the phase varies slowly, the constituent waves interfere constructively and the resulting amplitude is high. The maximum amplitude of a wave-packet therefore occurs when the phase is stationary:

$$\frac{d\,(kx - \omega\,(k)\,t)}{dk} = 0 \rightarrow x = \frac{d\omega\,(k)}{dk} t \tag{4.57}$$

The wave packet therefore *globally* moves at a speed v_g called the *group velocity* and given by:

$$v_g = \left| \frac{d\omega\,(k)}{dk} \right|_{k=k_0} \tag{4.58}$$

When propagation is non-dispersive, as in acoustics, the wave packet retains the same shape because each component propagates at the same speed. Group velocity and phase velocity are then equal. If, on the contrary, propagation is dispersive, the wave packet continuously changes shape. Group velocity is not equal to the phase velocity of the individual wave components. For example, the group velocity of beam bending waves is given by:

$$\omega = k^2 \sqrt{\frac{D}{M}} \rightarrow v_g = 2k_0 \sqrt{\frac{D}{M}} \tag{4.59}$$

4.6 Speed of sound

We all know that light travels faster than sound. That's why certain people appear bright until you hear them speak.
— **Albert Einstein** (1879-1955).

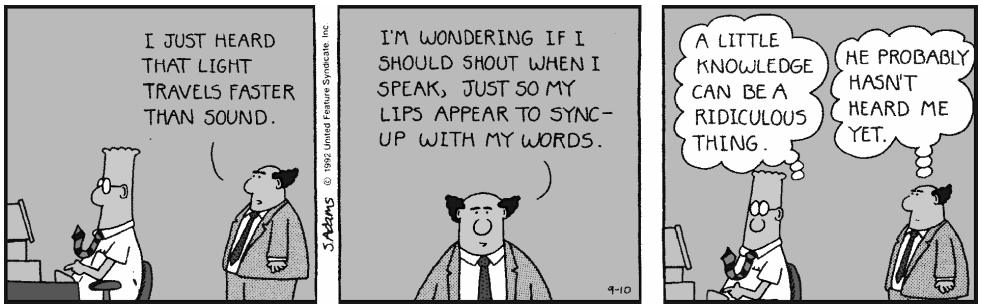

Figure 4.7: Speed of sound and speed of light in Dilbert's world.

4.6.1 Perfect gas

An expression for the speed of sound in ideal gas may be obtained using the appropriate thermodynamic relations. Pressure and density in an ideal gas undergoing an adiabatic transformation ($(p, \rho) \rightarrow (p_0, \rho_0)$) are related by:

$$\left(\frac{p}{p_0}\right) = \left(\frac{\rho}{\rho_0}\right)^{\gamma} \tag{4.60}$$

where γ is the ratio of specific heat at constant pressure and constant volume (c_p and c_v). Applying Equation 4.9 gives the speed of sound:

$$c^2 = \left(\frac{dp}{d\rho}\right)_{\rho=\rho_0} = \frac{\gamma p_0}{\rho_0} \tag{4.61}$$

We also know that:

$$p_0 = \rho_0 RT \tag{4.62}$$

where $R = c_p - c_v$. We therefore find:

$$c = \sqrt{\gamma RT} \tag{4.63}$$

While the dependency of sound speed with temperature may be neglected in most applications, it is important in some cases:

- refraction due to thermal gradients in the atmosphere (see Chapter 16);
- propagation of sound waves through the exhaust line of internal combustion engines where temperature ranges from 700°C (c=625 m/s) at the valve to 60°C (c=366 m/s) at the tailpipe.

The relationship between sound speed and temperature may be linearised to provide a simple calculation rule at usual temperatures (Figure 4.8):

$$c \simeq 331.3 + 0.6 \cdot t \tag{4.64}$$

where t is the temperature in Celsius. Speed of sound is given below for some other gases:

- water vapour: 402 m/s
- helium: 970 m/s
- hydrogen at 0°C: 1270 m/s

4.6.2 Liquids

The speed of sound in liquids depends on the adiabatic compressibility modulus κ_s (Newton-Laplace relationship):

$$c = \sqrt{\frac{\kappa_s}{\rho}} \tag{4.65}$$

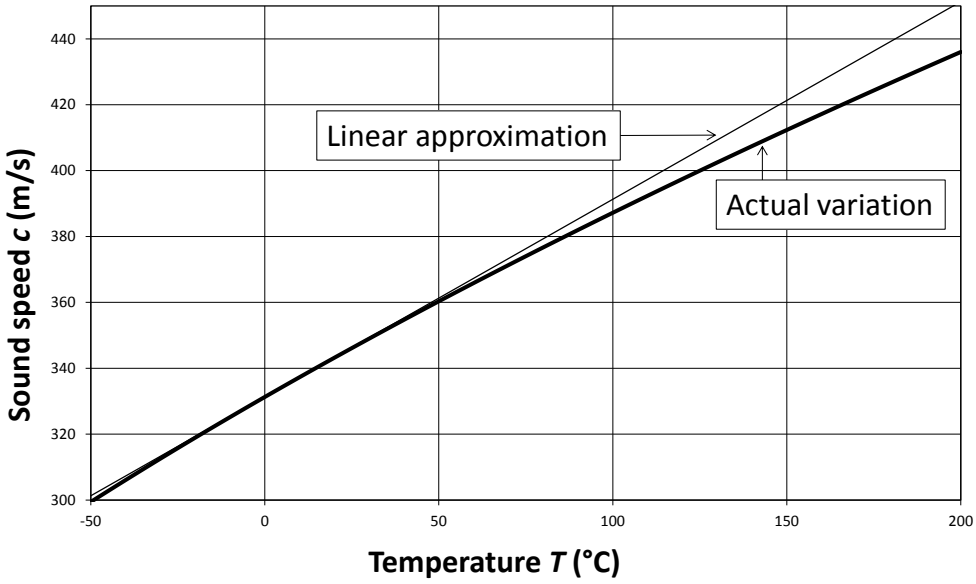

Figure 4.8: Variation of sound speed with temperature. The bold line shows the actual variation, the thin line displays the linear approximation valid at usual temperatures (Equation 4.64).

An empirical relationship exists for water:

$$c = 1407 + 4 \cdot t + 1.6 \cdot 10^{-6} \cdot p \tag{4.66}$$

where t is the temperature in Celsius and p the hydrostatic pressure in Pa (remember the order of magnitude of 1,500 m/s). For oceanic propagation, we have to take into account the temperature t (in Celsius), salinity s (in ppm) and depth z (in meters). Mackenzie[6] proposes an empirical formula:

$$\begin{aligned} c\,(t,s,z) &= a_1 + a_2 t + a_3 t^2 + a_4 t^3 + a_5 (s-35) \\ &+ a_6 z + a_7 z^2 + a_8 t (s-35) + a_9 t z^3 \end{aligned} \tag{4.67}$$

where the coefficients have the following values:

$a_1 = 1448.96$, $a_2 = 4.591$, $a_3 = -5.304 \cdot 10^{-2}$, $a_4 = 2.374 \cdot 10^{-4}$, $a_5 = 1.340$, $a_6 = 1.630 \cdot 10^{-2}$, $a_7 = 1.675 \cdot 10^{-7}$, $a_8 = -1.025 \cdot 10^{-2}$, $a_9 = -7.139 \cdot 10^{-13}$.

[6] **Mackenzie, Kenneth V.** (1981), *Discussion of sea-water sound-speed determinations*, Journal of the Acoustical Society of America, 70 (3), pp. 801-806.

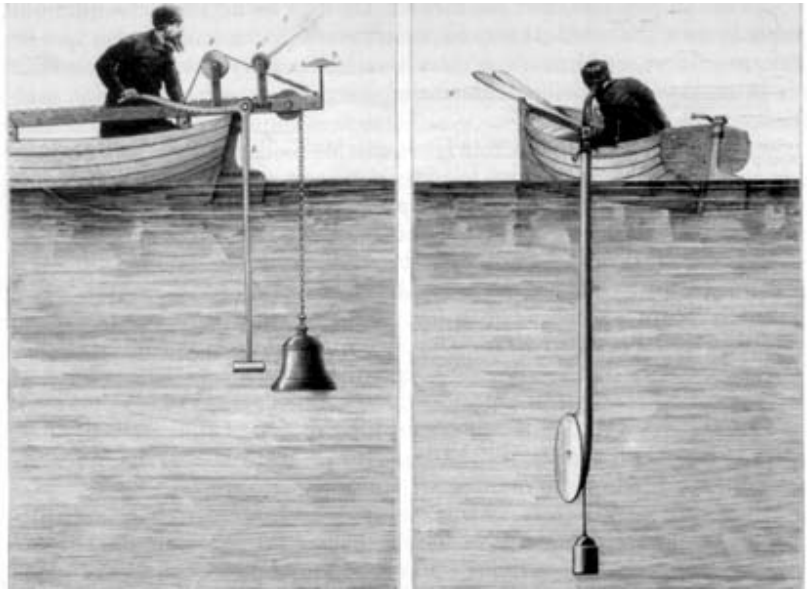

Figure 4.9: In 1828, Jean-Daniel Colladon and Charles Sturm measured, for the first time, the speed of sound in water in Lake Geneva.

4.6.3 Solids

The speed at which **compression** waves propagate in one-dimensional solids (e.g. rods) is given by:

$$c = \sqrt{\frac{E}{\rho}} \tag{4.68}$$

where E is Young's modulus. As an example, this formula gives 5,182 m/s for steel ($E = 2.1 \cdot 10^{11} N/m^2$ and $\rho = 7820 kg/m^3$). Other values are:

- soft rubber: 70 m/s
- concrete: 3,000 m/s
- glass: 5,000 m/s

For three-dimensional solids, taking shear effects into account, the formula becomes:

$$c = \sqrt{\frac{E}{\rho} \frac{(1-\nu)}{(1+\nu)(1-2\nu)}} \tag{4.69}$$

where ν is Poisson's ratio. Other types of elastic waves exist in solids. They have different propagation speeds and usually display a dispersive behaviour. Bending waves in plates for example propagate at a speed:

$$c_{bending} = \sqrt{\omega h \sqrt{\frac{E}{12\rho(1-\nu^2)}}} \tag{4.70}$$

where ω is the pulsation ($\omega = 2\pi f$), ν Poisson's coefficient and h the thickness of the plate.

5

Fourier analysis

The in-depth study of nature is the most fertile source of mathematical discoveries.
— **Joseph Fourier** (1768-1830), Preliminary discourse to the analytical theory of heat (1822).

Contents

5.1 Combination of simple signals 57
5.2 Fourier series 67
5.3 Fourier transform 76
5.4 Convolution product 79
5.5 Properties of the Fourier transform 81
5.6 Summary of the chapter 87

Figure 5.1: Portrait of Joseph Fourier. Drawn by Julien Léopold Boilly and engraved by Amédée Félix Barthélemy Geille, Portraits et histoire des hommes utiles, a collection of fifty portraits edited by Société Montyon & Franklin (1839-1840).

Chapter 2 presented sound as a small variation of pressure around a reference value and Chapter 4 showed that this pressure fluctuation obeys a wave or d'Alembert equation. A sound is described, at a particular point, by the local variation of pressure with time: $p(t)$. This *time-domain* description of sound may be complemented by a *spectral* or *frequency-domain* description. This chapter compiles a number of important results concerning Fourier[1] analysis. Before introducing this mathematical tool let us look at the combination of several simple sinusoidal signals.

[1]The French physicist Jean-Baptiste **Joseph Fourier** was born in March 1768 in Auxerre and died in May 1830 in Paris. His scientific and cultural interests were very broad, but he is best known for his participation in the Egyptian campaign of Napoleon Bonaparte in 1798 and for his essay on heat transfer presented to the Academy of Sciences in 1807. It is within this essay that he introduces for the first time the trigonometric series that are named after him. They were then introduced, ironically, in a *static* context and not, as we could have expected, in a *harmonic* context. Fourier is also the first scientist to have shed light on the atmospheric greenhouse effect.

5.1 Combination of simple signals

5.1.1 Signals with identical frequencies

Consider two monochromatic[2] signals of identical frequency, but different phases:

$$p_a(t) = P_a \cos(\phi_a + \omega t) \tag{5.1}$$

$$p_b(t) = P_b \cos(\phi_b + \omega t) \tag{5.2}$$

The properties of the combined signal:

$$p_c(t) = p_a(t) + p_b(t) \tag{5.3}$$

can be obtained by expanding the expressions for p_a and p_b:

$$p_c(t) = P_a \cos(\phi_a + \omega t) + P_b \cos(\phi_b + \omega t) \tag{5.4}$$

Simpson's formula yields:

$$\begin{aligned} p_c(t) = P_a \cos(\phi_a) \cos(\omega t) \quad &- \quad P_a \sin(\phi_a) \sin(\omega t) + \\ P_b \cos(\phi_b) \cos(\omega t) \quad &- \quad P_b \sin(\phi_b) \sin(\omega t) \end{aligned} \tag{5.5}$$

We can write the coefficients of $\cos(\omega t)$ and $\sin(\omega t)$ in the form:

$$P_a \cos(\phi_a) + P_b \cos(\phi_b) \doteq P_c \cos(\phi_c) \tag{5.6}$$

$$P_a \sin(\phi_a) + P_b \sin(\phi_b) \doteq P_c \sin(\phi_c) \tag{5.7}$$

in such a way that:

$$p_c(t) = P_c \cos(\phi_c + \omega t) \tag{5.8}$$

[2] From the ancient Greek word $\chi\rho\omega\mu\alpha\tau o\varsigma$: colour. This terminology was originally introduced in optics to designate a light of a single colour whose spectrum, by definition, is composed of a single frequency. It is now used in all disciplines where harmonic phenomena are observed.

The sum of two monochromatic signals of pulsation ω is another monochromatic signal of pulsation ω. The amplitude P_c of the combined signal can be obtained by adding the square of equations 5.6 and 5.7:

$$P_c^2 = P_a^2 + P_b^2 + 2P_aP_b\cos(\phi_a - \phi_b) \tag{5.9}$$

The ratio of the same two equations yields the phase ϕ_c of the combined signal:

$$\tan(\phi_c) = \frac{P_a\cos(\phi_a) + P_b\cos(\phi_b)}{P_a\sin(\phi_a) + P_b\sin(\phi_b)} \tag{5.10}$$

The amplitude of the combined signal is a function of the phase difference between the two elementary signals (see Figures 5.2 and 5.4). It is maximal when $\phi_a - \phi_b = 0$ and in this case (*constructive interference*, Figure 5.4):

$$P_c = P_a + P_b \tag{5.11}$$

It is minimal when $\phi_a - \phi_b = \pi$ and in that case (*destructive interference*, Figure 5.4):

$$P_c = P_a - P_b \tag{5.12}$$

The average value of P_c for all possible values of the phase difference is:

$$\left\langle P_c^2 \right\rangle = P_a^2 + P_b^2 \tag{5.13}$$

When $P_a = P_b$ and $\phi_a - \phi_b = \pi$, there is no resultant field ($P_c = 0$). Active Noise Control (ANC) uses this property. In order to control a primary sound field, we add a secondary field which is, in a given zone and at given frequencies, equal in amplitude and opposite in phase to the primary field. Figures 5.5 and 5.6 show the active control principle applied to an audio headset and to the passenger compartment of a car.

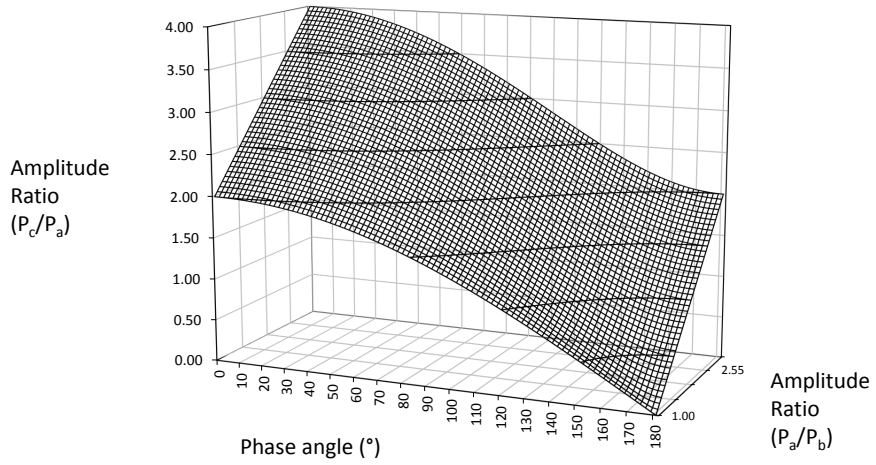

Figure 5.2: Combination of a sound A of unit amplitude with a sound B whose amplitude varies between 1 and 3. The phase difference between the two signals varies from 0 to 180°. The diagram gives the amplitude of the resulting signal.

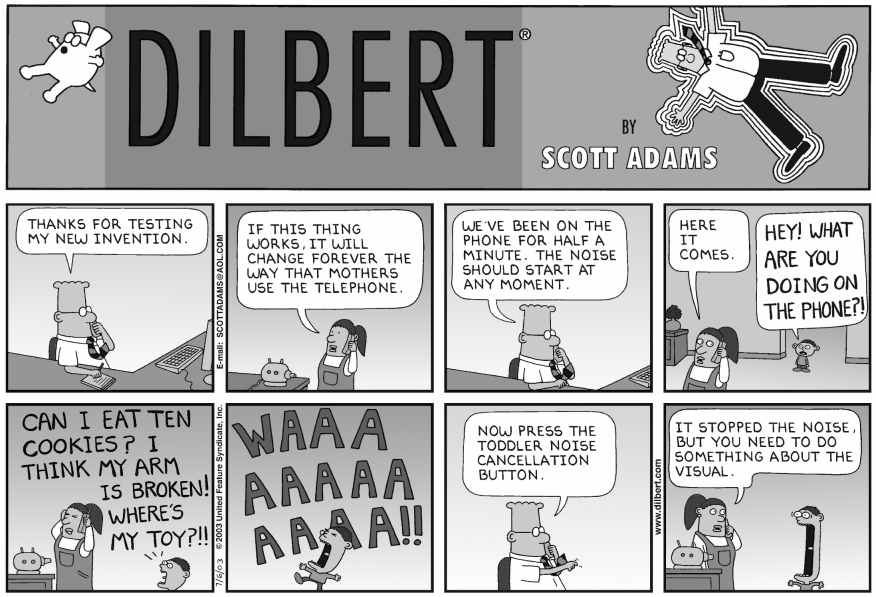

Figure 5.3: Active noise control according to Dilbert.

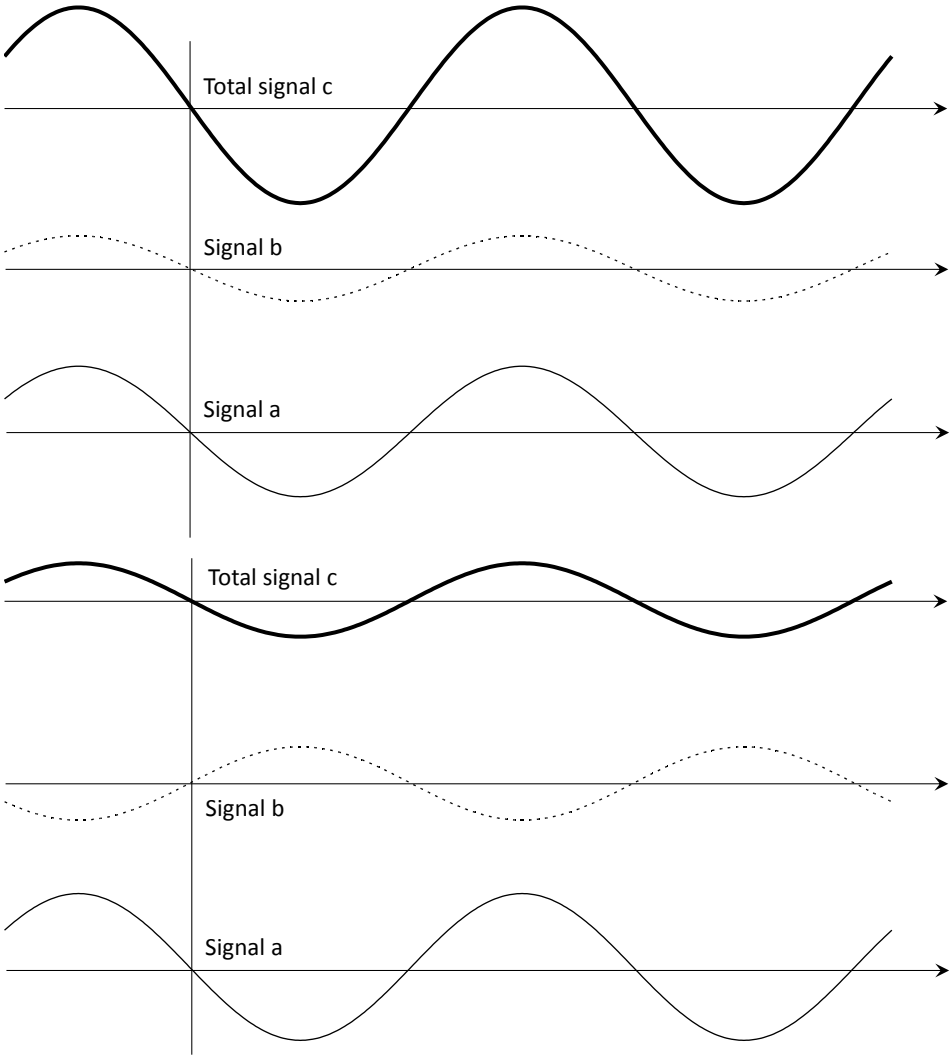

Figure 5.4: Combination of two monochromatic signals of identical frequencies: constructive interference (upper graph) and destructive interference (lower graph).

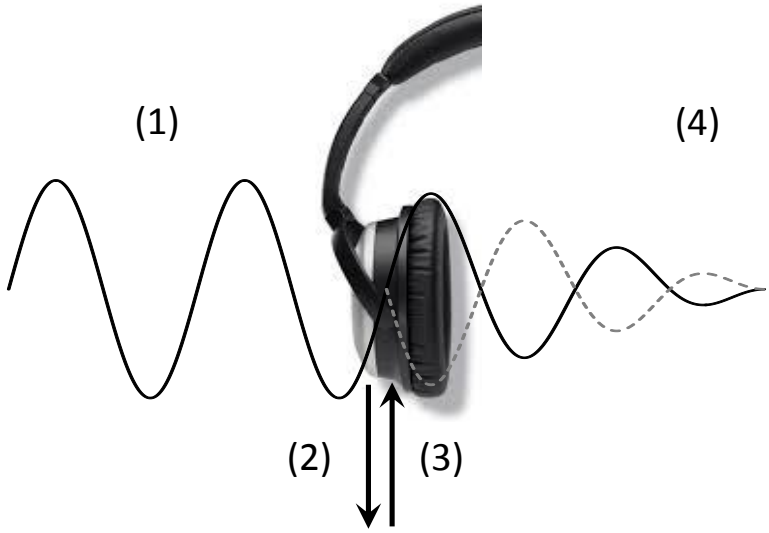

Figure 5.5: Working principle of an active control headset: the primary sound field (solid line) enters the headset (1), the signal is captured by a microphone and sent to a control unit (2) which calculates and then produces the secondary sound field (3, dotted line). Primary and secondary fields partially cancel each other (4).

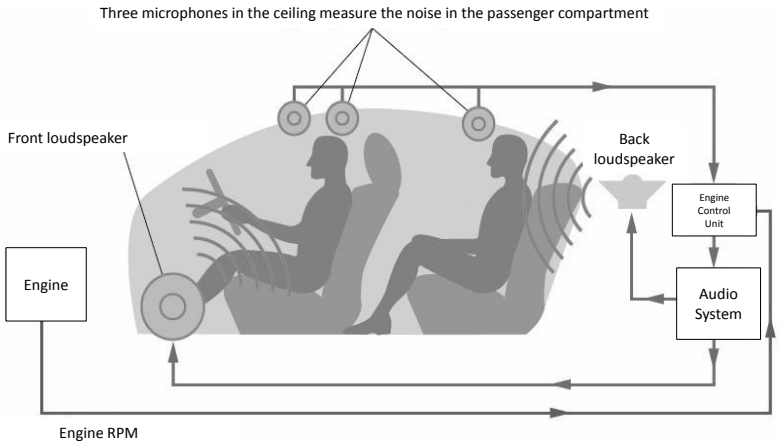

Based on a diagram initially published in © GM Techlink

Figure 5.6: Working principle of an active noise control system in passenger cars.

5.1.2 Signals with different frequencies

Two monochromatic signals of different frequencies f_1 and f_2 yield a periodic signal only if their frequency ratio is a rational number which requires that:

$$\exists\ (m,n)\ \in \mathbb{N} \mid \frac{m}{f_1} = \frac{n}{f_2} \doteq T_0 = \frac{1}{f_0} \tag{5.14}$$

Indeed, in this case, n periods of signal 2 correspond exactly to m periods of signal 1 (Figure 5.7, top graph). If m and n are the smallest integers fulfilling condition 5.14 then T_0 is the period of the resulting signal and f_0 its fundamental frequency. On the other hand, if the frequency ratio is irrational, the combined signal is aperiodic (Figure 5.7, bottom graph). Generally, the signal $p(t)$ resulting from the combination of n monochromatic signals whose frequencies are integer multiple of the same *fundamental* frequency f_0:

$$p(t) = \sum_{i=1.n} P_i \cos\left(\phi_i + 2i\pi f_0 t\right) \tag{5.15}$$

is periodic of period $T_0 = \frac{1}{f_0}$. Figures 5.8 and 5.9 show a combination of a fundamental and its harmonics and illustrate the progressive complexification of the signal when the number of harmonics increases. Figure 5.10 (upper graph) shows that adding a phase difference between the signals changes the shape of the global signal, but not its period. Figure 5.10 (lower graph)shows that the absence of the fundamental does not change the periodicity. Indeed, $2f_0$ and $3f_0$ are integer multiples of f_0 and not integer multiples of one another. The fundamental frequency is therefore *not necessarily* the lowest frequency of the spectrum of a periodic signal.

The combination of signals whose frequency is a multiple of a fundamental f_0 is characterised by the period T_0. The reverse is also true: any signal of period T_0 can be described as a linear combination of a finite or infinite number of monochromatic signals whose frequencies are multiples of $f_0 = \frac{1}{T_0}$. The extraction of these components of the composite signal is discussed in the next section.

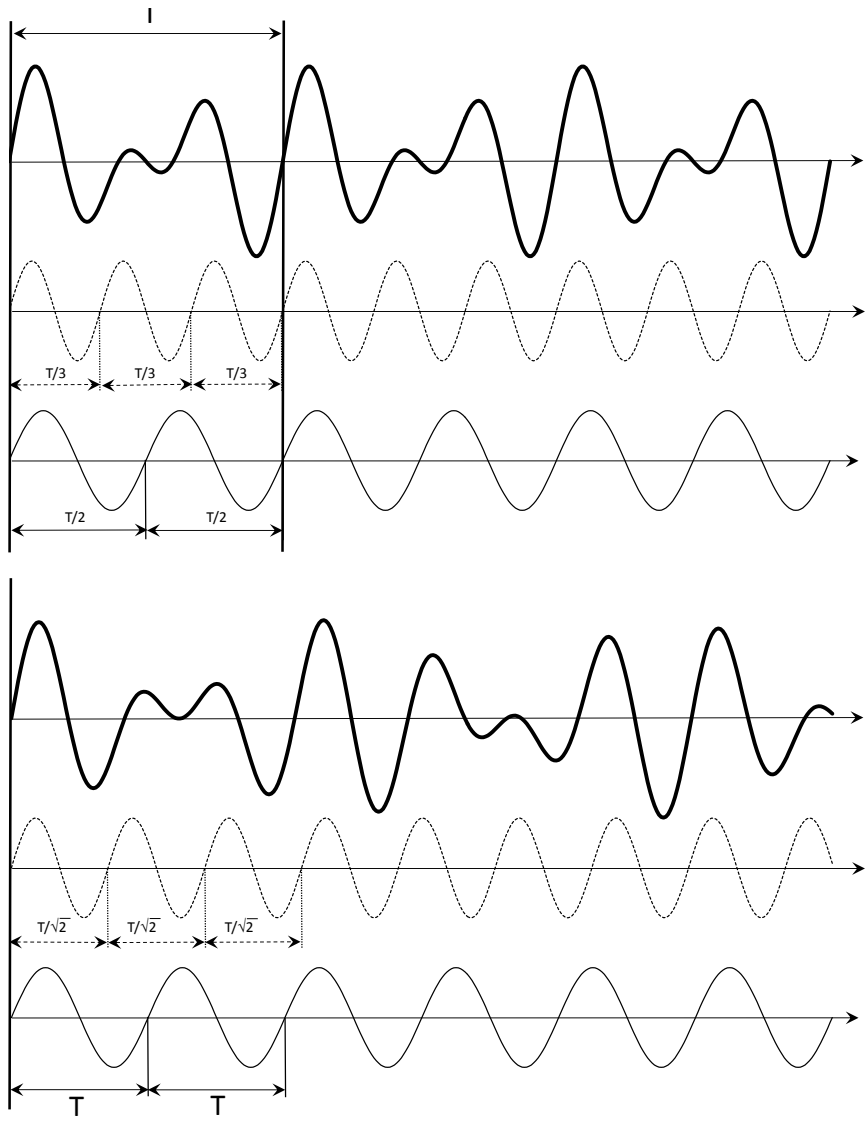

Figure 5.7: Upper graph: the combination of two monochromatic signals whose frequency ratio is rational (here $\frac{3}{2}$) yields a periodic signal. Lower graph: the combination of two monochromatic signals whose frequency ratio is irrational (here $\sqrt{2}$) yields a non-periodic signal.

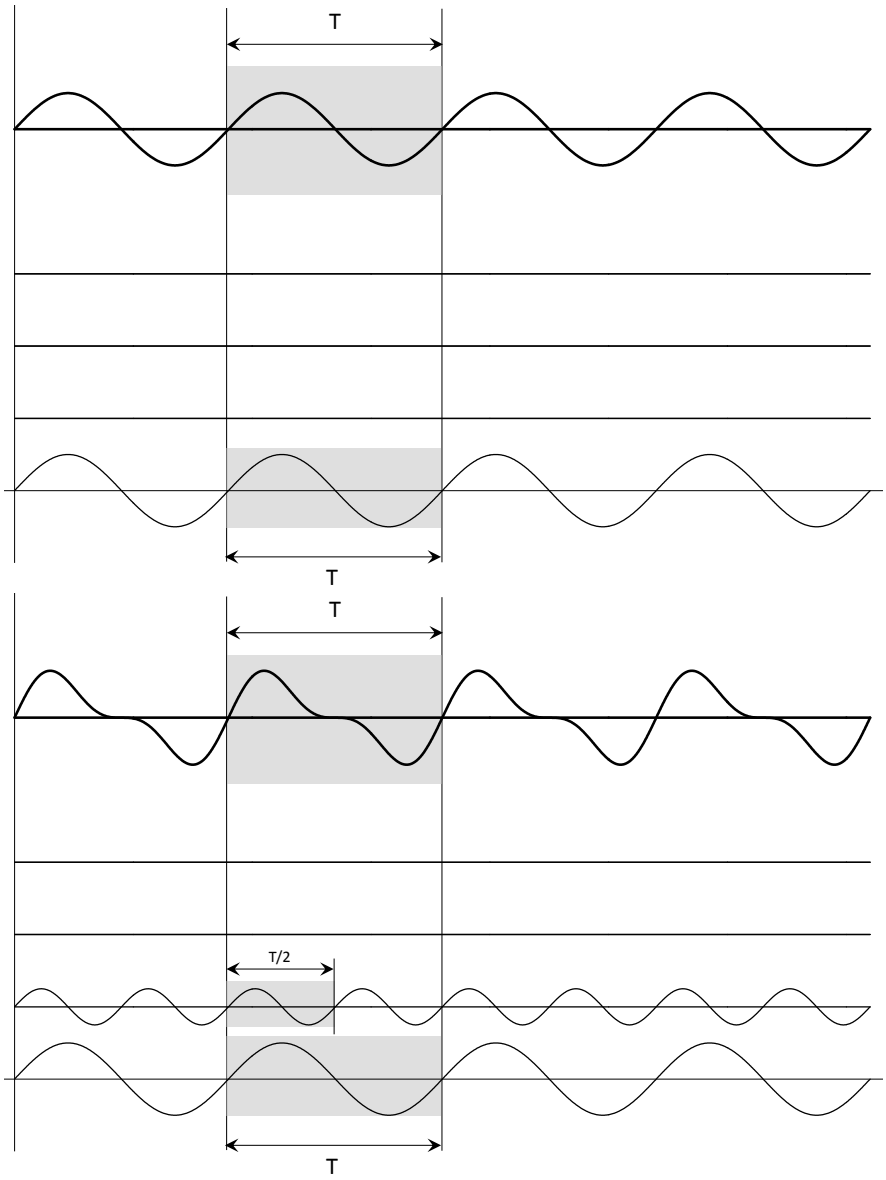

Figure 5.8: Combination of signals whose frequencies are all integer multiples of the same fundamental frequency. Upper graph: fundamental alone. Lower graph: fundamental and first harmonic.

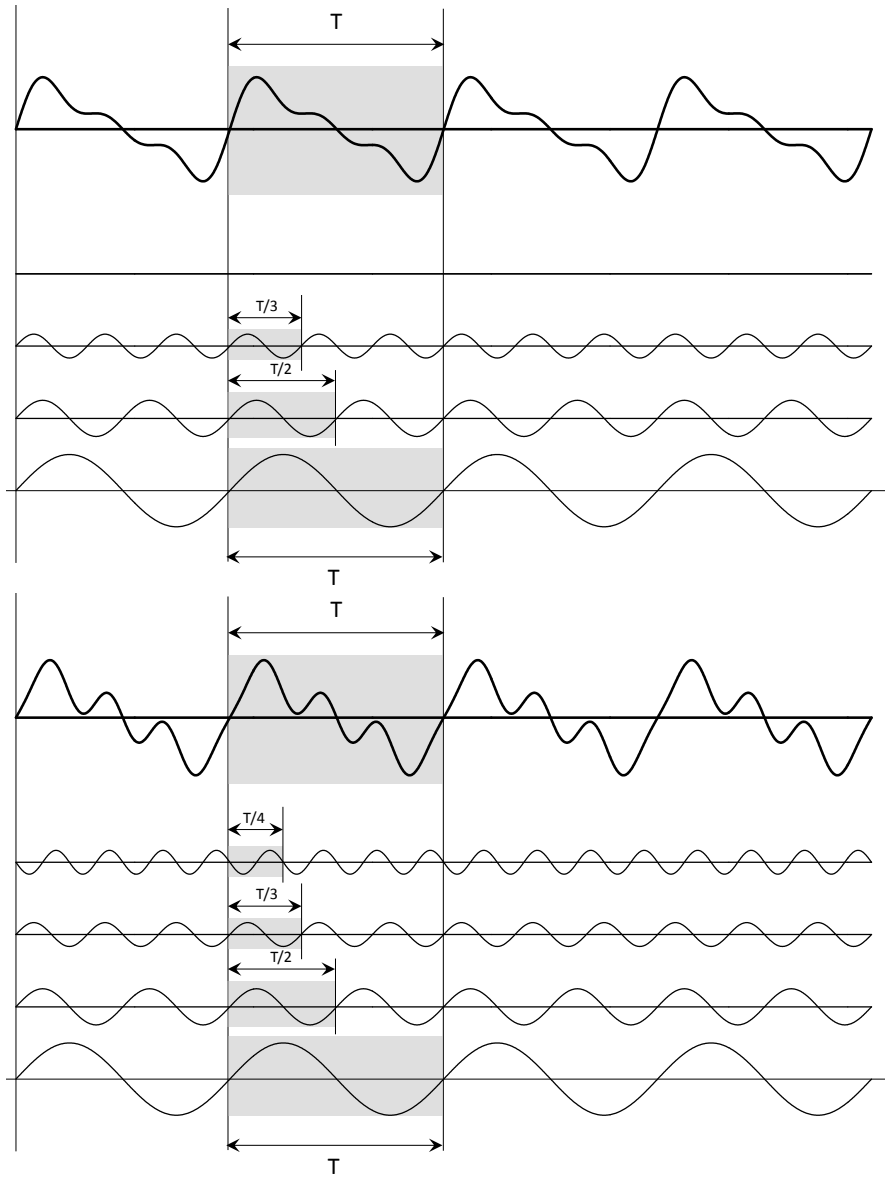

Figure 5.9: Combination of signals whose frequencies are all integer multiples of the same fundamental frequency. Upper graph: fundamental and first two harmonics. Lower graph: fundamental and harmonics 1 to 3.

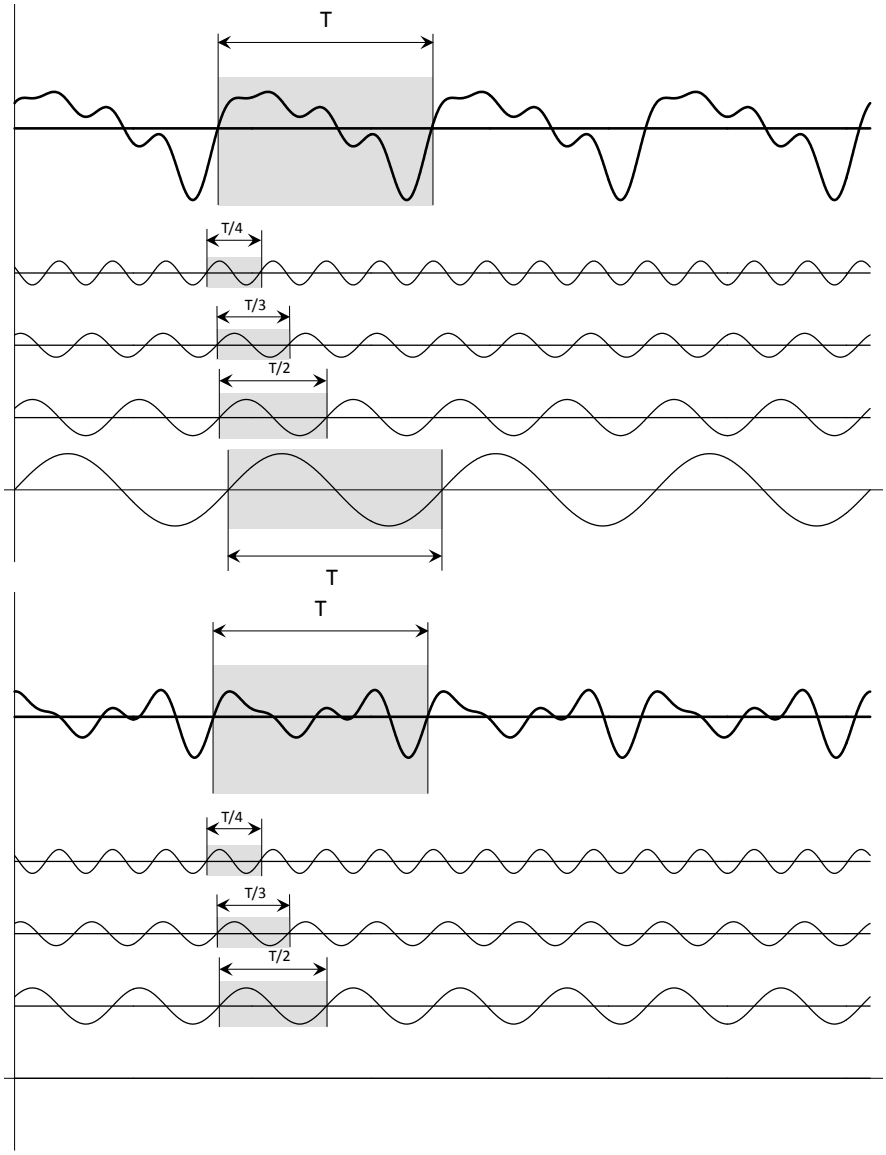

Figure 5.10: Combination of signals whose frequencies are all integer multiples of the same fundamental frequency. Upper graph: fundamental and all harmonics are now out of phase, the shape of the combined signal is modified, but not its period. Lower graph: the amplitude of the fundamental is now zero, but the period of the combined signal is not altered.

5.2 Fourier series

A signal $p(t)$ is periodic if:

$$\exists\, T : \forall t : p(t+T) = p(t) \tag{5.16}$$

Such a signal can be represented by its Fourier series which is written as[3]:

$$p(t) = \sum_{n=0,\infty} A_n \cos \omega_n t - \sum_{n=0,\infty} B_n \sin \omega_n t \tag{5.17}$$

with $\omega_n = 2n\pi/T$. If $p(t)$ designates the total pressure then, in an acoustic context, A_0 is the atmospheric pressure. If $p(t)$ designates the acoustic disturbance, assumed to be of zero mean, $A_0 = 0$. The acoustic pressure is a real quantity, and so are the coefficients A_n and B_n. B_0 is an arbitrary constant introduced only to make notations symmetrical. We can write this series in various other ways. For example by posing:

$$\begin{aligned} A_n &= C_n \cos \phi_n \\ B_n &= C_n \sin \phi_n \end{aligned} \tag{5.18}$$

with:

$$\begin{aligned} C_n &= \sqrt{A_n^2 + B_n^2} \\ \tan \phi_n &= \frac{B_n}{A_n} \end{aligned} \tag{5.19}$$

The Fourier series is then written (second form):

$$p(t) = \sum_{n=0,\infty} C_n \left(\cos \phi_n \cos \omega_n t - \sin \phi_n \sin \omega_n t\right) = \sum_{n=0,\infty} C_n \cos\left(\omega_n t + \phi_n\right) \tag{5.20}$$

or, introducing a complex exponential:

$$p(t) = \Re\left(\sum_{n=0,\infty} C_n e^{i\phi_n} e^{i\omega_n t}\right) \tag{5.21}$$

[3]The negative sign in front of the sine series is arbitrary, but simplifies later notations.

Defining the complex amplitude:

$$D_n = C_n e^{i\phi_n} = A_n + iB_n \tag{5.22}$$

yields the third form:

$$p(t) = \Re\left(\sum_{n=0,\infty} D_n e^{i\omega_n t}\right) \tag{5.23}$$

But the real part of a complex number is equal to half of the sum of this number and its complex conjugate:

$$p(t) = \sum_{n=0,\infty} \frac{D_n}{2} e^{i\omega_n t} + \sum_{n=0,\infty} \frac{D_n^*}{2} e^{-i\omega_n t} \tag{5.24}$$

Finally, introducing the coefficients E_n:

$$\begin{aligned} E_n &= \frac{D_n}{2} \quad pour \quad n > 0 \\ E_0 &= D_0 \\ E_n &= \frac{D_n^*}{2} \quad pour \quad n < 0 \end{aligned} \tag{5.25}$$

we find (fourth form):

$$p(t) = \sum_{n=-\infty,\infty} E_n e^{i\omega_n t} \tag{5.26}$$

E_n is a complex number and the above series defines a real function only because the following condition is satisfied:

$$E_{-n} = E_n^* \tag{5.27}$$

The m^{th} coefficient of the Fourier series (E_m) is calculated by multiplying both sides of Equation 5.26 by $e^{-i\omega_m t}$ and then by integrating over a period (t_0 is an arbitrary time value):

$$\int_{t_0}^{t_0+T} p(t) e^{-i\omega_m t} dt = \sum_{n=-\infty,\infty} E_n \int_{t_0}^{t_0+T} e^{i(\omega_n - \omega_m)t} dt \tag{5.28}$$

but:

$$\int_{t_0}^{t_0+T} e^{i(\omega_n - \omega_m)t} dt = T\delta_{nm} \tag{5.29}$$

where δ_{nm} is Kronecker's delta symbol (Section 3.2). We therefore obtain:

$$E_m = \frac{1}{T}\int_{t_0}^{t_0+T} p(t)e^{-i\omega_m t}dt \tag{5.30}$$

and, for the other Fourier coefficients:

$$D_0 = A_0 = \frac{1}{T}\int_{t_0}^{t_0+T} p(t)dt \tag{5.31}$$

$$D_m = \frac{2}{T}\int_{t_0}^{t_0+T} p(t)e^{-i\omega_m t}dt \tag{5.32}$$

$$A_m = \Re(D_m) = \frac{2}{T}\int_{t_0}^{t_0+T} p(t)\cos\omega_m t dt \tag{5.33}$$

$$B_m = \Im(D_m) = -\frac{2}{T}\int_{t_0}^{t_0+T} p(t)\sin\omega_m t dt \tag{5.34}$$

5.2.1 Square wave and Gibbs phenomenon

In (Figure 5.11), consider as an example the function of period 2π defined on the interval $[-\pi/2.3\pi/2]$ by:

$$\begin{aligned} p(t) &= 1 \quad for \quad -\frac{\pi}{2} < t < \frac{\pi}{2} \\ p(t) &= -1 \quad for \quad \frac{\pi}{2} < t < \frac{3\pi}{2} \end{aligned} \tag{5.35}$$

The function has a zero mean ($A_0 = 0$) and is symmetrical ($B_m = 0$). The harmonics have pulsations $\omega_m = m$. The coefficients A_m are given by:

$$\begin{aligned} A_m &= \frac{2}{2\pi}\left(\int_{\frac{-\pi}{2}}^{\frac{\pi}{2}} \cos mtdt - \int_{\frac{\pi}{2}}^{\frac{3\pi}{2}} \cos mtdt\right) \\ &= \frac{1}{m\pi}\left(3\sin\frac{m\pi}{2} - \sin\frac{3m\pi}{2}\right) \end{aligned} \tag{5.36}$$

We therefore find the development:

$$p(t) = \frac{4}{\pi}\left(\frac{\cos t}{1} - \frac{\cos 3t}{3} + \frac{\cos 5t}{5} - \frac{\cos 7t}{7} + \frac{\cos 9t}{9} + \ldots\right) \tag{5.37}$$

The Fourier series, truncated at order 50, is shown on Figure 5.12. It correctly approximates the two *plateau*, but does not converge at the two discontinuities (*Gibbs phenomenon*): for $n \to \infty$ the Fourier series at $t = \pi/2$ and $t = 3\pi/2$ tends, in this specific case, towards 1.17.

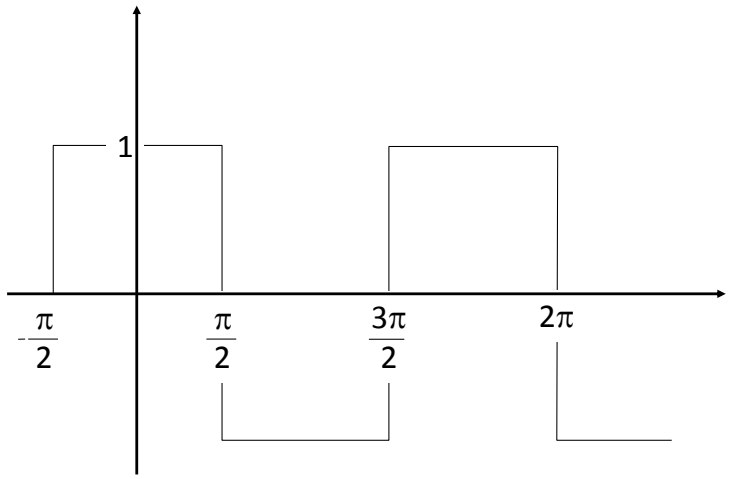

Figure 5.11: Square wave.

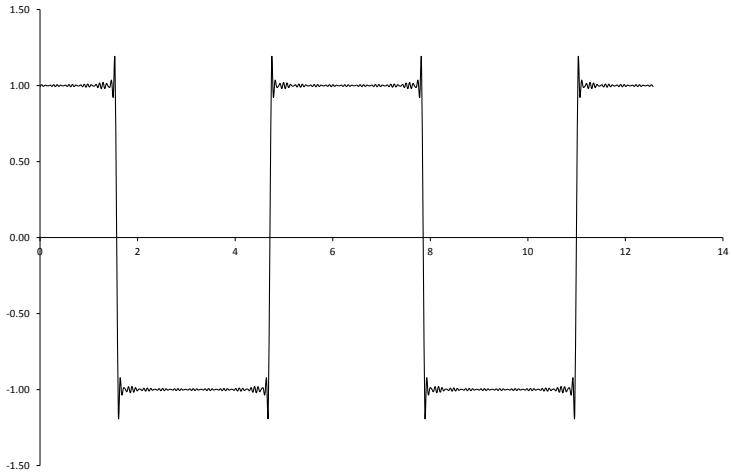

Figure 5.12: Gibbs phenomenon: the Fourier series does not converge at the points of discontinuity of the square wave.

5.2.2 Spectra and complex amplitudes

Any periodic signal is a linear combination of a finite (Figure 5.9) or infinite (Figure 5.12) number of monochromatic signals whose frequency is a multiple of the fundamental $\frac{1}{T}$. The amplitude of harmonic n can be defined by one of the pairs of real numbers (A_n, B_n), (C_n, ϕ_n) or by one of the complex numbers D_n or E_n. The decomposition of a periodic signal in harmonics may be graphically displayed as a *spectrum*. Various *spectra* associated to the signal of Figure 5.14 are plotted in Figures 5.15 to 5.17. The value of the different coefficients is given in Table 5.13.

The decomposition of a signal in its monochromatic components of complex amplitudes is very useful and will be used throughout the book. The sentence *the amplitude of sound at 100 Hz is* $(1+2i)$ is a shortcut of *the signal contains a harmonic component at 100 Hz whose complex amplitude is* $(1+2i)$:

$$p_{100}(t) = \Re\Big[(1+2i)e^{i200\pi t}\Big] = \cos(200\pi t) - 2\sin(200\pi t) \tag{5.38}$$

	5Hz	10Hz	15 Hz	20 Hz
A_n	2	1	1	-1
B_n	-2	-1	1	-1
C_n	$2\sqrt{2}$	$\sqrt{2}$	$\sqrt{2}$	$\sqrt{2}$
ϕ_n	$-\frac{\pi}{4}$	$-\frac{\pi}{4}$	$\frac{\pi}{4}$	$\frac{\pi}{4}$
D_n	$2-2i$	$1-i$	$1+i$	$-1-i$
E_n	$1-i$	$\frac{1-i}{2}$	$\frac{1+i}{2}$	$-\frac{1+i}{2}$
E_n^*	$1+i$	$\frac{1+i}{2}$	$\frac{1-i}{2}$	$-\frac{1-i}{2}$

Figure 5.13: Amplitude of the spectral components of the signal of Figure 5.14.

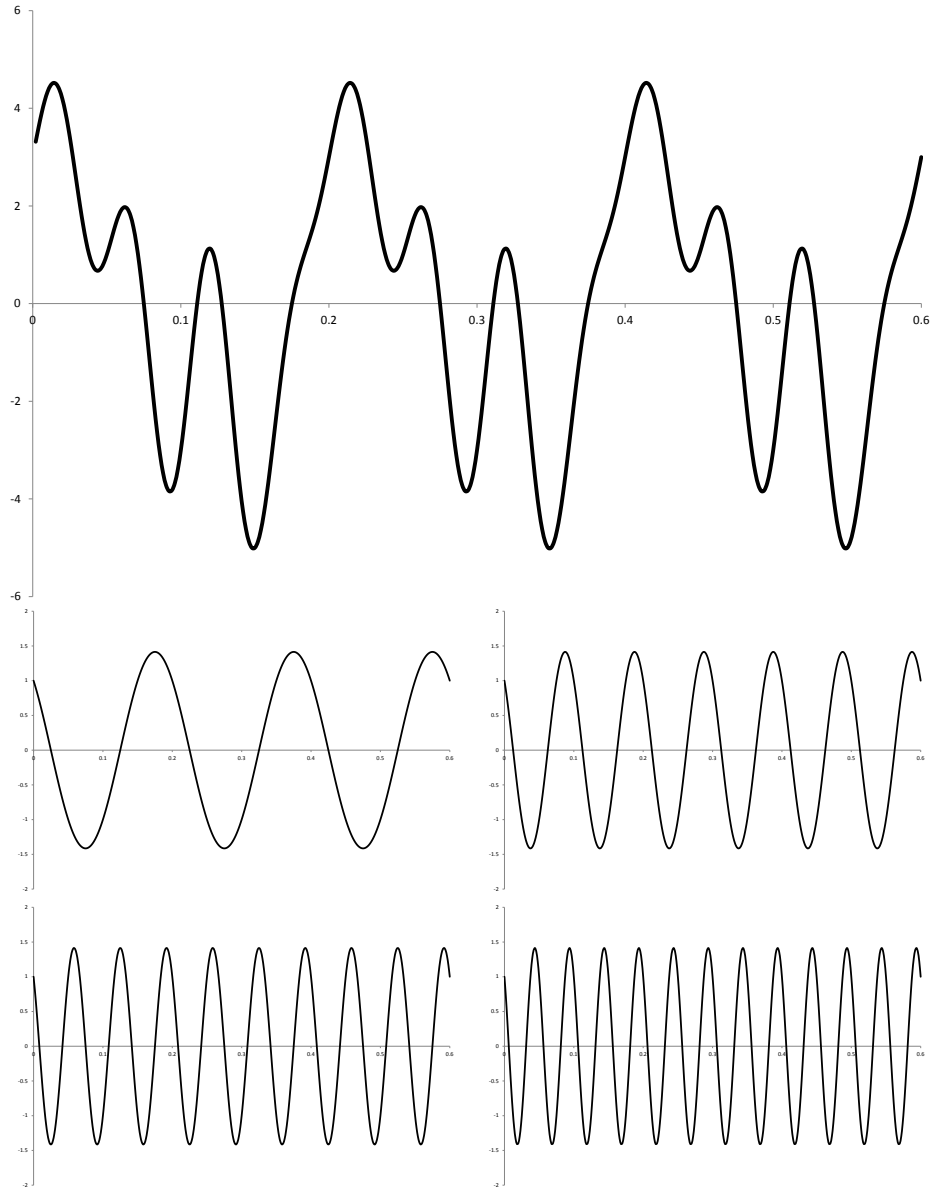

Figure 5.14: Periodic signal and its spectral components.

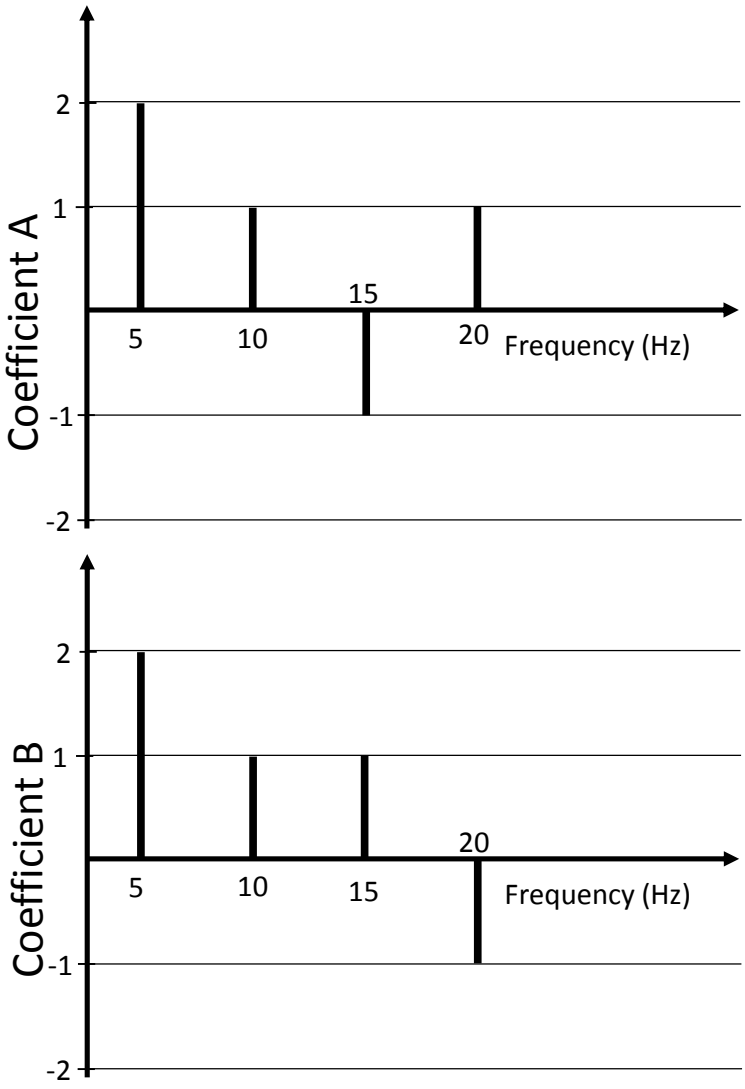

Figure 5.15: (A,B) spectrum of the signal of Figure 5.14.

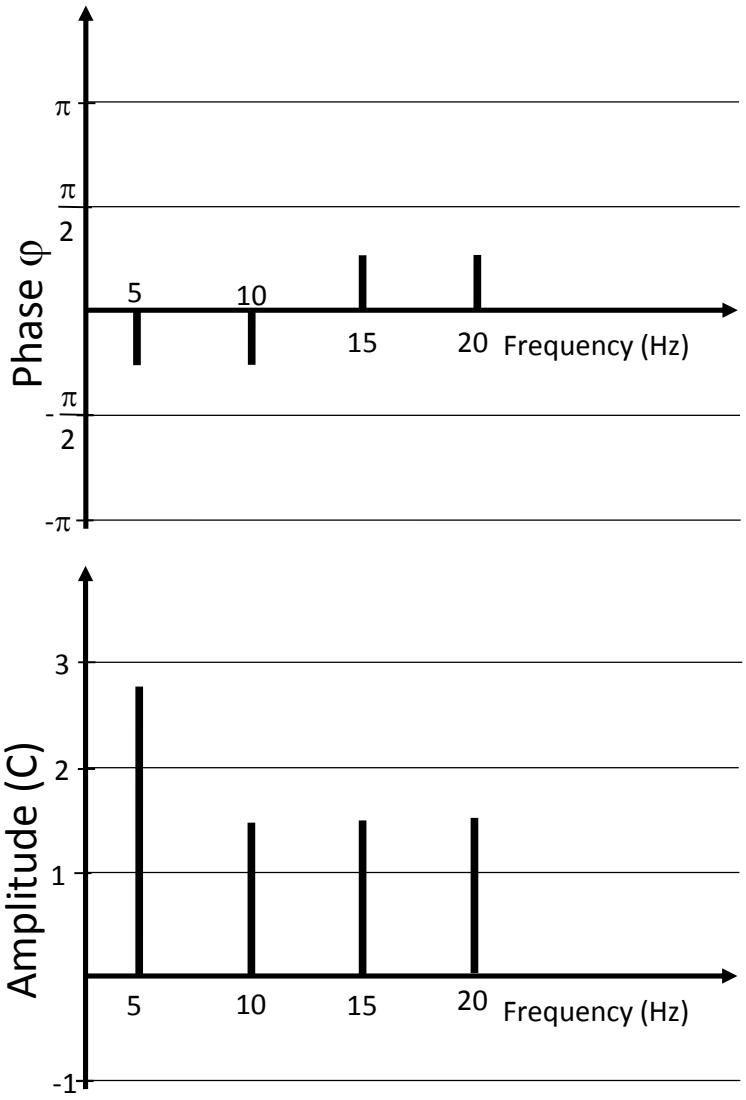

Figure 5.16: (C,ϕ) spectrum of the signal of Figure 5.14.

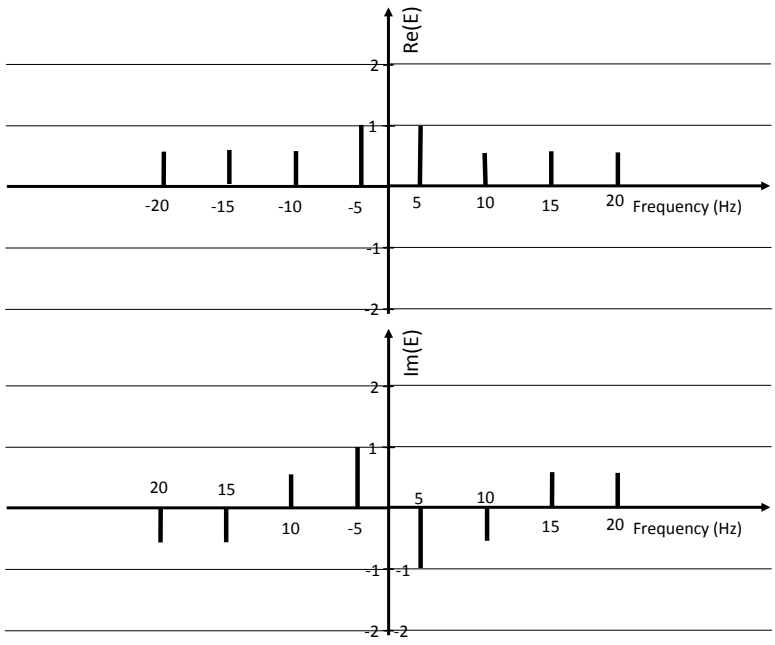

Figure 5.17: $(\Re(E), \Im(E))$ spectrum of the signal of Figure 5.14.

5.3 Fourier transform

Consider again equations 5.26 and 5.30, but with modified, symmetrical, integration bounds:

$$p(t) = \sum_{n=-\infty,\infty} E_n e^{i\omega_n t} \tag{5.39}$$

$$E_m = \frac{1}{T} \int_{t_0-\frac{T}{2}}^{t_0+\frac{T}{2}} p(t) e^{-i\omega_m t} dt \tag{5.40}$$

and let the period T of the signal grow progressively. The integration range grows and the distance between two successive harmonics decreases with T. If $T \to \infty$, the domain of integration stretches from $-\infty$ to $+\infty$ and the harmonics become infinitely close to one another creating a *frequency continuum*:

$$p(t) = \int_{-\infty}^{\infty} P(\omega) e^{i\omega t} df \tag{5.41}$$

$$P(\omega) = \int_{-\infty}^{\infty} p(t) e^{-i\omega t} dt \tag{5.42}$$

$P(\omega)$ is, by definition, the **Fourier transform** of the signal $p(t)$ and $p(t)$ is the **inverse Fourier transform** of the spectrum $P(\omega)$. Two remarks:

- If $p(t)$ has units of Pascal, $P(\omega)$ has units of $Pa \cdot s$ or Pa/Hz.
- The pulsation ω is often used as integration variable instead of the frequency f in 5.41:

$$p(t) = \frac{1}{2\pi} \int_{-\infty}^{\infty} P(\omega) e^{i\omega t} d\omega \tag{5.43}$$

5.3.1 Hermitian character of the spectrum

The Fourier transform can be used in a very general mathematical context and $p(t)$ could, for example, be a function of $\mathbb{C} \to \mathbb{C}$. We limit ourselves to

cases where $p(t)$ represents a time variation of pressure and is a function of $\mathbb{R} \to \mathbb{R}$. In this case we note that:

$$P(-\omega) = \int_{-\infty}^{\infty} p(t) e^{i\omega t} dt = P^*(\omega) \tag{5.44}$$

where P^* designates the complex conjugate of P. It is useful to compare this expression with Equation 5.27.

5.3.2 One-sided spectrum

Taking the hermitian character of the spectrum into account yields an alternative form of the inverse Fourier transform:

$$\begin{aligned} p(t) &= \int_{-\infty}^{\infty} P(\omega) e^{i\omega t} df \\ &= \int_{0}^{\infty} P(\omega) e^{i\omega t} df + \int_{0}^{\infty} P(-\omega) e^{-i\omega t} df \\ &= \int_{0}^{\infty} \left(P(\omega) e^{i\omega t} + \left(P(\omega) e^{i\omega t} \right)^* \right) df \\ &= 2\Re \left(\int_{0}^{\infty} P(\omega) e^{i\omega t} df \right) \end{aligned} \tag{5.45}$$

This expression let's us define a *one-sided spectrum* $P^+(\omega)$:

$$\begin{aligned} P^+(\omega) &= 2P(\omega) \quad for \;\; \omega > 0 \\ &= 0 \qquad for \;\; \omega < 0 \end{aligned} \tag{5.46}$$

With this modified spectrum the inverse Fourier transform is written:

$$p(t) = \Re \left(\int_{0}^{\infty} P^+(\omega) e^{i\omega t} df \right) \tag{5.47}$$

The *complete* spectrum P is the continuous equivalent to the E_n coefficients of the Fourier series. The one-sided spectrum P^+ is the continuous equivalent

to the coefficients D_n:

$$p(t) = \int_{-\infty}^{\infty} P(\omega) e^{i\omega t} df \quad \leftrightarrow \quad p(t) = \sum_{n=-\infty,\infty} E_n e^{i\omega_n t}$$

$$p(t) = \Re\left(\int_{0}^{\infty} P^{+}(\omega) e^{i\omega t} df\right) \quad \leftrightarrow \quad p(t) = \Re\left(\sum_{n=0,\infty} D_n e^{i\omega_n t}\right) \tag{5.48}$$

As the full spectrum is hermitian ($P(-\omega) = P^*(\omega)$), only the right half ($f > 0$) is usually represented. One must be careful when using such one-sided spectrum as they could represent either P or P^+ (see both spectra on Figure 5.18).

Application to a periodic function

If $p(t)$ is a periodic function it can be represented by a Fourier series (Equation 5.26):

$$p(t) = \sum_{n=-\infty,\infty} E_n e^{i\omega_n t} \tag{5.49}$$

and its Fourier transform is:

$$P(\omega) = \sum_{n=-\infty,\infty} E_n \int_{-\infty}^{\infty} e^{-i(\omega-\omega_n)t} dt \tag{5.50}$$

We know that:

$$\int_{-\infty}^{\infty} e^{-i(\omega-\omega_n)t} dt = 2\pi\delta\left(\omega - \omega_n\right) \tag{5.51}$$

where δ is the Dirac distribution whose value is zero everywhere, except when $\omega = \omega_n$ where δ has an infinite value. The Dirac distribution is defined in such a way that its integral over any interval containing ω_n is equal to one. We therefore find:

$$P(\omega) = 2\pi \sum_{n=-\infty,\infty} E_n \delta\left(\omega - \omega_n\right) \tag{5.52}$$

5.4 Convolution product

5.4.1 Definition

The convolution product of two signals $f(t)$ and $g(t)$ is defined as follows:

$$x(t) = \int_{-\infty}^{\infty} f(\tau) \cdot g(t-\tau) \cdot d\tau \tag{5.53}$$

and is denoted $f \otimes g$. Replacing f and g by their respective inverse Fourier transform in the expression of the convolution product we obtain:

$$\begin{aligned} x(t) &= \frac{1}{4\pi^2} \int_{-\infty}^{\infty} \left[\int_{-\infty}^{\infty} F(\omega) e^{i\omega\tau} d\omega \cdot \int_{-\infty}^{\infty} G(\sigma) e^{i\sigma(t-\tau)} d\sigma \right] d\tau \\ &= \frac{1}{4\pi^2} \int_{-\infty}^{\infty} \int_{-\infty}^{\infty} \int_{-\infty}^{\infty} F(\omega) G(\sigma) e^{i\sigma t} e^{i(\omega-\sigma)\tau} d\omega d\sigma d\tau \end{aligned} \tag{5.54}$$

but:

$$\frac{1}{2\pi} \int_{-\infty}^{\infty} e^{i(\omega-\sigma)\tau} d\tau = \delta(\omega - \sigma) \tag{5.55}$$

so that:

$$x(t) = \frac{1}{2\pi} \int_{-\infty}^{\infty} F(\omega) \cdot G(\omega) \cdot e^{i\omega t} d\omega \tag{5.56}$$

The Fourier transform of $x(t)$ is therefore equal to the product of the Fourier transforms of f and g:

$$x(t) = f(t) \otimes g(t) \Leftrightarrow X(\omega) = F(\omega) \cdot G(\omega) \tag{5.57}$$

Symmetrically, if a signal $x(t)$ is defined as the product of two signals $y(t)$ and $z(t)$, the Fourier transform of $x(t)$ is the convolution product of $Y(\omega)$ and $Z(\omega)$:

$$x(t) = f(t) \cdot g(t) \Leftrightarrow X(\omega) = F(\omega) \otimes G(\omega) \tag{5.58}$$

with

$$X(\omega) = \frac{1}{2\pi} \int_{-\infty}^{\infty} Y(\sigma) \cdot Z(\omega - \sigma) d\sigma \tag{5.59}$$

5.4.2 Windowing of a signal

A rectangular window (Figure 5.18) is defined by:

$$\begin{aligned} w(t) &= A \quad for|t| < \tau \\ &= 0 \quad for|t| > \tau \end{aligned} \tag{5.60}$$

and its Fourier transform is given by:

$$W(\omega) = A\int_{-\tau}^{\tau} e^{-i\omega t}dt = A\frac{e^{-i\omega\tau} - e^{i\omega\tau}}{-i\omega} = 2A\tau\frac{\sin\omega\tau}{\omega\tau} \tag{5.61}$$

The *windowed* signal $\bar{p}$ is defined as the signal p seen through the window w:

$$\bar{p}\,(t) = w\,(t - t_0)\cdot p\,(t) \tag{5.62}$$

its Fourier transform is therefore:

$$\bar{P}\,(\omega) = \left(W\,(\omega)\cdot e^{-i\omega t_0}\right) \otimes P\,(\omega) \tag{5.63}$$

The spectrum of the windowed signal is the convolution of the spectra of the original signal and the window.

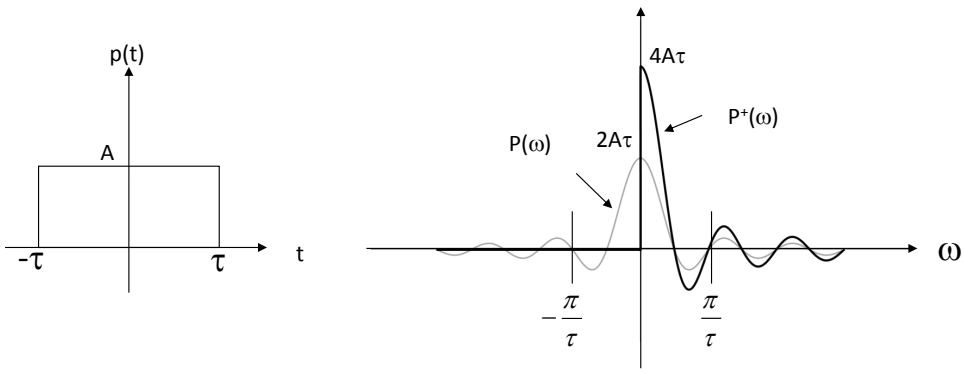

Figure 5.18: Rectangular window and its Fourier transform.

5.4.3 Filtering of a signal

If a filter $F(\omega)$ is applied to the spectrum of a signal:

$$\bar{P}(\omega) = F(\omega) \cdot P(\omega) \tag{5.64}$$

The filtered signal appears as the convolution of the original signal $p(t)$ by the impulse response of the filter ($f(t) \Leftrightarrow F(\omega)$):

$$\bar{p}(t) = f(t) \otimes p(t) \tag{5.65}$$

5.5 Properties of the Fourier transform

5.5.1 Time shift

The fact that $P(\omega)$ is the Fourier transform of $p(t)$ will be noted:

$$p(t) \Leftrightarrow P(\omega) \tag{5.66}$$

The *time-shift* property of the Fourier transform expresses that:

$$p(t - t_0) \Leftrightarrow P(\omega)e^{-i\omega t_0} \tag{5.67}$$

This property can, for example, qualitatively explain the spectra represented in Figure 5.19. The two curves compare measured and calculated vibration spectra of a structure excited by a shock hammer. The measured spectrum displays strong oscillations that are not present in the calculated spectrum. They are the result of a double impact of the hammer on the structure due to elastic rebound. Instead of the expected excitation $f(t)$, the structure is loaded with:

$$f(t) + \alpha f(t - t_0) \tag{5.68}$$

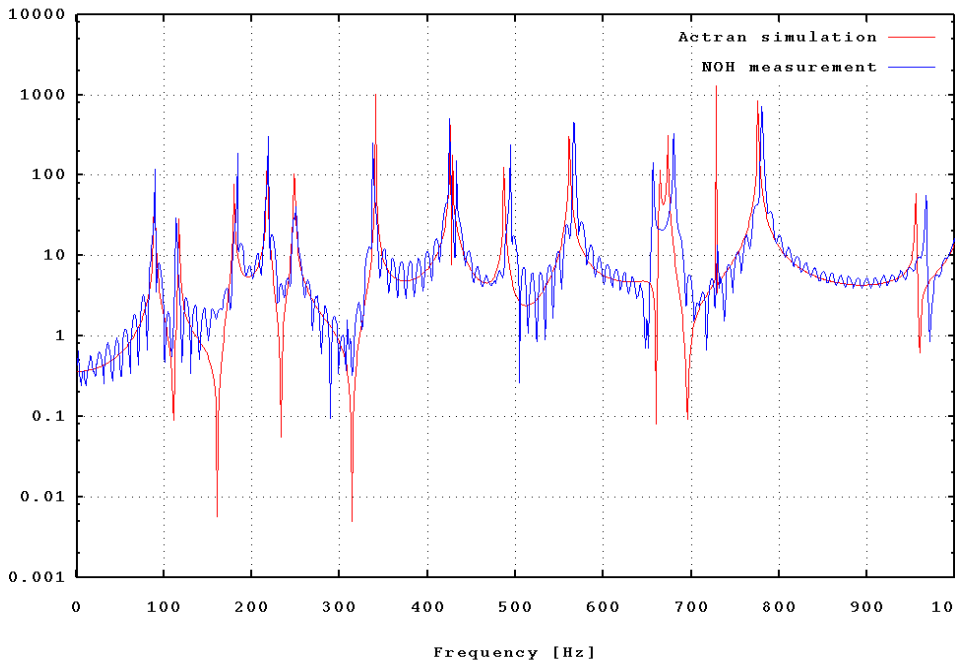

Figure 5.19: Echo effect.

where α measures the relative amplitude of the two impacts and t_0 represents the time delay between them. The excitation spectrum is given by ($f(t) \Leftrightarrow F(\omega)$):

$$F(\omega) \cdot \left(1 + \alpha e^{i\omega t_0}\right) \tag{5.69}$$

The modulus of the excitation is therefore that of a single impact modulated by the function:

$$\sqrt{1 + \alpha^2 + 2\alpha \cos \omega t_0} \tag{5.70}$$

This is the modulation observed in Figure 5.19.

5.5.2 Time and frequency scaling

The time and frequency scaling property of the Fourier transform states that:

$$p(at) \Leftrightarrow \frac{1}{|a|} P(\frac{\omega}{a}) \tag{5.71}$$

This property relates the spectra of two signals with identical shapes, but different durations (e.g. a 33 rpm long-playing record played at 45 rpm). It also schematically explains the dynamic behaviour of a vehicle travelling over a hump in the road. At a low speed, the excitation spectrum is concentrated in the low frequency range and the suspension behaves almost statically. As soon as the speed exceeds a certain threshold, the excitation necessarily includes a component at the resonance frequency of the suspension and the dynamic response of the vehicle is amplified. At very high speed the spectrum has a very low, nearly constant amplitude and the vertical response of the car remains limited. Figure 5.20 compares the dynamic amplification factors of the suspension with the spectrum of the vertical displacement (Equation 5.60) experienced by the tyre rolling at 10 and 60 km/h over a rectangular obstacle 10 cm high and 60 cm long.

5.5.3 Time derivatives

The Fourier transform of a function and its time derivatives are related by:

$$\frac{dp(t)}{dt} \Leftrightarrow i\omega P(\omega) \tag{5.72}$$

$$\frac{d^2p(t)}{dt^2} \Leftrightarrow -\omega^2 P(\omega) \tag{5.73}$$

$$\frac{d^np(t)}{dt^n} \Leftrightarrow (i\omega)^n P(\omega) \tag{5.74}$$

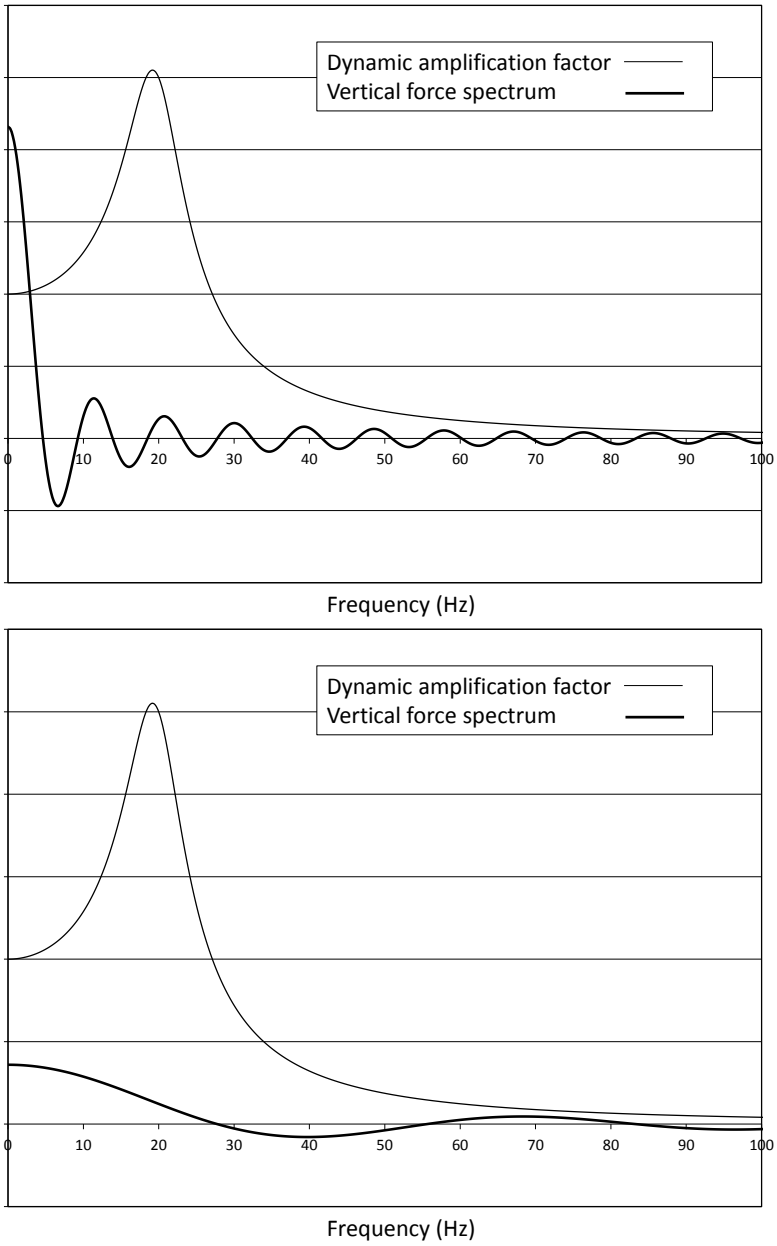

Figure 5.20: Spectrum of the rectangular obstacle and frequency response of the mass-spring system modelling the suspension and car. Vehicle velocity: 10 km/h (upper graph) and 60 km/h (lower graph).

With these properties, any linear differential equation may be transformed into a scalar equation:

$$\sum_{i=1.n} a_n \frac{d^n p(t)}{dt^n} = f(t) \Rightarrow \sum_{i=1.n} a_n (i\omega)^n P(\omega) = F(\omega) \tag{5.75}$$

from which we obtain:

$$P(\omega) = \frac{F(\omega)}{\sum_{i=1.n} a_n (i\omega)^n} \tag{5.76}$$

$p(t)$ is then found by taking the inverse Fourier transform of $P(\omega)$:

$$p(t) = \frac{1}{2\pi} \int_{-\infty}^{\infty} \frac{F(\omega) e^{i\omega t}}{\sum_{i=1.n} a_n (i\omega)^n} d\omega \tag{5.77}$$

5.5.4 Signal and spectrum width

The rectangular window (Equation 5.60) can be used to highlight another important property of the Fourier transform: the relationship between signal and spectrum width. The window has a width $\Delta\tau = 2\tau$ and its spectrum has a conventional width $\Delta\omega = \frac{2\pi}{\tau}$ (Figure 5.18). Their product is constant:

$$\Delta\tau \cdot \Delta\omega = 4\pi \tag{5.78}$$

From this we draw the following conclusions:

- A signal with a small temporal extension, i.e. with a well defined time localisation ($\Delta\tau$ small) has a wide frequency spectrum ($\Delta\omega$ large).
- A narrow spectrum ($\Delta\omega$ small) corresponds to a broad time signal ($\Delta\tau$ large). Figure 5.21 clearly shows that the spectrum becomes narrower when the time span of the signal increases.
- If $\tau \to 0$ and $A \to \infty$, while keeping $2A\tau = 1$, the rectangular signal becomes a Dirac distribution. Its Fourier transform has a constant modulus (Figure 5.22). Conversely, if $\tau \to \infty$ and $A \to 0$, while keeping $2A\tau = 1$, then $P(\omega) \to \delta(\omega)$.

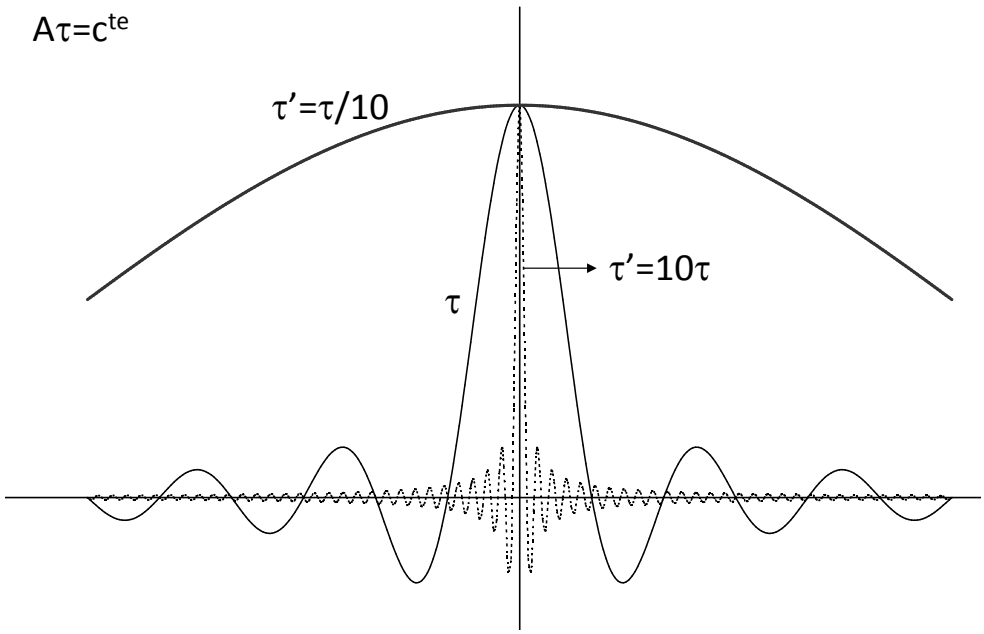

Figure 5.21: Relationship between signal and spectrum width.

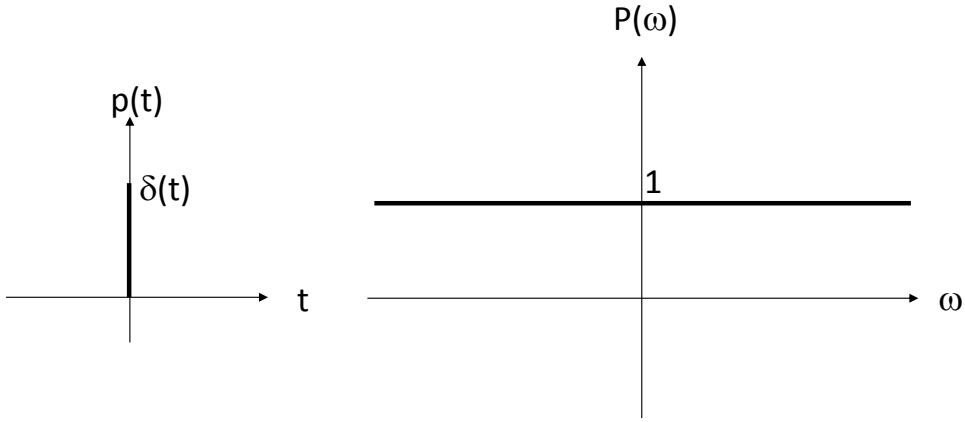

Figure 5.22: Impulsive signal and its Fourier transform.

5.6 Summary of the chapter

A sound is described by the history $p(t)$ of the acoustic pressure (pressure signal). Fourier theory shows that any signal can be analysed as the superposition of elementary periodic signals (sine and cosine). The amplitude of the elementary signals as a function of frequency is called the spectrum of the signal. For a periodic signal, the spectrum is discrete and is composed of a finite or infinite number of equally spaced *harmonics* ($\Delta f = 1/T$). The elementary signal of period T is called the *fundamental* and that of period T/m the harmonic $(m-1)$. For a non-periodic signal the spectrum is generally continuous and the contribution of each frequency to the signal is infinitesimal. Nevertheless, we have seen that the combination of two pure tones whose frequency ratio is irrational produces a non-periodic signal even if their spectrum is discrete (Figure 5.7).

The amplitude of the spectrum at a given frequency is a complex number; the corresponding elementary component of the signal is given by:

$$\begin{aligned} p_\omega(t) &= P(\omega)\cdot e^{i\omega t} + P(-\omega)\cdot e^{-i\omega t} \\ &= 2\Re\left(P(\omega)\cdot e^{i\omega t}\right) \\ &= \Re\left(P^+(\omega)\cdot e^{i\omega t}\right) \end{aligned} \tag{5.79}$$

If $p(t)$ is non-periodic, then p_ω is a *power spectral density* and the amplitude of the spectrum at frequency ω is $p_\omega d\omega$.

The signal and its Fourier transform provide two complementary descriptions of the same phenomenon. The signal records the actual physical phenomenon, while the spectrum provides a more readable and useful representation for the engineer.

6

Equations of acoustics in harmonic regime

Whoever, in the pursuit of science, seeks after immediate practical utility, may generally rest assured that he will seek in vain.
— **Hermann von Helmholtz** (1821-1894), Science (1922).
cited by Max Planck (1858-1947), Scientific autobiography (1948)

Contents

6.1 Helmholtz equation 90
6.2 Pressure-velocity relationship 90
6.3 Acoustic impedance 91
6.4 Sound intensity 92
6.5 Plane waves 97
6.6 Spherical waves 101

6.1 Helmholtz equation

We showed in Chapter 4 that the acoustic pressure field obeys a wave equation:

$$\Delta p - \frac{1}{c^2}\frac{\partial^2 p}{\partial t^2} = 0 \tag{6.1}$$

Taking the Fourier transform of this equation yields Helmholtz' equation[1] for the sound pressure spectrum $P(\omega)$ (with $p(t) \Leftrightarrow P(\omega)$):

$$\Delta P(\omega) + \frac{\omega^2}{c^2}P(\omega) = 0 \tag{6.2}$$

or:

$$\Delta P(\omega) + k^2 P(\omega) = 0 \tag{6.3}$$

where $k = \omega/c$ is the wave number (Section 4.5.1).

6.2 Pressure-velocity relationship

Equation 4.26 relates the velocity v_i of air particles to the pressure gradient:

$$\partial_j p(t) = -\rho \partial_t v_j(t) \tag{6.4}$$

Applying the Fourier transform yields a new relation linking the spectrum of the pressure gradient to the spectrum of the particle velocity:

$$\partial_j P(\omega) = -i\rho\omega V_j(\omega) \tag{6.5}$$

or:

$$V_j(\omega) = \frac{i}{\rho\omega}\partial_j P(\omega) \tag{6.6}$$

[1] **Hermann Ludwig Ferdinand von Helmholtz** was born in 1821 and died in 1884 in Potsdam. He is known for his work applying physics to physiology and for his contributions to thermodynamics. In the field of acoustics, he partly elucidated the physiological mechanism by which the ear perceives the height of a sound (*tonotopy*).

6.3 Acoustic impedance

The acoustic impedance[2] at a given point and in a given direction is defined as the ratio between the complex amplitude of the pressure and velocity spectra:

$$Z_j(\omega) = \frac{P(\omega)}{V_j(\omega)} \tag{6.7}$$

where j indicates direction. $Z_j(\omega)$ is a complex quantity, usually frequency dependent. The acoustical absorption of a boundary is characterised by its normal impedance (Chapter 8):

$$Z_n(\omega) = \frac{P(\omega)}{V_n(\omega)} \tag{6.8}$$

A perfectly rigid wall is characterised by an infinite impedance ($v_n = 0$, $Z_n = \infty$) while a perfectly soft surface ($p = 0$) has an impedance of zero. The inverse of impedance is called admittance:

$$A_n(\omega) = \frac{V_n(\omega)}{P(\omega)} \tag{6.9}$$

Impedance and admittance relate pressure and velocity spectra. The time-dependent ratio of the pressure and velocity signals has no physical relevance. Impedance is a general concept in the physics of harmonic phenomena. In the field of electricity, impedance is the generalisation of resistance to alternating currents (ratio of tension to current). In structural dynamics impedance has several definitions: force to displacement, force to velocity or force to acceleration ratio. Impedance is always the ratio (transfer function) between a cause (force, tension, acoustic pressure) and the associated effect (displacement, current or acoustic velocity). Impedance is, in general, a complex and frequency dependent quantity.

[2]From the latin *impedire*, to hinder.

6.4 Sound intensity

An air particle moves at a velocity $v(t)$ in a sound field characterised by a pressure $p(t)$. This movement requires a specific power (power per unit area) which is the product of pressure and velocity:

$$i(t) = p(t) \cdot v(t) \tag{6.10}$$

$i(t)$ is called *instantaneous sound intensity.*

6.4.1 Monochromatic signal

Consider a monochromatic signal with pulsation ω:

$$\begin{aligned} p(t) &= P_a \cos(\omega t + \phi_p) = \Re\left(P e^{i\omega t}\right) \\ v(t) &= V_a \cos(\omega t + \phi_v) = \Re\left(V e^{i\omega t}\right) \end{aligned} \tag{6.11}$$

The instantaneous intensity:

$$\begin{aligned} i(t) &= P_a V_a \cos(\omega t + \phi_p) \cos(\omega t + \phi_v) \\ &= \frac{P_a V_a}{2} \left[\cos(\phi_p - \phi_v) + \cos(2\omega t + \phi_p + \phi_v)\right] \\ &= \Re\left(\frac{PV^*}{2} + \frac{PV e^{2i\omega t}}{2}\right) \end{aligned} \tag{6.12}$$

appears as the sum of two terms (Figure 6.1). The first term, constant in time, is the **active intensity** and represents a net flux of power from the source to the receiver. The second term, of zero mean and characterised by a pulsation of 2ω, is the **reactive intensity**. Active intensity is maximum when pressure and velocity are in phase (Figure 6.2) as in a plane wave propagating in free field (Section 6.5.3). Active intensity is zero when pressure and velocity have a phase difference of 90° (Figure 6.3) as in a standing wave (Chapter 9).

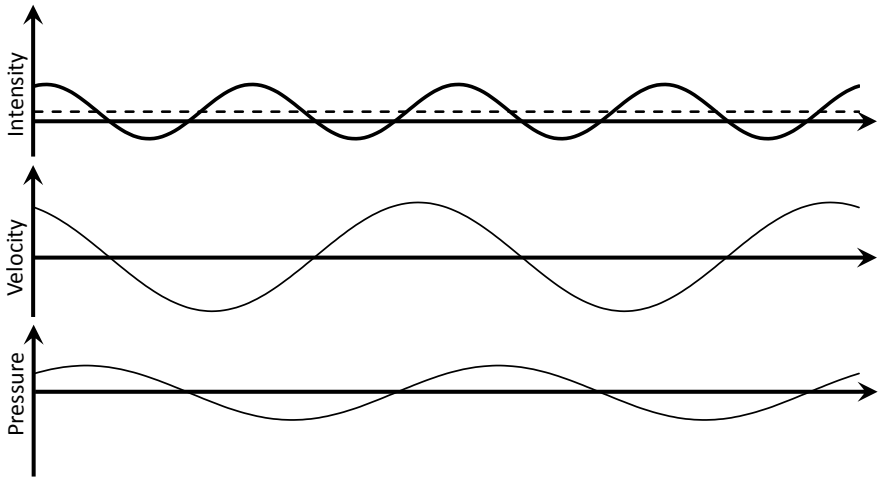

Figure 6.1: Sound intensity: general case. Active (dotted line) and reactive intensity (solid line).

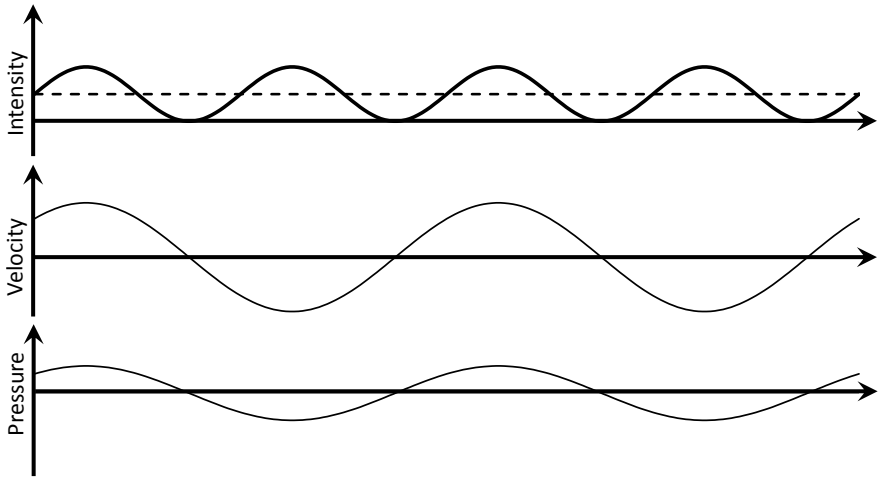

Figure 6.2: Sound intensity: pressure and velocity are in phase, impedance is real, active intensity is maximum.

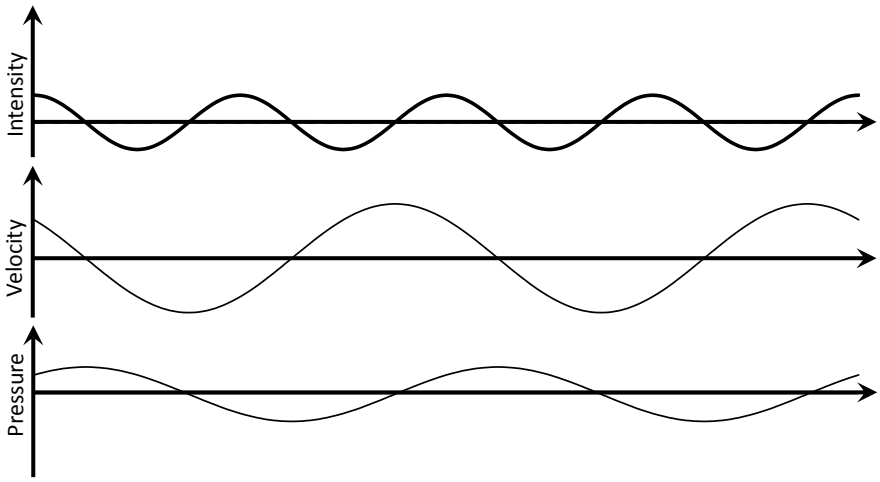

Figure 6.3: Sound intensity: pressure and velocity have a phase difference of 90°, impedance is imaginary, active intensity is zero.

6.4.2 General periodic signal

Consider now a periodic signal made of N monochromatic signals of pulsations $\omega_m = m\omega_0$:

$$\begin{aligned} p(t) &= \sum_{m=1}^{N} P_{am} \cos\left(m\omega_0 t + \phi_{pm}\right) \\ v(t) &= \sum_{m=1}^{N} V_{an} \cos\left(n\omega_0 t + \phi_{vn}\right) \end{aligned} \tag{6.13}$$

The instantaneous intensity is given by:

$$\begin{aligned} i(t) &= \sum_{n=1}^{N}\sum_{m=1}^{N} P_{am}V_{an} \cos\left(m\omega_0 t + \phi_{pm}\right)\cos\left(n\omega_0 t + \phi_{vn}\right) \\ &= \sum_{n=1}^{N}\sum_{m=1}^{N} \frac{P_{am}V_{an}}{2} \left[\begin{array}{l} \cos\left(\left(m-n\right)\omega_0 t + \phi_{pm} - \phi_{vn}\right) + \\ \cos\left(\left(m+n\right)\omega_0 t + \phi_{pm} + \phi_{vn}\right) \end{array} \right] \end{aligned} \tag{6.14}$$

The spectrum $I(\omega)$ associated with $i(t)$ contains all harmonics ranging from $-(N-1)$ to $2N$, including an active component corresponding to the $m = n$ term:

$$I_{active} = \sum_{m=1}^{N} \frac{P_{am} V_{am}}{2} \cos\left(\phi_{pm} - \phi_{vm}\right) \tag{6.15}$$

or, introducing the complex pressure (P_m) and velocity (V_m) amplitudes of harmonic m:

$$I_{active} = \Re\left(\sum_{m=1}^{N} \left(\frac{P_m V_m^*}{2}\right)\right) \tag{6.16}$$

6.4.3 General signal

Consider finally the most general signal. Intensity being the product of two signals, its spectrum is the convolution product of the related spectra:

$$I(\omega) = \frac{1}{2\pi} \int_{-\infty}^{\infty} P(\sigma) \cdot V(\omega - \sigma) d\sigma \tag{6.17}$$

The reactive intensity component with pulsation ω results from the power spent by the particles to oscillate at the pulsation $\omega - \sigma$ in a pressure field of pulsation σ and this for all values of σ. The spectrum of $i(t)$ also has a constant component $I(0)$ which is the **active intensity**:

$$\begin{aligned} I(0) &= \frac{1}{2\pi} \int_{-\infty}^{\infty} P(\sigma) \cdot V(-\sigma) d\sigma \\ &= \frac{1}{2\pi} \int_{-\infty}^{\infty} P(\sigma) \cdot V^*(\sigma) d\sigma \\ &= \frac{1}{2\pi} \Re\left(\int_{0}^{\infty} 2P(\sigma) \cdot V^*(\sigma) d\sigma\right) \\ &= \frac{1}{2\pi} \Re\left(\int_{0}^{\infty} \frac{P^+(\sigma) \cdot V^{+*}(\sigma)}{2} d\sigma\right) \end{aligned} \tag{6.18}$$

Note once again the possible ambiguity resulting from the use of a full spectrum vs. a one-sided spectrum. As active intensity is constant in time, it is inaccurate to talk about the active intensity *at pulsation* ω. This expression

is nevertheless often used to designate the spectral density of intensity:

$$I(\omega) = \Re\left(\frac{P^+(\omega) \cdot V^{+*}(\omega)}{2}\right) \tag{6.19}$$

which is the contribution of the pressure and velocity components of pulsation ω to the total active intensity.

By introducing the local impedance $Z = Z_r + iZ_i$, we can express active intensity (or its spectral density) in the form:

$$I(\omega) = \Re\left(\frac{P^+(\omega) \cdot P^{+*}(\omega)}{2Z}\right) = \frac{Z_r}{Z_r^2 + Z_i^2}\frac{|P^+(\omega)|^2}{2} \tag{6.20}$$

or, introducing the RMS pressure:

$$I(\omega) = \frac{Z_r}{Z_r^2 + Z_i^2}|P^+_{RMS}(\omega)|^2 \tag{6.21}$$

with:

$$|P^+_{RMS}(\omega)| = \frac{|P^+(\omega)|}{\sqrt{2}} \tag{6.22}$$

This last expression shows that active intensity has the same sign as the real part of the impedance (see Section 8.4.1).

6.5 Plane waves

6.5.1 General solution in one-dimension

The general solution of the one-dimensional wave equation (Equation 4.31) is:

$$p\left(x,t\right)=f\left(t-\frac{x}{c}\right)+g\left(t+\frac{x}{c}\right) \tag{6.23}$$

Applying the time-shift property (Equation 5.67) we find (with $f(t) \Leftrightarrow F(\omega)$ and $g(t) \Leftrightarrow G(\omega)$):

$$P\left(x,\omega\right)=F\left(\omega\right)e^{-ikx}+G\left(\omega\right)e^{ikx} \tag{6.24}$$

The first term represents a wave travelling towards the positive x (note the negative sign in the complex exponential), while the second term represents a wave travelling towards the negative x (note the positive sign in the complex exponential).

Notes:

1. Until now, we have systematically used lower case letters to indicate time-domain signals and uppercase letters to indicate spectra (as in $p(t) \Leftrightarrow P(\omega)$). This is no longer necessary as the variable (t or ω) indicates the nature of the function.

2. We consider all spectra to be *one-sided* so that intensity can be calculated by Equation 6.18.

6.5.2 Characteristic impedance

Consider a plane wave propagating from left to right:

$$p(x,\omega)=F(\omega)e^{-ikx} \tag{6.25}$$

The oscillating velocity of air particles is (Equation 6.5):

$$v_x(x,\omega) = \frac{i}{\rho\omega}\frac{\partial p(x,\omega)}{\partial x} = \frac{F(\omega)}{\rho c}e^{-ikx} \tag{6.26}$$

The impedance (pressure to velocity ratio) is independent of the position x:

$$Z = \frac{p}{v_x} = \rho c \tag{6.27}$$

This impedance value is called the *characteristic impedance of the medium*. We will see in Section 8.1.3 that this impedance has a very particular status and is used as a reference.

6.5.3 Intensity

The active intensity propagated by a plane wave is easily computed:

$$I_a = \frac{1}{2}\Re\left(\int_0^\infty p(\sigma)\cdot v^*(\sigma)\frac{d\sigma}{2\pi}\right) = \frac{1}{2\rho c}\int_0^\infty |p(\sigma)|^2\frac{d\sigma}{2\pi} \tag{6.28}$$

or, for a monochromatic signal:

$$I_a = \frac{|p|^2}{2\rho c} \tag{6.29}$$

Pressure is in phase with velocity and there is no reactive intensity. These are two characteristics of a purely propagative sound field.

6.5.4 Attenuation

We have assumed (Section 4.1) that the media in which the sound wave propagates is non-viscous. In such a fluid an acoustic wave propagates without any loss. In practice there is always some dissipation of energy in the fluid and the amplitude of the wave decays exponentially with distance:

$$p = Ae^{-\alpha x}e^{-ikx} \tag{6.30}$$

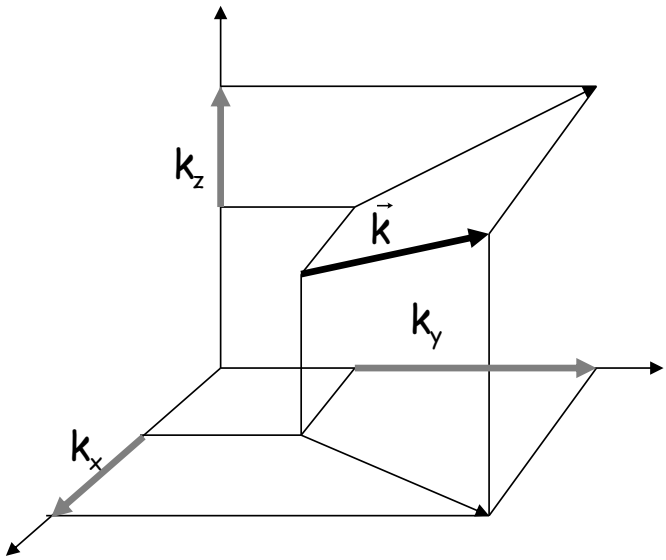

Figure 6.4: Components of the wave vector associated with a plane wave of arbitrary incidence.

where α is a coefficient of attenuation. We can rewrite the above equation by introducing a complex wave number $\tilde{k}$:

$$p = Ae^{-i\tilde{k}x} \rightarrow \tilde{k} = k - i\alpha = \frac{\omega - i\alpha c}{c} \simeq \frac{\omega}{c\left(1 + \frac{i\alpha c}{\omega}\right)} \tag{6.31}$$

The last expression defines a complex speed of sound $\tilde{c}$:

$$\tilde{c} = c\left(1 + i\frac{\alpha c}{\omega}\right) \tag{6.32}$$

Attenuation can therefore be modelled by adding a small imaginary component to the speed of sound. This coefficient depends on the nature of the fluid and of frequency. The ratio $\alpha c/\omega$ has an order of magnitude of 0.005 in air at audible frequencies.

6.5.5 Plane wave with arbitrary incidence

Let us consider the three-dimensional Helmholtz equation:

$$\frac{\partial^2 p(\vec{r},\omega)}{\partial x^2} + \frac{\partial^2 p(\vec{r},\omega)}{\partial y^2} + \frac{\partial^2 p(\vec{r},\omega)}{\partial z^2} + k^2 p(\vec{r},\omega) = 0 \tag{6.33}$$

and let us consider solutions of the form:

$$p\left(\vec{r},\omega\right) = X(x)\cdot Y(y)\cdot Z(z) \tag{6.34}$$

Introducing this solution into the wave equation and dividing by $p(\vec{r},\omega)$ gives:

$$\frac{1}{X}\frac{d^2X(x)}{dx^2} + \frac{1}{Y}\frac{d^2Y(y)}{dy^2} + \frac{1}{Z}\frac{d^2Z(z)}{dz^2} + k^2 = 0 \tag{6.35}$$

Each term of this equation involves a single coordinate and must be constant for the sum to be zero:

$$\frac{1}{X}\frac{d^2X(x)}{dx^2} = -k_x^2 \Rightarrow X(x) = Ae^{-ik_x x} \tag{6.36}$$

$$\frac{1}{Y}\frac{d^2Y(y)}{dy^2} = -k_y^2 \Rightarrow Y(y) = Be^{-ik_y y} \tag{6.37}$$

$$\frac{1}{Z}\frac{d^2Z(z)}{dz^2} = -k_z^2 \Rightarrow Z(z) = Ce^{-ik_z z} \tag{6.38}$$

The function:

$$p(\vec{r},\omega) = P\cdot e^{-i(k_x x + k_y y + k_z z)} \tag{6.39}$$

is the solution of the Helmholtz equation provided that the *dispersion relation* holds:

$$k^2 = k_x^2 + k_y^2 + k_y^2 \tag{6.40}$$

The solution may be rewritten in a more compact form by introducing the wave vector $\vec{k}$ or components (k_x, k_y, k_z):

$$p(\vec{r},\omega) = Pe^{-i\vec{k}\cdot\vec{r}} \tag{6.41}$$

The pressure p is constant on a plane defined by the equation:

$$\vec{k} \cdot \vec{r} = constant \tag{6.42}$$

$Pe^{-i\vec{k}\cdot\vec{r}}$ is indeed a plane wave (Figure 6.4). It propagates in the direction of the vector $\vec{k}$. The wavefronts are perpendicular to $\vec{k}$.

6.6 Spherical waves

As the rain pelted the surface of the river, the Counselor, standing atop an altar of barrels, spoke of something, the war perhaps, in a voice that those closest to him could barely hear, but what they heard they repeated to those behind them, who passed it on to those further back, and so on, in a series of concentric circles.
— **Mario Vargas Llosa** (1936-), The war of the end of the world (1981).
English translation by Helen Lane (1985).

6.6.1 Monopoles

The wave equation in spherical coordinates is written:

$$\frac{1}{r^2}\frac{\partial}{\partial r}\left(r^2\frac{\partial p}{\partial r}\right) + \frac{1}{r^2\sin\theta}\frac{\partial}{\partial\theta}\left(\sin\theta\frac{\partial p}{\partial\theta}\right) + \frac{1}{r^2\sin^2\theta}\frac{\partial^2 p}{\partial\phi^2} - \frac{1}{c^2}\frac{\partial^2 p}{\partial t^2} = 0 \tag{6.43}$$

A purely radial solution (independent of θ and ϕ) obeys the equation:

$$\frac{1}{r^2}\frac{\partial}{\partial r}\left(r^2\frac{\partial p}{\partial r}\right) - \frac{1}{c^2}\frac{\partial^2 p}{\partial t^2} = 0 \tag{6.44}$$

which can be rewritten in the following way:

$$\frac{\partial^2 (pr)}{\partial r^2} - \frac{1}{c^2}\frac{\partial^2 (pr)}{\partial t^2} = 0 \tag{6.45}$$

by analogy with (Equation 4.31), the general solution is,

$$p\left(r,t\right)=\frac{f\left(t-\frac{r}{c}\right)}{r}+\frac{g\left(t+\frac{r}{c}\right)}{r} \tag{6.46}$$

This solution is the sum of two radial waves, one divergent and the other convergent. Taking the Fourier transform, we get the general solution of the spherical Helmholtz equation:

$$p\left(r,\omega\right)=F\left(\omega\right)\frac{e^{-ikr}}{r}+G\left(\omega\right)\frac{e^{ikr}}{r} \tag{6.47}$$

In almost all cases the converging wave is incompatible with the boundary conditions and we will only retain the first term (Figure 6.5):

$$p\left(r,\omega\right)=F\left(\omega\right)\frac{e^{-ikr}}{r} \tag{6.48}$$

The radial velocity of the air particles in a monopole field is given by:

$$v_r\left(r,\omega\right)=\frac{i}{\rho\omega}\frac{dp\left(x,\omega\right)}{dr}=\frac{1}{\rho c}\cdot\left(1+\frac{1}{ikr}\right)\cdot F\left(\omega\right)\frac{e^{-ikr}}{r} \tag{6.49}$$

The radial impedance is:

$$Z_r\left(r,\omega\right)=\frac{\rho c}{1+\frac{1}{ikr}} \tag{6.50}$$

and tends towards ρc when $r\to\infty$. The real and imaginary parts are represented in Figure 6.6. The acoustic intensity is given by:

$$I_r\left(r,\omega\right)=\frac{\left|F\left(\omega\right)\right|^2}{2\rho c r^2} \tag{6.51}$$

The power radiated by the source through a sphere of radius R is independent of R (energy conservation):

$$W\left(R,\omega\right)=4\pi R^2\frac{\left|F\left(\omega\right)\right|^2}{2\rho c R^2}=2\pi\frac{\left|F\left(\omega\right)\right|^2}{\rho c} \tag{6.52}$$

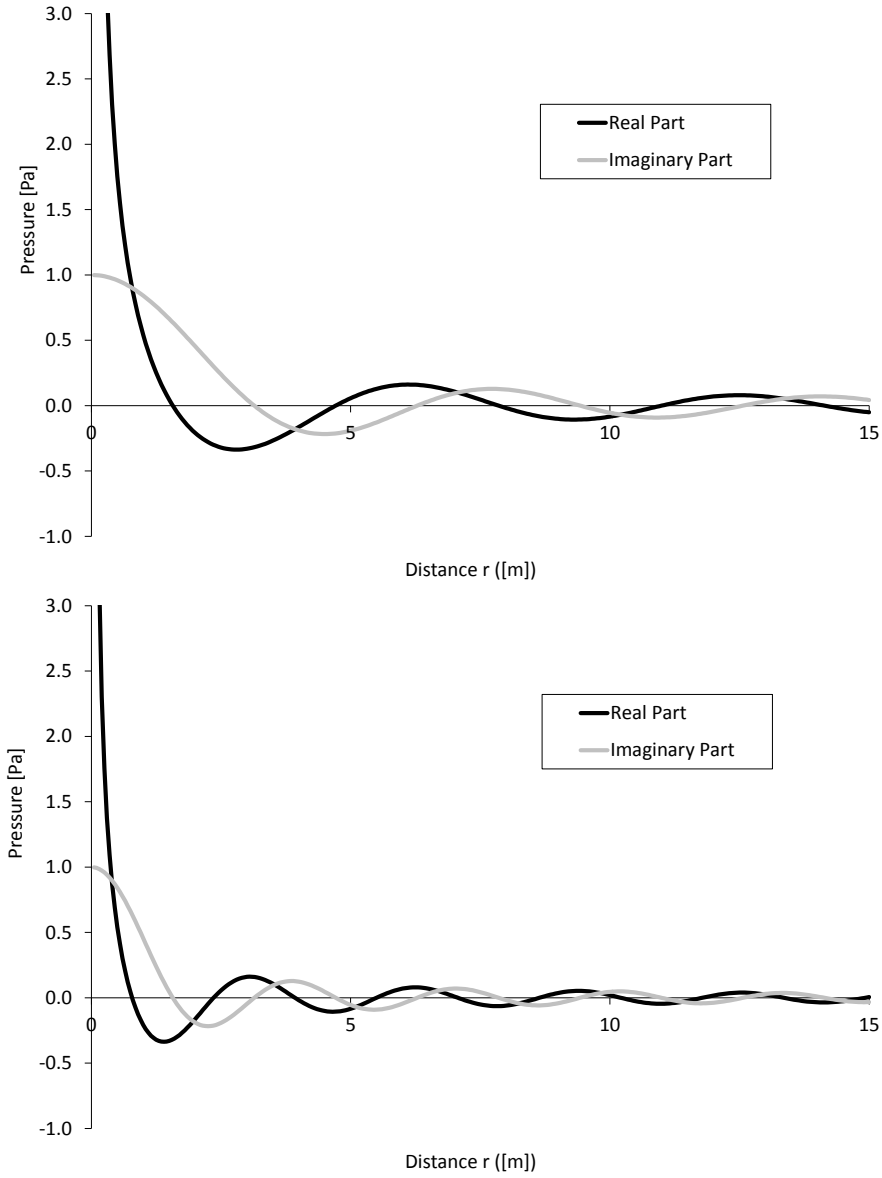

Figure 6.5: Radial variation of the real and imaginary parts of the acoustic pressure induced by a monopole. Graphs are shown for two different values of the wave number ($k = 1$ and $k = 2$).

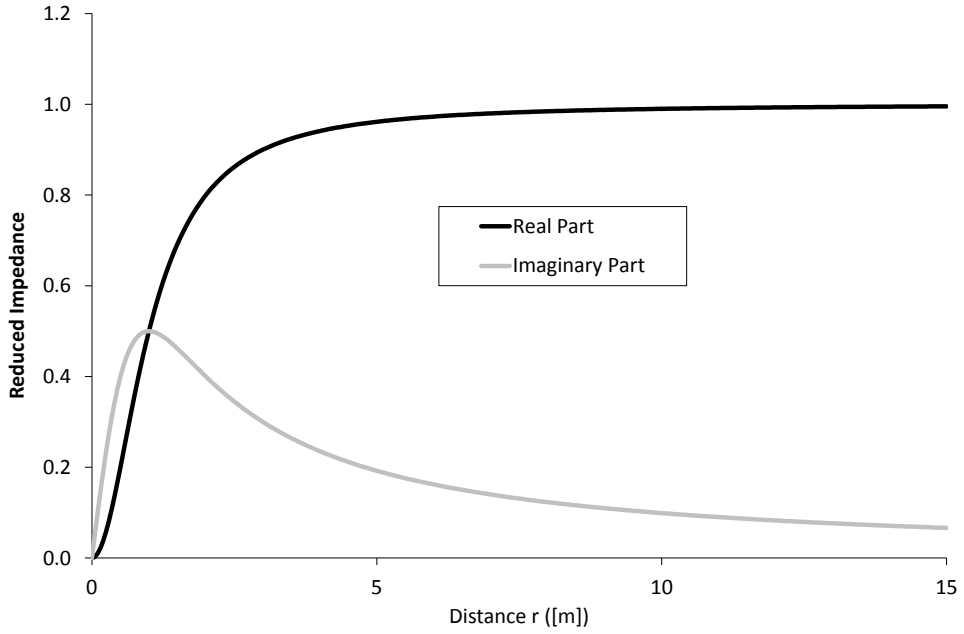

Figure 6.6: Radial variation of the real and imaginary parts of the radial impedance in the acoustic field induced by a monopole.

6.6.2 Volume flow of a source

Consider a pulsating sphere vibrating with a uniform normal velocity v. Let a be the radius of the sphere. The acoustic field induced by these vibrations is spherically symmetric:

$$p\left(r,\omega\right) = A\frac{e^{-ikr}}{r} \tag{6.53}$$

Acoustic velocity in $r = a$ must be equal to v:

$$v = A\frac{1}{\rho c}\frac{1+ika}{ika}\frac{e^{-ika}}{a} \tag{6.54}$$

This provides a relationship between A and v, from which we obtain:

$$p\left(r,\omega\right) = \frac{i\rho\omega v a^2}{1+ika}\frac{e^{-ik(r-a)}}{r} \tag{6.55}$$

When a tends to 0 while keeping the product $4\pi a^2 v$ constant and equal to q, which we define as the *volume flow* of the source, we find:

$$p\left(r,\omega\right) = i\rho\omega q\frac{e^{-ikr}}{4\pi r} \tag{6.56}$$

The amplitude $F(\omega)$ and volume flow $q(\omega)$ of a point source are therefore linked by:

$$p\left(r,\omega\right) = F\left(\omega\right)\frac{e^{-ikr}}{r} \Leftrightarrow p\left(r,\omega\right) = i\rho\omega q\left(\omega\right)\frac{e^{-ikr}}{4\pi r} \tag{6.57}$$

$$q\left(\omega\right) = \frac{4\pi F\left(\omega\right)}{i\rho\omega} \tag{6.58}$$

7

Sound levels

When one door closes, another door opens; but we so often look so long and regretfully upon the closed door that we do not see the one which has opened for us.
— **Alexander Graham Bell** (1847-1922)

Contents

7.1 The decibel scale 108
7.2 Adding levels 114
7.3 Octaves and third-octaves 117
7.4 Corrected and cumulative levels 123

7.1 The decibel scale

7.1.1 Definition

The relative power of two sources is often described by a *level difference* measured in decibels.[1] If the sources are respectively characterised by powers P_1 and P_2, their *relative* power level in decibels is given by:

$$L_2 - L_1 = 10 \log \frac{P_2}{P_1} \tag{7.1}$$

We can also define an *absolute* power level by introducing a *conventional* reference power P_{ref}. The *level* of a power source P is then given by :

$$L = 10 \log \frac{P}{P_{ref}} \tag{7.2}$$

In acoustics, we measure the sound level at a given point by comparing the sound intensity at that point with a reference intensity ($I_{ref} = 10^{-12}$ W/m^2):

$$L_I = 10 \log \frac{I}{I_{ref}} \tag{7.3}$$

But sound intensity can always be written in the form (Equation 6.21):

$$I = p_{RMS}^2 \frac{Z_r}{|Z|^2} \tag{7.4}$$

From which we derive a definition of the sound level in terms of acoustic pressure amplitude :

$$L_p = 20 \log \frac{p_{RMS}}{p_{ref}} = 20 \log \frac{p}{\sqrt{2} p_{ref}} \tag{7.5}$$

[1] The decibel, or tenth of Bel, is a non-standard unit named in honour of **Alexander Graham Bell**. Bell, who was born in Edinburgh in 1847 and died in Beinn Breagh (Canada) in 1922, is known for his invention of the telephone (1876), but also for numerous contributions to phonology.

where the reference pressure p_{ref} is of $2.10^{-5}Pa$ in air and $1\mu Pa$ in water. We easily see that:

- doubling pressure leads to an increase of the sound pressure level by 6 dB ($20\log 2 = 6$);
- doubling intensity leads to an increase of the sound intensity level by 3 dB ($10\log 2 = 3$).

In air, and for a plane wave of unit amplitude, the sound pressure level L_p is:

$$L_p = 20\log\frac{p}{\sqrt{2}p_{ref}} = 20\log\frac{1}{\sqrt{2}\times 2\cdot 10^{-5}} = 90.97\ dB \tag{7.6}$$

While the intensity of a plane wave is the square of the pressure amplitude divided by $2\rho c$ (Equation 6.29) so that the intensity level is:

$$L_I = 10\log\frac{I}{I_{ref}} = 10\log\frac{\frac{1^2}{2\cdot 1.225\cdot 340}}{10^{-12}} = 90.79\ dB \tag{7.7}$$

L_p and L_I are therefore nearly identical for a plane wave in air. In all other cases L_p and L_I will have different values. The intensity level can be seen as the cause of the sound field, while the pressure level measures the effect associated with this cause. The two levels are connected by the local acoustic impedance.

The levels associated with various typical noise sources are given in Figures 7.2 and 7.3.

Note: Sound level is associated with the sound spectrum and not with the sound signal. We cannot calculate the *instantaneous level* of a sound. Sound level is associated with sound intensity which is a quantity averaged over a cycle. A time-dependent sound level can however be calculated on the basis of successive short samples from a longer signal.

Media	Quantity	Reference value	Unit
Gas	Sound pressure	$2 \cdot 10^{-5}$	[Pa]
Liquid	Sound pressure	10^{-6}	[Pa]
Any media	Sound intensity	10^{-12}	$[W/m^2]$
Solid	Force	10^{-6}	$[N]$
Any media	Displacement	must be specified	$[m]$
Any media	Speed	10^{-9}	$[m/s]$
Any media	Acceleration	10^{-6}	$[m/s^2]$

Figure 7.1: Reference values for different physical quantities.

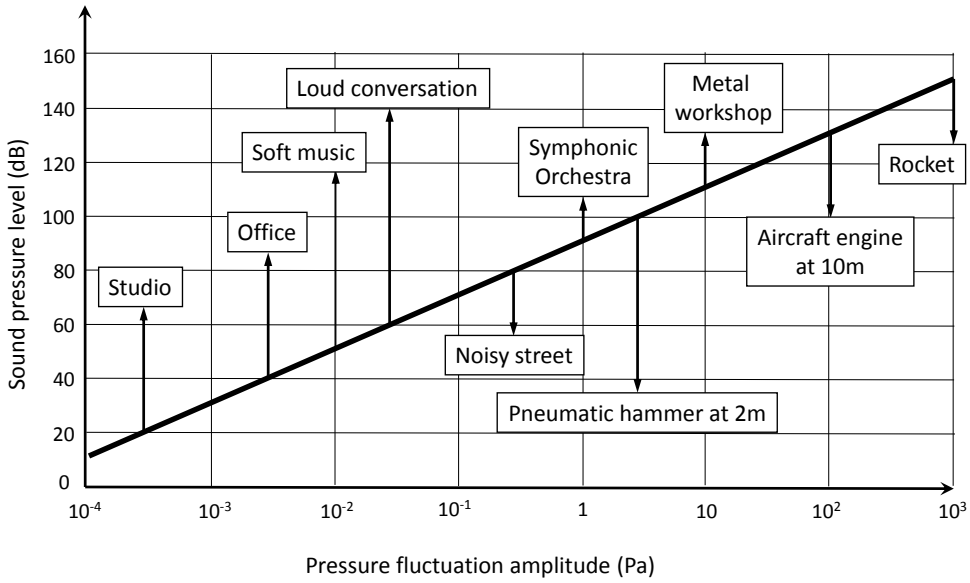

Figure 7.2: Relationship between sound pressure and sound pressure level with examples of characteristic sound levels.

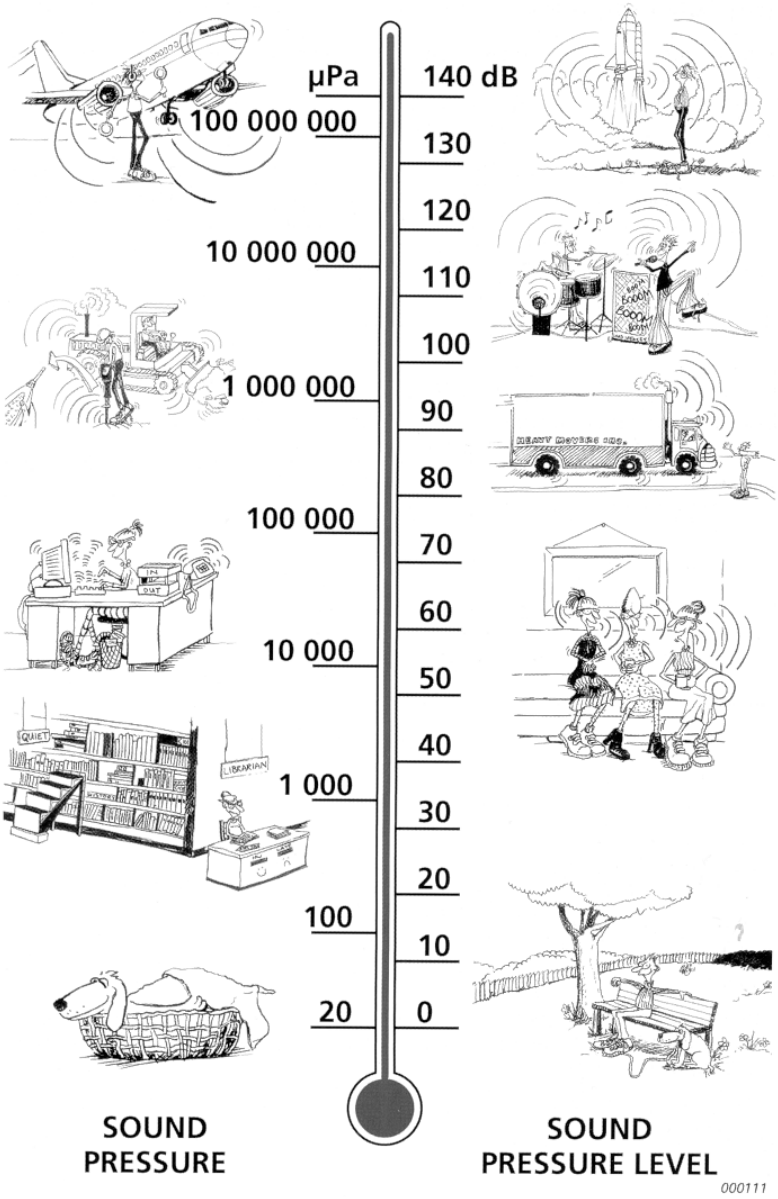

Figure 7.3: Relationship between sound pressure and sound pressure level with examples of characteristic sound levels.

7.1.2 Weber and Fechner laws

Logarithmic scale is used for sound levels due to the necessity to compress the scale of acoustic pressure. Pressure values associated with audible sounds indeed extend across eight orders of magnitude (10^{-5} to 10^{3} Pa). The logarithmic scale is also justified by the laws of Weber and Fechner:[2]

- **Weber** was interested in the lowest level L_2 that an individual is able to distinguish from a baseline level L_1. He observed that the difference $L_2 - L_1$ (called the *difference limen* or smallest perceptible level difference) is not constant, but proportional to L_1. Such behaviour is common when it comes to subjective perception. For example, an additional million dollars represents a radical change for the average individual, but has little impact for a multinational company whose turnover amounts to billions of dollars.
- **Fechner** formulated the hypothesis that a listener unconsciously estimates the perceived sound level by counting the difference limen i.e. by *integrating* the relative magnitudes $\frac{\Delta I}{I}$. This led him to conclude that the perceived level is proportional to the logarithm of the intensity (Figure 7.5).

The Weber and Fechner laws are first level approximations of the actual perception of sound by the human ear which is in fact much more complex[3].

[2] **Ernst Heinrich Weber** (1795-1878), a German physiologist and psychologist, is known as the founder of experimental psychology. He was a professor at the University of Leipzig from 1821 until 1871. **Gustav Fechner** (1801-1887), a German philosopher and physicist, is known as the father of psycho-physics.

[3] For an accessible discussion giving a thorough description of sound perception, see **William Morris Hartmann**, *Signal, Sound, sensation*, AIP Press, 1997.

Figure 7.4: Ernst Heinrich Weber and Gustav Fechner.

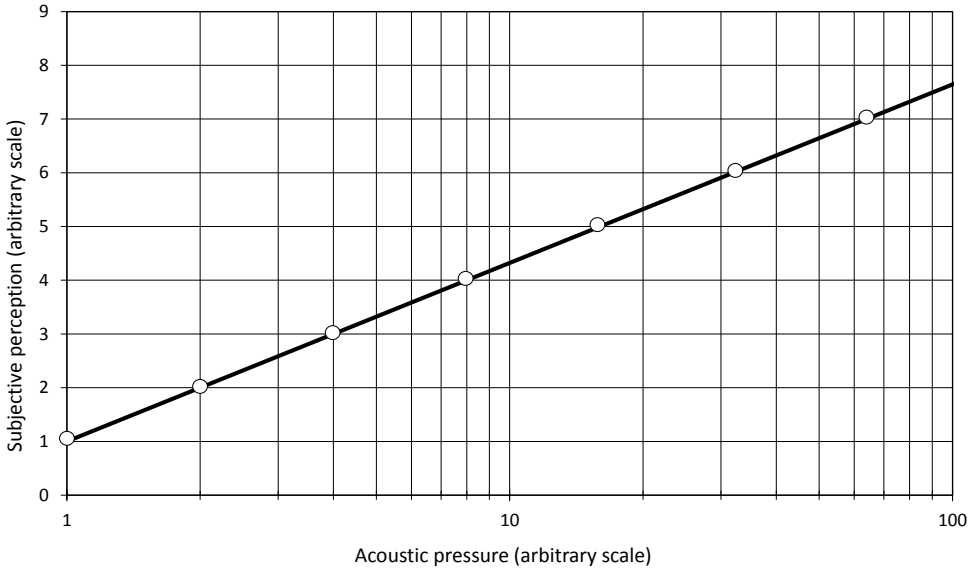

Figure 7.5: Schematic representation of the Weber-Fechner law: if pressure amplitudes form a *geometric* sequence (p_0, $p_1 = p_0\delta$, $\ldots$ $p_n = p_0\delta^n$) then the sound pressure levels form an *arithmetic* sequence (L_0, $L_1 = L_0 + \Delta$, $\ldots$ $L_n = L_0 + n\Delta$).

7.2 Adding levels

7.2.1 General principle

Consider two sources A and B which induce, separately, at a given point, the levels L_A and L_B. The sound level induced at that same point by both sources acting simultaneously is calculated by considering that the two sources combine their **intensities**. Intensity being proportional to the square of the pressure (Equation 6.21) we obtain:

$$\begin{aligned} L_C &= L_A \oplus L_B \\ &= 10 \log \left(\frac{p_{Aeff}^2}{p_{ref}^2} + \frac{p_{Beff}^2}{p_{ref}^2} \right) \\ &= 10 \log \left(10^{\frac{L_A}{10}} + 10^{\frac{L_B}{10}} \right) \end{aligned} \tag{7.8}$$

We can express the total level as a function of the highest of the two levels (say L_A) and of the level difference $\Delta L = L_A - L_B$:

$$L_C = L_A \oplus L_B = 10 \log \left[10^{\frac{L_A}{10}} \left(1 + 10^{\frac{\Delta L}{10}} \right) \right] = L_A + 10 \log \left(1 + 10^{\frac{\Delta L}{10}} \right) \tag{7.9}$$

The last term, which gives a correction to be added to level L_A to find L_C, is graphically depicted on Figure 7.6. As an example, we see that the combination of two identical levels ($\Delta L = 0$) adds 3 dB to this level (Figure 7.7):

$$L_A \oplus L_A = L_A + 3 \; dB \tag{7.10}$$

Figure 7.7 is correct because the sound of the two lawn-mowers is not coherent. If the two sources were perfectly identical in amplitude and phase, the resulting pressure would have been doubled and the sound level raised by $20 \log 2 = 6$ dB. If both sources were exactly in opposition of phase, the resulting pressure would be zero and the combined level $-\infty$ dB.

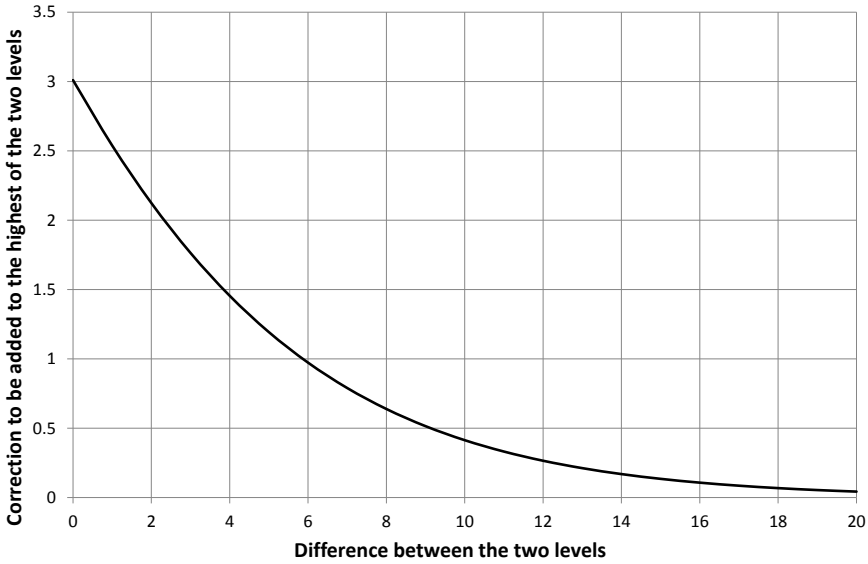

Figure 7.6: Diagram giving the correction to apply to the highest of two levels to calculate their sum based on their difference.

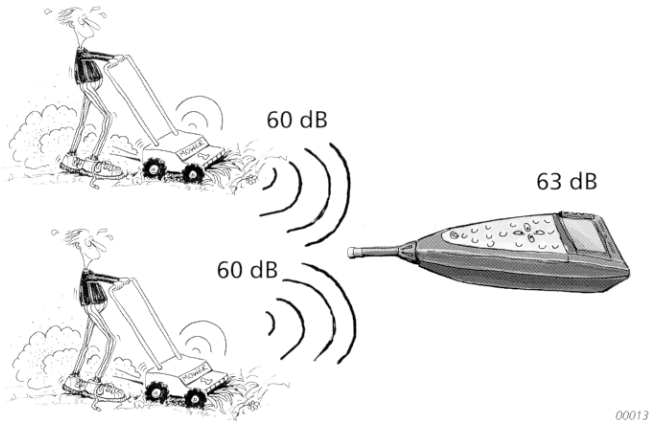

Figure 7.7: Two sources of equal intensity generate together a sound pressure level that is 3dB higher than the sound pressure level of a single source.

7.2.2 Masking

When two sources have very different sound levels, only the dominant source is really perceptible (the correction ΔL tends to zero when the level difference increases). This *masking effect* by which the dominant source hides other sources is a key practical issue in acoustics. Consider a hypothetical machine featuring three noise sources A, B and C ($L_A = 80$ dB, $L_B = 75$ dB and $L_C = 73$ dB). The total level is 81.8 dB. Naive engineers given the task of reducing noise might focus their efforts on the main source. Suppose they manage to lower source A from 80 to 70 dB. The result would be disappointing because the total sound level is only 4 dB lower ($(70 \oplus 75 \oplus 73 = 77.9$ dB). A better approach would consist in acting on source A until it reaches the level of source B and then to reduce A and B simultaneously. Finally, when A and B reach the level of C, all three sources should be lowered simultaneously.

L_A	$L_A \oplus L_B \oplus L_C$	Marginal gain
80	81.81	
79	81.17	-0.63
78	80.59	-0.58
77	80.07	-0.52
76	79.61	-0.46
75	79.20	-0.41
74	78.85	-0.35
73	78.54	-0.30
72	78.29	-0.26
71	78.07	-0.22
70	77.89	-0.18

This game of hide-and-seek where every improvement on any source reveals another source is typical in automotive and aerospace engineering. For a long time, automotive engineers were preoccupied with engine noise. Now that substantial progress has been achieved, rolling noise has become the major concern. Once rolling noise is under control, wind noise will become the main issue. Aircraft jet engines provide another example. Modern bypass engines are characterised by high *bypass ratio* (ratio between the total air flow

and the fraction passing through the combustion chamber) to reduce average ejection speed and jet noise. The strategy has paid off and jet noise has been significantly reduced ... and fan noise is now the predominant source!

7.3 Octaves and third-octaves

The audible frequency range is often broken down into octave or third-octave bands (see Tables 7.9 and 7.10). According to the definition of a musical octave, the central frequency is doubled between one octave band and the next. The central frequencies of a third-octave band and the next are in a ratio of $\sqrt[3]{2}$. The ISO standard rounds off the frequency values defining the bands. With this rounding-off, the decade value of central frequencies ($10 \log_{10} f_c$) are integers (see last column of Table 7.10) providing a natural numbering for the bands. For instance, the third-octave band centered on 10 kHz carries the number 40.

7.3.1 Band level

The sound level in a given frequency band is obtained by calculating the total energy of the acoustic signal in this frequency band. If the spectrum is continuous, the band level is calculated by integrating the spectrum in the band. If the spectrum is discrete, the band level is the sum of the quadratic pressures of each tone in the band. The spectrum $P(\omega)$ is called the *narrow band spectrum*, while the histogram representing the levels in each frequency band is called the *octave or third-octave band spectrum*. In practice, a band-pass filter (Figure 7.8) is applied to the spectrum before calculating the band-level. This filter, which is continuous and infinitely differentiable, avoids a brutal truncation on both sides of the band. A tonal component close to a band's bounding frequency will therefore partly contribute to both bands.

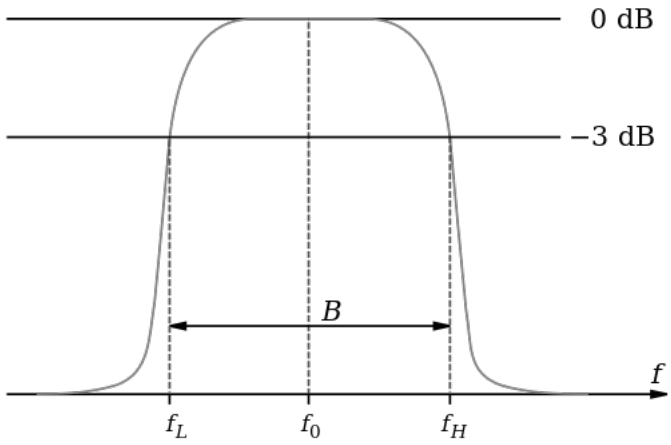

Figure 7.8: Band-pass filter.

Standardised octave bands			
Number	f_{center}	f_{min}	f_{max}
1	16	0	22.4
2	31.5	22.4	45
3	63	45	90
4	125	90	180
5	250	180	355
6	500	355	710
7	1.000	710	1.400
8	2.000	1.400	2.800
9	4.000	2.800	5.600
10	8.000	5.600	11.200
11	16.000	11.200	22.400
12	31.500	22.400	-

Figure 7.9: Normalised definition of octave bands.

Normalised third-octave bands				
Number	f_{center}	f_{min}	f_{max}	$10 \log_{10} f_c$
1	16	-	18	12.0
2	20	18	22.4	13.0
3	25	22.4	28	14.0
4	31.5	28	35.5	15.0
5	40	35.5	45	16.0
6	50	45	56	17.0
7	63	56	71	18.0
8	80	71	90	19.0
9	100	90	112	20.0
10	125	112	140	21.0
11	160	140	180	22.0
12	200	180	224	23.0
13	250	224	280	24.0
14	315	280	355	25.0
15	400	355	450	26.0
16	500	450	560	27.0
17	630	560	710	28.0
18	800	710	900	29.0
19	1.000	900	1.120	30.0
20	1.250	1.120	1.400	31.0
21	1.600	1.400	1.800	32.0
22	2.000	1.800	2.240	33.0
23	2.500	2.240	2.800	34.0
24	3.150	2.800	3.550	35.0
25	4.000	3.550	4.500	36.0
26	5.000	4.500	5.600	37.0
27	6.300	5.600	7.100	38.0
28	8.000	7.100	9.000	39.0
29	10.000	9.000	11.200	40.0
30	12.500	11.200	14.000	41.0
31	16.000	14.000	18.000	42.0
32	20.000	18.000	22.400	43.0
33	25.000	22.400	28.000	44.0
34	31.500	28.000	-	45.0

Figure 7.10: Normalised definition of third-octave bands.

7.3.2 White, pink and brown noise

White noise is characterised by a constant narrow-band spectrum (Figure 7.11). The level in octave band $n-1$ is 3 dB lower than that in band n, which is twice as wide. Pink noise has a narrow-band spectrum that decreases with frequency ($\frac{1}{f}$) so that the octave band level is constant. Brown noise[4] is characterised by a steeper decrease (typically $\frac{1}{f^2}$). The spectrum of synthetic signals approaching white, pink and brown noise are displayed in Figures 7.12, 7.13 and 7.14.

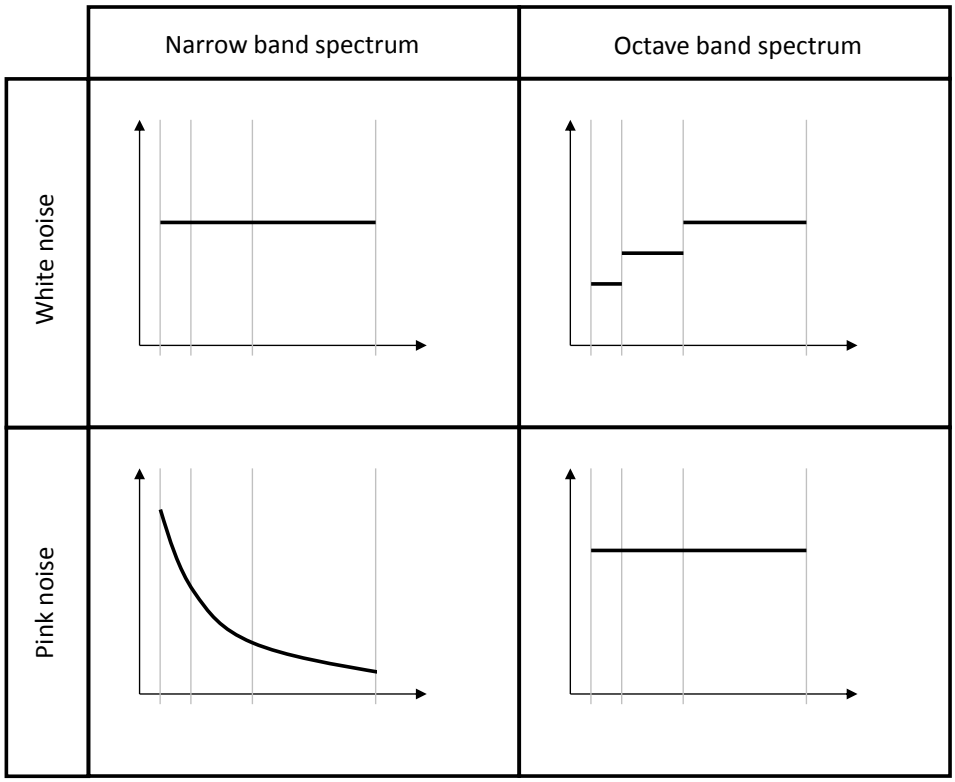

Figure 7.11: Narrow band and octave band spectra of white and pink noise.

[4] *Brown* does not refer to a colour, but to the *brownian* motion, named after the Scottish botanist Robert Brown (1773-1858), whose random behaviour is characterised by a quadratic decrease of the power spectral density with frequency.

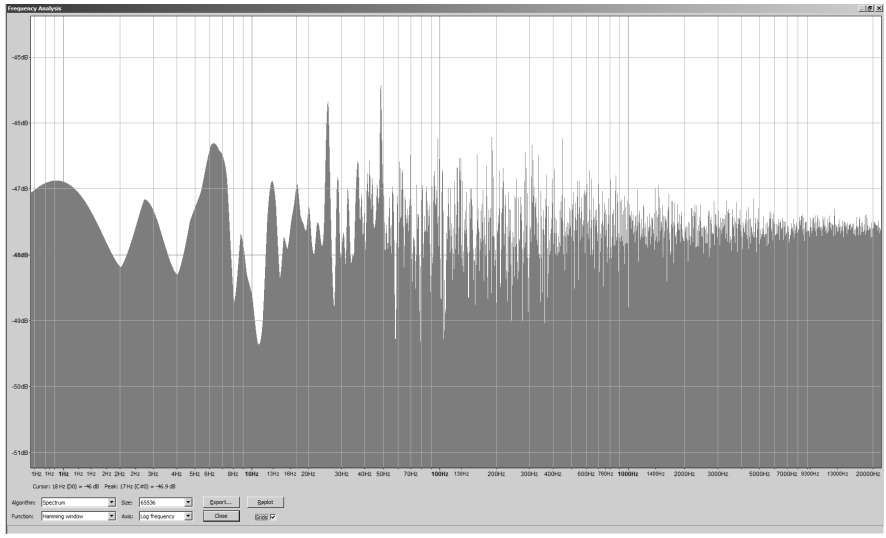

Figure 7.12: Narrow-band spectrum of a synthetic signal approaching white noise.

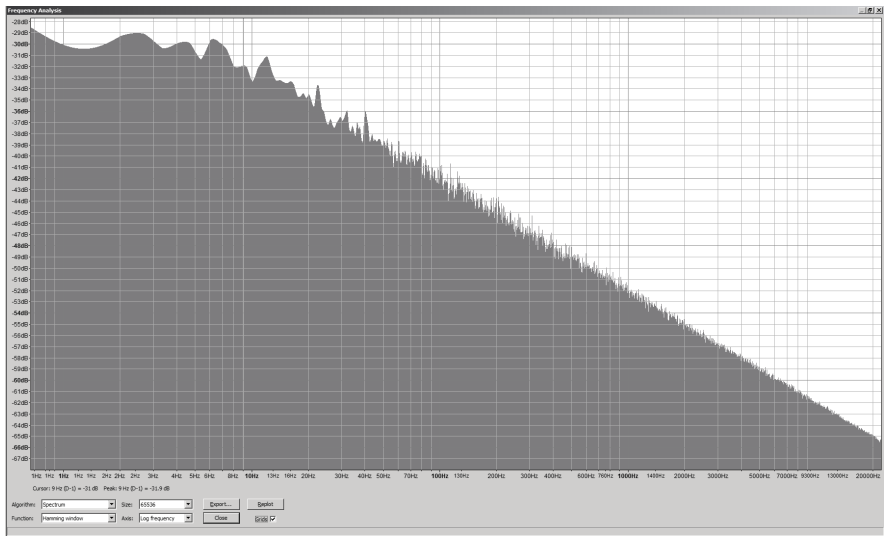

Figure 7.13: Narrow-band spectrum of a synthetic signal approaching pink noise.

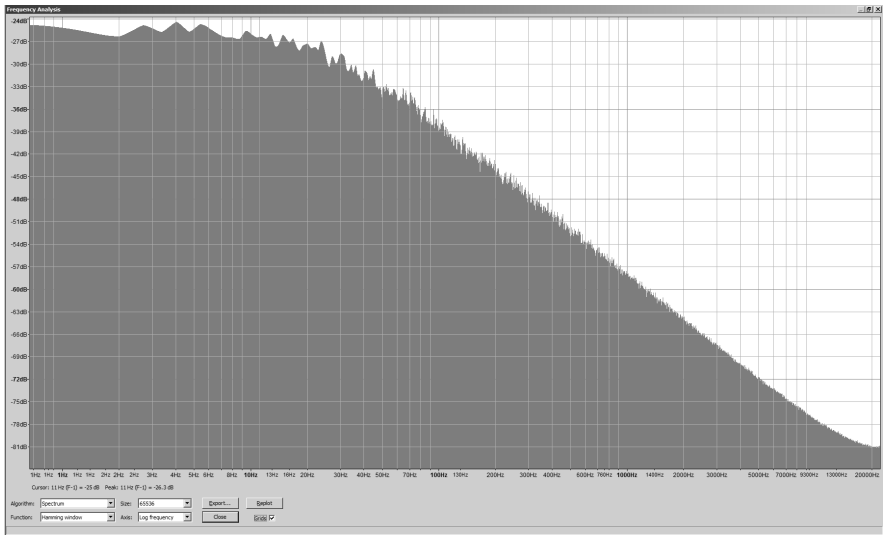

Figure 7.14: Narrow-band spectrum of a synthetic signal approaching brown noise.

7.4 Corrected and cumulative levels

Loudness measures the strength of an auditory sensation. Although the choice of a logarithmic scale for the sound level is partially based on psychophysiological motivations (Weber-Fechner's law), experiments show that loudness and level are not identical. This section will describe several measures of loudness:

- dbA and related filtered levels;
- equivalent levels;
- EPNdB level;
- NR indicator.

7.4.1 Fletcher and Munson curves

The fact that the ear is not equally sensitive to all frequencies has been highlighted in many experiments. Fletcher and Munson[5] used the following experimental protocol in their pioneering work:

- participants listen to a reference tone (frequency 1 kHz, level L) and then to a tone of different frequency;
- the level of the second tone is then adjusted until it appears to have the same subjective level as the reference tone.

When carried out on many participants across all audible frequencies and at various reference levels, curves of equal *loudness*, graduated in phones, are obtained (Figure 7.15). The main characteristics of these curves are:

- low sensitivity of the ear at low and high-frequency;

[5] **Fletcher H., Munson W.A.**. *Loudness, its definition, measurement and calculation.* J.Acoust.Soc.Am. 5 (1933), pp.82-108.

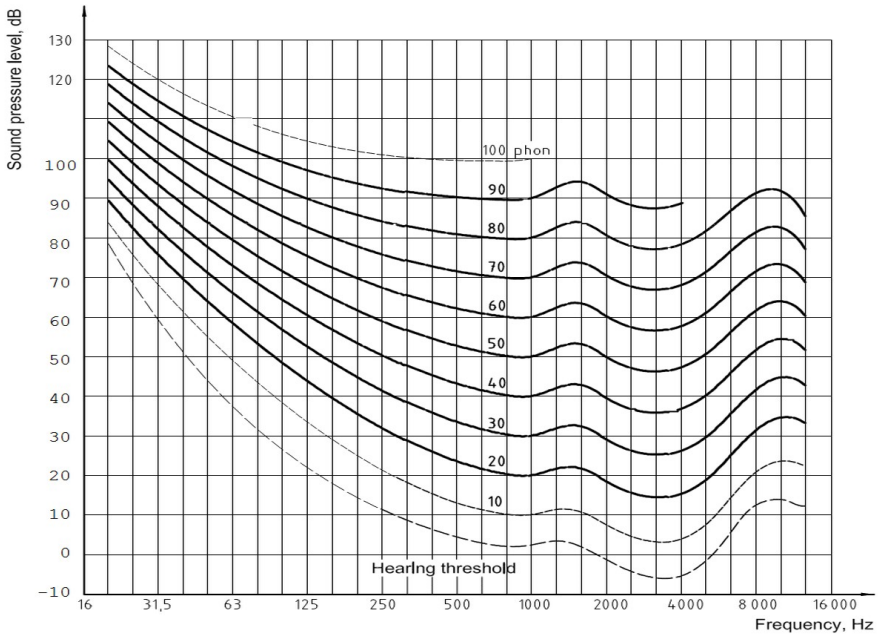

Figure 7.15: Curves of equal loudness as defined by the ISO226-2003 standard.

- maximum sensitivity between 3 and 4 kHz corresponding to a quarter-wavelength resonance of the ear canal ($f = 3.400\ Hz \rightarrow \lambda/4 = 2.5cm$, see Section 10.2.4);

- flattening of the loudness curves when the reference level increases;

- the sound level in dB and the loudness in phones coincide at 1 kHz which was chosen as the reference frequency.

The artificial nature of the experimental protocol has been widely criticised. The ear and the brain indeed react quite differently to pure and continuous tones as opposed to complex, multi-frequency, time-varying sounds.

7.4.2 Filters

Noise measuring devices (sound-level meters) are generally equipped with filters tagged A, B, C, D and U. The specification of filters A, B, C and D is given in Figure 7.16 and filters A, C and U in Figure 7.17. Filters A, B and C approximate the Fletcher and Munson curves for 40, 70 and 100 dB. Filter D was originally developed for the specific needs of airport nuisance, but is now usually replaced by the EPNdB levels (Section 7.4.5). Filter U was introduced recently for measuring audible sounds in the presence of ultrasound. It can be combined with the A filter to form the AU filter. Today the A filter, in spite of obvious shortcomings, is very widely used in environmental acoustics. The A filter is formally defined as follows:

$$A(f) = \frac{12200^2 f^4}{(f^2 + 20.6^2)(f^2 + 12200^2)\sqrt{(f^2 + 107.7^2)(f^2 + 737.9^2)}} \tag{7.11}$$

where f is the frequency in Hz. The correction in dB is therefore given by (no correction at 1,000 Hz):

$$20 \log \left(\frac{A(f)}{A(1000)} \right) \tag{7.12}$$

The same applies for the other filters:

$$B(f) = \frac{12200^2 f^3}{(f^2 + 20.6^2)(f^2 + 12200^2)\sqrt{(f^2 + 158.5^2)}} \tag{7.13}$$

$$C(f) = \frac{12200^2 f^2}{(f^2 + 20.6^2)(f^2 + 12200^2)} \tag{7.14}$$

$$D(f) = \frac{f}{6.89669 \cdot 10^{-5}} \sqrt{\frac{h(f)}{(f^2 + 79919.29^2)(f^2 + 1345600)}} \tag{7.15}$$

where, in the last expression, $h(f)$ is defined by:

$$h(f) = \frac{(1037918.48 - f^2)^2 + 1080768.16 f^2}{(9837328 - f^2)^2 + 11723776 f^2} \tag{7.16}$$

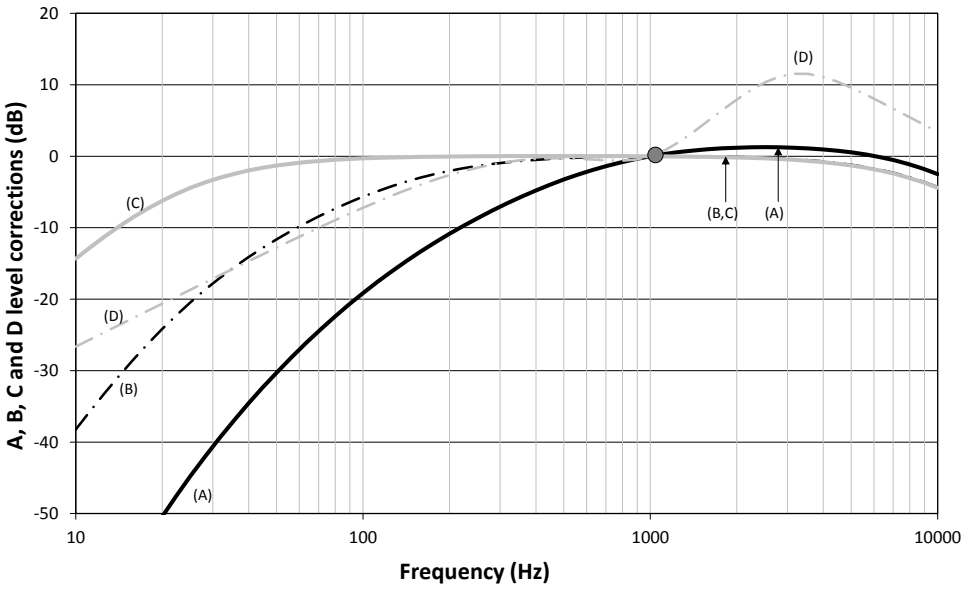

Figure 7.16: Correction to be applied to the dB level to obtain the dBA, dBB, dBC or dBD levels.

The correction functions defined above are in fact filters to which an impulse response can be associated. Applying the A-filter to a time signal $p(t)$ therefore yields the filtered signal $p_A(t)$:

$$p_A(t) = \int_{-\infty}^{\infty} p(\tau) \cdot a(t-\tau) \cdot d\tau \;\; with \;\; a(t) = \frac{1}{2\pi} \int_{-\infty}^{\infty} A(\omega) e^{i\omega t} d\omega \qquad (7.17)$$

Conventional Freq. [Hz]	Exact Freq. [Hz]	Correction A [dB]	Correction C [dB]	Correction U [dB]
10	10.00	-70.4	-14.3	0.0
12.5	12.59	-63.4	-11.2	0.0
16	15.85	-56.7	- 8.5	0.0
20	19.95	-50.5	- 6.2	0.0
25	25.12	-44.7	- 4.4	0.0
31.5	31.62	-39.4	- 3.0	0.0
40	39.81	-34.6	- 2.0	0.0
50	50.12	-30.2	- 1.3	0.0
63	63.10	-26.2	- 0.8	0.0
80	79.43	-22.5	- 0.5	0.0
100	100.00	-19.1	- 0.3	0.0
125	125.90	-16.1	- 0.2	0.0
160	158.50	-13.4	- 0.1	0.0
200	199.50	-10.9	0.0	0.0
250	251.20	- 8.6	0.0	0.0
315	316.20	- 6.6	0.0	0.0
400	398.10	- 4.8	0.0	0.0
500	501.20	- 3.2	0.0	0.0
630	631.00	- 1.9	0.0	0.0
800	794.30	- 0.8	0.0	0.0
1,000	1000.00	0.0	0.0	0.0
1,250	1259.00	+ 0.6	0.0	0.0
1,600	1585.00	+ 1.0	- 0.1	0.0
2,000	1995.00	+ 1.2	- 0.2	0.0
2,500	2512.00	+ 1.3	- 0.3	0.0
3,150	3162.00	+ 1.2	- 0.5	0.0
4,000	3981.00	+ 1.0	- 0.8	0.0
5,000	5012.00	+ 0.5	- 1.3	0.0
6,300	6310.00	- 0.1	- 2.0	0.0
8,000	7943.00	- 1.1	- 3.0	0.0
10,000	10000.00	- 2.5	- 4.4	0.0
12,500	12590.00	- 4.3	- 6.2	- 2.8
16,000	15850.00	- 6.6	- 8.5	-13.0
20,000	19950.00	- 9.3	-11.2	-25.3

Figure 7.17: Correction factors associated with A, C and U filters.

7.4.3 Equivalent and statistical levels

The *instantaneous* level, calculated using the spectrum of a short recording, is not representative of the nuisance experienced by an individual subjected to a sound of variable amplitude during a long period. The equivalent noise level $L_{eq}(T)$ is the level of a continuous signal which, within a certain duration T, contains the same energy as the fluctuating signal:

$$L_{eq}(T) = 10 \cdot log \int_0^T \frac{p_{RMS}^2}{p_{ref}^2} dt \tag{7.18}$$

Some remarks:

- The equivalent level is a characteristic of the overall time signal and is not related to a specific frequency band. An equivalent level by frequency band can be obtained by filtering the signal using the appropriate band-filter.
- The equivalent level is often expressed in dBA. This requires the preliminary filtering of the temporal signal by the A-filter.
- The duration of the reference period T can vary from a fraction of a second to a year. Standard durations include $t_{slow} = 1s$, $t_{fast} = 0.125s$ and $t_{peak} = 0.035s$.

The L_{Amax} level is defined as the maximum of $L_{Aeq}(t_{slow})$ over a duration $T \gg t_{slow}$. Statistical level L_{AN} is the level exceeded during N percent of the measurement time. Statistical levels in common use are L_{A10} (*average maximum noise level*) and L_{A90} (*minimum average background noise level*). These equivalent and statistical levels are highlighted in Figure 7.18 on an urban noise recording sample.

7.4.4 L_{den}

The European Union has defined a weighted equivalent level that is now used throughout Europe to characterise long-term sound environments. This level,

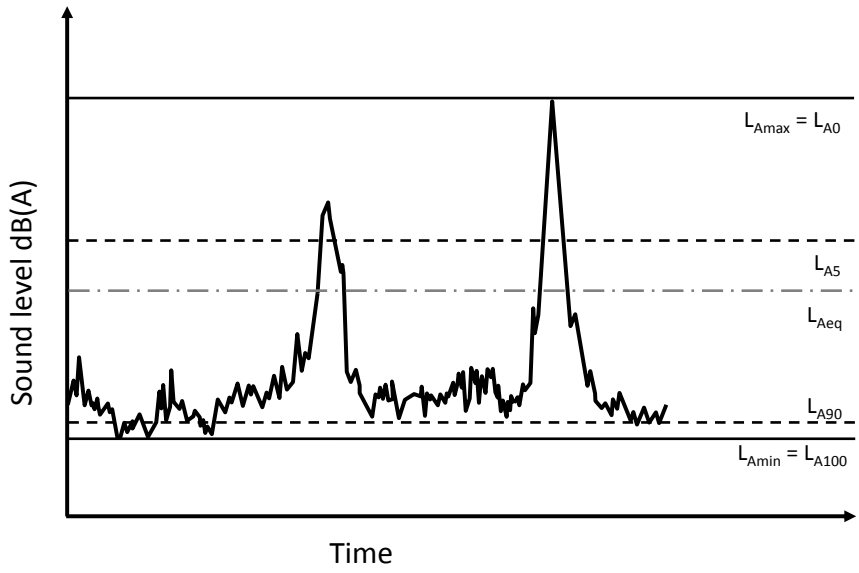

Figure 7.18: Equivalent and statistical levels.

called L_{den} (for *day, evening, night*) is calculated as follows:

$$L_{den} = 10log\frac{12 \cdot 10^{\frac{L_{AD}}{10}} + 4 \cdot 10^{\frac{L_{AE}+5}{10}} + 8 \cdot 10^{\frac{L_{AN}+10}{10}}}{24} \tag{7.19}$$

where L_{AD}, L_{AE}, L_{AN} are the continuous equivalent level measured in dBA over a full year between, respectively, 7AM and 7PM (D=day), 7PM and 11PM (E=evening) and 11PM and 7AM (N=night). The logic behind the definition of L_{den} is the following:

- the equivalent level measured during one of the three periods is weighted by the duration of this period.

- the equivalent level measured in the evening is increased by 5 dB and that of the night by 10 dBn as the subjective nuisance is considered to be higher at these times of day when subjective tolerance of noise is lower.

7.4.5 EPNdB

Airport noise is assessed using the EPNdB scale (for *Effective Perceived Noise Level*). The calculation method is not presented here.[6]

7.4.6 Noise Rating (NR)

The NR level (Noise Rating, ISO standard) is defined by a series of curves onto which the octave-band sound level spectrum is plotted (Figure 7.19). The NR rating is the highest NR curve touched by the octave-band spectrum. The NR-level is used in architectural acoustics to define acceptable levels according to type of use: NR 10-20 for audiometric measurements, 20-30 for classrooms, 30-40 for quiet offices, 60-70 for industrial premises.

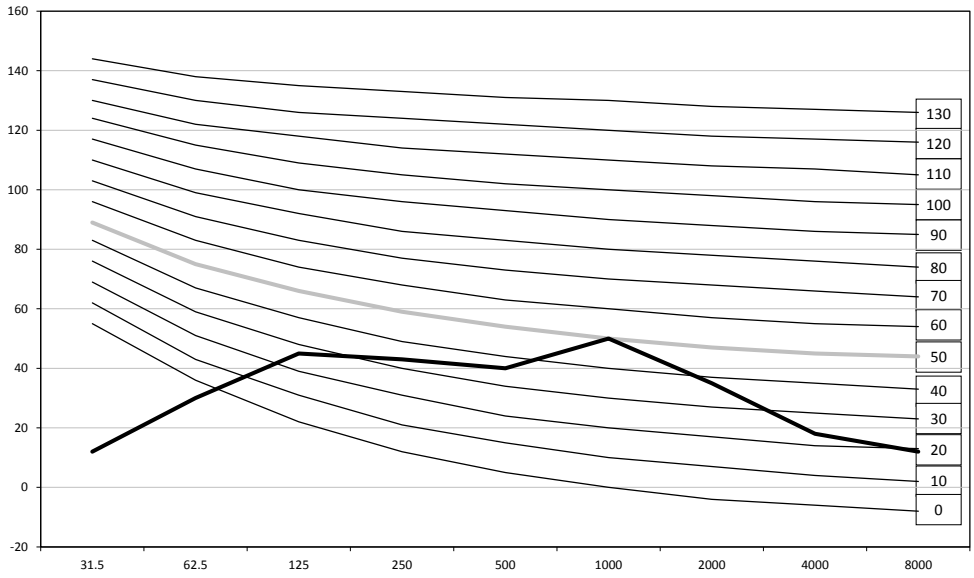

Figure 7.19: NR curves: the highest NR curve (grey lines) reached by the spectrum (bold black line) is NR50. The noise rating is therefore NR50.

[6]See *Federal Aviation Regulation, Part 3, Section A36.4.*

Part II

Fundamental phenomena
of linear acoustics

8

Reflection and absorption

His last word ran down the right row of tables to reach the landlady at her counter, from where it returned with new momentum, along the left row, before dying away at the door.
— **Marcel Aymé** (1902-1967), Brûlebois (1930).
Author's own translation from French to English.

Contents

8.1 Reflection under normal incidence 134
8.2 Reflection under oblique incidence 143
8.3 Reflection of a monopole source 147
8.4 Notes on the concept of impedance 162
8.5 Reverberation time 172

This chapter presents the physics of sound wave reflection and introduces the concept of absorption. The main principles of room acoustics are also covered.

8.1 Reflection under normal incidence

8.1.1 Rigid surface (zero velocity)

Time domain analysis

Equation 4.26 shows that, in the absence of sources, the pressure gradient is directly proportional to the acceleration of the fluid particles. At a fixed wall, this acceleration must be zero and so must the pressure gradient. The corresponding pressure field is a special case of the general one-dimensional solution:

$$p\left(x,t\right)=p^{+}\left(t-\frac{x}{c}\right)+p^{-}\left(t+\frac{x}{c}\right) \tag{8.1}$$

with the additional condition that:

$$\left(\frac{\partial p\left(x,t\right)}{\partial x}\right)_{x=x_0}=0 \tag{8.2}$$

The derivative of a symmetric function is antisymmetric. Therefore if we take p^{-} as the symmetric of p^{+} with respect to x_0, the derivative of $(p^{+}+p^{-})$ vanishes at $x=x_0$. The general solution of the one-dimensional wave equation in the presence of a perfectly rigid wall at $x=x_0$ is therefore (noting $p_i \doteq p^{+}=p^{-}$):

$$p\left(x,t\right)=p_i\left(t-\frac{x}{c}\right)+p_i\left(t+\frac{x-2x_0}{c}\right) \tag{8.3}$$

Or, if $x_0=0$:

$$p\left(x,t\right)=p_i\left(t-\frac{x}{c}\right)+p_i\left(t+\frac{x}{c}\right) \tag{8.4}$$

A particular case is shown in Figure 8.1 where we see an acoustical disturbance progressing towards the wall, hitting it and then coming back. In accordance with Equation 8.3, this solution can be analysed as the combination of two waves whose profiles are symmetrical with respect to $x = x_0$, one propagating from left to right and the other from right to left. When a wave hits a rigid wall, it is as though the incident wave were entering the wall while an image wave, perfectly symmetrical to the incident wave, were simultaneously leaving the wall.

Frequency domain analysis

Consider an incident wave propagating along the x axis, from left to right, towards a rigid plane (zero velocity condition) located at $x = 0$ (Figure 8.2). The one-dimensional acoustic pressure distribution is of the form:

$$p(x,\omega) = p^+(\omega)e^{-ikx} + p^-(\omega)e^{ikx} \tag{8.5}$$

Velocity is given by:

$$v_x(x,\omega) = \frac{p^+(\omega)}{\rho c}e^{-ikx} - \frac{p^-(\omega)}{\rho c}e^{ikx} \tag{8.6}$$

but since velocity must be zero at $x = 0$, we see that:

$$v_x(0,\omega) = \frac{p^+(\omega) - p^-(\omega)}{\rho c} = 0 \rightarrow p^+ = p^- \doteq p_i \tag{8.7}$$

from which we obtain:

$$p(x,\omega) = p_i(\omega)\left(e^{-ikx} + e^{ikx}\right) = 2p_i(\omega)\cos kx \tag{8.8}$$

which is indeed the Fourier transform of Equation 8.4. Velocity is finally given by:

$$v_x(x,\omega) = \frac{p_i}{\rho c}\left(e^{-ikx} - e^{ikx}\right) = \frac{-2ip_i(\omega)}{\rho c}\sin kx \tag{8.9}$$

while acoustic impedance is given by:

$$Z_x(x,\omega) = \frac{p\,(x,\omega)}{v_x\,(x,\omega)} = i\rho c\frac{\cos kx}{\sin kx} \tag{8.10}$$

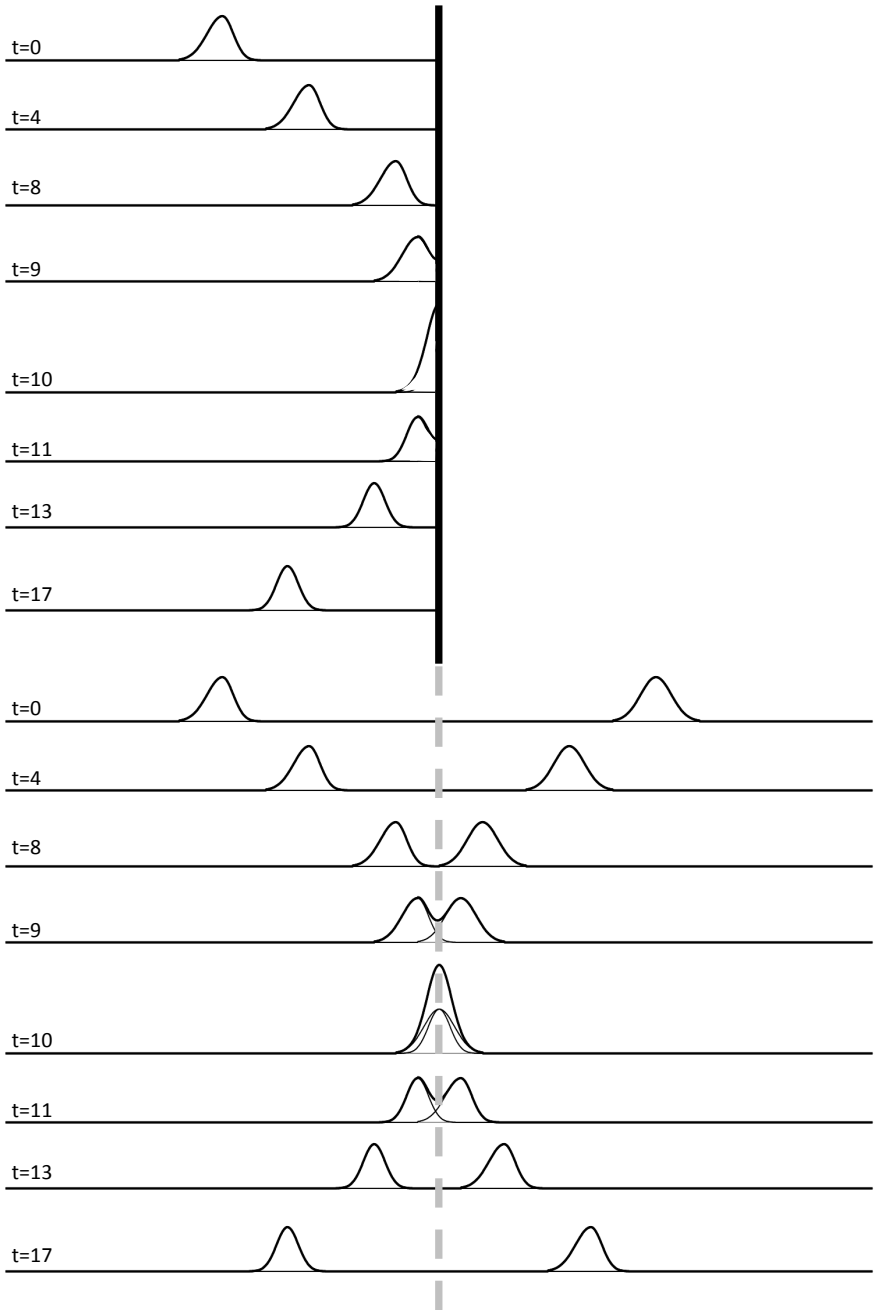

Figure 8.1: Reflection of a plane wave on a rigid wall (upper graph). The wall acts as a mirror, superimposing a reflected wave, symmetrical to the incident wave (lower graph).

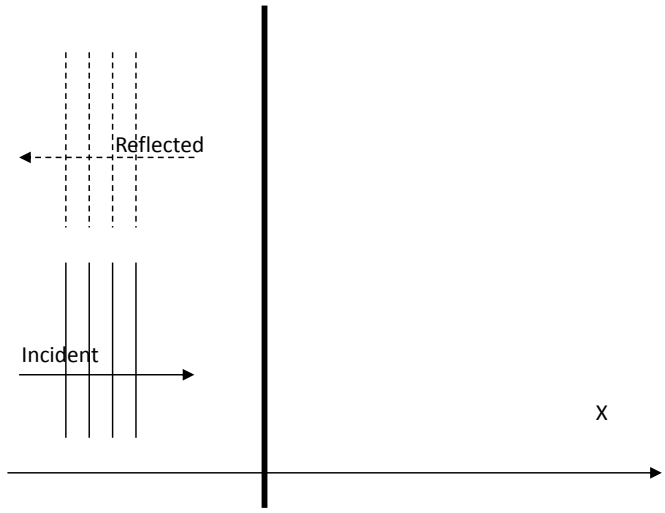

Figure 8.2: Reflection of a plane wave on a rigid surface (normal incidence).

The impedance value is *purely imaginary* because pressure and speed have a phase difference of 90°. Active intensity is zero because the intensity propagated from left to right by the incident wave is exactly equal to the intensity carried from right to left by the reflected wave: both waves combine to form a stationary wave. At the rigid surface, the acoustic pressure is double that of the incident wave:

$$p(0, \omega) = 2p_i(\omega) \tag{8.11}$$

Absorption, material thickness and wavelength

Energy dissipation in most absorbing materials is proportional to acoustic velocity. We have seen above that maximum velocity occurs a quarter of a wavelength away from the wall ($x = \lambda/4$). We can therefore draw the following intuitive conclusions:

1. A layer of absorbing material is efficient, at a given frequency, only if it is at least a quarter of a wavelength thick.

2. The efficiency of such materials depends on frequency: a 1 cm-thick carpet will, for instance, only be efficient above 8 kHz.

3. A thin layer of material at a distance $\lambda/4$ from the wall is more efficient than the same layer directly applied on the surface.

8.1.2 Free surface (zero pressure)

Time domain

Suppose we want to impose a zero pressure condition at $x = x_0$. The sum of any two **antisymmetrical** functions (with respect to $x = x_0$) is a general solution of this problem:

$$p\,(x,t) = p_i\left(t - \frac{x}{c}\right) - p_i\left(t + \frac{x - 2x_0}{c}\right) \tag{8.12}$$

A zero-pressure condition acts as an *anti-mirror* (Figure 8.3): it is as though an antisymmetrical image wave was overlapping with the original wave to guarantee that the zero-pressure condition is respected at the wall. A zero acoustic pressure condition is rarely met in practice. However, the free surface of a fluid is modelled by such a condition. The open end of a tube, like that of a flute, is also well approximated by a zero pressure condition provided that the wavelength is significantly larger than the diameter of the tube.

Frequency domain

The solution in the frequency domain is simply written as:

$$p(x,\omega) = p_i(\omega)\left(e^{-ikx} - e^{ikx}\right) = -2ip_i(\omega)\sin kx \tag{8.13}$$

The reflected wave has the same amplitude as the incident wave, but the two waves have a phase difference of π.

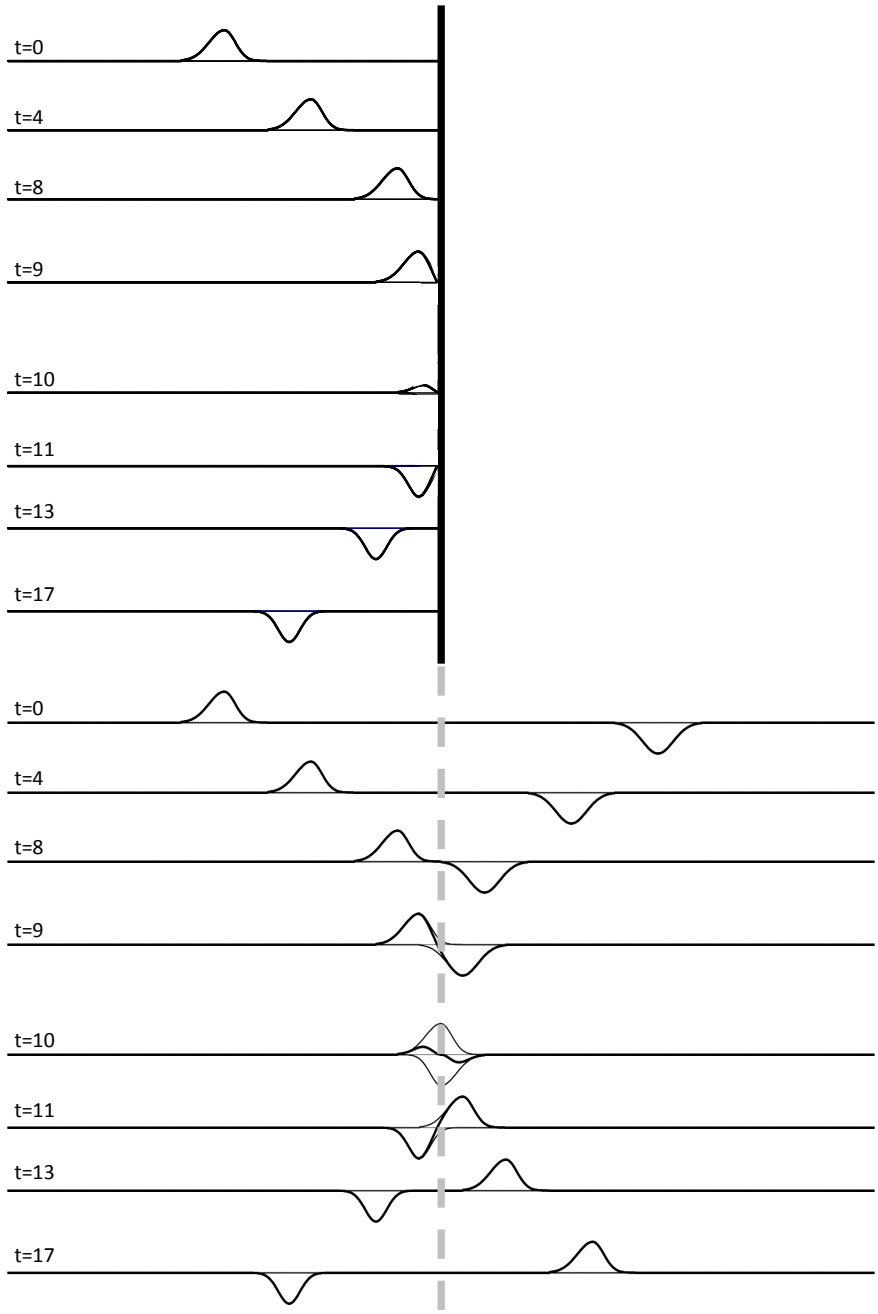

Figure 8.3: Reflection of a plane wave on a zero-pressure surface (upper graph). The surface acts as a mirror superimposing an antisymmetrical reflected wave to the incident wave (lower graph).

8.1.3 Absorbing surface

Frequency domain

Consider an intermediate case where the reflecting surface is partially absorbing. Our starting point is always the general one-dimensional solution:

$$p(x,\omega) = p^+(\omega)e^{-ikx} + p^-(\omega)e^{ikx} \tag{8.14}$$

Velocity at the wall is given by:

$$v_x(0,\omega) = \frac{p^+(\omega) - p^-(\omega)}{\rho c} \tag{8.15}$$

and pressure at the wall by:

$$p(0,\omega) = p^+(\omega) + p^-(\omega) \tag{8.16}$$

The impedance at the wall is the ratio of pressure to velocity:

$$Z(\omega) = \rho c \frac{p^+(\omega) + p^-(\omega)}{p^+(\omega) - p^-(\omega)} \tag{8.17}$$

Introducing the reflection factor $R(\omega)$:

$$R(\omega) = \frac{p^-(\omega)}{p^+(\omega)} \tag{8.18}$$

the impedance can be written as:

$$Z(\omega) = \rho c \frac{1 + R(\omega)}{1 - R(\omega)} \tag{8.19}$$

This relationship can be inverted to yield:

$$R(\omega) = \frac{Z(\omega) - \rho c}{Z(\omega) + \rho c} \tag{8.20}$$

The incident intensity is given by:

$$I_{inc} = \frac{|p^+(\omega)|^2}{2\rho c} \tag{8.21}$$

while the reflected intensity is given by

$$I_{ref} = \frac{|p^+(\omega)|^2 |R(\omega)|^2}{2\rho c} \tag{8.22}$$

The absorbed intensity is the difference between the incident and reflected intensity:

$$I_{abs} = I_{inc} - I_{ref} = \frac{|p^+(\omega)|^2 (1 - |R(\omega)|^2)}{2\rho c} \tag{8.23}$$

The ratio between absorbed and incident intensities defines the *absorption coefficient* α:

$$\alpha = \frac{I_{abs}}{I_{inc}} = 1 - |R(\omega)|^2 \tag{8.24}$$

while the ratio of reflected and incident intensities defines the coefficient of reflection r:

$$r = \frac{I_{ref}}{I_{inc}} = |R(\omega)|^2 = 1 - \alpha \tag{8.25}$$

Note that:

$$\alpha + r = 1 \tag{8.26}$$

Differences between Z_n, R, α and r

Partial reflection and absorption of an acoustic wave at the wall may be characterised by each of the following coefficients: normal impedance Z_n, reflection factor R, coefficient of absorption α, coefficient of reflection r. Impedance and reflection factor are *complex* quantities and represent the effect of the material covering the surface on both the amplitude and phase of the incident wave. The absorption and reflection coefficients are *real* quantities providing information about the intensity level of the reflected wave, but not about its phase.

Characteristic and reduced impedance

If the normal impedance of the surface is equal to ρc, the reflection factor R, the coefficient of reflection r and the reflected intensity are all equal to zero, while the coefficient of absorption α is equal to 1 and the absorbed intensity is equal to the incident intensity. Under normal incidence, a wave hitting a wall carrying this impedance is therefore completely absorbed. The impedance ρc is called the **characteristic impedance** of the medium. The impedance of a given material is often compared to this characteristic value and the reduced impedance coefficient z is defined as the ratio:

$$z = \frac{Z}{\rho c} \tag{8.27}$$

Time domain

Equation 8.14 can be rewritten:

$$p = p_i \left(e^{-ikx} + Re^{ikx} \right) \tag{8.28}$$

The time history of the pressure, at a given point, is obtained by taking the inverse Fourier transform of the above expression:

$$p(x,t) = p_i(t - \frac{x}{c}) + p_i(t + \frac{x}{c}) \otimes r(t + \frac{x}{c}) \tag{8.29}$$

where the symbol $\otimes$ indicates the convolution product and where $r(t)$ designates the impulse response of the reflection factor ($r(t) \Leftrightarrow R(\omega)$).

8.2 Reflection under oblique incidence

8.2.1 Rigid surface and Descartes law

Consider now a plane wave, of wave vector $(k_x, -k_y, 0)$, incident on a rigid plane $y = 0$ (Figure 8.4). The normal to the plane is conventionally defined as entering the plane and its components are $(0, -1, 0)$. The incident wave interferes with the reflected wave of wave vector $(k_x^r, k_y^r, 0)$:

$$p(\vec{r}, \omega) = p_i(\omega) e^{-i(k_x x - k_y y)} + p_i(\omega) R(\omega) e^{-i(k_x^r x + k_y^r y)} \tag{8.30}$$

The normal velocity at the wall is given by:

$$v_n(x, 0, z, \omega) = -v_y(x, 0, z, \omega) = \frac{k_y p_i(\omega)}{\rho\omega} e^{-ik_x x} - \frac{k_y^r p_i(\omega) R(\omega)}{\rho\omega} e^{-ik_x^r x} \tag{8.31}$$

One easily sees that this velocity can be zero *for all* x only if two conditions are fulfilled:

$$k_x^r = k_x \tag{8.32}$$

$$k_y^r R(\omega) = k_y \tag{8.33}$$

But the dispersion relation further imposes that:

$$k_x^{r\,2} + k_y^{r\,2} = k_x^2 + k_y^2 = k^2 \tag{8.34}$$

Consequently:

$$k_y^r = k_y \tag{8.35}$$

$$R(\omega) = 1 \tag{8.36}$$

The total pressure is then given by:

$$p(\vec{r}, \omega) = p_i(\omega) \left(e^{-i(k_x x - k_y y)} + e^{-i(k_x x + k_y y)} \right) \tag{8.37}$$

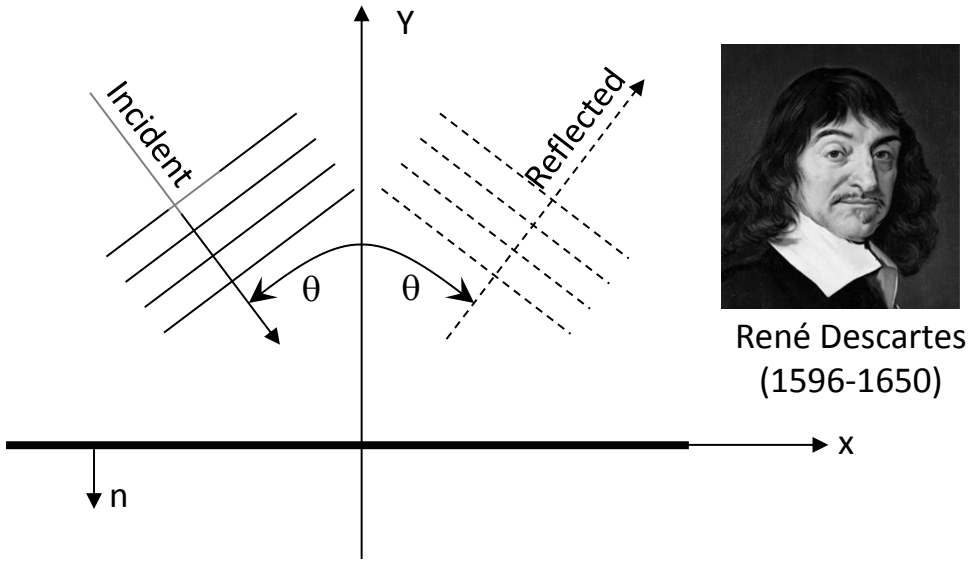

Figure 8.4: Reflection of a plane wave on a rigid wall under oblique incidence.

This is known as **Descartes' law**[1] which expresses that the incident wave and the reflected wave form the same angle with the normal to the reflecting plane.

8.2.2 Absorbing surface

Consider an absorbing wall characterised by a reflection factor R. We can easily demonstrate that the law of Descartes remains valid in this case. The total pressure can therefore be written:

$$p(\vec{r},\omega) = p_i(\omega)\left(e^{-i(k_x x - k_y y)} + R(\omega)e^{-i(k_x x + k_y y)}\right) \tag{8.38}$$

[1] **René Descartes**, French philosopher, physicist and mathematician, was born in La Haye (Indre-et-Loire, a city now called Descartes) in 1596 and died in Stockholm in 1650. He made several key contributions to optics and mathematics, but is best known for his systematic method of scientific questioning, later called *cartesian*, which departs from medieval scholastics.

An alternative form can be obtained by introducing the angle θ formed by the incident and reflected waves with the y axis ($\cos\theta = k_y/k$):

$$p(\vec{r},\omega) = p_i(\omega)\left(e^{-ik(x\sin\theta - y\cos\theta)} + R(\omega)e^{-ik(x\sin\theta + y\cos\theta)}\right) \tag{8.39}$$

Pressure, normal velocity and impedance to the wall are then given by:

$$p(x,0,\omega) = p_i(\omega)(1+R(\omega))e^{-ikx\sin\theta} \tag{8.40}$$

$$v_n(x,0,\omega) = -v_y(x,0,\omega) = \frac{p_i(\omega)}{\rho c}(1-R(\omega))\cos\theta e^{-ikx\sin\theta} \tag{8.41}$$

$$Z(\omega) = \rho c\frac{1+R(\omega)}{1-R(\omega)}\frac{1}{\cos\theta} \tag{8.42}$$

The last relationship can be inverted:

$$R(\omega) = \frac{Z(\omega)\cos\theta - \rho c}{Z(\omega)\cos\theta + \rho c} \tag{8.43}$$

For a surface of given normal impedance, the reflection factor *depends on the angle of incidence*. The absorption coefficient α can be calculated explicitly by introducing the real and imaginary components of the impedance $Z = \rho c(z_r + iz_i)$:

$$\alpha(\omega.\theta) = 1 - |R(\omega)|^2 = \frac{4z_r(\omega)\cos\theta}{(1+z_r(\omega)\cos\theta)^2 + z_i^2(\omega)\cos^2\theta} \tag{8.44}$$

Figure 8.5 gives the variation of $\alpha(\theta)$ for various impedance values. For $|z| > 1$, we observe the growth of α with θ until a maximum α_m is reached for an angle of incidence θ_m. The maximum is followed by a sharp decline and a zero absorption is obtained at grazing incidence. If Z is purely real, the angle of incidence $\theta_m(\omega)$ is given by:

$$\cos\theta_m(\omega) = \frac{1}{z_r(\omega)} \tag{8.45}$$

and $\alpha_m = 1$. If impedance is complex, absorption is never complete ($\alpha_m < 1$). For $|z| \leq 1$, absorption uniformly decreases with θ.

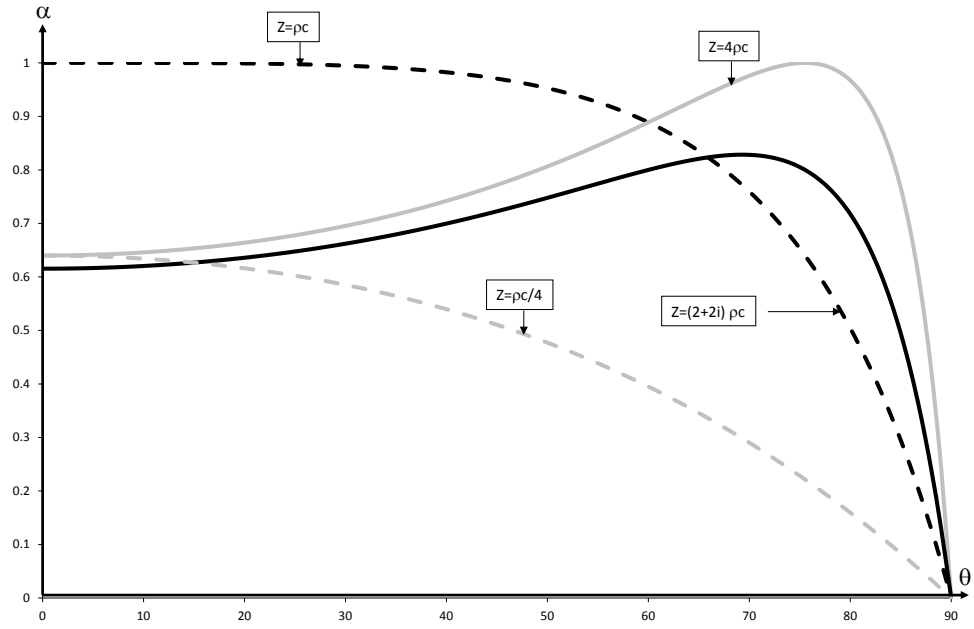

Figure 8.5: Variation of the absorption coefficient with the angle of incidence for different values of the normal impedance.

8.3 Reflection of a monopole source

8.3.1 Image source

The results obtained in previous paragraphs can be described in terms of image sources: the presence of the plane creates a source, symmetrical to the original source, and of amplitude $p^+(\omega)R(\omega)$ (Figure 8.6 and 8.7). The incident wave *penetrates* into the plane and the *reflected* field is generated by the image source.

Consider now a monopole located at a point P over a rigid plane S (Figure 8.8a). The pressure field generated by the monopole at point Q, in free field, is given by (Section 6.6.1):

$$p(Q) = A\frac{e^{-ikr}}{r} \tag{8.46}$$

where r is the distance between P and Q. This field is not compatible with the rigid condition on S. By analogy with the plane wave case, we add an image source at P', symmetric of P with respect to S, (Figure 8.8b) and obtain:

$$p(Q) = A\frac{e^{-ikr}}{r} + A\frac{e^{-ikr'}}{r'} \tag{8.47}$$

We intuitively understand, and easily verify, that the zero normal velocity condition on S is now satisfied (Figure 8.8c) as the vertical velocity components induced by both sources are equal and opposite.

Absorbing surface

For plane waves, the concept of image source is general and also applies when S is covered by an absorbing material (finite impedance boundary condition). To account for absorption, we simply give a reduced amplitude (factor R) to

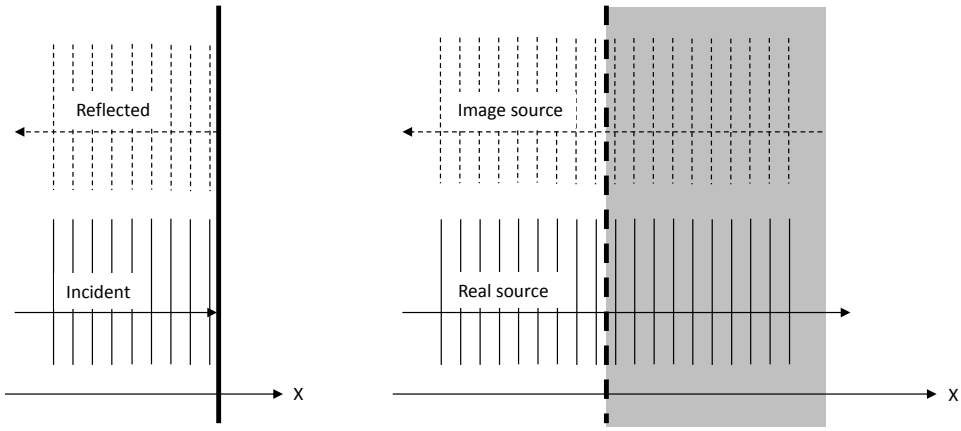

Figure 8.6: Reflection and image source (normal incidence).

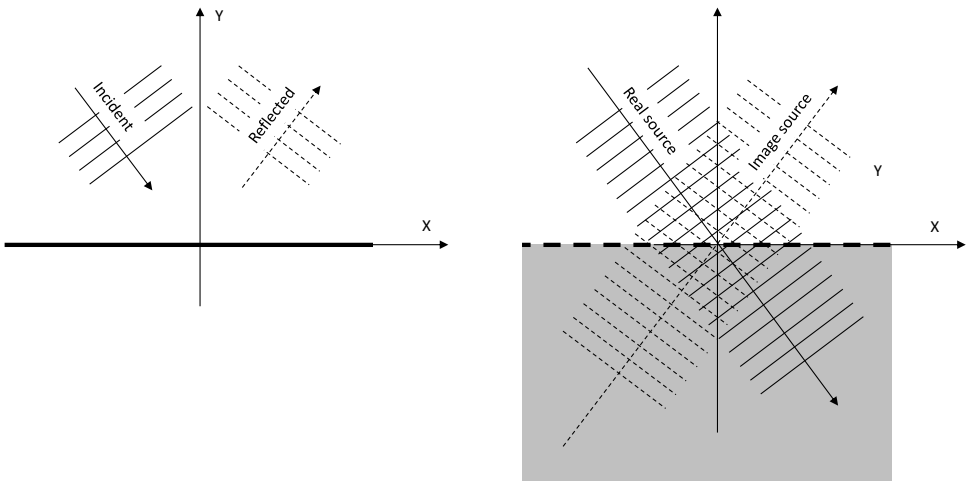

Figure 8.7: Reflection and image source (oblique incidence).

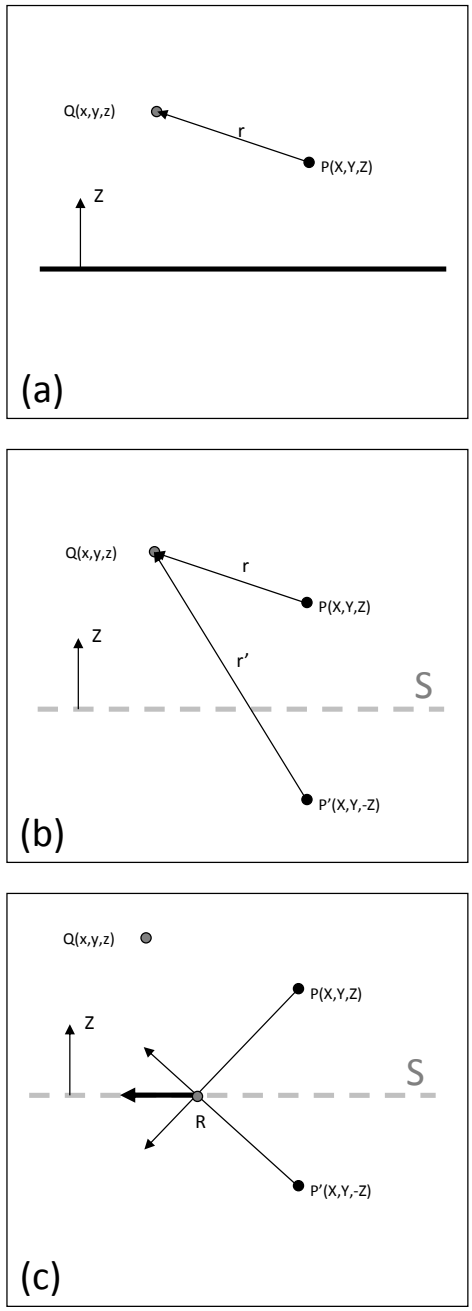

Figure 8.8: Reflection of a monopole on a rigid surface: real and image sources.

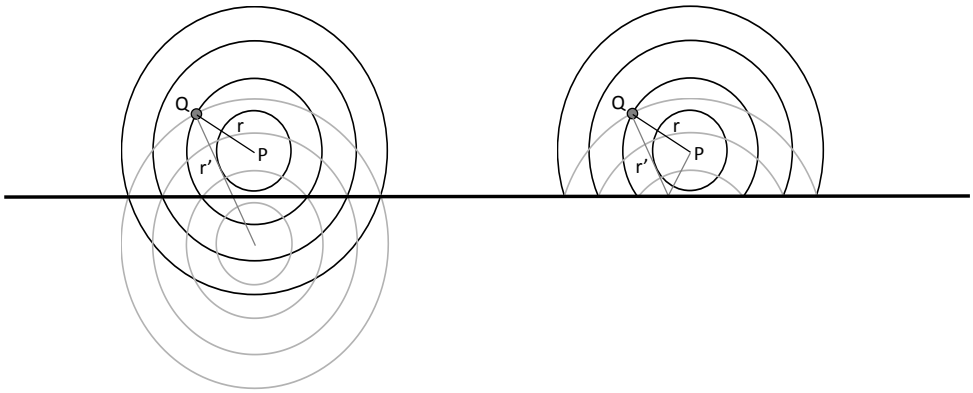

Figure 8.9: Reflection of a monopole on a rigid plane. Left: wave fronts from the source and its image in free field. Right: real wave fronts.

the image source. This does not work in the case of a spherical source. We indeed easily verify that the pressure field:

$$p(Q) = A\frac{e^{-ikr}}{r} + A \cdot R\frac{e^{-ikr'}}{r'} \tag{8.48}$$

is characterised by a non-constant value of the ratio p/v_n on the symmetry plane S.

8.3.2 Reflectogram

Single wall

Consider two impulsive sources located at point P and P'. Figure 8.9 shows the wave fronts associated to the source and its image (left) and the real wave fronts (right). The sound at point Q is perceived twice:

- firstly as the wave front of the real source reaches Q after a travel time $\frac{r}{c}$;
- secondly when the sound of the image source reaches Q at time $\frac{r'}{c}$.

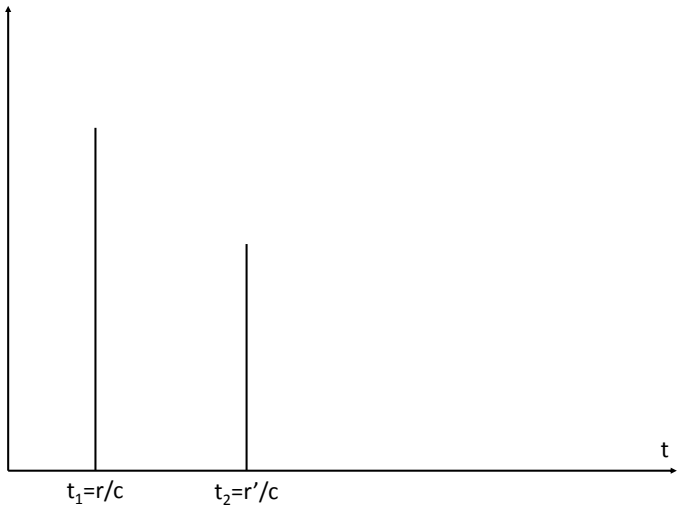

Figure 8.10: Reflectogram for the single wall case.

There is a delay between the *direct sound* and the *reflected sound*, but also an amplitude difference (ratio $\frac{r}{r'}$). The reflected wave propagates over a longer distance and its energy is distributed over a wider wave front. We can represent the acoustic events at point Q by a reflectogram (Figure 8.10) showing the successive impulses in terms of amplitude and arrival time.

Two rigid perpendicular walls

Consider the case of a source P placed near two perpendicular rigid walls S_1 and S_2 (Figure 8.11). To ensure zero-velocity conditions we must create two image sources P_1 and P_2, but also a source P_{12}. Indeed, on S_1, the velocity associated with P is compensated by P_1, but P_2 also induces a non-zero horizontal velocity component which is compensated by P_{12}. The same analysis can be made for S_2. The image of the source with respect to each wall must be considered, but also the image of each image. The sound field generated at Q by a source located at P therefore appears as the combination of four contributions (Figure 8.12) and the corresponding reflectogram shows four distinct impulses of decreasing amplitudes (Figure 8.13). The wave fronts at the four times of arrival are shown in Figure 8.14.

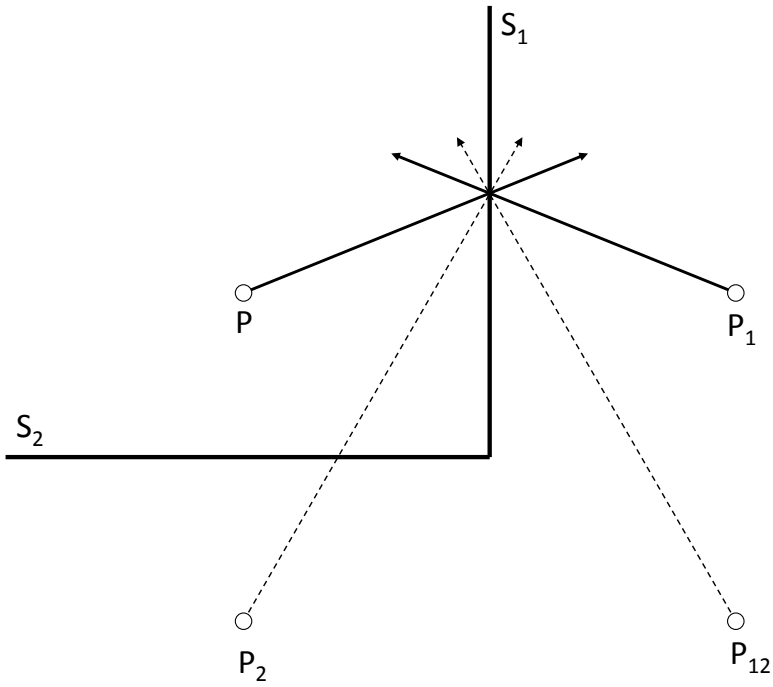

Figure 8.11: Image sources in the case of two perpendicular planes.

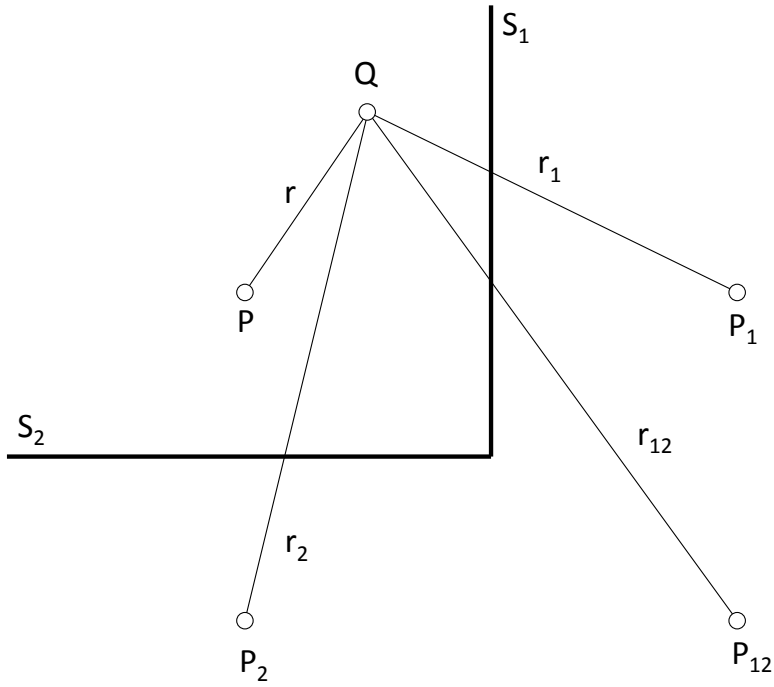

Figure 8.12: The sound at point Q is contributed by four distinct sources.

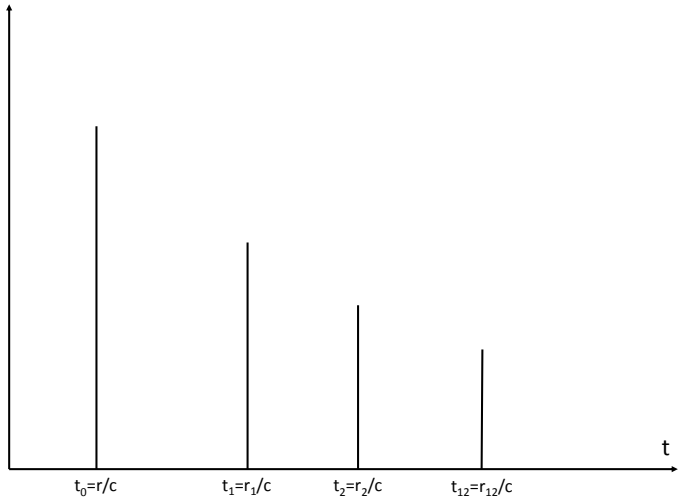

Figure 8.13: The reflectogram shows four successive impulses.

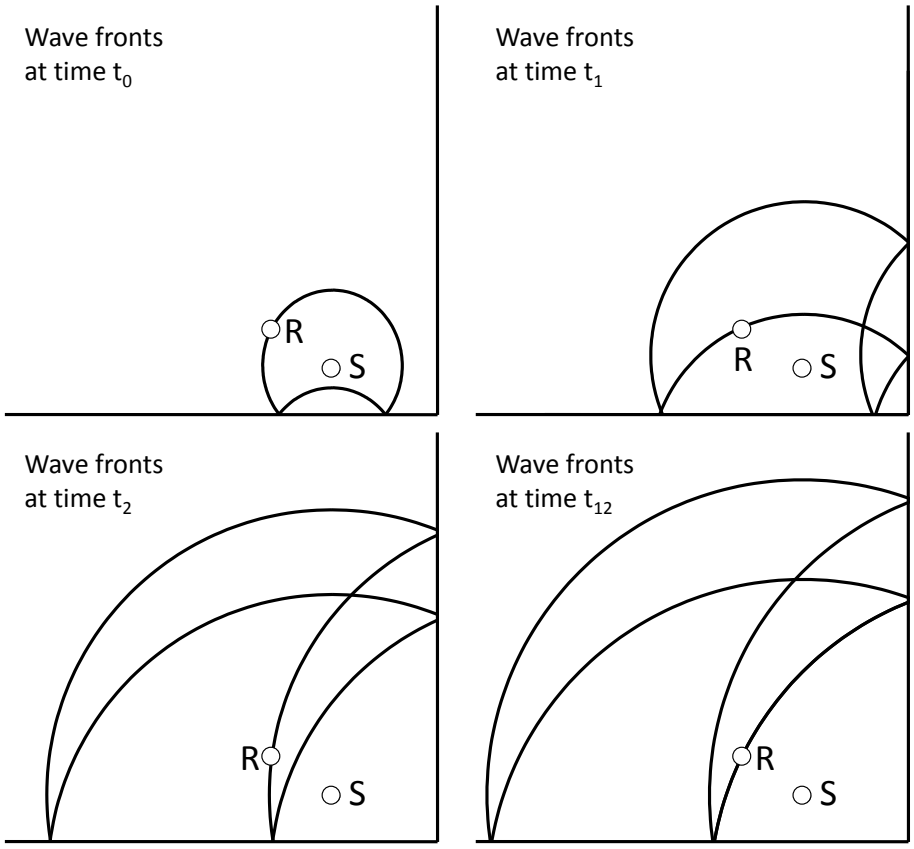

Figure 8.14: Wave fronts at times t_0, t_1, t_2 and t_{12} where the impulse emitted by source S reaches receiver R.

Closed rectangular cavity

If we consider a two-dimensional rectangular cavity (Figure 8.15), the image of the source must be taken with respect to each wall (order 1). The image of each image must then also be considered (order 2) and so on (orders 3, 4 ...). There are an infinite number of image sources and, consequently, an infinite number of impulses in the reflectogram (Figure 8.21).

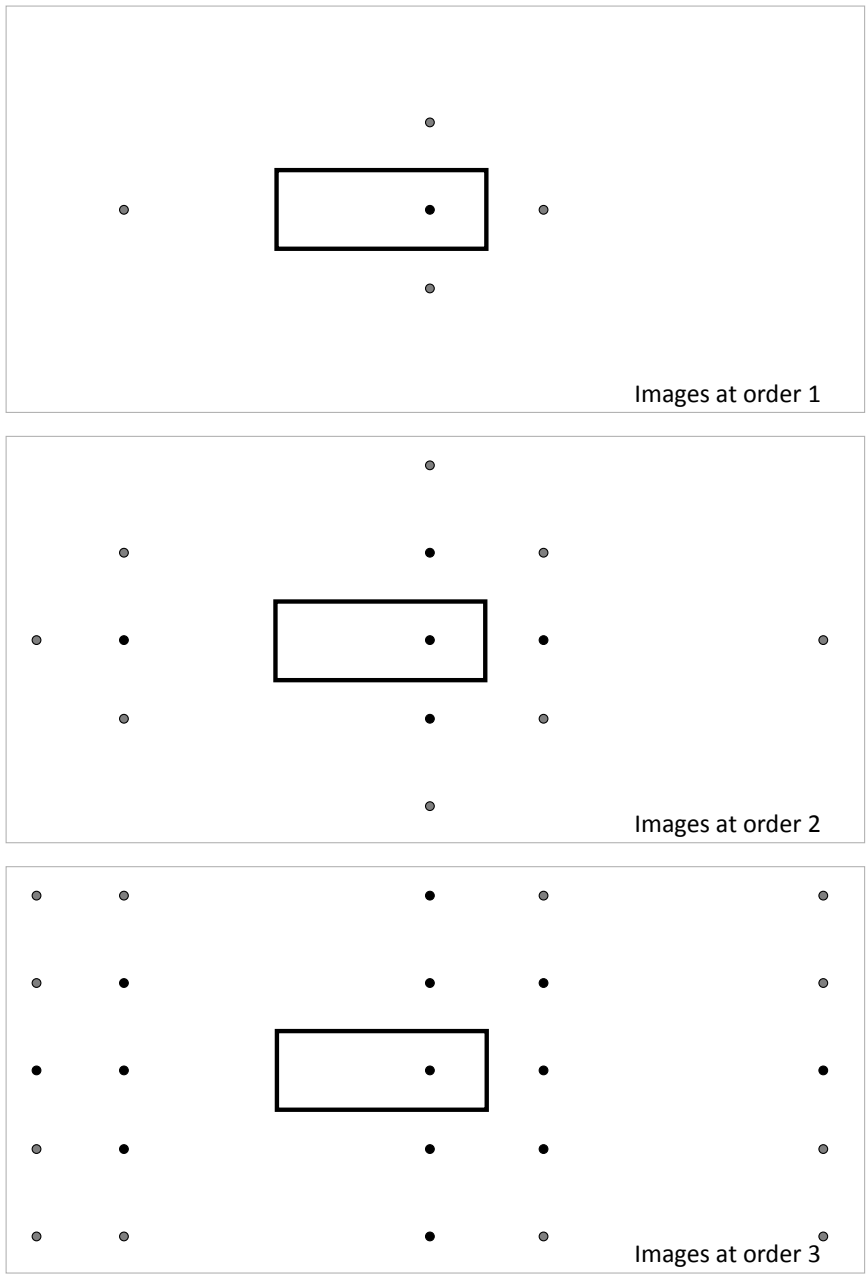

Figure 8.15: Image sources in the case of a rectangular cavity.

8.3.3 Ray tracing method

The image source method works well for rectangular cavities. As soon as the geometry becomes more complex, it is necessary to manage the fact that each image source only radiates over a determined range of angles. This complicates the method, making it very impractical. Fortunately, the ray tracing method avoids these difficulties and is widely used in room acoustics.

In Figure 8.16 we observe that the angles formed by the normal to the spherical wave fronts, before and after reflection, follow the law of Descartes. An infinitesimal element of the spherical wave front behaves as a plane wave. Figure 8.17 also shows that the reflection of a source on two perpendicular planes can be analysed in terms of specularly reflected rays. The four impulses appearing on the reflectogram of Figure 8.13 correspond to the four *paths*: P-Q, P-(2)-Q, P-(3)-Q, P-(4a)-(4b)-Q. In a general context the ray tracing method is based on the following steps:

1. the positioning of the source and of one or more receivers (zones of small extension centered on a point where we wish to evaluate the sound level) are defined;

2. a material is assigned to each wall and its absorption coefficient α defined (in practice α has a different value in each octave band);

3. the source is replaced by an even spatial distribution of a high number of rays (typically several tens of thousands), each carrying a fraction of the total energy of the source (the distribution can be homogeneous or integrate a certain directivity of the source);

4. each individual ray is tracked during its specular reflections on the walls (Figure 8.18);

5. when a ray passes through a receiver, an impulse is recorded in the reflectogram:

    - the arrival time is simply the total travelled distance (r) divided by the speed of sound (c);

- the energy brought to the receiver by the ray is the original energy carried by the ray decreased by three factors:
  - a factor $\frac{1}{r^2}$ due to spherical divergence (the longer the path, the wider the surface on which the energy is distributed);
  - the product of the coefficients $(1-\alpha)$ of all the walls encountered along the way and
  - a coefficient $e^{-\gamma r}$ taking into account the attenuation (dissipation in the propagation media).

6. we can then trace the reflectogram (Figure 8.21), but also, if enough receivers are defined, *maps* representing the spatial distribution of various acoustic parameters (Figure 8.20).

Some remarks on the ray tracing method:

1. Small receivers are required to achieve a good spatial resolution of the acoustic field. The number of rays passing through a receiver being inversely proportional to the size of the receiver, it is necessary to increase the number of rays. The computational cost of the method is therefore also increased. To solve this problem, an improved version of the method has been proposed using point receivers and tracking *cones* rather than rays (Figure 8.22). Sound intensity within a cone follows a gaussian distribution to ensure a homogeneous distribution of sound intensity around the source.

2. The classical ray tracing method ignores the effects of coherence and rays have an arbitrary phase relationship. In practice there is always a certain degree of coherence, in particular during the first reflections. More sophisticated versions of the ray tracing method take coherence into account. The materials must then be characterised by their impedance and not only by their absorption factor.

3. The reflection of a sound wave on a real material combines a specular part (Descartes law) and a diffuse part. The specular reflection dominates at low frequency (as long as the geometrical irregularities of the material are significantly smaller than the wavelength) while the importance of diffuse reflection gradually increases with frequency. Diffuse reflection can be taken into account, in a simplified way, by re-emitting

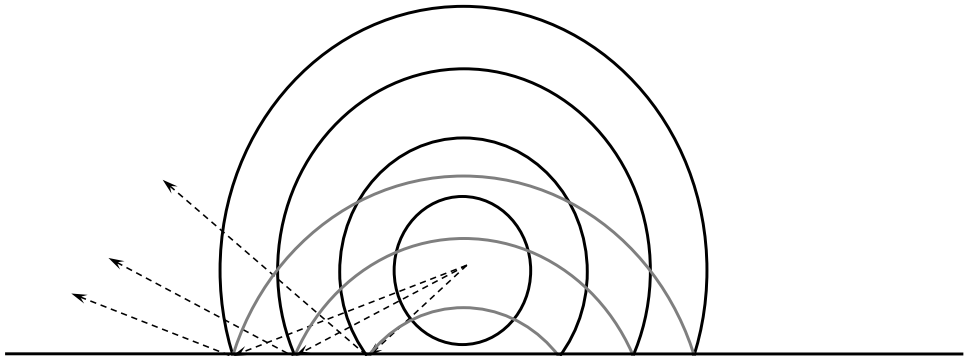

Figure 8.16: The normal vector to the spherical wave fronts follows Descartes specular reflection law.

a fraction of the incident energy in one or several randomly selected directions. An incident ray is then split into several reflected rays which considerably increases the calculation time.

4. Diffraction is often treated in the same way: when a ray strikes a diffracting edge, its energy is distributed over several diffracted rays.

5. Tracking ceases when the ray has lost a pre-defined fraction η of its energy by attenuation, absorption and spherical divergence. The residual energy is statistically distributed along the tail of the reflectogram. At that stage, the acoustic field has become *diffuse*. A diffuse sound field is a field where all directions of propagation have the same probability.

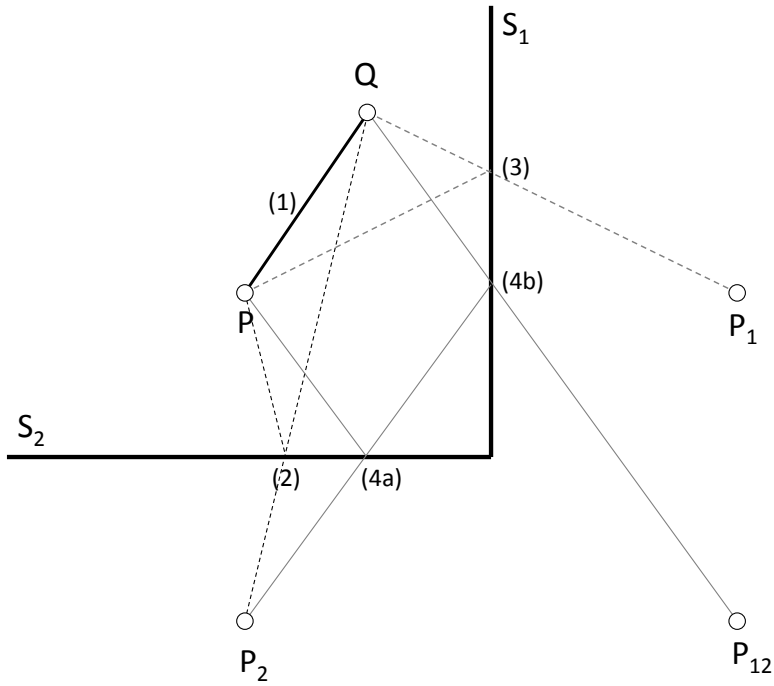

Figure 8.17: The method of image source may be analysed in terms of rays.

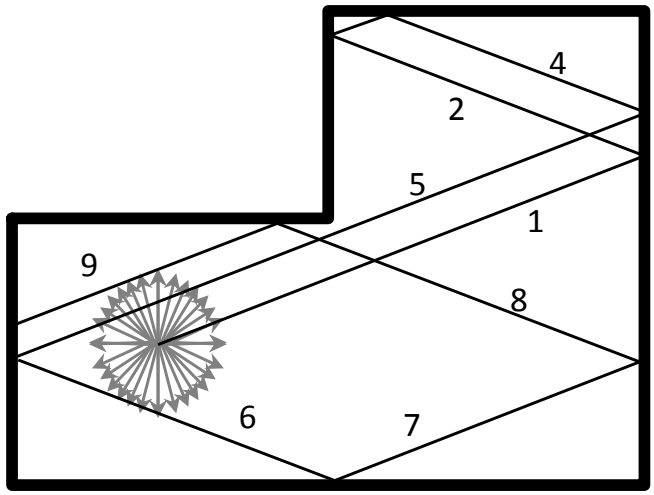

Figure 8.18: Ray path in an L-shaped cavity.

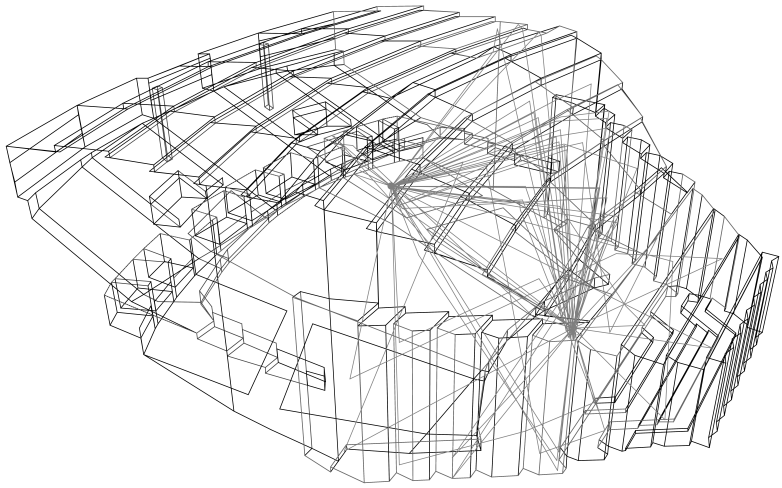

Figure 8.19: Ray path in a concert hall.

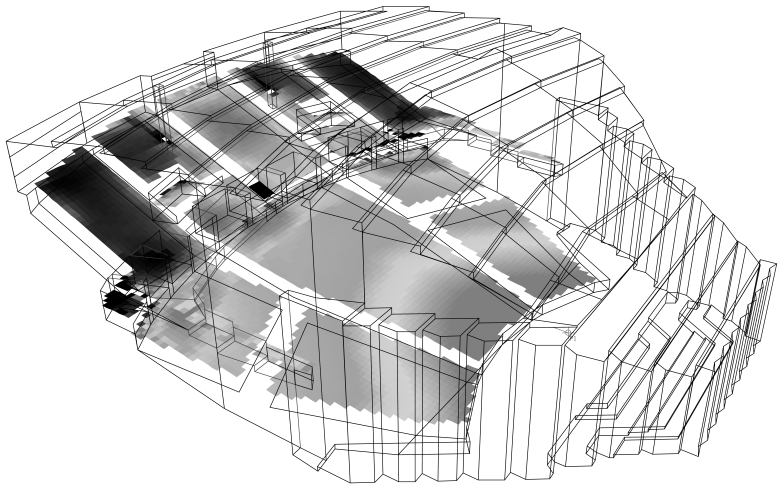

Figure 8.20: Map of sound pressure level (SPL) in a concert hall.

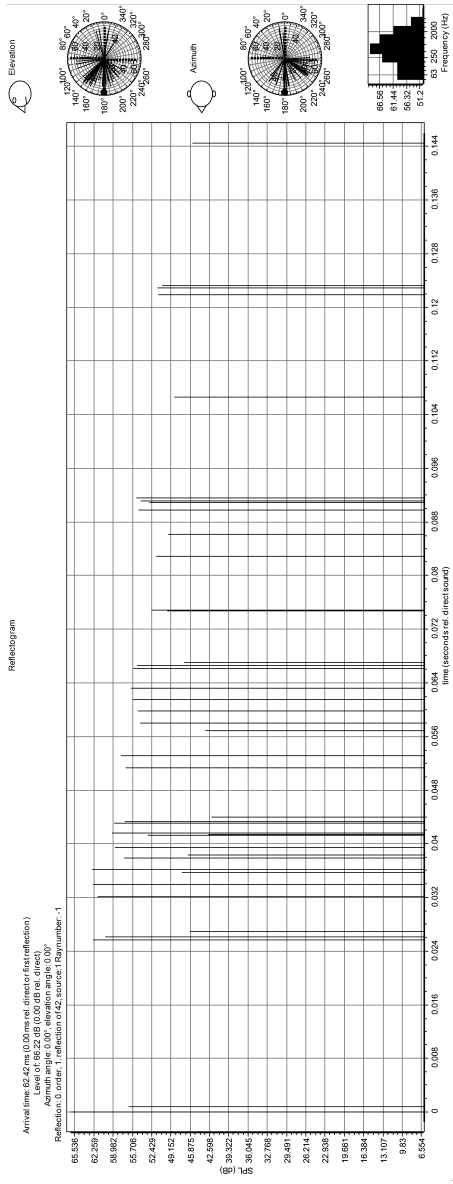

Figure 8.21: Reflectogram of a concert hall calculated by the ray tracing method. The angle at which each ray reaches a given receiver is depicted on the small diagrams on the side of the reflectogram. The small faces, with ears and nose, next to these diagrams provide a reference orientation.

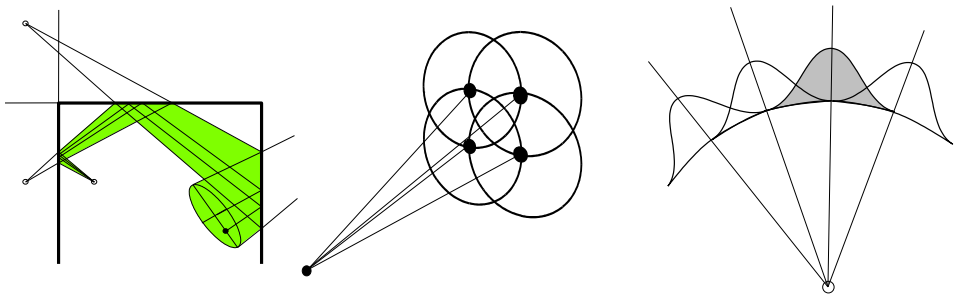

Figure 8.22: Replacing rays by cones improves the spatial resolution of the method.

8.4 Notes on the concept of impedance

8.4.1 Sign of the impedance coefficient

This Madonna, like some regret deep-rooted in the flesh, must have given the wrong sign to the pitiful algebra that sometimes haunted Aurélie's brain.
— **Marcel Aymé** (1902-1967), The hollow field (1929).
English translation by Helen Waddell (1933).

Impedance is defined as the ratio of pressure to velocity and therefore depends on the direction along which the velocity is measured. One can be interested in the impedance in the x, y or z direction or in the normal impedance on a given surface. This last concept is appropriate when considering the absorption properties of the surface. Let Z_n be the normal impedance on a surface and let p be the acoustic pressure at a point of this surface. The normal acoustical intensity at this point is given by:

$$I_n = \frac{\Re(Z_n)}{|Z_n|^2} \frac{|p|^2}{2} \tag{8.49}$$

The normal intensity is oriented along the normal vector if the real part of the normal impedance is positive and has the opposite direction if the real part is negative (Figure 8.23). Absorption occurs when there is a transfer

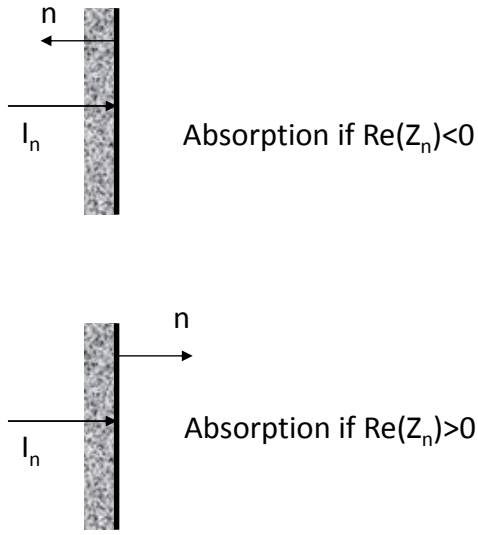

Figure 8.23: The sign of the impedance coefficient depends on the orientation of the normal vector.

of energy from the acoustic fluid to the absorbing surface: either the normal points towards the fluid and $\Re(Z_n)$ is negative, or the normal points towards the absorbing surface and $\Re(Z_n)$ is positive.

8.4.2 Frequency dependency of the impedance

The variation of impedance with frequency indicates that the pressure-velocity relationship is not local in time: the instantaneous velocity depends on the temporal evolution of pressure and vice-versa. Indeed, the proportionality between the pressure and velocity spectra translates into a convolution integral in the time domain:

$$p(t) = \int_{-\infty}^{\infty} z(\tau) \cdot v(t-\tau) \cdot d\tau \tag{8.50}$$

$$v(t) = \int_{-\infty}^{\infty} a(\tau) \cdot p(t-\tau) \cdot d\tau \tag{8.51}$$

with

$$z(t) = \frac{1}{2\pi}\int_{-\infty}^{\infty} Z(\omega)e^{i\omega t}d\omega \tag{8.52}$$

and

$$a(t) = \frac{1}{2\pi}\int_{-\infty}^{\infty} \frac{1}{Z(\omega)}e^{i\omega t}d\omega \tag{8.53}$$

Pressure at time t cannot depend on the future velocity and vice-versa (causality principle). Impulse responses $z(t)$ and $a(t)$ therefore must be zero for $t < 0$. This restricts the way $Z(\omega)$ and $A(\omega)$ may vary with frequency. If the variation of impedance with ω is regular enough, it can be approximated by the ratio of two polynomials in $(i\omega)$ (Padé approximations):

$$\tilde{Z}(\omega) = \frac{\sum_{j=1}^{n} A_j \cdot (i\omega)^j}{\sum_{k=1}^{m} B_k \cdot (i\omega)^k} \tag{8.54}$$

The pressure-velocity relationship can then be written as:

$$p(\omega) \cdot \sum_{k=1}^{m} B_k \cdot (i\omega)^k = v(\omega) \cdot \sum_{j=1}^{n} A_j \cdot (i\omega)^j \tag{8.55}$$

or, by applying the inverse Fourier transform to both sides:

$$\sum_{k=1}^{m} B_k \frac{d^k p(t)}{dt^k} = \sum_{j=1}^{n} A_j \frac{d^j v(t)}{dt^j} \tag{8.56}$$

The impedance frequency dependency (when it is defined as a Padé approximation) becomes, in the time domain, a linear relationship between pressure, velocity and their time derivatives.

8.4.3 Vibrating and absorbing panel

From a purely mathematical point of view, the Helmholtz equation accepts, at a given point, the specification of one of the following three boundary condition types:

- Dirichlet: fixed pressure (p);
- Neumann: normal pressure gradient ($\partial_n p$) or normal velocity (v_n);

- Robin: linear relationship between pressure and normal velocity ($ap + bv_n = c$).

Normal impedance boundary conditions are a special case of the Robin condition ($a = 1$, $b = -Z_n$, $c = 0$). The case of a boundary that is both flexible and absorbing is a straightforward generalisation. If the wall vibrates with a normal velocity v_s, and if the material covering the wall has an impedance Z_n, the relationship between the acoustic pressure p and the velocity v_f of the fluid particles is as follows:

$$Z_n = \frac{p}{v_f - v_s} \tag{8.57}$$

The finite value of the impedance coefficient creates a velocity difference between the solid boundary and the neighbouring fluid.

8.4.4 Locally and non-locally reacting material

The impedance boundary condition is usually directly applied on the boundary surface. The phenomenon is considered to be *local*: the material imposes a local relationship between pressure and normal velocity at each point. In reality, an absorbing layer always has a definite, non-zero, thickness (Figure 8.24). Energy dissipation indeed only occurs when there is interaction between the sound field and a bulky dissipative media (Chapter 14). In order to accurately model the absorbing media, we must choose one of the following strategies:

- Create a model involving two different materials: air and an absorbing layer.[2] A continuity condition is defined at the interface between the two materials. A boundary condition is defined to represent the surface on which the absorbing material is laid or glued (Figure 8.24.A).

- Create a single-material model (air) and define, at the interface between the air and the absorbing layer, a boundary condition representing the complex phenomena associated to this material (Figure 8.24.B). Ideally,

[2] Models representing the propagation of sound waves in porous media (Craggs, Biot) are discussed in Chapter 14.

a condition of this type must be *non-local*, because the wave leaving the material at point Q results from waves entering the material at more than one point (P and P' for example, see Figure 8.24.D).

In practice, we often model a material by its local impedance, therefore neglecting the non-locally reacting character of the material and its finite thickness (Figure 8.24.C). Figure 8.5 shows that the absorption tends to 0 at grazing incidence ($\theta = 90°$). This is due to the fact that the model assumes that the acoustic treatment has no thickness. Under grazing incidence, the normal velocity is zero at the wall and the sound field does not interact with the infinitely thin material covering the wall: there is no dissipation, whatever the impedance value. In reality, a material has a thickness and there is interaction. Also, the wavefronts, initially plane, deform due to the difference in propagation speed between the two media.

8.4.5 Impedance measurement with a Kundt tube

The impedance of a material is measured using a Kundt tube.[3] The measurement principle is introduced below.

Analytical solution

Consider a tube of length ℓ, excited at its left end by an oscillating piston. At the right end lies a sample of material of (unknown) impedance $Z = z \cdot \rho c$ (Figure 8.26). The acoustic pressure in the tube is given by:

$$p(\omega) = p^+(\omega)e^{-ikx} + p^-(\omega)e^{ikx} \tag{8.58}$$

[3] **August Kundt**, a German physicist, was born in Schwerin on November 18, 1839 and died on May 21, 1894 in Lübeck. Though mainly known for his eponymous tube that is used to make sound waves visible, Kundt worked in numerous domains and notably demonstrated the mono-atomic character of mercury. He was the assistant of Hermann von Helmholtz and had a famous assistant himself: Wilhelm Conrad Röntgen discovered X-rays and became, in 1901, the first recipient of the Nobel Prize in Physics.

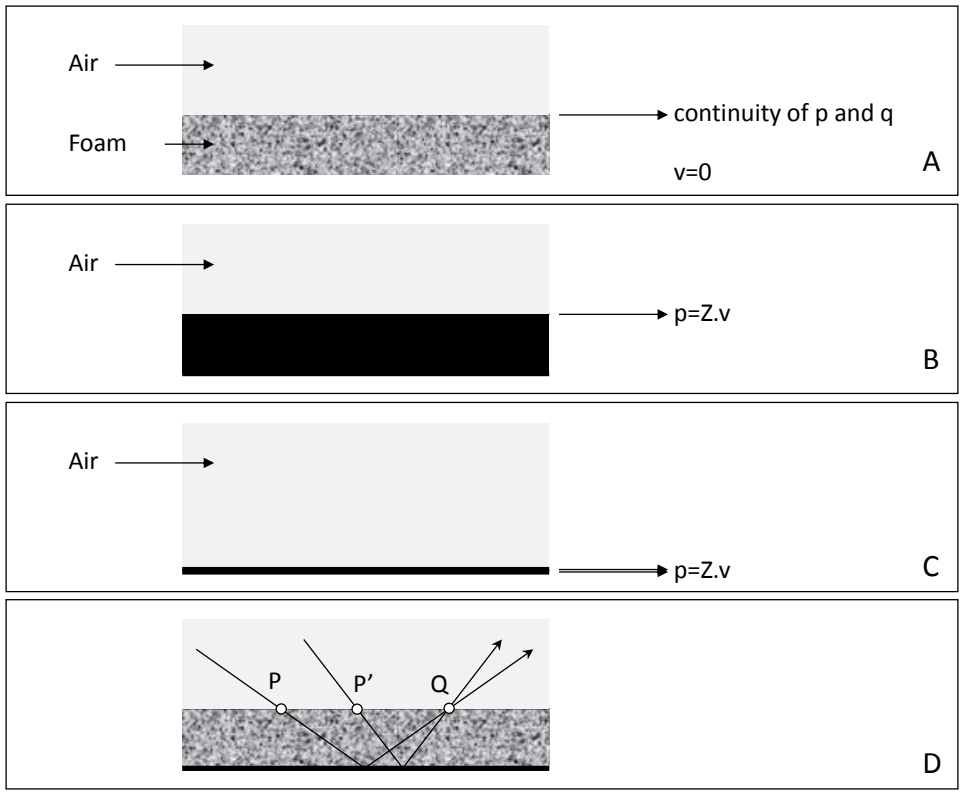

Figure 8.24: Locally and non-locally reacting materials. In (A), the symbol q designates the acoustic flow i.e. v on the air side and $\Omega \cdot v$ on the absorbing material side (Ω is the porosity defined in Section 14.3.2).

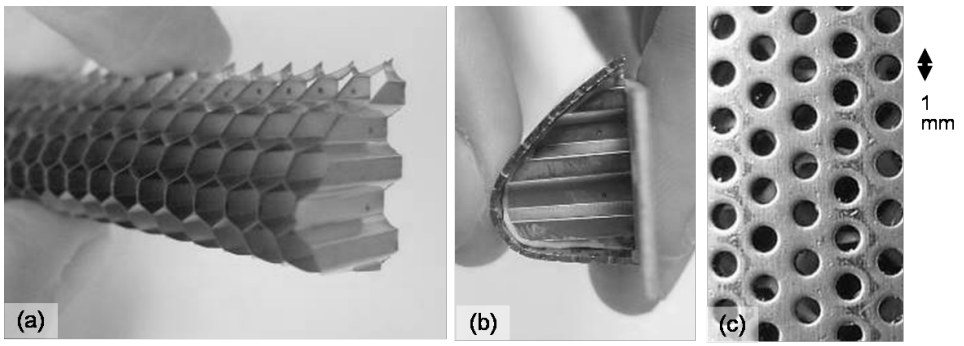

Figure 8.25: Example of locally reacting acoustic treatment using a honeycomb material covered by a perforated plate.

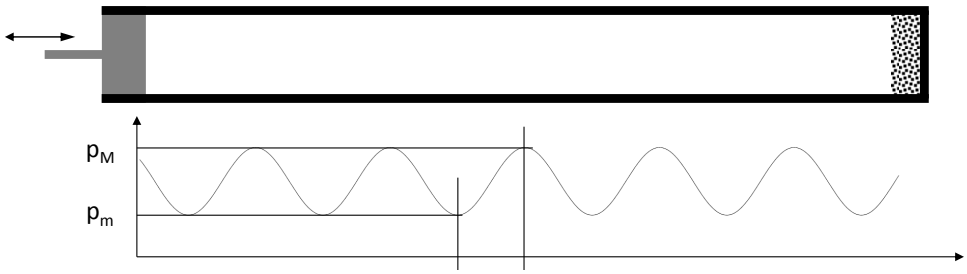

Figure 8.26: Impedance measurement with a Kundt tube.

The boundary conditions are:

$$\begin{aligned} v_x(0) &= \frac{i}{\rho\omega}\left[\frac{dp}{dx}\right]_{x=0} = \bar{v}(\omega) \\ Z \cdot v_x(\ell) = p(\ell) &\Leftrightarrow \frac{iZ}{\rho\omega}\left[\frac{dp}{dx}\right]_{x=\ell} = p(\ell) \end{aligned} \tag{8.59}$$

or:

$$\begin{aligned} p^+ - p^- &= \rho c\bar{v} \\ z\left(p^+ e^{-ik\ell} - p^- e^{ik\ell}\right) &= p^+ e^{-ik\ell} + p^- e^{ik\ell} \end{aligned} \tag{8.60}$$

Solving this system of equations yields:

$$p = i\rho c\bar{v}\frac{\sin k(\ell - x) - iz\cos k(\ell - x)}{\cos k\ell + iz\sin k\ell} \tag{8.61}$$

The pressure distribution in an *open-ended tube* is obtained by setting $z = 0$:

$$p = i\rho c\bar{v}\frac{\sin k(\ell - x)}{\cos k\ell} \tag{8.62}$$

When $z \to \infty$, we obtain the sound field in a *closed tube*:

$$p = -i\rho c\bar{v}\frac{\cos k(\ell - x)}{\sin k\ell} \tag{8.63}$$

For $z = 1$ ($Z = \rho c$), we find:

$$p = \rho c\bar{v}e^{-ikx} \tag{8.64}$$

which represents perfect absorption (no reflected component: $p^- = 0$).

Measurement procedure

The measurement procedure involves a mobile microphone located inside the tube. The operator locates the points (x_m and x_M) where quadratic pressure is maximum and minimum ($|p_m|^2$ and $|p_M|^2$). Two coefficients are then calculated:

$$\alpha \doteq \tan 2k(\ell - x_m) = \tan 2k(\ell - x_M) \tag{8.65}$$

$$\beta \doteq \frac{|p_m|^2}{|p_M|^2} \tag{8.66}$$

Quadratic pressure in the tube is given by (introducing the real and imaginary parts as well as the modulus of the impedance: z_r, z_i and $|z|$):

$$|p|^2 = \rho^2 c^2 |\bar{v}|^2 \frac{(|z|^2+1) + (|z|^2-1)\cos 2k(\ell - x) + 2z_i \sin 2k(\ell - x)}{(|z|^2+1) - (|z|^2-1)\cos 2k\ell - 2z_i \sin 2k\ell} \tag{8.67}$$

Maximum quadratic pressure occurs when:

$$\tan 2k(\ell - x) = \frac{2z_i}{(z^2-1)} \tag{8.68}$$

From this we obtain:

$$z_i = \frac{\alpha}{2}(z^2 - 1) \tag{8.69}$$

We can now calculate the β coefficient, taking the above relation into consideration:

$$\beta = \frac{|p_m|^2}{|p_M|^2} = \frac{\left(\begin{array}{l} (|z|^2+1) + (|z|^2-1)\cos 2k(\ell - x_m) \\ +\alpha(|z|^2-1)\sin 2k(\ell - x_m) \end{array} \right)}{\left(\begin{array}{l} (|z|^2+1) + (|z|^2-1)\cos 2k(\ell - x_M) \\ +\alpha(|z|^2-1)\sin 2k(\ell - x_M) \end{array} \right)} \tag{8.70}$$

This relation can be inverted to yield the impedance modulus:

$$|z|^2 = \frac{\left(\begin{array}{l} 1 - \beta - \cos 2k(\ell - x_m) + \beta \cos 2k(\ell - x_M) \\ -\alpha \sin 2k(\ell - x_m) + \alpha\beta \sin 2k(\ell - x_M) \end{array} \right)}{\left(\begin{array}{l} 1 - \beta + \cos 2k(\ell - x_m) - \beta \cos 2k(\ell - x_M) \\ +\alpha \sin 2k(\ell - x_m) - \alpha\beta \sin 2k(\ell - x_M) \end{array} \right)} \tag{8.71}$$

The real and imaginary parts are then:

$$z_i = \frac{\alpha}{2}(z^2 - 1) \tag{8.72}$$

$$z_r = +\sqrt{|z|^2 - z_i^2} \tag{8.73}$$

The positive root is chosen to ensure power dissipation at $x = \ell$ (Section 8.4.1).

To summarise:

1. measure x_m, x_M, p_m and p_M;
2. calculate α (Equation 8.65) and β (Equation 8.66);
3. calculate $|z|^2$ as a function of β, x_m and x_M (Equation 8.71);
4. calculate z_i knowing $|z|^2$ and α (Equation 8.72);
5. calculate z_r knowing $|z|^2$ and z_i (Equation 8.73).

The impedance of a material is frequency dependent. The measurement procedure must be repeated for each frequency of interest. The *manual* process described above is no longer used today. The modern version of the Kundt tube features several fixed microphones simultaneously recording the pressure signal, across the entire frequency range. Digital processing of these signals instantly gives the impedance values.

8.5 Reverberation time

> *We were allowed to talk in the refectory in the evening. There were only a hundred and fifty of us, but the noise rose steadily,* proprio motu*, since everyone had to keep raising his voice to make himself heard. When it reached its full flowering the racket formed an edifice of sound that exactly filled the big room, and the master in charge would bring it tumbling down with a single blast on his whistle. There was something vertiginous about the ensuing silence.*
>
> — **Michel Tournier** (1924-2016), The Erl-King (1970).
>
> English translation by Barbara Bray (1972).

When a sound is emitted in a sufficiently reverberant room, after a certain time, the successive reflections create a *diffuse* sound field. The energy density is uniform and all propagation directions have equal probability. A simple model for the build-up and extinction of sound in a room can be built based on the diffuse sound field hypothesis.

8.5.1 Sound build-up

Consider a room of volume V and boundary area S. The sound field is described by its uniform energy density ε [J/m^3]. A source of power E [W] is switched on at time $t = 0$ ($\varepsilon(0) = 0$). The energy produced by the source during the time dt is Edt and the energy density in the room increases by $d\varepsilon$. They are related by:

$$Edt = Vd\varepsilon \rightarrow \frac{d\varepsilon}{dt} = \frac{E}{V} \rightarrow \varepsilon = e^{\frac{Et}{V}} - 1 \tag{8.74}$$

Energy density would increase indefinitely if part of the emitted power were not absorbed at the wall. The energy absorbed during time dt is:

$$dE_{abs} = \alpha SIdt \tag{8.75}$$

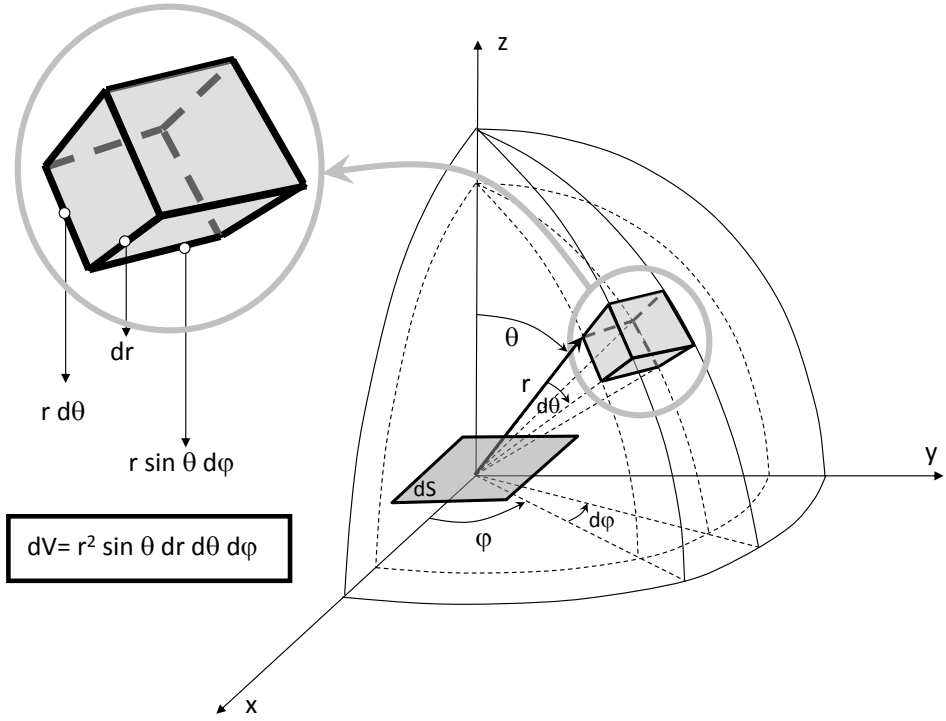

Figure 8.27: Power emitted by volume element dV and intercepted by surface element dS.

where:

- α is the average absorption coefficient of the walls ($\alpha S = \sum \alpha_i S_i$ where S_i is the area and α_i the absorption coefficient of wall i);
- I is the normal intensity at the wall, which we assume to be uniform.

The intensity intercepted by the surface element dS during the time dt is the integral of contributions received from every volume element dV (Figure 8.27). The integral is calculated on a sphere Σ of radius $c \cdot dt$. Indeed, the contribution of the volume located outside Σ has not yet reached dS at time dt.

$$I \cdot dt \cdot dS = \int_{\Sigma} \frac{\varepsilon \cdot dV}{4\pi r^2} \cos\theta \cdot dS \tag{8.76}$$

In spherical coordinates (Figure 8.27):

$$dV = r^2 \sin\theta \cdot dr \cdot d\theta \cdot d\phi \tag{8.77}$$

so that:

$$\begin{aligned} I \cdot dt \cdot dS &= \int_0^{c\cdot dt} \int_0^{\frac{\pi}{2}} \int_0^{2\pi} \frac{\varepsilon}{4\pi} \sin\theta\cos\theta \cdot dr \cdot d\theta \cdot d\phi \\ &= \frac{\varepsilon c}{4} \cdot dt \cdot dS \end{aligned} \tag{8.78}$$

and:

$$I = \frac{\varepsilon c}{4} \tag{8.79}$$

The energy balance of the room is therefore written:

$$Edt = Vd\varepsilon + \frac{\varepsilon c}{4}\alpha S dt \tag{8.80}$$

or

$$V\frac{d\varepsilon}{dt} + \frac{\alpha S c}{4}\varepsilon = E \rightarrow \varepsilon = \frac{4E}{\alpha S c}\left(1 - e^{-\frac{\alpha S c}{4V}t}\right) \tag{8.81}$$

After a sufficiently long time, asymptotic conditions are reached. The energy density tends to:

$$\varepsilon_{max} = \frac{4E}{\alpha S c} \tag{8.82}$$

and the total intensity dissipated at the wall is equal to the power injected by the source:

$$I_{max} = \frac{\varepsilon_{max} c}{4} \rightarrow \alpha S I_{max} = E \tag{8.83}$$

8.5.2 Sound extinction

At time t_e, after ε has reached its asymptotic value ε_{max}, if the source is switched off, ε will evolve according to the following equation:

$$V\frac{d\varepsilon}{dt} + \frac{\alpha S c}{4}\varepsilon = 0 \rightarrow \varepsilon = \frac{4E}{\alpha S c} e^{-\frac{\alpha S c}{4V}(t - t_e)} \tag{8.84}$$

Both solutions (build-up and extinction) are represented in Figure 8.28.

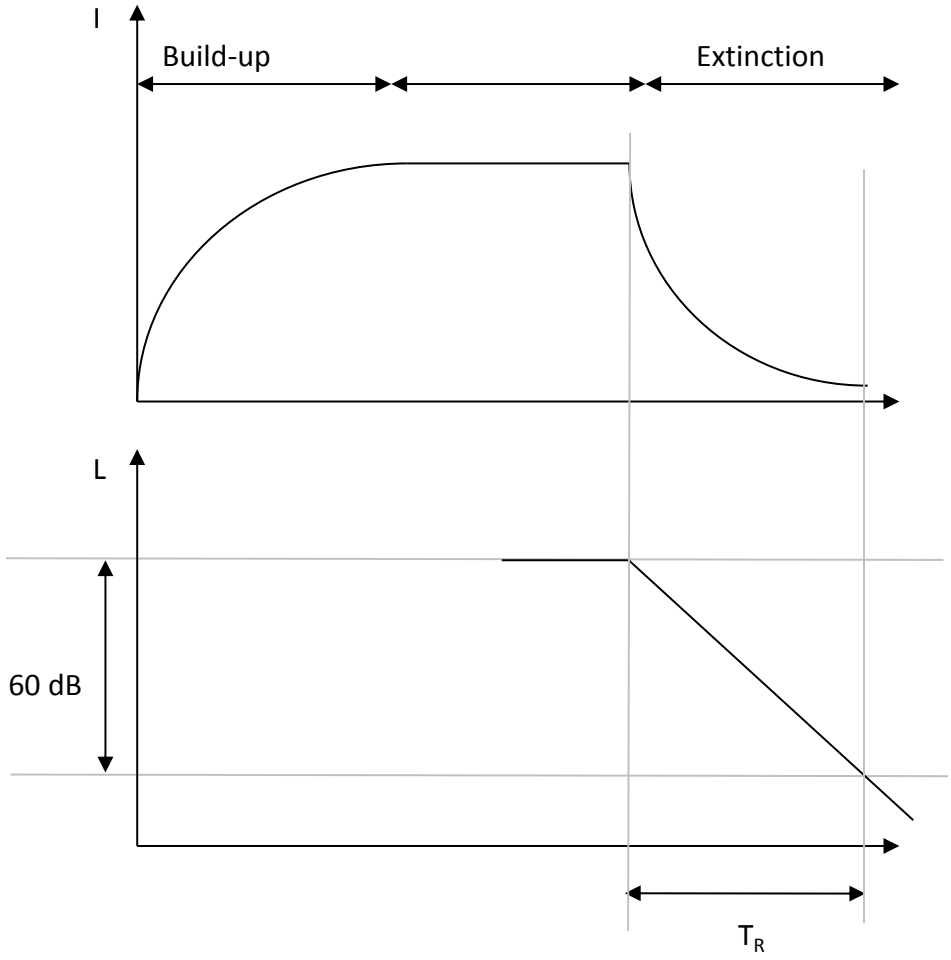

Figure 8.28: Build-up and extinction of sound in a room.

8.5.3 Sabine law

By definition, the reverberation time T_R is the time required for the sound level to decrease by 60 dB after the source has been switched off:

$$10 \log \frac{\varepsilon(t_e)}{\varepsilon(t_e + T_R)} = 60 \tag{8.85}$$

but:

$$\frac{\varepsilon(t_e)}{\varepsilon(t_e + T_R)} = e^{\frac{\alpha S c T_R}{4V}} \tag{8.86}$$

so that:

$$10 \log \frac{\varepsilon(t_e)}{\varepsilon(t_e + T_T)} = \frac{\alpha S c T_R}{4V} 10 \log e = 60 \tag{8.87}$$

We finally obtain:

$$T_R = \frac{60}{10 \log e} \cdot \frac{4}{c} \cdot \frac{V}{\alpha S} = 0.16 \frac{V}{\alpha S} = 0.16 \frac{V}{\sum_i \alpha_i S_i} \tag{8.88}$$

This is Sabine's formula (Figure 8.29), which can be rewritten as:

$$T_R = 0.16 \frac{V}{A} \tag{8.89}$$

where

$$A = \sum_i \alpha_i S_i \tag{8.90}$$

A is called the absorption area of the room.

Remarks:

- This expression assumes homogeneous distribution of acoustic energy in the room. In practice the distribution is always somewhat heterogeneous.

- Coefficients α_i are generally frequency dependent which means that reverberation time is also frequency dependent (Figure 8.30). An average reverberation time can of course be calculated, but it is often more appropriate to consider different T_R values in each octave band.

Figure 8.29: Wallace Sabine (1868-1919).

- T_R decreases with A. A can be increased by using materials with higher absorption (larger α) or by increasing the treated surface (Figure 8.31).
- Sabine did not develop his expression using the theoretical schema discussed above, but by an experimental approach. In 1895, while teaching at Harvard, he was asked to find a solution to the very poor acoustics of the Fogg Art Museum's auditorium. During this study, he realised that the product of the reverberation time by the absorption area was proportional to the volume of the room. The theory presented is an *a posteriori* justification of this experimental law.

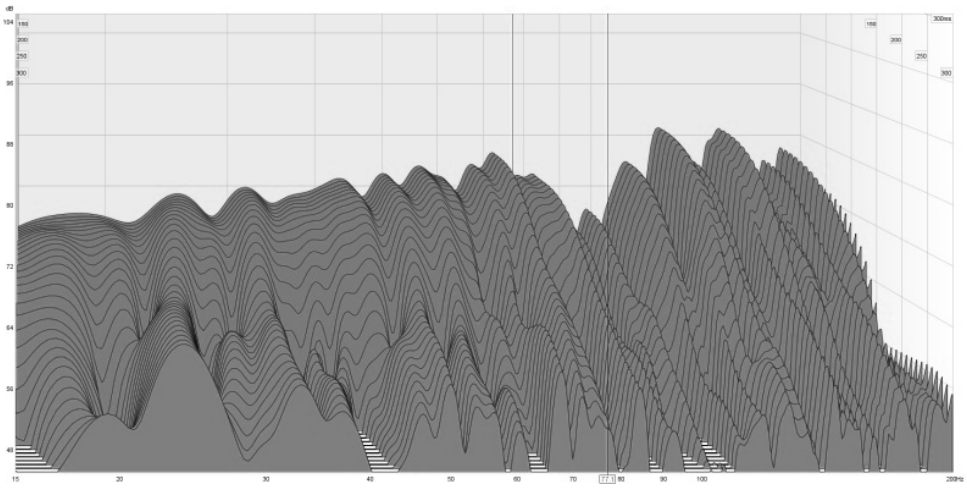

Figure 8.30: Sound extinction in a real room: reverberation time differs in different frequency bands.

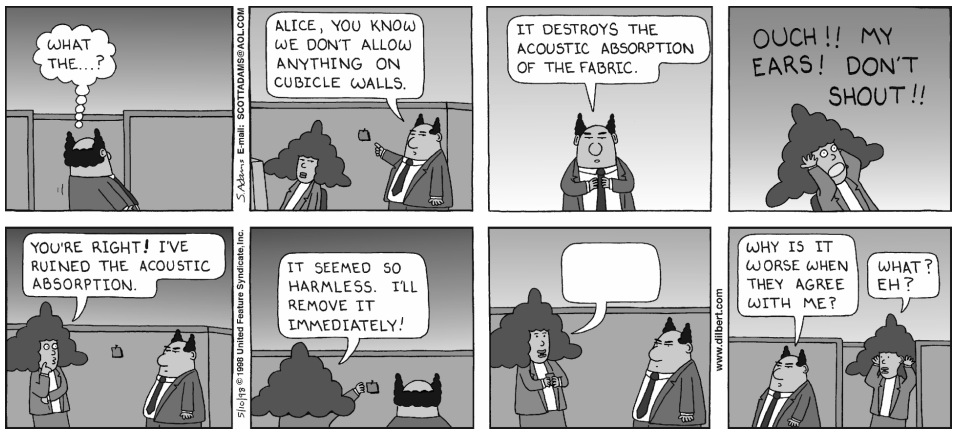

Figure 8.31: Absorption in Dilbert's cubicle: a matter of area.

8.5.4 Anechoic and reverberant chambers

Acousticians perform most of their experiments in one of three different types of room:

- All walls in **anechoic rooms** (Figure 8.32) are covered with cones of absorbing material chosen for its high α coefficient. The conical shape increases the absorbing area S. The reverberation time is therefore extremely short. An anechoic room approximates *free field* conditions (no reflections).

- A **reverberant chamber** (Figure 8.33) aims at maximizing the reverberation time. The sound field in a reverberant chamber is almost perfectly diffuse. The walls of a reverberant room are never parallel and diffusors are usually hanging from the ceiling to avoid privileged propagation direction. Walls are made of hard materials with very low absorption coefficient ($\alpha \simeq 0$).

- The **semi-anechoic rooms** (Figure 8.34) often used in the automobile industry display a reflective ground and absorbing walls and ceiling. These rooms approximate road conditions with free propagation in all directions, but reflection on the ground.

8.5.5 Eyring and Millington formulas

For a room with perfectly reflecting walls ($\alpha = 0$), Sabine's law consistently gives an infinite reverberation time. However, for perfectly absorbing walls ($\alpha = 1$), one finds a reverberation time of $0.16\frac{V}{S}$ whereas this should in fact be very close to zero. To correct this problem, Eyring[4] and Millington[5] proposed

[4] **Eyring C.F.**, *Reverberation time in dead rooms*, Journal of the Acoustical Society of America, pp, 217-241, 1930. Carl Ferdinand Eyring (1889-1951) is the uncle of the chemist Henry Eyring (1901-1981), famous for the kinetic theory of Eyring-Polanyi.

[5] **Millington G.**, *A Modified Formula for Reverberation*, Journal of the Acoustical Society of America, 69-82, 1932.

Figure 8.32: Anechoic room.

Figure 8.33: Reverberant chamber.

Figure 8.34: Semi-anechoic room.

modified expressions adapted to very absorbing environments (Figure 8.35):

$$A_{Eyring} = -S \ln \left(1 - \frac{\sum_i \alpha_i S_i}{S}\right) \tag{8.91}$$

$$A_{Millington} = -\sum_i S_i \ln \left(1 - \alpha_i\right) \tag{8.92}$$

8.5.6 Absorption coefficient measurement

Sabine's formula provides a simple way to measure the α coefficient of a material. Consider a reverberant chamber characterised by a reverberation time T_{R1}. Knowing its total area S_r, we can estimate an average absorption coefficient α_r from the reverberation time:

$$\alpha_r = \frac{0.16V}{T_{R1} S_r} \tag{8.93}$$

If we place a sample of material on the ground (area S_s and unknown absorption coefficient α_s) and measure the reverberation time once again, we can write:

$$T_{R2} = \frac{0.16V}{\alpha_s S_s + \alpha_r \left(S_r - S_s\right)} \tag{8.94}$$

from which we obtain:

$$\alpha_s = \frac{0.16V \left(S_r T_{R1} - \left(S_r - S_s\right) T_{R2}\right)}{S_r T_{R1} S_s T_{R2}} \tag{8.95}$$

This is the most commonly used method for measuring absorption coefficients. It is indeed extremely fast and simple and only requires the measurement of two reverberation times. The sample does not need to have a specific shape or dimension and may simply be put on the floor.

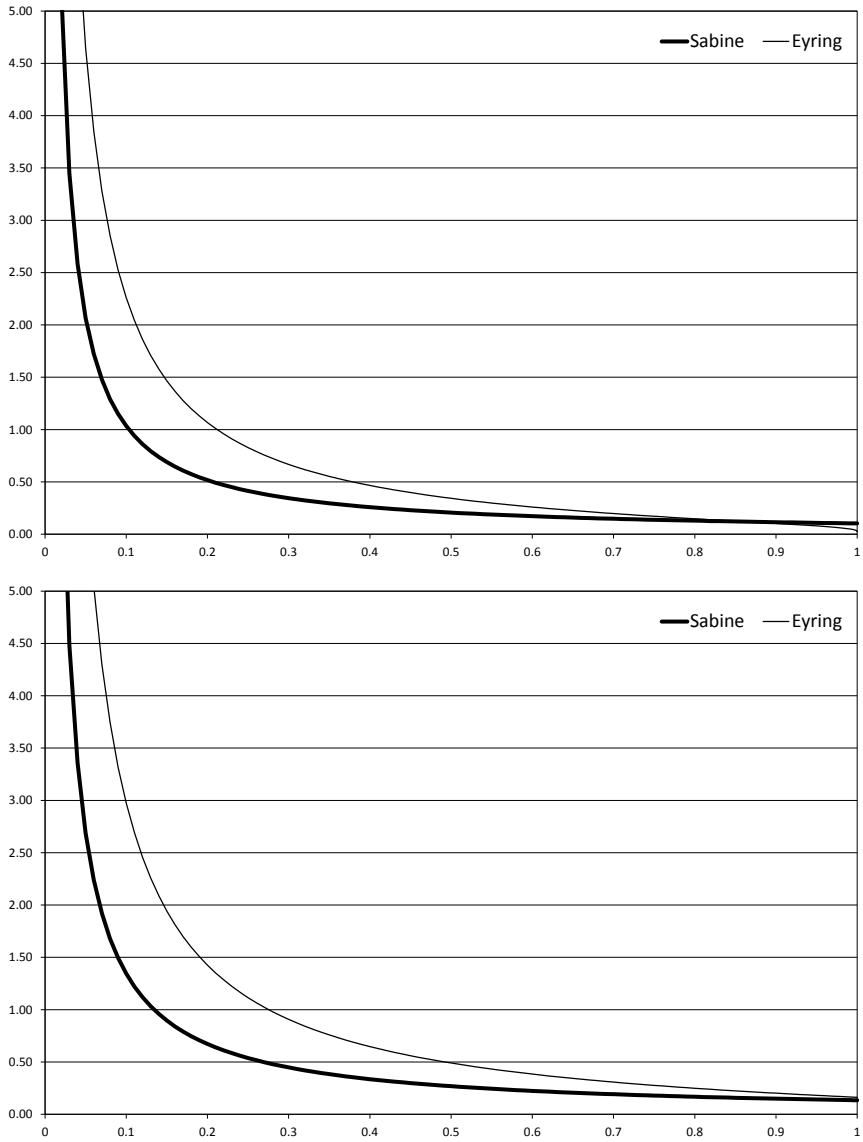

Figure 8.35: Reverberation time according to Eyring and Sabine formulas. The room has dimensions of 6 x 4 x 2.80 meters. In the first graph, all walls are covered with the same material whose absorption coefficient varies from 0 to 1. Reverberation time should tend to 0 for $\alpha = 1$. In the second graph, only the ground and walls are covered with an absorbing material, the ceiling being perfectly reflecting ($\alpha = 0$).

9

Resonance

And the more souls who resonate together, the greater the intensity of their love, for mirror-like, each soul reflects the others.
— **Dante Alighieri** (1265-1321), The Divine Comedy (composed between 1307 and 1321).

English translation by Stephen Mitchell (1993).

'Do you know that [Caruso] could sing to a wine-glass and shatter it?' he demanded.
'I always thought that was a fable,' said Mr Satterthwaite smiling.
'No, it's gospel truth, I believe. The thing's quite possible. It's a question of resonance.'
— **Agatha Christie** (1890-1976), The Face of Helen *in* The Mysterious Mr Quin (1930).

Contents

9.1 Resonance of a closed tube 186
9.2 Eigenmodes and eigenfrequencies 190
9.3 Modal superposition 194
9.4 Box-shaped cavity 197
9.5 Resonance of an arbitrary cavity 199

In this chapter we show that acoustic resonance occurs naturally in all enclosed sound fields. A simple tube is used as an example to introduce the concepts of eigenfrequencies and eigenmodes.

We also show how the acoustic field in a tube can be expressed as a linear combination of its eigenmodes which is commonly referred to as modal superposition. The same concepts are used to obtain an analytical description of the sound field in a box-shaped cavity. Arbitrarily shaped cavities are analysed using numerical techniques. Resonators such as Helmholtz and quarter-wavelength are presented in Chapter 10.

9.1 Resonance of a closed tube

9.1.1 Velocity source

Consider the horizontal tube of length ℓ shown on the upper part of Figure 9.1. The left end of the tube oscillates with a horizontal velocity $\bar{v}(\omega)$. The other walls are rigid (zero normal velocity). Assuming that the sound field is one-dimensional, the acoustic pressure distribution takes the form:

$$p(\omega, x) = p^+(\omega)e^{-ikx} + p^-(\omega)e^{ikx} \tag{9.1}$$

and the associated velocity distribution is:

$$v_x(\omega, x) = \frac{i}{\rho\omega}\frac{dp}{dx} = \frac{p^+}{\rho c}(\omega)e^{-ikx} - \frac{p^-}{\rho c}(\omega)e^{ikx} \tag{9.2}$$

The boundary conditions for this velocity-driven scenario are:

$$\begin{aligned} v_x(x=0) &= \bar{v}(\omega) \\ v_x(x=\ell) &= 0 \end{aligned} \tag{9.3}$$

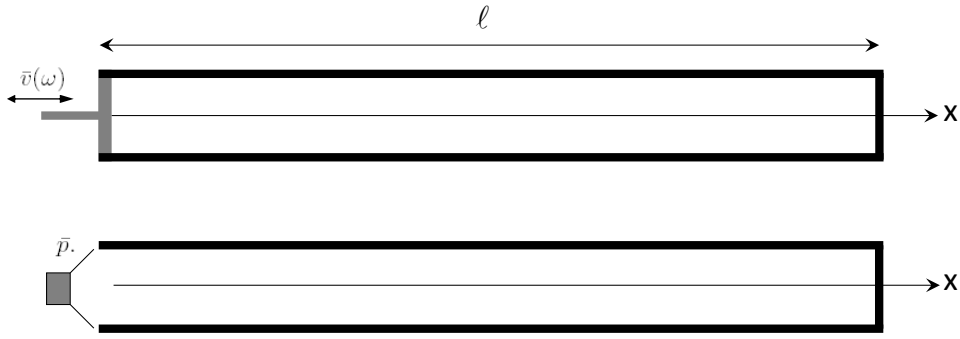

Figure 9.1: Closed tubes excited by a velocity source (top) or a pressure source (bottom).

They can be expressed using the two unknown amplitudes p^+ and p^-:

$$\begin{aligned} p^+ - p^- &= \rho c \bar{v} \\ p^+ e^{-ik\ell} - p^- e^{ik\ell} &= 0 \end{aligned} \tag{9.4}$$

Solving this system of equations for p^+ and p^- yields the following pressure and velocity distributions:

$$p(\omega, x) = -i\rho c \bar{v} \frac{\cos k\,(\ell - x)}{\sin k\ell} \tag{9.5}$$

$$v(\omega, x) = \bar{v} \frac{\sin k\,(\ell - x)}{\sin k\ell} \tag{9.6}$$

The pressure in the tube tends to infinity when $\sin kl$ tends to zero or when:

$$k\ell = n\pi \Leftrightarrow f = n\frac{c}{2\ell} \Leftrightarrow \ell = n\frac{\lambda}{2} \tag{9.7}$$

Resonance therefore occurs whenever the tube length equals an integer multiple of half-wavelength.

9.1.2 Pressure source

Consider the same tube equipped with a different source at the left end. Instead of a vibrating surface imposing a fixed normal velocity amplitude, we have a device that imposes a fixed pressure fluctuation amplitude $\bar{p}(\omega)$. The pressure and velocity fields in the duct are still of the form:

$$p(\omega, x) = p^+(\omega)e^{-ikx} + p^-(\omega)e^{ikx} \tag{9.8}$$

$$v_x(\omega, x) = \frac{i}{\rho\omega}\frac{dp}{dx} = \frac{p^+}{\rho c}(\omega)e^{-ikx} - \frac{p^-}{\rho c}(\omega)e^{ikx} \tag{9.9}$$

Yet, the boundary conditions are now:

$$\begin{aligned} p(x=0) &= \bar{p} \\ v_x(x=\ell) &= 0 \end{aligned} \tag{9.10}$$

or

$$\begin{aligned} p^+ + p^- &= \bar{p} \\ p^+e^{-ik\ell} - p^-e^{ik\ell} &= 0 \end{aligned} \tag{9.11}$$

The solution of this system of equations yields values of p^+ and p^- that, inserted in the expression for $p(\omega, x)$, give the pressure and velocity fields in a tube excited by a pressure source:

$$p(\omega, x) = \bar{p}\frac{\cos k\,(\ell - x)}{\cos k\ell} \tag{9.12}$$

$$v(\omega, x) = \frac{i\bar{p}}{\rho c}\frac{\sin k\,(\ell - x)}{\cos k\ell} \tag{9.13}$$

Under this new condition, the pressure tends to infinity when $\cos k\ell$ tends to zero which occurs when:

$$k\ell = (2n-1)\frac{\pi}{2} \Leftrightarrow f = (2n-1)\frac{c}{4\ell} \Leftrightarrow \ell = (2n-1)\frac{\lambda}{4} \tag{9.14}$$

Resonance now appears whenever the tube length equals an odd integer multiple of quarter-wavelength.

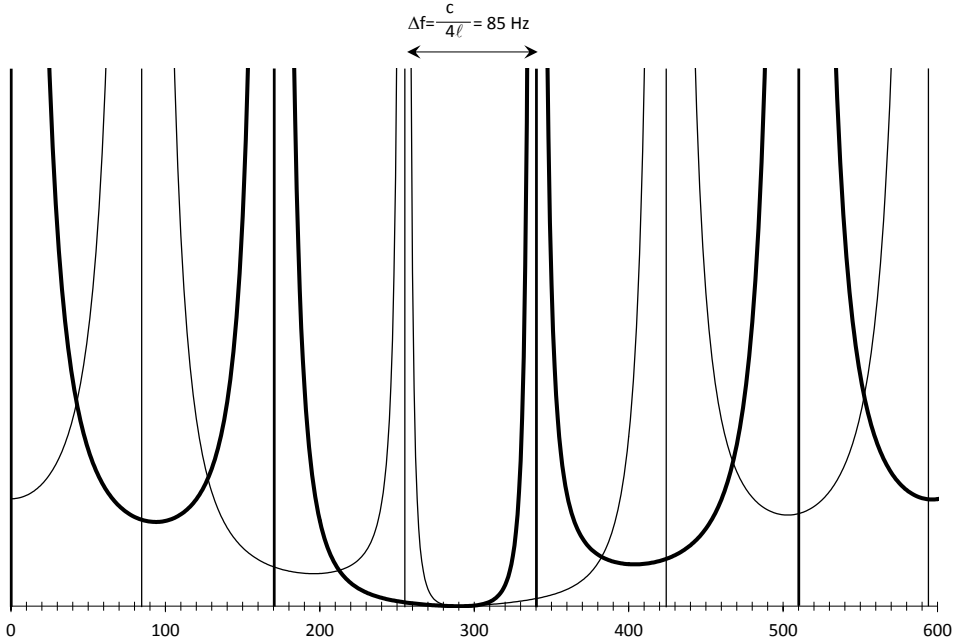

Figure 9.2: Frequency response of acoustic pressure in a closed tube (length $\ell = 1$ m, speed of sound $c = 340$ m/s, pressure is calculated at $x = \frac{\sqrt{2}}{2}$). Bold line: velocity source. Thin line: pressure source.

9.1.3 Comparison of the pressure and velocity sources

The impedance Z is an intrinsic property of the closed tube and is the same for both pressure and velocity sources:

$$Z(\omega, x = 0) = \frac{p(\omega, x = 0)}{v(\omega, x = 0)} = -i\rho c \frac{\cos k\ell}{\sin k\ell} \tag{9.15}$$

The resonance frequencies depend on the properties of the tube *and* the nature of the source. When comparing the velocity- and pressure-stimulated eigenfrequencies derived in Equations 9.7 and 9.14, we realise that they are separated by an interval of $\frac{c}{4\ell}$ as illustrated in Figure 9.2, which gives the sound spectrum in the tube. To understand the difference between the two sources, we need to investigate the cause of the infinite pressure at resonance.

Consider first the case of the velocity source. The incident field generated by the source ($p_i e^{-ikx}$) interferes with the reflected field at the left end of the tube ($p_i e^{+ikx}$). The incident and reflected fields also interfere with the *reflection of the reflection* on the piston ($p_i e^{-ikx}$). This pattern repeats through many higher order reflections. The successive reflections interfere in a globally *destructive* manner and the magnitude of the pressure field remains finite. At the resonance frequency, however, they all interfere *constructively* and the magnitude of the acoustic pressure field tends to infinity. Constructive interference occurs when the length of the return trip (down the tube and back) is a multiple of the wavelength. Resonance therefore occurs when the length of the tube is an integer number of half-wavelength.

In the pressure source case the incident wave ($p_i e^{-ikx}$) is reflected at the right end ($p_i e^{+ikx}$). However this reflected wave is itself reflected on the source with a 180-degree phase shift ($-p_i e^{-ikx}$). The *reflection of the reflection* is only synchronised with the incident field if the length of the return trip is an odd number of half-wavelength. Resonance therefore occurs when the length of the tube is equal to an odd number of quarter-wavelength. In a certain sense we can say that the reflection on the pressure source instantaneously adds half a wavelength to the propagation distance.

Note: the concept of pressure and velocity sources will be discussed in more detail in Section 10.4.1 where the concept of *source impedance* is presented.

9.2 Eigenmodes and eigenfrequencies

Tube closed at both ends

Consider a rigid tube that is capped at both ends. There is no excitation and the boundary conditions are:

$$\begin{aligned} p^+ - p^- &= 0 \\ p^+ e^{-ik\ell} - p^- e^{ik\ell} &= 0 \end{aligned} \tag{9.16}$$

This system of two equations can be satisfied by the trivial solution $p^+ = p^- = 0$, but also, more interestingly, when $p^+ = p^-$ and $e^{-ik\ell} = e^{ik\ell}$. The last condition is met when:

$$\sin k\ell = 0 \Leftrightarrow k\ell = n\pi \Leftrightarrow f = n\frac{c}{2\ell} \Leftrightarrow \ell = n\frac{\lambda}{2} \tag{9.17}$$

Resonance frequencies are therefore frequencies where an acoustic field may exist even without any source. In practical terms, these are frequencies at which a sound can persist indefinitely even after the source has been switched off.

The pressure distributions in the tube at the n^{th} resonance frequency is defined by:

$$p_n(x) = A\cos\frac{n\pi x}{\ell} \tag{9.18}$$

where A is a scaling coefficient and $p_n(x)$ is the normal mode corresponding to the natural frequencies $f = \frac{nc}{2\ell}$.

Tube open on one side and closed on the other

At low frequency, an open end may be approximated by a zero pressure condition. The boundary conditions for the acoustic field in a tube open at its left end and rigidly closed at its right end are:

$$\begin{aligned} p(x=0) &= 0 \\ v_x(x=\ell) &= 0 \end{aligned} \tag{9.19}$$

or:

$$\begin{aligned} p^+ + p^- &= 0 \\ \frac{1}{\rho c}\left(p^+ e^{-ik\ell} - p^- e^{ik\ell}\right) &= 0 \end{aligned} \tag{9.20}$$

which is satisfied by the trivial solution $p^+ = p^- = 0$ and where $p^+ = p^-$ and $e^{-ik\ell} + e^{ik\ell} = 0$. The last condition is met when:

$$\begin{aligned} \cos k\ell = 0 \Leftrightarrow k\ell &= (2n-1)\frac{\pi}{2} \\ \Leftrightarrow f = (2n-1)\frac{c}{4\ell} \Leftrightarrow \ell &= (2n-1)\frac{\lambda}{4} \end{aligned} \tag{9.21}$$

The corresponding natural modes are:

$$p = A \sin \frac{(2n-1)\pi x}{2\ell} \tag{9.22}$$

Tube open on both sides

For a tube open on both ends, the boundary conditions are:

$$\begin{aligned} p(x=0) &= 0 \\ p(x=\ell) &= 0 \end{aligned} \tag{9.23}$$

or:

$$\begin{aligned} p^+ + p^- &= 0 \\ p^+ e^{-ik\ell} + p^- e^{ik\ell} &= 0 \end{aligned} \tag{9.24}$$

which is satisfied by the trivial solution $p^+ = p^- = 0$ and where $p^+ = p^-$ and $e^{-ik\ell} = e^{ik\ell}$. The last condition is met when:

$$\sin k\ell = 0 \Leftrightarrow k\ell = n\pi \Leftrightarrow f = n\frac{c}{2\ell} \Leftrightarrow \ell = n\frac{\lambda}{2} \tag{9.25}$$

The corresponding natural modes are:

$$p = A \sin \frac{n\pi x}{\ell} \tag{9.26}$$

The natural modes of the closed-closed, closed-open and open-open tubes are presented in Figure 9.3.

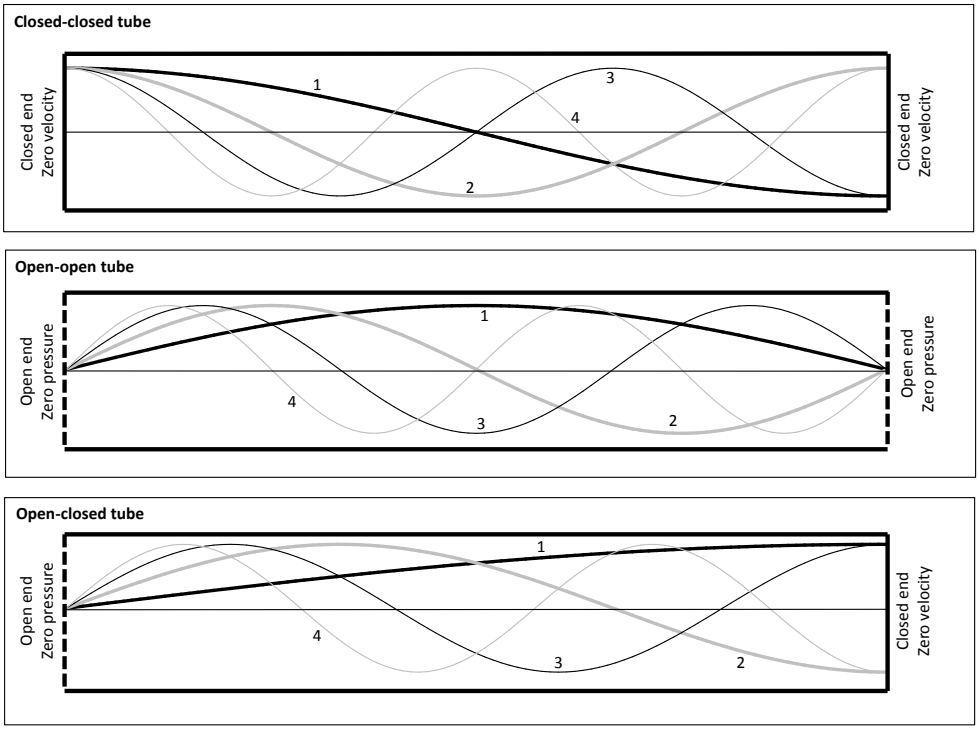

Figure 9.3: Pressure distribution of the first four natural modes of closed-closed, open-closed and open-open tubes.

9.3 Modal superposition

The pressure in a tube that is closed on the right and excited by a velocity source on the left is given by:

$$p(\omega, x) = -i\rho c\bar{v}\frac{\cos k\,(\ell - x)}{\sin k\ell} \tag{9.27}$$

This pressure distribution can be approximated by a linear combination of the natural modes of the closed-closed tube:

$$p(\omega, x) \simeq \sum_{n=1}^{\infty} A_n(\omega)\cos\frac{n\pi x}{\ell} \tag{9.28}$$

To find the modal participation factors A_n, multiply both sides by $\cos\frac{m\pi x}{\ell}$ and integrate over the interval $[0, \ell]$. Considering that the integral:

$$\int_0^\ell \cos\frac{m\pi x}{\ell}\cos\frac{n\pi x}{\ell}dx \tag{9.29}$$

is equal to zero when $m \neq n$, to $\frac{\ell}{2}$ when $m = n \neq 0$ and to ℓ when $m = n = 0$, we find:

$$A_0(\omega) = \frac{-i\rho c\bar{v}}{\sin k\ell}\int_0^\ell \cos k\,(\ell - x)dx = \frac{-i\rho c\bar{v}}{k\ell} \tag{9.30}$$

$$\begin{aligned} A_m(\omega) &= \frac{-2i\rho c\bar{v}}{\ell \sin k\ell}\int_0^\ell \cos k\,(\ell - x)\cos\frac{m\pi x}{\ell}dx \\ &= \frac{-i\rho c\bar{v}}{\sin k\ell}\left(\frac{\sin k\ell + \sin m\pi}{k\ell + m\pi} + \frac{\sin k\ell - \sin m\pi}{k\ell - m\pi}\right) \end{aligned} \tag{9.31}$$

Figure 9.4 shows the exact pressure field and its approximation by modal superposition. The modal development quickly converges towards the exact solution except at $x = 0$. The individual modes were indeed calculated with a zero velocity condition at $x = 0$ and are unable to superimpose to the non-zero normal velocity value $\bar{v}$. Non-convergence at $x = 0$ is even more pronounced in the velocity field shown in Figure 9.5.

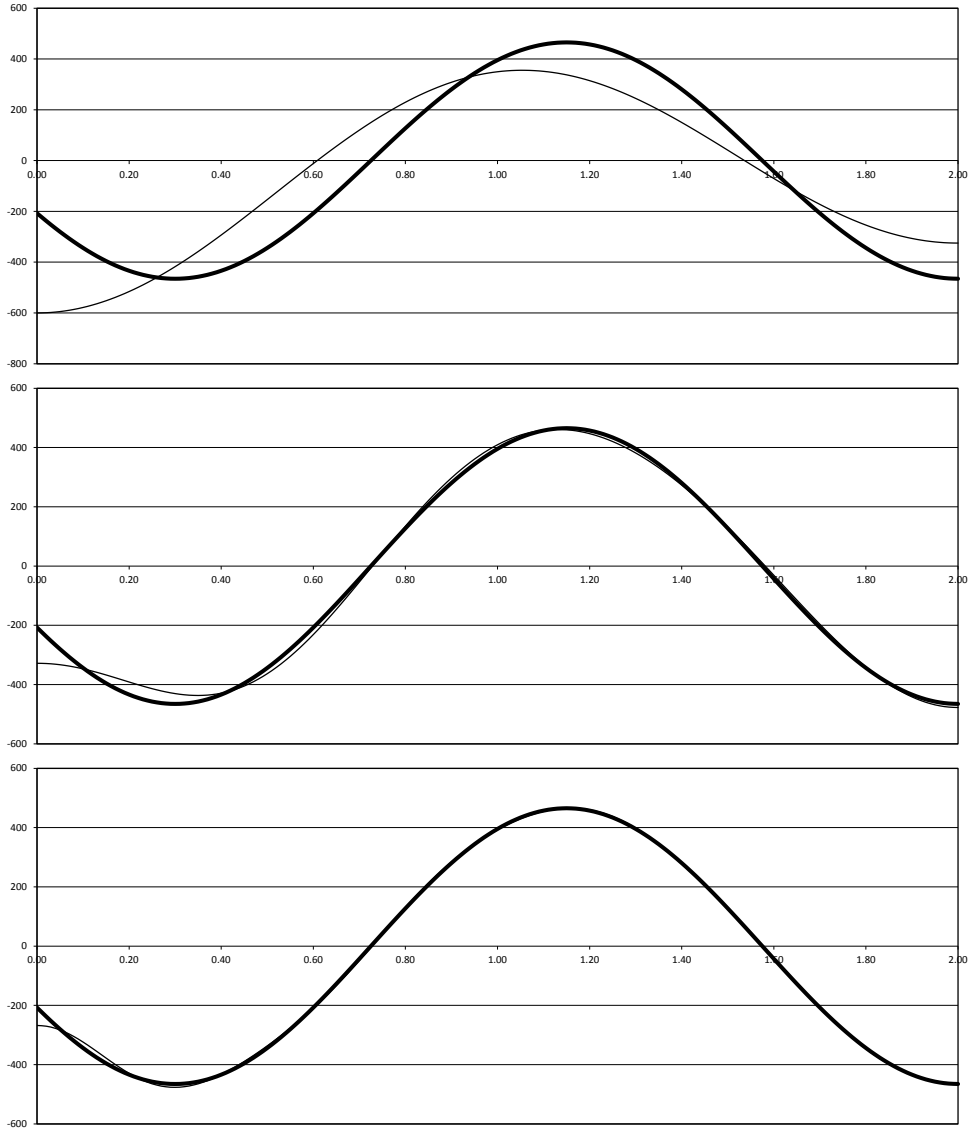

Figure 9.4: Pressure distribution in a tube ($\ell = 2$ m, $f = 200$ Hz, $\bar{v} = 1$ m/s): comparison of the exact and modal superposition solution (top: 2 modes, middle: 5 modes, bottom: 10 modes).

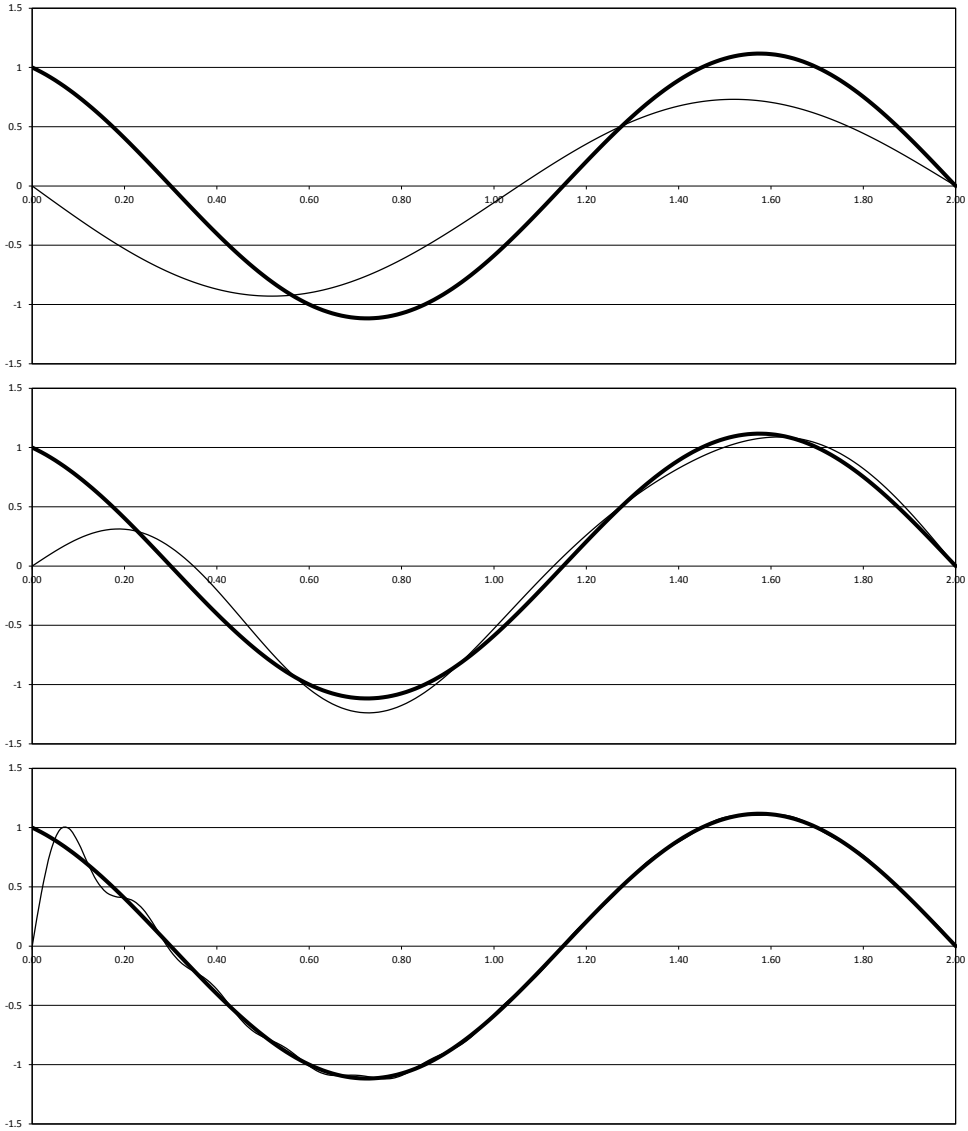

Figure 9.5: Velocity distribution in a tube ($\ell = 2$ m, $f = 200$ Hz, $\bar{v} = 1$ m/s): comparison of the exact and modal superposition solution (top: 2 modes, middle: 5 modes, bottom: 10 modes).

9.4 Box-shaped cavity

To calculate the resonance of a box-shaped cavity with rigid walls of dimensions $a \times b \times d$, we need to consider the three-dimensional Helmholtz equation:

$$\frac{\partial^2 p}{\partial x^2} + \frac{\partial^2 p}{\partial y^2} + \frac{\partial^2 p}{\partial z^2} + k^2 p = 0 \tag{9.32}$$

with the following boundary conditions:

$$\begin{aligned} \left[\frac{\partial p}{\partial x}\right]_{x=0} &= \left[\frac{\partial p}{\partial x}\right]_{x=a} = 0 \\ \left[\frac{\partial p}{\partial y}\right]_{y=0} &= \left[\frac{\partial p}{\partial y}\right]_{y=b} = 0 \\ \left[\frac{\partial p}{\partial z}\right]_{z=0} &= \left[\frac{\partial p}{\partial z}\right]_{z=d} = 0 \end{aligned} \tag{9.33}$$

This problem admits the trivial solution $p = 0$ and solutions of the form:

$$A \cos k_x x \cos k_y y \cos k_z z \tag{9.34}$$

provided that:

$$k_x^2 + k_y^2 + k_z^2 = k^2 \tag{9.35}$$

They comply with the boundary conditions if the three wave numbers can be expressed as follows:

$$\begin{aligned} k_x &= i\frac{\pi}{a} \\ k_y &= j\frac{\pi}{b} \\ k_z &= m\frac{\pi}{d} \end{aligned} \tag{9.36}$$

Each triplet (i, j, m) corresponds to a specific mode:

$$\phi_{ijm} = \cos\frac{i\pi x}{a} \cos\frac{j\pi y}{b} \cos\frac{m\pi z}{d} \tag{9.37}$$

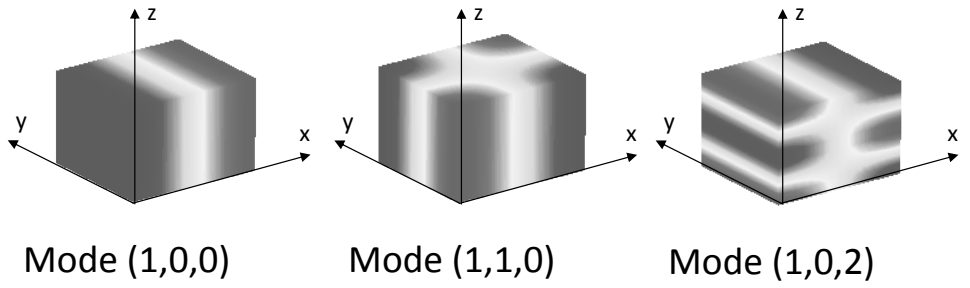

Figure 9.6: Three modes of a box-shaped cavity.

whose natural frequency is given by:

$$f_{ijm} = \frac{kc}{2\pi} = \frac{c}{2}\sqrt{\left(\frac{i}{a}\right)^2 + \left(\frac{j}{b}\right)^2 + \left(\frac{m}{d}\right)^2} \tag{9.38}$$

Figure 9.6 exemplifies the pressure distribution of such modes in a rectangular cavity.

Zero-frequency mode

The natural mode corresponding to $i = j = m = 0$ is characterised by a constant pressure distribution and a zero resonance frequency. It is the acoustic equivalent of the *rigid body modes* encountered in structural dynamics. The high acoustic response at low frequency visible in Figure 9.2 results from that constant pressure mode.

9.5 Resonance of an arbitrary cavity

The resonance of an arbitrarily shaped cavity can be calculated using the finite element method. Consider a domain Ω with a rigid boundary. The system of equations resulting from the finite element discretisation of Ω is written as:[1]

$$\left[K + i\omega C - \omega^2 M\right](p(\omega)) = (F(\omega)) \tag{9.39}$$

where K, C and M are the respective stiffness, damping and mass matrices, p the vector of unknown nodal acoustic pressure values and F the excitation vector. Without damping and excitation, the system simplifies to:

$$\left[K - \omega^2 M\right](p(\omega)) = 0 \tag{9.40}$$

This homogeneous system has non-trivial solutions for a discrete set of values $\omega = \omega_i$ called eigenvalues. Each eigenvalue associates with a specific pressure distribution ϕ_i called eigenmode. The corresponding natural frequencies are $f_i = \omega_i/2\pi$. For example, Figure 9.7 depicts an acoustic mode of the inner cavity of an automotive air conditioning unit which was computed using the finite element method.

[1] The principles of the finite element method are considered as known. Only a high-level description of the acoustic modal analysis using finite element analysis (FEA) is given here.

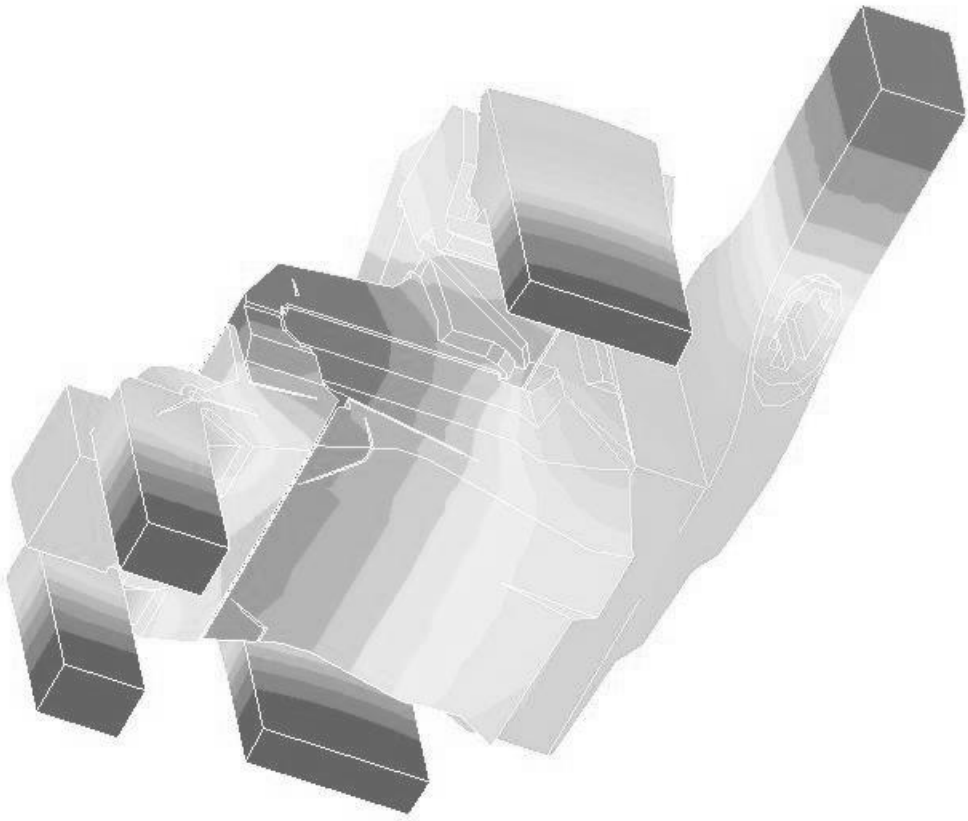

Figure 9.7: Acoustic mode of the inner cavity of an air-conditioning unit with a resonance frequency of 444 Hz.

10

Guided propagation

Contents

10.1 Cutoff frequency 202
10.2 Transfer matrices 204
10.3 Transmission Loss (TL) 218
10.4 Insertion Loss (IL) 222
10.5 Circular ducts 226
10.6 Role of evanescent modes 230
10.7 Reactive and dissipative silencers 238

We now study the propagation of sound in ducts (e.g. engine air intake, exhaust, air conditioning ducts). We first demonstrate that, below the *cutoff* frequency, sound in the duct only propagates as plane waves. We then see how the propagation of plane waves in various kinds of duct configurations can be characterised by a simple transfer matrix. The concepts of *transmission loss* and *insertion loss* are then presented.

10.1 Cutoff frequency

Consider a tube of rectangular cross section ($a \times b$). The walls are rigid. The acoustic field in the tube obeys the Helmholtz equation:

$$\frac{\partial^2 p}{\partial x^2} + \frac{\partial^2 p}{\partial y^2} + \frac{\partial^2 p}{\partial z^2} + k^2 p = 0 \tag{10.1}$$

with the following boundary conditions:

$$\begin{aligned} \left[\frac{\partial p}{\partial x}\right]_{x=0} &= \left[\frac{\partial p}{\partial x}\right]_{x=a} = 0 \\ \left[\frac{\partial p}{\partial y}\right]_{y=0} &= \left[\frac{\partial p}{\partial y}\right]_{y=b} = 0 \end{aligned} \tag{10.2}$$

Any function of the form:

$$A \cos k_x x \cos k_y y e^{ik_z z} \tag{10.3}$$

is a solution of the equation, provided that:

$$k_x^2 + k_y^2 + k_z^2 = k^2 \tag{10.4}$$

and satisfies the boundary conditions if the two wavenumbers k_x and k_y are of the form:

$$\begin{aligned} k_x &= m\frac{\pi}{a} \\ k_y &= n\frac{\pi}{b} \end{aligned} \tag{10.5}$$

k_z is then obtained from the dispersion law:

$$k_z = \sqrt{k^2 - \frac{m^2\pi^2}{a^2} - \frac{n^2\pi^2}{b^2}} \tag{10.6}$$

Two situations may occur:

1. If k_z is real, the solution represents a wave: the mode (m,n) is said to be *propagative*.

2. If k_z is imaginary, the solution becomes ($k_z = ik_i$):

$$A \cos k_x x \cos k_y y e^{-k_i z} \tag{10.7}$$

   which represents a pressure distribution whose amplitude exponentially decreases with distance. The wave is *evanescent* and the mode (m,n) is *non-propagative* (see figure 10.1).

A different *cutoff frequency* f_{mn} is associated with each value of (m, n). Mode (m, n) propagates at frequencies higher than f_{mn} and is evanescent below that frequency. For rectangular cross section ducts, the cutoff frequency is given by:

$$f_{mn} = \sqrt{\frac{m^2c^2}{4a^2} + \frac{n^2c^2}{4b^2}} \tag{10.8}$$

A plane wave mode ($m = n = 0$) has a zero cutoff frequency ($f_{mn} = 0$) and propagates at all frequencies. The lowest non-zero cutoff frequency corresponds to mode (1,0) (assuming $a > b$):

$$f_{10} = \frac{c}{2a} \tag{10.9}$$

This frequency sets a limit to the transfer matrix method presented below. This method indeed assumes that the acoustic field may be described, at each and every point in the system, by a plane wave. To give an order of magnitude, consider a duct whose largest section has a width of 5 cm. The plane wave approximation is valid up to the first cutoff frequency ($f_{10} = 3,400\ Hz$).

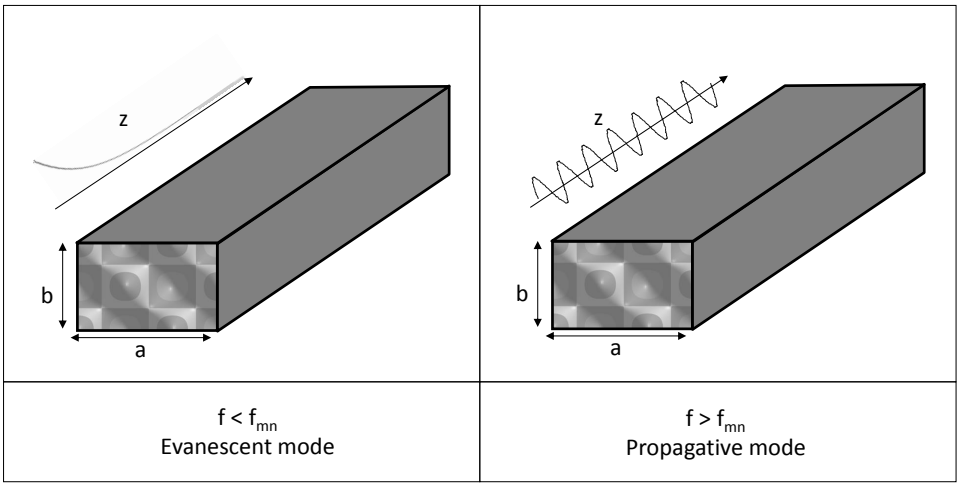

Figure 10.1: Cutoff frequency: evanescent and propagating modes.

10.2 Transfer matrices

10.2.1 Constant cross section ducts

Consider a plane wave propagating in a tube of length ℓ and constant cross section area S. The acoustic field in the *inlet* section is entirely characterised by the local acoustic pressure and velocity (p_e, v_e). Similarly, in the *outlet* section, the acoustic field is described by the couple (p_s, v_s). The fields in the inlet and outlet sections are linearly related:

$$\begin{aligned} p_e &= Ap_s + Bv_s \\ v_e &= Cp_s + Dv_s \end{aligned} \tag{10.10}$$

The matrix:

$$\begin{pmatrix} A & B \\ C & D \end{pmatrix} \tag{10.11}$$

is called the *transfer matrix* of the duct. Its coefficients can be calculated by considering two different sets of boundary conditions. We first choose to close the duct:

$$\begin{aligned} v_e &= 1 \\ v_s &= 0 \end{aligned} \tag{10.12}$$

In that case:

$$\begin{aligned} A &= \frac{p_e}{p_s} \\ C &= \frac{1}{p_s} \end{aligned} \tag{10.13}$$

but we know the analytical solution associated with a closed duct excited by an oscillating piston (Equation 9.5 with $\bar{v} = 1$):

$$p = -i\rho c \frac{\cos k(\ell - x)}{\sin k\ell} \tag{10.14}$$

We use it to calculate p_e and p_s and then to find A and C:

$$\begin{aligned} A &= \cos k\ell \\ C &= \frac{i}{\rho c} \sin k\ell \end{aligned} \tag{10.15}$$

The other set of boundary conditions is:

$$\begin{aligned} v_e &= 1 \\ p_s &= 0 \end{aligned} \tag{10.16}$$

In that case:

$$\begin{aligned} B &= \frac{p_e}{v_s} \\ D &= \frac{1}{v_s} \end{aligned} \tag{10.17}$$

The solution to this problem is also known (Equation 8.62 with $\bar{v} = 0$):

$$p = i\rho c \frac{\sin k(\ell - x)}{\cos k\ell} \tag{10.18}$$

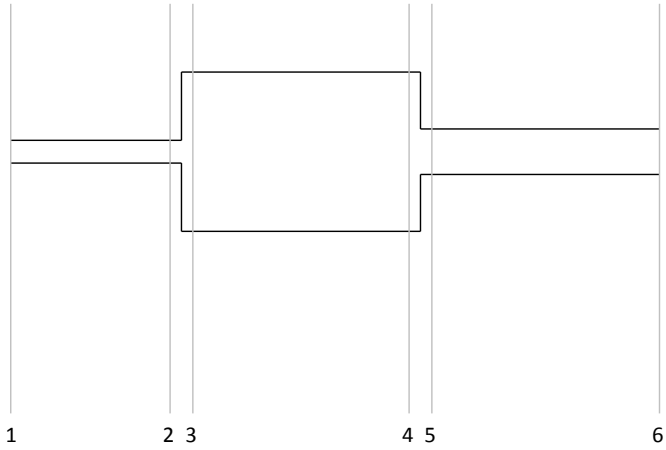

Figure 10.2: Three connected ducts.

We use it to calculate v_e and p_s and to find B and D:

$$\begin{aligned} B &= i\rho c \sin k\ell \\ D &= \cos k\ell \end{aligned} \tag{10.19}$$

The transfer matrix of a tube of constant cross section is therefore:

$$\begin{pmatrix} \cos k\ell & i\rho c \sin k\ell \\ \frac{i \sin k\ell}{\rho c} & \cos k\ell \end{pmatrix} \tag{10.20}$$

10.2.2 Transfer matrix of three connected ducts

Consider three connected ducts (Figure 10.2). They have length ℓ_a, ℓ_b and ℓ_c and cross-sectional area S_a, S_b and S_c. Sections 2 and 3 are located just before and after the cross section discontinuity between the first and second ducts. Sections 4 and 5 are located just before and after the cross section discontinuity between the second and third ducts. The transfer matrices linking pressure and velocity amplitudes in section 1 and 2, 3 and 4 and 5

and 6 are those calculated in the previous section:

$$T_{12} = \begin{pmatrix} \cos k\ell_a & i\rho c \sin k\ell_a \\ \frac{i \sin k\ell_a}{\rho c} & \cos k\ell_a \end{pmatrix} \tag{10.21}$$

$$T_{34} = \begin{pmatrix} \cos k\ell_b & i\rho c \sin k\ell_b \\ \frac{i \sin k\ell_b}{\rho c} & \cos k\ell_b \end{pmatrix} \tag{10.22}$$

$$T_{56} = \begin{pmatrix} \cos k\ell_c & i\rho c \sin k\ell_c \\ \frac{i \sin k\ell_c}{\rho c} & \cos k\ell_c \end{pmatrix} \tag{10.23}$$

The acoustic variables in sections 2 and 3 are related by:

$$\begin{aligned} p_2 &= p_3 \\ S_a v_2 &= S_b v_3 \end{aligned} \tag{10.24}$$

The transfer matrix associated with a change in cross section ($S_a \rightarrow S_b$) is therefore:

$$T_{23} = \begin{pmatrix} 1 & 0 \\ 0 & \frac{S_b}{S_a} \end{pmatrix} \tag{10.25}$$

Similarly we have:

$$T_{45} = \begin{pmatrix} 1 & 0 \\ 0 & \frac{S_c}{S_b} \end{pmatrix} \tag{10.26}$$

We can calculate the transfer matrix of the entire three-duct system by multiplying the five transfer matrices:

$$\begin{pmatrix} p_1 \\ v_1 \end{pmatrix} = T_{12} \cdot T_{23} \cdot T_{34} \cdot T_{45} \cdot T_{56} \cdot \begin{pmatrix} p_6 \\ v_6 \end{pmatrix} = T_{16} \cdot \begin{pmatrix} p_6 \\ v_6 \end{pmatrix} \tag{10.27}$$

This example illustrates the basic principles of the transfer matrix method:

- the system is broken down into elementary components for which transfer matrices are known;
- the global transfer matrix is calculated as the product of elementary matrices.

The fundamental hypothesis of the method is that the acoustic field is a plane wave at every point along the propagation path. This hypothesis is valid as long as frequency remains below the lowest cutoff frequency of the system.

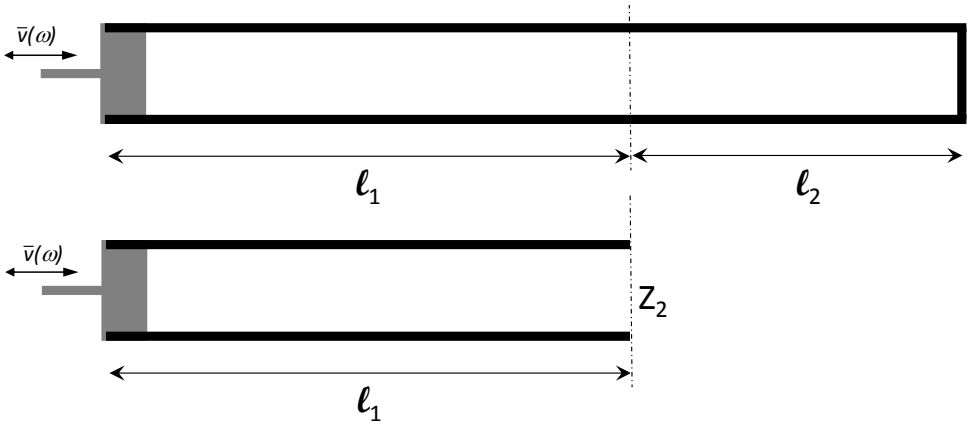

Figure 10.3: Thévenin's theorem applied to a closed duct excited by a velocity source.

10.2.3 T-connection

Thévenin's theorem

In electricity, the theorem of Thévenin[1] splits a circuit in two parts: the *active* part includes the source and a set of components (resistors, capacitors, inductors) while the *passive* part contains another set of components. As far as the active part is concerned (difference of potential between two points, intensity in each branch of the circuit), the passive part can be replaced by an equivalent impedance that is both complex and frequency dependent.

This theorem also applies to one-dimensional acoustic fields (plane wave). Consider again the problem of a closed duct excited by a piston. We divide the tube into two parts of lengths ℓ_1 and ℓ_2 ($\ell_1 + \ell_2 = \ell$, see figure 10.3). We know (Equation 9.15) that the impedance of the right side is given by:

$$Z_2 = Z(\omega, x = \ell_2) = -i\rho c \frac{\cos k\ell_2}{\sin k\ell_2} \tag{10.28}$$

[1] **Léon Charles Thévenin**, a French electrical engineer, was born in Meaux in 1857 and died in Paris in 1926.

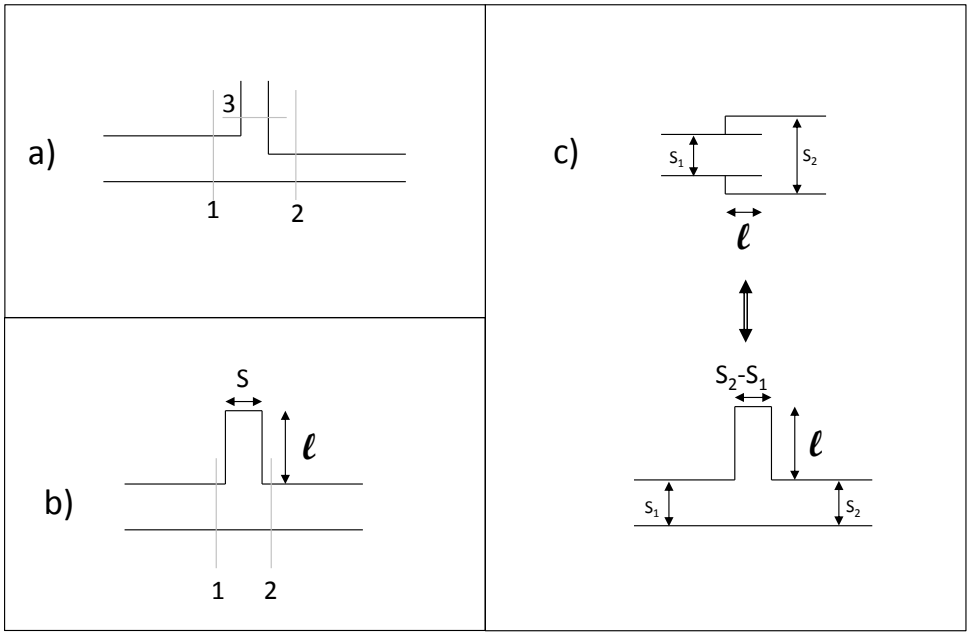

Figure 10.4: T-connections.

The acoustic field in a tube of length ℓ_1 excited by a velocity source and closed by a surface carrying an impedance Z_2 is given by (Equation 8.61):

$$p = i\rho c\bar{v}\frac{\sin k(\ell_1 - x) - iz\cos k(\ell_1 - x)}{\cos k\ell_1 + i\frac{Z_2}{\rho c}\sin k\ell_1} \tag{10.29}$$

Substituting Equation 10.28 into Equation 10.29 we find, after some calculations:

$$p(\omega, x) = -i\rho c\bar{v}\frac{\cos k\left(\ell - x\right)}{\sin k\ell} \tag{10.30}$$

This is identical to Equation 9.5. Seen from the left side of the tube, the two problems shown in Figure 10.3 are strictly equivalent. This important result will be used in the following section.

Transfer matrix of a T-connection

Consider the T-connection shown in Figure 10.4a. We can write the following relations between pressure and velocity in the different sections (that we consider infinitely close to each other):

$$\begin{aligned} p_1 &= p_2 = p_3 \\ S_1 v_1 &= S_2 v_2 + S_3 v_3 \end{aligned} \tag{10.31}$$

If branch 3 is connected to a component characterised by its impedance Z_3, we can write the second relation in the form:

$$v_1 = \frac{S_2}{S_1} v_2 + \frac{S_3}{Z_3 S_1} p_2 \tag{10.32}$$

The transfer matrix linking sections 1 and 2 is therefore:

$$\begin{pmatrix} p_1 \\ v_1 \end{pmatrix} = \begin{pmatrix} 1 & 0 \\ \frac{S_3}{Z_3 S_1} & \frac{S_2}{S_1} \end{pmatrix} \begin{pmatrix} p_2 \\ v_2 \end{pmatrix} \tag{10.33}$$

10.2.4 Quarter-wavelength resonator

Consider the case of a duct with a constant cross section connected to a resonator of length ℓ and cross section S (Figure 10.4b). The impedance of the resonator is given by:

$$Z_3 = -i\rho c \frac{\cos k\ell}{i \sin k\ell} \tag{10.34}$$

The transfer matrix between two sections located upstream and downstream of the resonator is given by:

$$\begin{pmatrix} p_1 \\ v_1 \end{pmatrix} = \begin{pmatrix} 1 & 0 \\ i \frac{S}{\rho c S_1} \tan k\ell & \frac{S_2}{S_1} \end{pmatrix} \begin{pmatrix} p_2 \\ v_2 \end{pmatrix} \tag{10.35}$$

But $Z_3 = 0$ when $\ell = \lambda/4$. In this case, the wave entering the resonator propagates over a quarter-wavelength, is reflected and then returns to its starting point after travelling another quarter-wavelength. Both the original

signal and the signal that travelled up and down the resonator have the same magnitude, but they are shifted by 180°. They therefore cancel each other out (Figure 10.5). These devices, named *quarter-wavelength resonators*, are frequently used in industry (Figure 10.6). A tube whose end extends into a larger tube (Figure 10.4c) is a particular example of quarter-wavelength resonator (cross section: $S_2 - S_1$, length: ℓ).

10.2.5 Helmholtz resonator

A Helmholtz resonator is an air cavity with volume V, a small neck of cross-sectional area S and height h (Figure 10.7). At low frequency, the resonator behaves as a mass-spring system where the air in the cavity is the mass-element ($m = \rho h S$) and the air in the neck is the spring-element. The spring stiffness k is evaluated by calculating the pressure rise in the cavity Δp due to a small displacement δ of the air in the neck:

$$\Delta p = \kappa \frac{\Delta V}{V} = \kappa \frac{\delta \cdot S}{V} \tag{10.36}$$

where $\kappa = \rho c^2$ is the air compressibility modulus. Stiffness is the ratio between the spring restoring force ($F = S\Delta p$) and the displacement δ:

$$k = \frac{F}{\delta} = \frac{\rho c^2 S^2}{V} \tag{10.37}$$

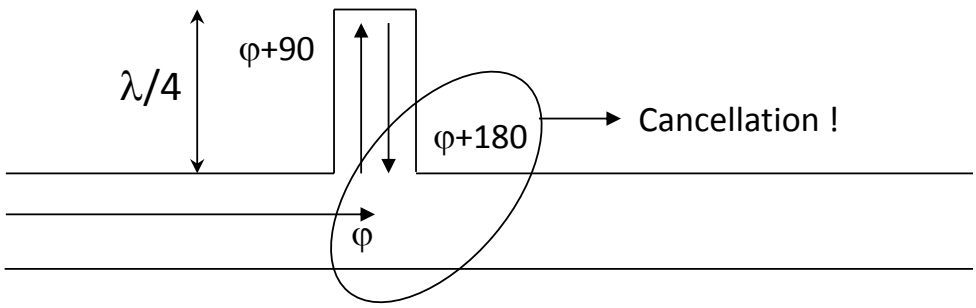

Figure 10.5: Principles of the quarter-wavelength resonator.

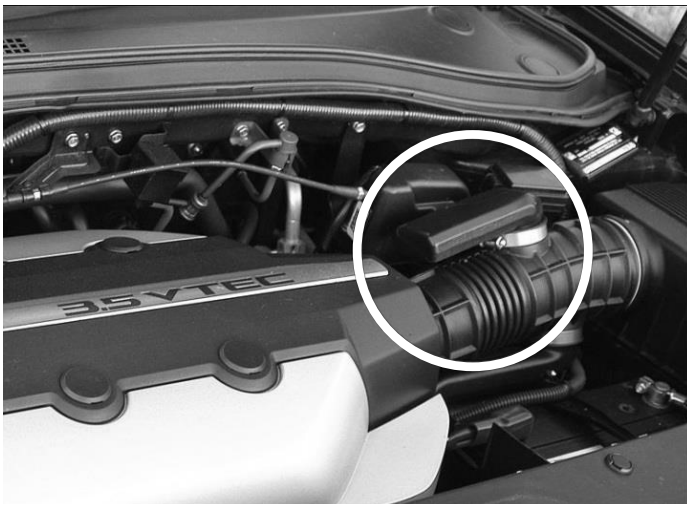

Figure 10.6: Quarter-wavelength resonator in the air intake circuit of a car engine.

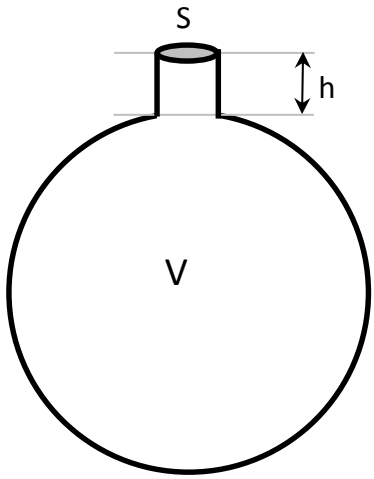

Figure 10.7: Helmholtz resonator.

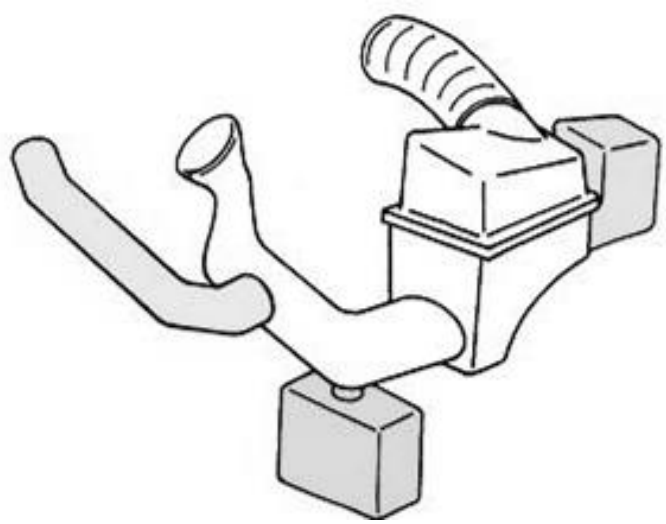

Figure 10.8: Helmholtz resonator in the air intake circuit of a car engine.

The resonance frequency of this mass-spring system is given by:

$$f_{res} = \frac{1}{2\pi}\sqrt{\frac{k}{m}} = \frac{c}{2\pi}\sqrt{\frac{S}{hV}} \tag{10.38}$$

The mechanical impedance (force over displacement) is:

$$Z_m = k - \omega^2 m = \frac{\rho c^2 S^2}{V} - \rho\omega^2 hS \tag{10.39}$$

If we connect a Helmholtz resonator to a duct, we locally impose an acoustic impedance (pressure over velocity):

$$Z_a = \frac{Z_m}{i\omega S} \tag{10.40}$$

This impedance is zero at the resonator's resonance. The resonator totally reflects the incident field towards the source: there is no transmitted field.

Dissipation in the resonator

To be accurate we should account for viscous dissipation (R_v) and for radiative loss (R_r) in the neck. The mechanical impedance of the resonator then has a real and an imaginary component:

$$Z_m = \left(\frac{\rho c^2 S^2}{V} - \rho \omega^2 h S \right) + i\omega \left(R_r + R_v \right) \tag{10.41}$$

Ingard[2] proposes the following expressions for R_r and R_v (a is the radius of the neck):

$$R_r = \frac{\rho c k^2 S^2}{2\pi} \tag{10.42}$$

$$R_v = 0.00166 \sqrt{f} \cdot S \cdot \frac{h + a}{\rho c a} \tag{10.43}$$

10.2.6 Alternative definitions of transfer matrices

We have assumed that the acoustic field is uniform in any cross section of the system. We can then characterise this field by three different pairs of variables:

- pressure p and velocity v as we have done until now;
- pressure p and acoustic flow $q = vS$ where S is the local cross-sectional area;
- the amplitudes p^+ and p^- of the forward and backward propagating waves.

A different definition of the transfer matrix is associated with each choice of variables:

$$\begin{pmatrix} p_e \\ v_e \end{pmatrix} = \begin{pmatrix} A & B \\ C & D \end{pmatrix} \begin{pmatrix} p_s \\ v_s \end{pmatrix} \tag{10.44}$$

[2] **Ingard U.**, *On the Theory and Design of Acoustic Resonators*, J. Acoust. Soc. Am. 25. 1037 (1953).

$$\begin{pmatrix} p_e \\ q_e \end{pmatrix} = \begin{pmatrix} A' & B' \\ C' & D' \end{pmatrix} \begin{pmatrix} p_s \\ q_s \end{pmatrix} \tag{10.45}$$

$$\begin{pmatrix} p_e^+ \\ p_e^- \end{pmatrix} = \begin{pmatrix} \alpha & \beta \\ \gamma & \delta \end{pmatrix} \begin{pmatrix} p_s^+ \\ p_s^- \end{pmatrix} \tag{10.46}$$

Each definition has its advantages: the first one is the most common, the second facilitates the handling of cross section changes (unit transfer matrix) while the third definition will be used to define an important property of a duct system, its *transmission loss*. One can easily switch from one definition to another. For example, we have:

$$\begin{aligned} A' &= A \\ B' &= \frac{B}{S_s} \\ C' &= S_e C \\ D' &= \frac{S_e}{S_s} D \end{aligned} \tag{10.47}$$

To find a relationship between the $[A, B, C, D]$ and $[\alpha, \beta, \gamma, \delta]$ coefficients, we note that:

$$p_e = p_e^+ + p_e^- \tag{10.48}$$

and

$$v_e = \frac{1}{\rho c}\left(p_e^+ - p_e^-\right) \tag{10.49}$$

from which we obtain, after a few calculations:

$$\begin{aligned} \alpha &= \frac{1}{2}\left(A + \frac{B}{\rho c} + \rho c C + D\right) \\ \beta &= \frac{1}{2}\left(A - \frac{B}{\rho c} + \rho c C - D\right) \\ \gamma &= \frac{1}{2}\left(A + \frac{B}{\rho c} - \rho c C - D\right) \\ \delta &= \frac{1}{2}\left(A - \frac{B}{\rho c} - \rho c C + D\right) \end{aligned} \tag{10.50}$$

10.2.7 Transfer matrix measurement procedure

The four coefficients of a transfer matrix can be measured by combining two sets of measurements obtained with two different impedance values (Z_a and Z_b) in the outlet section of the component. These impedances may, for example, correspond to open and closed conditions. The numerical values of these impedances does not need to be known. The method requires (Figure 10.9) two microphones (1 and 2) placed upstream of the inlet section (e) and two microphones (3 and 4) located downstream from the outlet section (s). The same distance δ separates sections 1 and 2, 2 and e, s and 3 and 3 and 4.

The pressures at the four microphones (p_1, p_2, p_3, p_4) are measured for the two different boundary conditions $(p_{1a}, p_{1b}, p_{2a}, \ldots)$. We can write the following relationships between the 8 measured pressures:

$$\begin{aligned}
p_{1a} &= p_{ea}^{+} e^{2ik\delta} + p_{ea}^{-} e^{-2ik\delta} \\
p_{2a} &= p_{ea}^{+} e^{ik\delta} + p_{ea}^{-} e^{-ik\delta} \\
p_{3a} &= p_{sa}^{+} e^{-ik\delta} + p_{sa}^{-} e^{ik\delta} \\
p_{4a} &= p_{sa}^{+} e^{-2ik\delta} + p_{sa}^{-} e^{2ik\delta} \\
p_{1b} &= p_{eb}^{+} e^{2ik\delta} + p_{eb}^{-} e^{-2ik\delta} \\
p_{2b} &= p_{eb}^{+} e^{ik\delta} + p_{eb}^{-} e^{-ik\delta} \\
p_{3b} &= p_{sb}^{+} e^{-ik\delta} + p_{sb}^{-} e^{ik\delta} \\
p_{4b} &= p_{sb}^{+} e^{-2ik\delta} + p_{sb}^{-} e^{2ik\delta}
\end{aligned} \tag{10.51}$$

Solving these two systems of four equations provides the amplitudes of the forward and backward propagating waves in the inlet and outlet sections for both configurations. With these, another system of four equations can be written. Solving the system gives the α, β, γ and δ coefficients:

$$\begin{aligned}
p_{ea}^{+} &= \alpha p_{sa}^{+} + \beta p_{sa}^{-} \\
p_{ea}^{-} &= \gamma p_{sa}^{+} + \delta p_{sa}^{-} \\
p_{eb}^{+} &= \alpha p_{sb}^{+} + \beta p_{sb}^{-} \\
p_{eb}^{-} &= \gamma p_{sb}^{+} + \delta p_{sb}^{-}
\end{aligned} \tag{10.52}$$

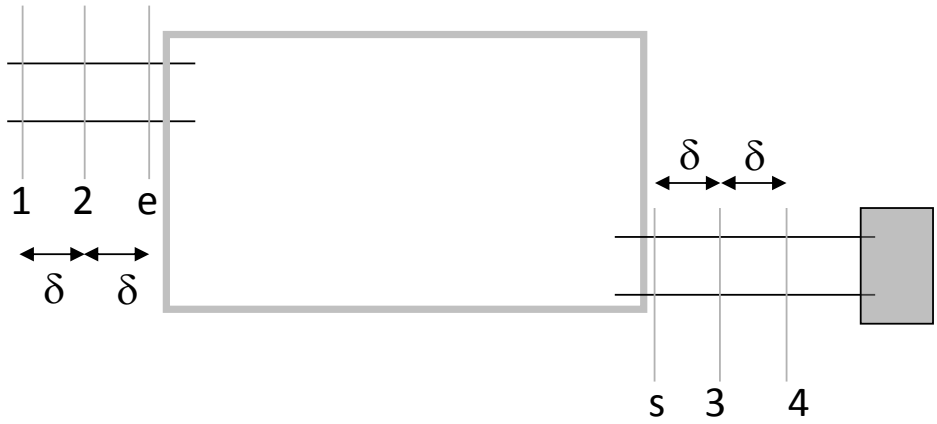

Figure 10.9: Measurement of the transfer matrix of a component using the four microphone technique: principle of the method.

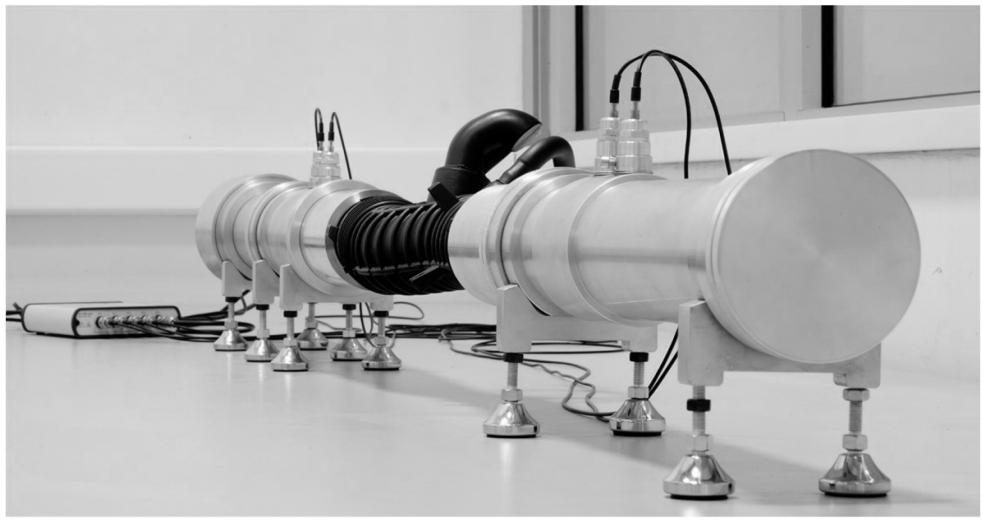

Figure 10.10: Measurement of the transfer matrix of a component using the four microphone technique: experimental set-up.

10.3 Transmission Loss (TL)

10.3.1 Definition

The α, β, γ and δ coefficients each have an important physical meaning. If the outlet section (s) is perfectly anechoic ($p_s^- = 0$), we have:

$$p_e^+ = \alpha p_s^+ \tag{10.53}$$

α therefore measures the ratio between the intensity leaving the system at section (s):

$$I_s^+ = \frac{|p_s|^{+2}}{2\rho c} \tag{10.54}$$

and the intensity entering at section (e):

$$I_e^+ = \frac{|p_e|^{+2}}{2\rho c} = |\alpha|^2 I_s^+ \tag{10.55}$$

The *transmission loss* (TL) is defined by:

$$TL = -10 \log \frac{I_s^+}{I_e^+} = 10 \log |\alpha|^2 = 20 \log \left[\frac{1}{2} |A + \frac{B}{\rho c} + \rho c C + D| \right] \tag{10.56}$$

The ratio of reflected to incident intensities (still assuming anechoic conditions in the outlet section) is given by:

$$\frac{I_e^-}{I_e^+} = \frac{|\gamma|^2}{|\alpha|^2} \tag{10.57}$$

In the case of a perfectly rigid termination ($p_s^+ = 0$), this ratio would be:

$$\frac{I_e^-}{I_e^+} = \frac{|\delta|^2}{|\beta|^2} \tag{10.58}$$

10.3.2 Transmission Loss of an expansion chamber

Consider a cylindrical cavity of cross section mS and length ℓ connected upstream and downstream to tubes of cross section S. The transfer matrix between the sections immediately upstream and downstream from the main cavity is given by:

$$\begin{aligned} T &= \begin{pmatrix} 1 & 0 \\ 0 & m \end{pmatrix} \cdot \begin{pmatrix} \cos k\ell & i\rho c \sin k\ell \\ \frac{i \sin k\ell}{\rho c} & \cos k\ell \end{pmatrix} \cdot \begin{pmatrix} 1 & 0 \\ 0 & \frac{1}{m} \end{pmatrix} \\ &= \begin{pmatrix} \cos k\ell & \frac{i\rho c}{m} \sin k\ell \\ \frac{im}{\rho c} \sin k\ell & \cos k\ell \end{pmatrix} \end{aligned} \tag{10.59}$$

and the transmission loss is (Figure 10.11):

$$TL = -10 \log \left[1 + \left(\frac{m^2 - 1}{2m} \sin k\ell \right)^2 \right] \tag{10.60}$$

As soon as the excitation frequency exceeds the lowest cutoff frequency of the system, the transmission loss is considerably affected by the presence of non-plane wave modes. Figure 10.12 shows the transmission loss of an expansion chamber comparing two calculations done with and without considering the contribution of non-plane wave modes.

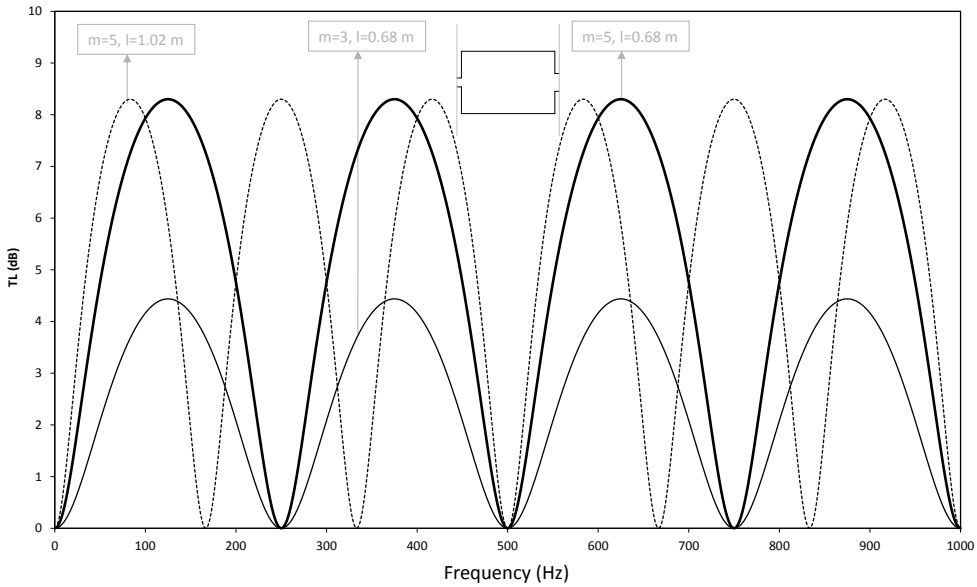

Figure 10.11: Transmission loss of an expansion chamber. The m coefficient influences the attenuation level. Length ℓ defines the set of frequencies where transmission is maximum or zero.

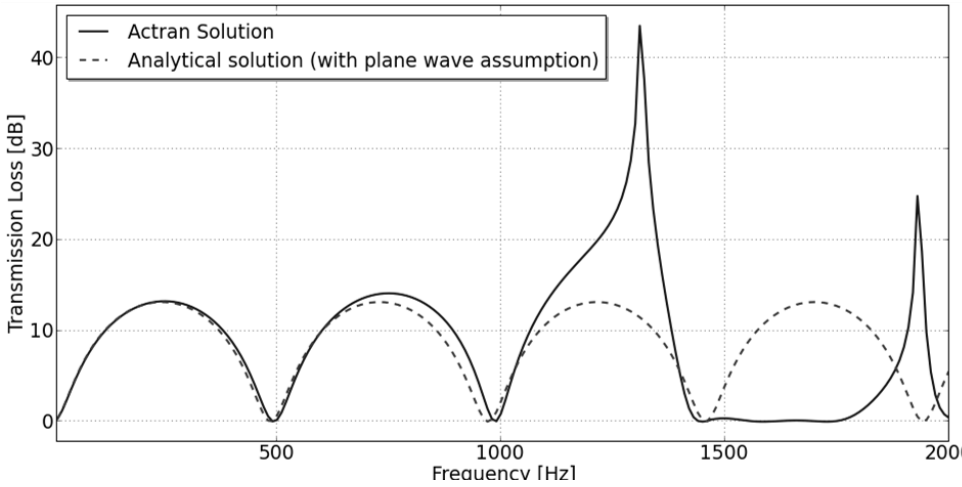

Figure 10.12: Effect of non-plane wave modes on the transmission loss of an expansion chamber: analytical (dashed line) and numerical solution (solid line). The two solutions start diverging at 1,000 Hz.

10.3.3 TL of a tube fitted with a resonator

Figure 10.13 compares the TL of a tube equipped with three different resonators of identical resonance frequency: two Helmholtz resonators of different dimensions and a quarter-wavelength resonator. We observe that:

- the frequency band in which the Helmholtz resonator is efficient is larger than that of the equivalent quarter-wavelength resonator;
- the frequency range in which a Helmholtz resonator is efficient depends, for a given resonance frequency, on the dimensions of the neck;
- Helmholtz resonators have a unique resonance,[3] while the quarter-wavelength resonator is resonant at all odd harmonics of its fundamental.

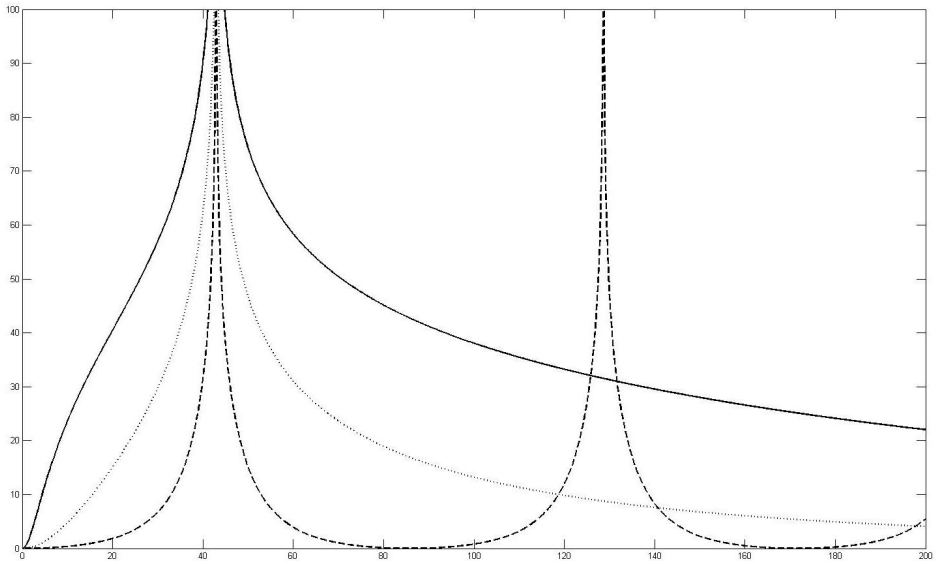

Figure 10.13: Comparison of the TL of a duct ($\ell = 1$) connected to three different resonators located halfway down the duct. Solid line: Helmholtz resonator (a=0.01, h=0.05, V=0.01, see Section 10.2.5). Dotted line: Helmholtz resonator (a=0.02, h=0.20, V=0.01). Dashed line: quarter-wavelength resonator. All resonate at 42.89 Hz.

[3] As long as the excitation frequency remains below the first resonance frequency of the resonator cavity. This is the normal working mode of a Helmholtz resonator.

10.4 Insertion Loss (IL)

We have seen that any silencer[4] can be described by a transfer matrix relating acoustic variables (p and v or p^+ and p^-) in the inlet and outlet cross sections. We now study the silencer inserted in its environment.

10.4.1 Source impedance

We place a general source upstream from the silencer. Pressure and velocity at the source are related by:

$$\frac{v_e}{\bar{v}} - \frac{p_e}{\bar{p}} = \bar{q} \tag{10.61}$$

$S = \frac{\bar{p}}{\bar{v}}$ is the impedance of the source. Note that when $\bar{q} = 0$, $\frac{p_e}{v_e} = S$. The special cases $\bar{p} = \infty$ and $\bar{v} = \infty$ respectively correspond to a velocity source ($v_e = \bar{q}\bar{v}$) and a pressure source ($p_e = -\bar{q}\bar{p}$).

10.4.2 Impedance matching

Suppose that the impedance of the acoustic system connected to the source is Z. We easily find that:

$$p_e = \bar{p}\bar{q}\frac{Z}{Z - S} \tag{10.62}$$

and

$$v_e = \bar{p}\bar{q}\frac{1}{Z - S} \tag{10.63}$$

[4]By *silencer* we mean a set of tubes and cavities with a single inlet and outlet section where the first cutoff frequency of each cross section is higher than the silencer's maximum working frequency.

The intensity injected by the source and transmitted through the impedance Z is therefore equal to:

$$I_{e1} = I_{s1} = \frac{\Re(Z)}{2} \left| \frac{\bar{p}\bar{q}}{Z - S} \right|^2 \tag{10.64}$$

This intensity is at its maximum when $Z = S$ (*adapted impedance*).

10.4.3 Generalised source connected to a silencer

The source is connected to a silencer of transfer matrix (A, B, C, D), itself connected to an element (exterior medium, cavity, anechoic ending) characterised by its impedance Z. We have four equations related to four acoustic variables:

$$p_e = Ap_s + Bv_s \tag{10.65}$$

$$v_e = Cp_s + Dv_s \tag{10.66}$$

$$\frac{v_e}{\bar{v}} - \frac{p_e}{\bar{p}} = \bar{q} \tag{10.67}$$

$$p_s = Zv_s \tag{10.68}$$

From which we find:

$$v_s = \frac{\bar{p}\bar{v}\bar{q}}{\bar{p}\,(CZ + D) - \bar{v}\,(AZ + B)} \tag{10.69}$$

$$p_e = (AZ + B) \cdot v_s \tag{10.70}$$

$$v_e = (CZ + D) \cdot v_s \tag{10.71}$$

$$p_s = Z \cdot v_s \tag{10.72}$$

The intensity coming out of the system is given by:

$$I_{s2} = \frac{1}{2}\Re(p_s v_s^*) = \frac{\Re(Z)}{2} |v_s|^2 \tag{10.73}$$

10.4.4 Insertion loss (IL)

The *insertion loss* is defined as the ratio of intensities coming out of the system, with and without silencer (Equations 10.64 and 10.73):

$$IL = 10 \log \frac{I_{s1}}{I_{s2}} = 10 \log \left| \frac{S\,(CZ + D) - (AZ + B)}{(Z - S)} \right|^2 \tag{10.74}$$

10.4.5 Comparing Insertion Loss and Transmission Loss

The transmission loss is a *conventional* measure of the efficiency of a component. It is an intrinsic property of this component, independent of the other components placed upstream (source, other silencer) and downstream (more silencers, outlet). On the other hand, the insertion loss characterises the efficiency of the component placed in a given environment. It is influenced by the elements placed upstream (S) or downstream (Z). Figure 10.14 summarises these differences.

Note that there are several alternative definitions of the insertion loss. In fact, any indicator comparing situations *with* and *without* a given device may be used as insertion loss. Consider for example an exhaust line in which we wish to insert an additional silencer. The sound level at the end of the line is L_1 without and L_2 with the additional silencer. A possible measure of the efficiency of that additional silencer is the difference $L_1 - L_2$.

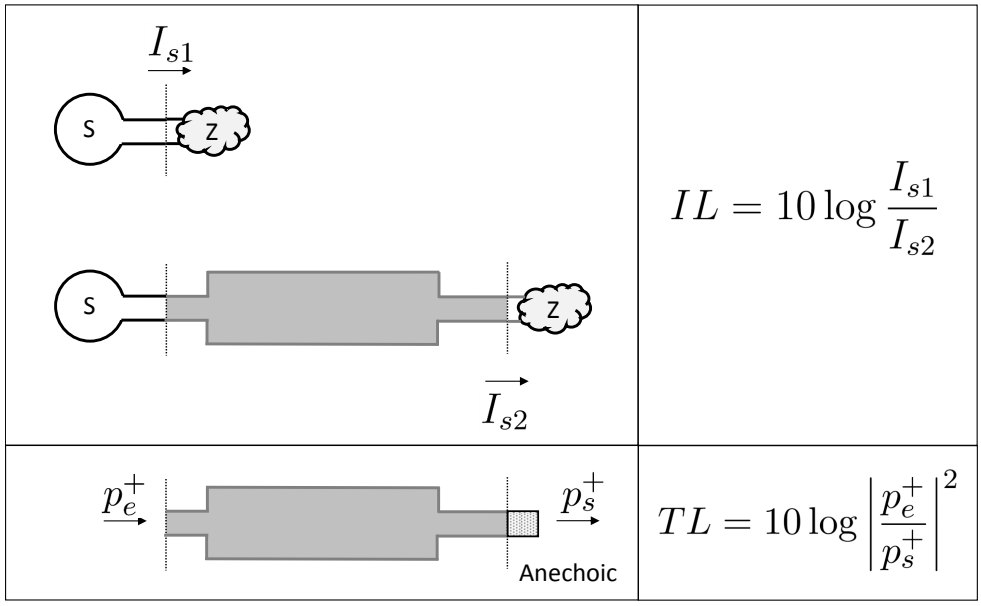

Figure 10.14: Comparison of *transmission loss* (TL) and *insertion loss* (IL). TL is a conventional measure of the efficiency of a component and independent of the environment. IL measures the efficiency of the component in a given (upstream and downstream) environment.

10.5 Cutoff frequency of circular ducts

10.5.1 Bessel equation and functions

The Helmholtz equation in spherical coordinates is:

$$\Delta p + k^2 p = 0 \rightarrow \frac{\partial^2 f}{\partial r^2} + \frac{1}{r}\frac{\partial f}{\partial r} + \frac{1}{r^2}\frac{\partial^2 f}{\partial \phi^2} + \frac{\partial^2 f}{\partial z^2} + k^2 p = 0 \tag{10.75}$$

We look for solutions of the form:

$$p\left(r, \phi, z; n, k_z\right) = J_n\left(r; k_z\right) \cdot e^{in\phi} \cdot e^{ik_z z} \tag{10.76}$$

and see that J must be a solution of the equation:

$$\frac{d^2 J_n}{dr^2} + \frac{1}{r}\frac{dJ_n}{dr} + \left(\left(k^2 - k_z^2\right) - \frac{n^2}{r^2}\right) \cdot J_n = 0 \tag{10.77}$$

Define $\xi = \kappa r$ where $\kappa = \sqrt{k^2 - k_z^2}$. The previous equation becomes:

$$\frac{\partial^2 J_n\left(\xi\right)}{\partial \xi^2} + \frac{1}{\xi}\frac{\partial J_n\left(\xi\right)}{\partial \xi} + \left(1 - \frac{n^2}{\xi^2}\right) J_n\left(\xi\right) = 0 \tag{10.78}$$

which is a Bessel equation[5] of order n. The solution of this equation is a Bessel function of the first kind of order n. This function is defined by:[6]

$$J_n\left(\xi\right) = \sum_{m=0}^{\infty} \frac{(-1)^m}{m!\ (m+n+1)!} \left(\frac{\xi}{2}\right)^{2m+n} \tag{10.79}$$

[5] **Friedrich Wilhelm Bessel**, a German astronomer and mathematician, was born in 1784 in Minden and died in 1846 in Konigsberg. Bessel is known for having been the first to accurately measure the distance of a star. He introduced his differential equation, and its associated functions, in the context of celestial mechanics.

[6] This definition and the properties which follow suppose that n is an integer (positive, negative or zero). Bessel functions can be extended to cases where n is real. See, for example, **Frank Bowman**, *Introduction to Bessel function*, Dover Publication Inc (1958).

Bessel functions of the first kind can also be defined by:

$$J_n(\xi) = \frac{1}{\pi}\int_0^{\pi} \cos(n\tau - \xi\sin\tau)\ d\tau = \frac{f1}{2\pi}\int_{-\pi}^{\pi} e^{i(n\tau-\xi\sin\tau)}\ d\tau \tag{10.80}$$

Figure 10.15 represents the Bessel functions of the first kind of order 0, 1, 2 and 3. The Bessel functions are related by a recurrence relation:

$$J_n(\xi) = \frac{\xi}{2n}\left[J_{n-1}(\xi) + J_{n+1}(\xi)\right] \tag{10.81}$$

and their derivative is obtained in the following way:

- for $n \neq 0$:

$$J'_n(\xi) = \frac{1}{2}\left[J_{n-1}(\xi) - J_{n+1}(\xi)\right] \tag{10.82}$$

- for $n = 0$:

$$J'_0(\xi) = -J_1(\xi) \tag{10.83}$$

10.5.2 Cutoff frequency

Consider a circular duct of radius R. The duct walls are assumed to be perfectly rigid. The acoustic field:

$$p(r,\phi,z,n,\kappa) = J_n(\kappa r)\cdot e^{in\phi}\cdot e^{ik_z z} \tag{10.84}$$

is a solution of the Helmholtz equation, but satisfies the boundary conditions only if:

$$J'_n(\kappa R) = 0 \tag{10.85}$$

Call ξ_{nm} the m^{th} zero of the function $J'_n(\xi)$ $(m = 0, 1, 2, 3, \ldots)$. These zeros are given in Table 10.16. The boundary conditions are satisfied only if:

$$\kappa R = \xi_{nm} \rightarrow k_z = \sqrt{k^2 - \left(\frac{\xi_{nm}}{R}\right)^2} \tag{10.86}$$

Two situations may occur:

1. If k_z is real, the pressure distribution $J_n\left(\xi_{nm}\frac{r}{R}\right)e^{in\phi}$ in a cross section of the duct propagates along the z axis with a wavenumber k_z. This happens when:
$$f \geq \frac{c \cdot \xi_{nm}}{2\pi R} \doteq f_{nm} \tag{10.87}$$

2. If f is below the cutoff frequency f_{nm}, k_z is imaginary: there is no propagation and the mode is evanescent.

We note that:

- for $n = 0$, $\xi_{00} = 0$ and the corresponding mode is plane:
$$J_0\left(\xi_{00}\frac{r}{R}\right) = J_0(0) = 1 \tag{10.88}$$
the cutoff frequency f_{00} is zero and the mode propagates at all frequencies;

- for n even, $\xi_{n0} = 0$, but this case is irrelevant since the corresponding mode has a zero amplitude (if $n > 0$, $J_n\left(\xi_{n0}\frac{r}{R}\right) = J_n(0) = 0$);

- the first cutoff frequency, under which only the plane wave mode propagates, is given in air at standard temperature by:
$$f_{11} = \frac{c \cdot \xi_{11}}{2\pi R} = \frac{340 \times 1.8412}{2\pi R} \simeq \frac{100}{R} \tag{10.89}$$

- for a given cross-sectional area S, a duct with square cross section ($S = a^2$) has a cutoff frequency slightly lower than a duct with circular cross section ($S = \pi R^2$):
$$f_{10}^{\square} = \frac{c}{2a} = \frac{c}{2\sqrt{S}} < f_{11}^{\bigcirc} = \frac{c}{\frac{2\sqrt{\pi}}{1.8412}\sqrt{S}} = \frac{c}{1.925\sqrt{S}} \tag{10.90}$$

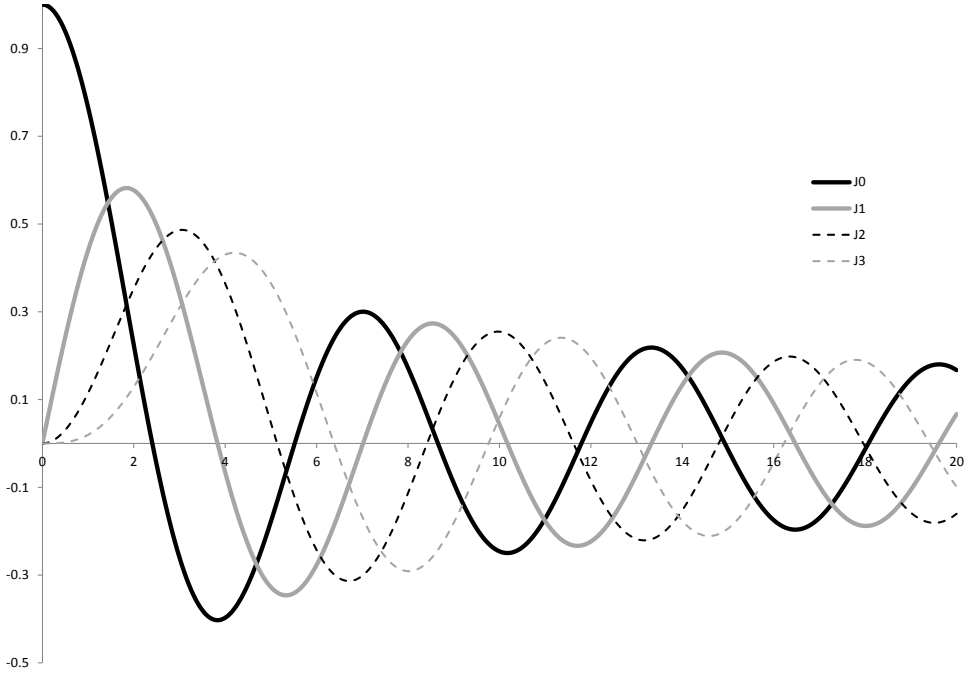

Figure 10.15: Graphs of Bessel functions $J_0(\xi)$, $J_1(\xi)$, $J_2(\xi)$ and $J_3(\xi)$.

m	ξ_{0m}	ξ_{1m}	ξ_{2m}	ξ_{3m}	ξ_{4m}	ξ_{5m}
0	0.0000	-	0.0000	-	0.0000	-
1	3.8317	1.8412	3.0542	4.2012	5.3175	6.4156
2	7.0156	5.3314	6.7061	8.0152	9.2824	10.5199
3	10.1735	8.5363	9.9695	11.3459	12.6819	13.9872
4	13.3237	11.7060	13.1704	14.5858	15.9641	17.3128
5	16.4706	14.8636	16.3475	17.7887	19.1960	20.5755

Figure 10.16: First zeros of functions $J_0'(\xi)$, $J_1'(\xi)$, $J_2'(\xi)$, $J_3'(\xi)$, $J_4'(\xi)$ and $J_5'(\xi)$.

10.6 Role of evanescent modes

Evanescent modes do not propagate, but they play an important role in the transition between two components. Consider for example (Figure 10.17) two semi-infinite ducts aligned on the y-axis and connected at $x = 0$. The tubes have dimensions a and b ($a > b$). We furthermore assume:

- that the out-of-plane dimension is very small (2D problem);
- that $k < \frac{\pi}{2a} < \frac{\pi}{2b}$, in order to remain below the first cutoff frequency, so that only plane wave modes are propagating, on both sides of the cross section change.

The acoustic field in the left duct can be written as a linear combination of the eigenmodes of the section:[7]

$$p_a(x, y) = \sum_{n=0}^{\infty} A_n(x) \cos\left[\frac{n\pi}{2a}(y + a)\right] \tag{10.91}$$

The evanescent modes have non-zero amplitudes, even if only plane wave modes propagate. Injecting this development into the Helmholtz equation,

[7] We include symmetric and anti-symmetric modes, although the latter, in the chosen context, are of zero magnitude.

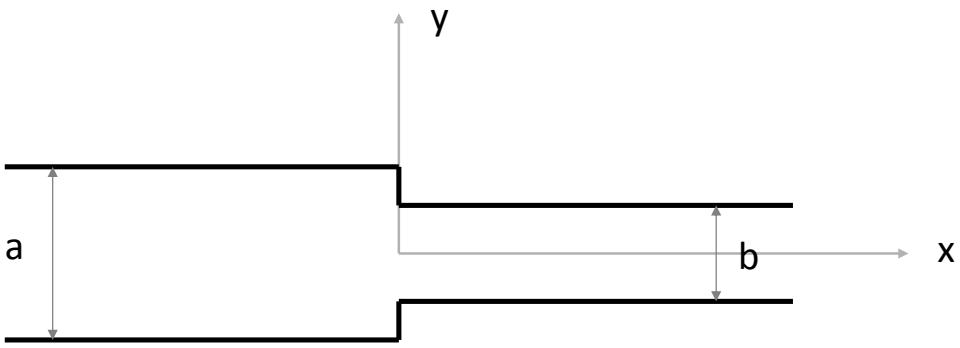

Figure 10.17: Schematic of cross section change.

we obtain an equation for the amplitude A_n of each mode ($n = 0, 1, 2, \ldots$):

$$\frac{d^2 A_n(x)}{dx^2} - \left(\left(\frac{n\pi}{2a} \right)^2 - k^2 \right) A_n(x) = 0 \tag{10.92}$$

The general solution of this equation has the form:

$$A_n(x) = A_n^+ e^{-\alpha_n x} + A_n^- e^{\alpha_n x} \tag{10.93}$$

with

$$\alpha_n = +\sqrt{\left(\frac{n\pi}{2a} \right)^2 - k^2} \tag{10.94}$$

α_0 is purely imaginary while, for $n > 0$, α_n is real. Consider that the terms A_n^+ are zero for $n > 0$ i.e. that the source, located on the left side of the cross section change, is a plane wave. We then find:

$$p_a(x, y) = A_0^+ e^{-ikx} + \sum_{n=0}^{\infty} A_n^- e^{\alpha_n x} \cos\left[\frac{n\pi}{2a} (y + a) \right] \tag{10.95}$$

from which we obtain the horizontal velocity u_a:

$$\begin{aligned} u_a(x, y) &= \frac{i}{\rho\omega} \frac{dp_a}{dx} \\ &= \frac{A_0^+}{\rho c} e^{-ikx} \\ &+ \sum_{n=0}^{\infty} \frac{i\alpha_n A_n^-}{\rho\omega} e^{\alpha_n x} \cos\left[\frac{n\pi}{2a} (y + a) \right] \end{aligned} \tag{10.96}$$

The pressure in the right duct is found in a similar way. Assuming that the right end is perfectly anechoic ($B_n^- = 0 \; \forall n$) we find:

$$p_b(x, y) = \sum_{n=0}^{\infty} B_n^+ e^{-\beta_n x} \cos\left[\frac{n\pi}{2b} (y + b) \right] \tag{10.97}$$

$$u_b(x, y) = -\sum_{n=0}^{\infty} \frac{i\beta_n B_n^+}{\rho\omega} e^{-\beta_n x} \cos\left[\frac{n\pi}{2b} (y + b) \right] \tag{10.98}$$

with:

$$\beta_n = +\sqrt{\left(\frac{n\pi}{2b} \right)^2 - k^2} \tag{10.99}$$

The following conditions apply at $x = 0$:

$$\begin{aligned} u_a(0,y) &= 0 \qquad for \quad |y| > b \\ &= u_b(0,y) \qquad for \quad |y| \le b \end{aligned} \tag{10.100}$$

and

$$p_a(0,y) = p_b(0,y) \;\; for\; |y| \le b \tag{10.101}$$

We therefore obtain the following equations:

$$A_0^+ + \sum_{n=0}^{\infty} A_n^- \cos\left[\frac{n\pi}{2a}(y+a)\right] = \sum_{n=0}^{\infty} B_n^+ \cos\left[\frac{n\pi}{2b}(y+b)\right] \tag{10.102}$$

$$\begin{aligned} &\frac{A_0^+}{\rho c} + \sum_{n=0}^{\infty} \frac{i\alpha_n A_n^-}{\rho\omega} \cos\left[\frac{n\pi}{2a}(y+a)\right] = \\ &-W(y,b) \cdot \sum_{n=0}^{\infty} \frac{i\beta_n B_n^+}{\rho\omega} \cos\left[\frac{n\pi}{2b}(y+b)\right] \end{aligned} \tag{10.103}$$

where $W(y,b)$ is a rectangular window of width $2b$:

$$\begin{aligned} W(y,b) &= 0 \qquad for \quad |y| > b \\ &= 1 \qquad for \quad |y| \le b \end{aligned} \tag{10.104}$$

Multiply both sides of the velocity continuity equation by $\cos\left[\frac{m\pi}{2a}(y+a)\right]$ and integrate on $[-a,a]$:

$$\begin{aligned} &\frac{A_0^+}{\rho c} \int_{-a}^{a} \cos\left[\frac{m\pi}{2a}(y+a)\right] dy + \\ &\sum_{n=0}^{\infty} \frac{i\alpha_n A_n^-}{\rho\omega} \int_{-a}^{a} \cos\left[\frac{n\pi}{2a}(y+a)\right] \cos\left[\frac{m\pi}{2a}(y+a)\right] dy = \\ &-\sum_{n=0}^{\infty} \frac{i\beta_n B_n^+}{\rho\omega} \int_{-b}^{b} \cos\left[\frac{n\pi}{2b}(y+b)\right] \cos\left[\frac{m\pi}{2a}(y+a)\right] dy \end{aligned} \tag{10.105}$$

The first two integrals are calculated as follows:

$$\int_{-a}^{a} \cos\left[\frac{m\pi}{2a}(y+a)\right] dy = 2a\delta_{m0} \tag{10.106}$$

$$\int_{-a}^{a} \cos\left[\frac{n\pi}{2a}(y+a)\right] \cos\left[\frac{m\pi}{2a}(y+a)\right] dy = \begin{array}{ll} 2a & m=n=0 \\ a\delta_{mn} & m \neq 0 \end{array} \tag{10.107}$$

To calculate the third integral, we define:

$$\begin{aligned} k_1 &= \frac{n\pi}{2a} + \frac{m\pi}{2b} \\ k_2 &= \frac{n\pi}{2a} - \frac{m\pi}{2b} \end{aligned} \tag{10.108}$$

and use the Simpson formula to split the integral into two components:

$$\begin{aligned} I_{mn} &= I_{mn}^{(1)} + I_{mn}^{(2)} \\ I_{mn}^{(1)} &= \frac{1}{2}\int_{-b}^{b} \cos\left[k_1 y + \frac{(m+n)\pi}{2}\right] dy \\ I_{mn}^{(2)} &= \frac{1}{2}\int_{-b}^{b} \cos\left[k_2 y + \frac{(m-n)\pi}{2}\right] dy \end{aligned} \tag{10.109}$$

The first term is:

- if $k_1 = 0$:

$$I_{mn}^{(1)} = b \cos\frac{(m+n)\pi}{2} \tag{10.110}$$

- if $k_1 \neq 0$:

$$I_{mn}^{(1)} = \frac{1}{2k_1}\left(\sin\left[k_1 b + \frac{(m+n)\pi}{2}\right] - \sin\left[-k_1 b + \frac{(m+n)\pi}{2}\right]\right) \tag{10.111}$$

and the second:

- if $k_2 = 0$:

$$I_{mn}^{(2)} = b \cos\frac{(m+n)\pi}{2} \tag{10.112}$$

- if $k_2 \neq 0$:

$$I_{mn}^{(2)} = \frac{1}{2k_2}\left(\sin\left[k_2 b + \frac{(m-n)\pi}{2}\right] - \sin\left[-k_2 b + \frac{(m-n)\pi}{2}\right]\right) \tag{10.113}$$

The velocity continuity equation projected on mode $m = 0$ is written:

$$\frac{2ia\alpha_0}{\rho\omega}A_0^- + \sum_{n=0}^{\infty}\frac{i\beta_n I_{0n}}{\rho\omega}B_n^+ = -\frac{2a}{\rho c}A_0^+ \tag{10.114}$$

and on the other modes ($m \neq 0$):

$$\frac{ia\alpha_m}{\rho\omega}A_m^- + \sum_{n=0}^{\infty}\frac{i\beta_n I_{mn}}{\rho\omega}B_n^+ = 0 \tag{10.115}$$

Multiply both sides of the pressure continuity equation by $\cos\left[\frac{m\pi}{2b}(y+b)\right]$ and integrate on $[-b, b]$:

$$\begin{aligned} &A_0^+\int_{-b}^{b}\cos\left[\frac{m\pi}{2b}(y+b)\right]dy + \\ &\sum_{n=0}^{\infty}A_n^-\int_{-b}^{b}\cos\left[\frac{n\pi}{2a}(y+a)\right]\cos\left[\frac{m\pi}{2b}(y+b)\right]dy = \\ &-\sum_{n=0}^{\infty}B_n^+\int_{-b}^{b}\cos\left[\frac{n\pi}{2b}(y+b)\right]\cos\left[\frac{m\pi}{2b}(y+b)\right]dy \end{aligned} \tag{10.116}$$

The three integrals are easily calculated:

$$\int_{-b}^{b}\cos\left[\frac{m\pi}{2b}(y+b)\right]dy = 2b\delta_{m0} \tag{10.117}$$

$$\int_{-b}^{b}\cos\left[\frac{n\pi}{2a}(y+a)\right]\cos\left[\frac{m\pi}{2b}(y+b)\right]dy = I_{nm} \tag{10.118}$$

$$\int_{-b}^{b}\cos\left[\frac{n\pi}{2b}(y+b)\right]\cos\left[\frac{m\pi}{2b}(y+b)\right]dy = \begin{array}{ll} 2b & m = n = 0 \\ b\delta_{mn} & m \neq 0 \end{array} \tag{10.119}$$

The pressure continuity equation projected on mode $m = 0$ is written:

$$\sum_{n=0}^{\infty}I_{n0}A_n^- + 2bB_0^+ = -2bA_0^+ \tag{10.120}$$

and on the other mode ($m \neq 0$):

$$\sum_{n=0}^{\infty}I_{nm}A_n^- + bB_m^+ = 0 \tag{10.121}$$

If we retain N non-planar modes, equations 10.114, 10.115, 10.120 and 10.121 form a system of $2(N+1)$ equations with $2(N+1)$ unknowns (the A_n^- and B_n^+). The solution of this system gives the pressure and velocity in both ducts. This solution is represented in Figures 10.18 and 10.19. Even below the first cutoff frequency, a very large number of modes must be considered to obtain an accurate solution because the discontinuous velocity profile $u_a(0, y)$ is difficult to approximate by a Fourier series. The series even diverges at the points of discontinuity (Gibbs phenomenon, Figure 10.19, see also Section 5.2.1). The effect of these higher order modes is however limited to the region where the cross section changes because their α_n or β_n coefficients are so high that their contributions are decreasing very rapidly as one moves away from $x = 0$.

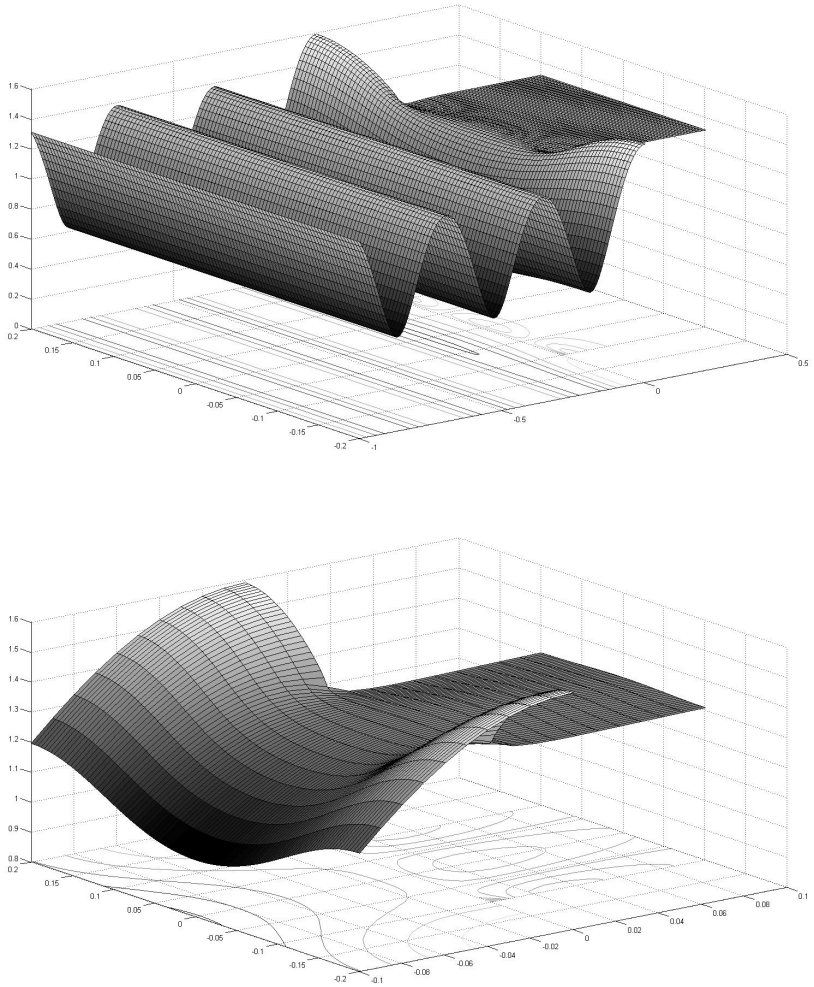

Figure 10.18: Pressure distribution near a cross section change: global view (above) and zoom on the transition (below). A stationary wave is observed in the left duct; it results from the interaction of the incident wave A_0^+ with the reflected waves A_n^-. The wave in the right duct is purely propagative because of the anechoic termination. Evanescent modes are only visible in the neighbourhood of the cross section change. Parameter values: $a = 0.1$, $b = 0.1$, $f = 400$, $N = 1,000$, $A_0^+ = 1$.

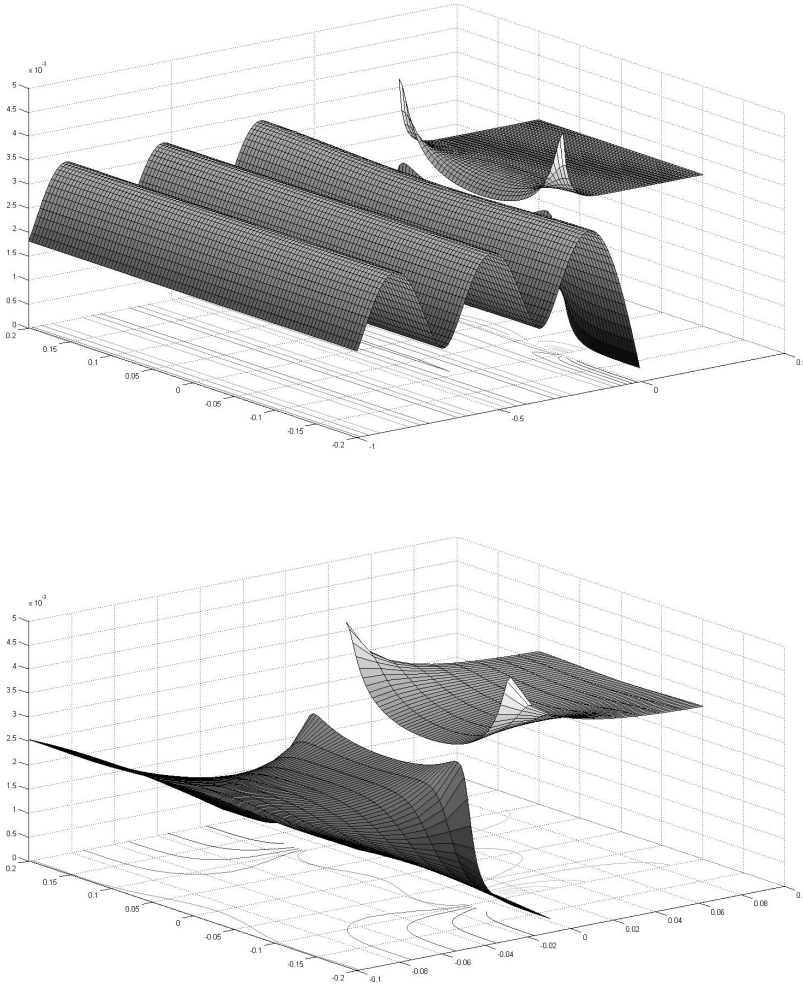

Figure 10.19: Horizontal velocity distribution near a cross section change: global view (above) and zoom on the transition (below). The zero velocity condition is respected, but the velocity discontinuity at $y = -b$ and $y = b$ induces a Gibbs phenomenon: the Fourier series for u_a is non-convergent at these points. Parameter values: $a = 0.1$, $b = 0.1$, $f = 400$, $N = 1,000$, $A_0^+ = 1$.

10.7 Reactive and dissipative silencers

The theory presented in this chapter applies to silencers and, in particular, to the components of motor vehicle exhaust lines. A silencer has been presented as a filter acting on the transmission of the sound between the inlet and outlet. The purpose of the silencer is to limit the transmission of intensity by maximizing the transmission loss. The portion of incident intensity that is not transmitted is reflected back towards the source. Such a silencer is purely reactive: there is no energy dissipation.

In practice, silencers associate this reactive behavior with a dissipation mechanism. Certain cavities of the silencer are filled with porous material within which the sound field loses part of its energy. The different cavities are often connected through perforated walls which provide an additional source of dissipation.

11

Sound radiation

The goal of life is not to possess power, but to radiate it.
— **Henry Miller** (1891-1980), Sunday After the War (1944).

Contents

11.1 Dipoles and quadrupoles 240
11.2 Multipole expansion 249
11.3 Helmholtz integral equation 258
11.4 Power, efficiency and impedance 270

This chapter will investigate *acoustic radiation* and provide tools to describe the acoustic field created by a vibrating structure radiating in an unbounded domain with no obstacle (*free field radiation*). Two analysis methods will be presented: multipole analysis and the Helmlholtz integral equation.

Multipole analysis provides a general analysis framework for radiated acoustic fields. It shows that any acoustic source can be represented by a cloud of monopoles and that this cloud can be reduced to a single monopole, three dipoles, six quadrupoles, and more multipoles of higher order. Multipole analysis shows that the directivity of the sound field, that is the spatial distribution of the acoustic field on a sphere surrounding the radiating object, is a linear combination of canonical elementary directivity diagrams. It also predicts how directivity evolves with frequency and distance. Multipole analysis forms the basis of an important extension of the finite element method to unbounded domains: the infinite element method. The Helmholtz partial differential equation can be recast into a **boundary integral equation** which relates the acoustic field in the domain to the acoustic pressure and normal velocity distribution on the radiating surface. The Helmholtz integral equation forms the basis of an important numerical method in acoustics: the boundary element method.

11.1 Dipoles and quadrupoles

11.1.1 Dipoles

> *...something more complex and disconcerting than the harmony of spheres: a couple.*
> — **Julien Gracq** (1910-2007), A dark stranger (1945).
> Author's own translation from French to English.

Consider (Figure 11.1) two sources of opposite amplitudes (A and $-A$) positioned symmetrically with respect to a point Q of coordinates $(x, 0, 0)$. The

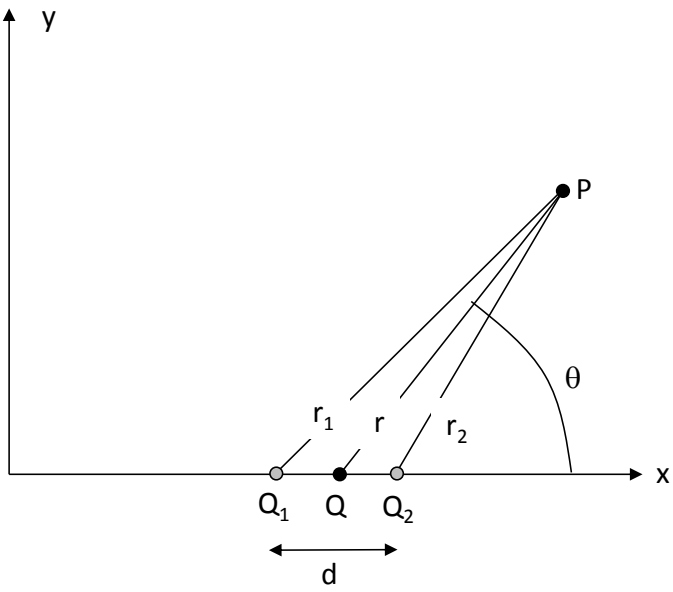

Figure 11.1: Dipole.

acoustic field induced by these two sources at point P of coordinates (X, Y, Z) is:

$$p = A\left(\frac{e^{-ikr_2}}{r_2} - \frac{e^{-ikr_1}}{r_1}\right) \tag{11.1}$$

If the distance between the two sources is small, we can express the total acoustic pressure as a function of the distance r between P and Q and of the distance d between the two sources:

$$\begin{aligned}\frac{e^{-ikr_2}}{r_2} &= \frac{e^{-ikr}}{r} - \frac{d}{2}\frac{\partial}{\partial x}\left(\frac{e^{-ikr}}{r}\right) + o(d^2) \\ &= \frac{e^{-ikr}}{r} - \frac{d}{2}\frac{\partial r}{\partial x}\frac{d}{dr}\left(\frac{e^{-ikr}}{r}\right) + o(d^2) \\ &= \frac{e^{-ikr}}{r} - \frac{d}{2}\cos\theta\frac{e^{-ikr}}{r}\left(\frac{-1-ikr}{r}\right) + o(d^2) \end{aligned} \tag{11.2}$$

$$\frac{e^{-ikr_1}}{r_1} = \frac{e^{-ikr}}{r} + \frac{d}{2}\cos\theta\frac{e^{-ikr}}{r}\left(\frac{-1-ikr}{r}\right) + o(d^2) \tag{11.3}$$

$$p = Ad\cos\theta\frac{e^{-ikr}}{r}\left(\frac{1+ikr}{r}\right) + o(d^2) \tag{11.4}$$

Or, if d tends to 0 while keeping the *dipole moment* $D = Ad$ constant:

$$\begin{aligned} p &= D\cos\theta\frac{e^{-ikr}}{r}\left(\frac{1+ikr}{r}\right) \\ &= ikD\cdot\frac{e^{-ikr}}{r}\cdot\cos\theta\cdot\left(1+\frac{1}{ikr}\right) \end{aligned} \tag{11.5}$$

The acoustic field of the dipole appears as the product of four terms:

1. an amplitude ikD, itself the product of two terms: the dipole moment D and a factor ik characteristic of a dipole;
2. a monopole field of unit amplitude $\frac{e^{-ikr}}{r}$;
3. a *directivity* term $\cos\theta$ (Figure 11.3);
4. a polynomial in $\frac{1}{ikr}$ (here of order 1) which tends to 1 when kr tends to infinity.

The directivity of the dipole is characterised by two lobes of opposite phase ($\cos\theta = -\cos(\pi-\theta)$) aligned on the dipole axis (Figure 11.3) and by a zero acoustic pressure on the symmetry plane ($\theta = \frac{\pi}{2}$). The radial acoustic velocity is easily obtained:

$$v_r = \frac{i}{\rho\omega}\frac{\partial p}{\partial r} = \frac{ikD}{\rho c}\cos\theta\frac{e^{-ikr}}{r}\left(1+\frac{2}{ikr}+\frac{2}{(ikr)^2}\right) \tag{11.6}$$

And the tangential velocity component is:

$$v_\theta = \frac{i}{\rho\omega}\frac{1}{r}\frac{\partial p}{\partial\theta} = \frac{ikD}{\rho c}\sin\theta\frac{e^{-ikr}}{r}\left(\frac{1}{ikr}+\frac{1}{(ikr)^2}\right) \tag{11.7}$$

The radial intensity is therefore obtained as follows:

$$I_r = \frac{1}{2}\Re(p_r v_r^*) = \frac{(kD\cos\theta)^2}{2\rho c r^2} \tag{11.8}$$

and the power radiated through a sphere of radius r centered on Q is:

$$W_r = \frac{(kD)^2}{2\rho c r^2}\int_0^{2\pi}\cos^2\theta\int_0^{\pi} r^2\sin\phi\, d\phi\, d\theta = \frac{\pi(kD)^2}{\rho c} \tag{11.9}$$

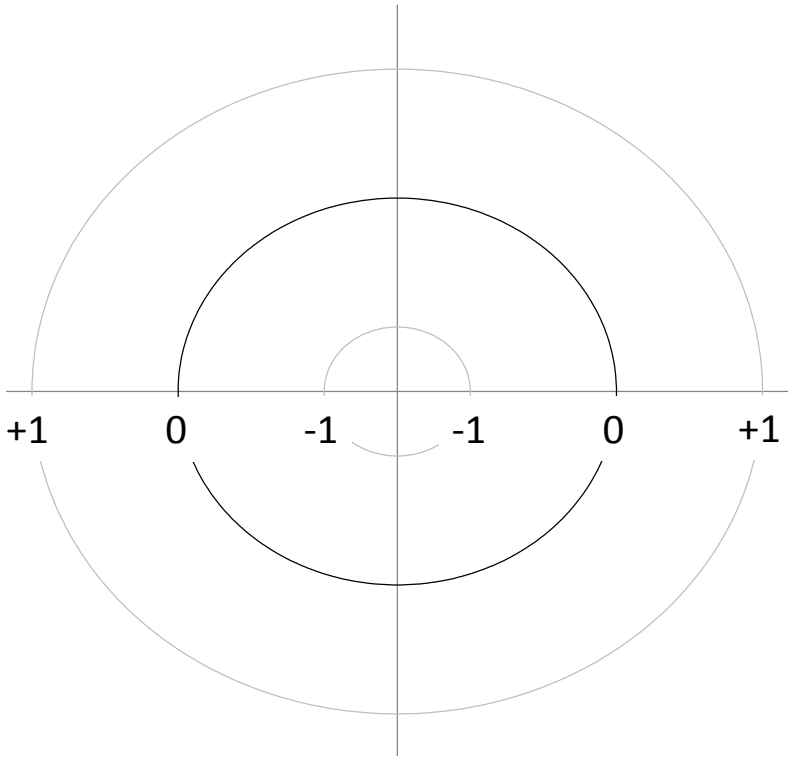

Figure 11.2: Conventions for directivity diagrams used in this chapter: the inner circle corresponds to $p = -1$, the outer circle to $p = +1$ and the middle circle to $p = 0$.

Unsurprisingly, the power is independent of r.

11.1.2 Longitudinal quadrupole

Consider again Figure 11.1, but let us place two sources of identical amplitudes A at Q_1 and Q_2 and a third source of amplitude $-2A$ at Q. The total field generated at point P by these three sources is given by:

$$p = A\left(\frac{e^{-ikr_2}}{r_2} - 2\frac{e^{-ikr}}{r} + \frac{e^{-ikr_1}}{r_1}\right) \tag{11.10}$$

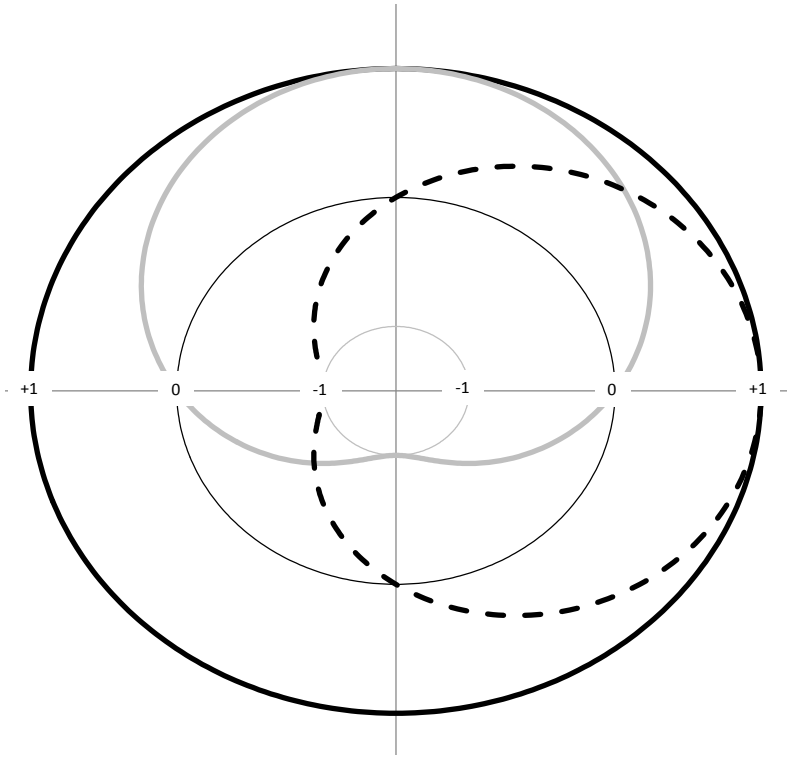

Figure 11.3: Directivity diagrams of a monopole (solid black line), a dipole aligned on the x-axis (dashed black line), and a dipole aligned on the y-axis (solid grey line). Conventions are those defined in Figure 11.2.

But we can write:

$$\frac{e^{-ikr_1}}{r_1} = \frac{e^{-ikr}}{r} + \frac{d}{2}\frac{\partial}{\partial x}\left(\frac{e^{-ikr}}{r}\right) + \frac{d^2}{4}\frac{\partial^2}{\partial x^2}\left(\frac{e^{-ikr}}{r}\right) + o(d^3) \tag{11.11}$$

$$\frac{e^{-ikr_2}}{r_2} = \frac{e^{-ikr}}{r} - \frac{d}{2}\frac{\partial}{\partial x}\left(\frac{e^{-ikr}}{r}\right) + \frac{d^2}{4}\frac{\partial^2}{\partial x^2}\left(\frac{e^{-ikr}}{r}\right) + o(d^3) \tag{11.12}$$

As the distance d approaches 0 while the *quadrupole moment* $Q = \frac{Ad^2}{2}$ remains constant, we find:

$$\begin{aligned} p &= Q\frac{\partial^2}{\partial x^2}\left(\frac{e^{-ikr}}{r}\right) \\ &= (ik)^2 Q \cdot \frac{e^{-ikr}}{r} \cdot \cos^2\theta \cdot \left(1 + \frac{2}{ikr} + \frac{2}{(ikr)^2}\right) \end{aligned} \tag{11.13}$$

The sound field of the quadrupole displays a symmetry with respect to plane $x = x_Q$ (this was an antisymmetry plane for the dipole field) and is zero on that plane (Figure 11.5). The sound field of the quadrupole appears again as the product of four terms:

1. an amplitude $(ik)^2 Q = -k^2 Q$, itself the product of two terms: the quadrupole moment Q and a factor $(ik)^2$ characteristic of a quadrupole;

2. a monopole field of unit amplitude $\frac{e^{-ikr}}{r}$;

3. a *directivity* term $\cos^2\theta$ (Figure 11.5);

4. a polynomial in $\frac{1}{ikr}$ (here of second order) which tends to 1 when kr tends to infinity.

11.1.3 Lateral quadrupole

Consider four sources located at the apex of a square (Figure 11.4). Sources 1 and 4 have amplitudes A, the other two have amplitudes $-A$. The total

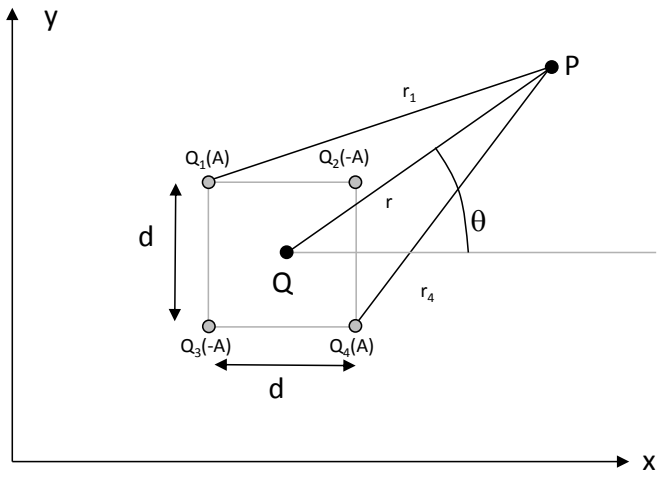

Figure 11.4: Lateral quadrupole.

pressure at P is:

$$p = A\left(-\frac{e^{-ikr_1}}{r_1} + \frac{e^{-ikr_2}}{r_2} + \frac{e^{-ikr_3}}{r_3} - \frac{e^{-ikr_4}}{r_4}\right) \tag{11.14}$$

but:

$$\begin{aligned}\frac{e^{-ikr_1}}{r_1} &= \frac{e^{-ikr}}{r} - \frac{d}{2}\frac{\partial}{\partial x}\left(\frac{e^{-ikr}}{r}\right) + \frac{d}{2}\frac{\partial}{\partial y}\left(\frac{e^{-ikr}}{r}\right) + \frac{d^2}{4}\frac{\partial^2}{\partial x^2}\left(\frac{e^{-ikr}}{r}\right) \\ &- \frac{d^2}{4}\frac{\partial^2}{\partial x \partial y}\left(\frac{e^{-ikr}}{r}\right) + \frac{d^2}{4}\frac{\partial^2}{\partial y^2}\left(\frac{e^{-ikr}}{r}\right) + o(d^3)\end{aligned} \tag{11.15}$$

$$\begin{aligned}\frac{e^{-ikr_2}}{r_2} &= \frac{e^{-ikr}}{r} + \frac{d}{2}\frac{\partial}{\partial x}\left(\frac{e^{-ikr}}{r}\right) + \frac{d}{2}\frac{\partial}{\partial y}\left(\frac{e^{-ikr}}{r}\right) + \frac{d^2}{4}\frac{\partial^2}{\partial x^2}\left(\frac{e^{-ikr}}{r}\right) \\ &+ \frac{d^2}{4}\frac{\partial^2}{\partial x \partial y}\left(\frac{e^{-ikr}}{r}\right) + \frac{d^2}{4}\frac{\partial^2}{\partial y^2}\left(\frac{e^{-ikr}}{r}\right) + o(d^3)\end{aligned} \tag{11.16}$$

$$\begin{aligned}\frac{e^{-ikr_3}}{r_3} &= \frac{e^{-ikr}}{r} - \frac{d}{2}\frac{\partial}{\partial x}\left(\frac{e^{-ikr}}{r}\right) - \frac{d}{2}\frac{\partial}{\partial y}\left(\frac{e^{-ikr}}{r}\right) + \frac{d^2}{4}\frac{\partial^2}{\partial x^2}\left(\frac{e^{-ikr}}{r}\right) \\ &+ \frac{d^2}{4}\frac{\partial^2}{\partial x \partial y}\left(\frac{e^{-ikr}}{r}\right) + \frac{d^2}{4}\frac{\partial^2}{\partial y^2}\left(\frac{e^{-ikr}}{r}\right) + o(d^3) \qquad (11.17)\end{aligned}$$

$$\begin{aligned}\frac{e^{-ikr_4}}{r_4} &= \frac{e^{-ikr}}{r} + \frac{d}{2}\frac{\partial}{\partial x}\left(\frac{e^{-ikr}}{r}\right) - \frac{d}{2}\frac{\partial}{\partial y}\left(\frac{e^{-ikr}}{r}\right) + \frac{d^2}{4}\frac{\partial^2}{\partial x^2}\left(\frac{e^{-ikr}}{r}\right) \\ &- \frac{d^2}{4}\frac{\partial^2}{\partial x \partial y}\left(\frac{e^{-ikr}}{r}\right) + \frac{d^2}{4}\frac{\partial^2}{\partial y^2}\left(\frac{e^{-ikr}}{r}\right) + o(d^3) \qquad (11.18)\end{aligned}$$

From which we obtain, after letting d tend to zero while keeping $Q = \frac{Ad^2}{2}$ constant:

$$\begin{aligned}p &= Q\frac{\partial^2}{\partial x \partial y}\left(\frac{e^{-ikr}}{r}\right) \\ &= (ik)^2 Q \cdot \frac{e^{-ikr}}{r} \cdot \sin\theta\cos\theta \cdot \left(1 + \frac{2}{ikr} + \frac{2}{(ikr)^2}\right) \qquad (11.19)\end{aligned}$$

The sound field of this quadrupole has two antisymmetry planes ($x = x_Q$ and $y = y_Q$) and is zero on these two planes (Figure 11.5).

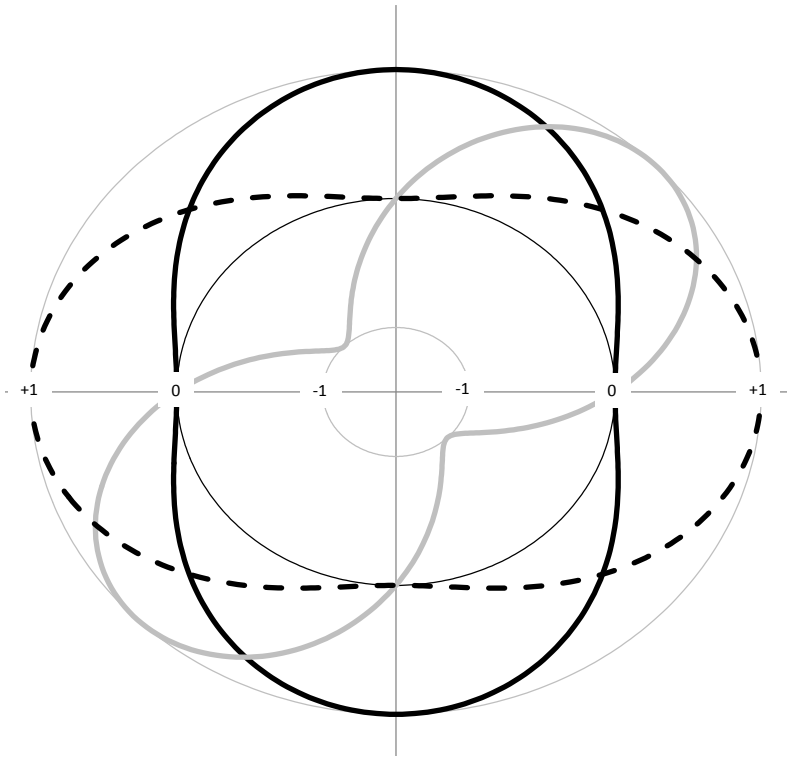

Figure 11.5: Directivity diagrams of three quadrupoles: longitudinal quadrupole aligned on the y-axis (solid black line), longitudinal quadrupole aligned on the x-axis (dashed black line) and lateral quadrupole (solid grey line).

11.2 Multipole expansion

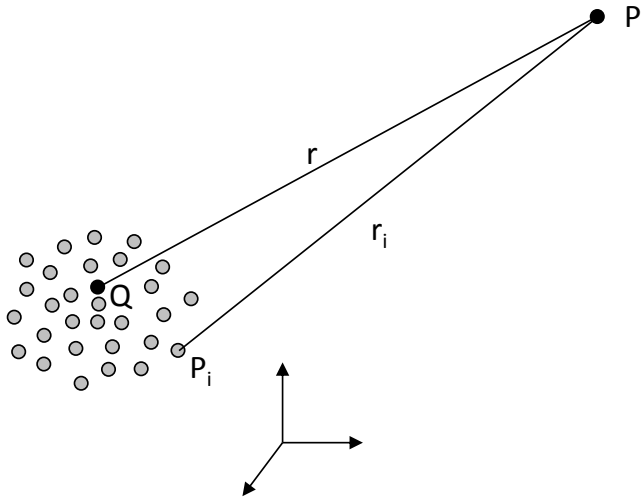

Figure 11.6: Notation used while deriving the multipole expansion of sound fields.

Consider n point sources of amplitude $A_i (i = 1, n)$ located at points P_i with coordinates $x_j^{(i)} (j = 1, 3)$. Together they generate at point P of coordinates X_j a pressure (Figure 11.6):

$$p = \sum_{i=1,n} A_i \frac{e^{-ikr_i}}{r_i} \tag{11.20}$$

where r_i is the distance between P and P_i. We then choose a point Q of coordinates x_j and define:[1]

$$G = \frac{e^{-ikr}}{r} \tag{11.21}$$

$$r = \sqrt{(x_j - X_j)\,(x_j - X_j)} \tag{11.22}$$

For each source, the term $\frac{e^{-ikr_i}}{r_i}$ may be developed in Taylor series around the

[1]Einstein's convention of implicit summation on repeated indices will be used in this development. See Section 3.2.

point Q:

$$\begin{aligned}\frac{e^{-ikr_i}}{r_i} &= G + \frac{x_j^{(i)} - x_j}{1!}\partial_j G + \frac{\left(x_j^{(i)} - x_j\right)\left(x_k^{(i)} - x_k\right)}{2!}\partial_{jk} G \\ &+ \frac{\left(x_j^{(i)} - x_j\right)\left(x_k^{(i)} - x_k\right)\left(x_l^{(i)} - x_l\right)}{3!}\partial_{jkl} G + \ldots \end{aligned} \tag{11.23}$$

The pressure p can therefore be expressed as:

$$\begin{aligned} p &= \underbrace{\left(\sum_i A_i\right)}_{M} \cdot G + \underbrace{\left(\sum_i A_i \frac{x_j^{(i)} - x_j}{1!}\right)}_{D_j} \cdot \partial_j G \\ &+ \underbrace{\left(\sum_i A_i \frac{\left(x_j^{(i)} - x_j\right)\left(x_k^{(i)} - x_k\right)}{2!}\right)}_{Q_{jk}} \partial_{jk} G \\ &+ \underbrace{\left(\sum_i A_i \frac{\left(x_j^{(i)} - x_j\right)\left(x_k^{(i)} - x_k\right)\left(x_l^{(i)} - x_l\right)}{3!}\right)}_{O_{jkl}} \partial_{jkl} G \\ &+ \ldots \end{aligned} \tag{11.24}$$

This development may be written in a more compact form:

$$p = M \cdot G + D_j \cdot \partial_j G + Q_{jk} \cdot \partial_{jk} G + O_{jkl} \cdot \partial_{jkl} G + \ldots \tag{11.25}$$

where M, D_j, Q_{jk} and O_{jkl} are the multipole moments of order 1 (monopole), 2 (dipole), 3 (quadrupole) and 4 (octupole).

Partial derivatives of G

The successive partial derivatives of G are calculated below, denoting $G^{(n)} = \frac{\partial^n G}{\partial r^n}$:

$$\partial_j G = G^{(1)} \partial_j r \tag{11.26}$$

$$\partial_{jk} G = G^{(2)} \partial_j r \partial_k r + G^{(1)} \partial_{jk} r \tag{11.27}$$

$$\begin{aligned}\partial_{jkl}G &= G^{(3)}\partial_j r\cdot\partial_k r\cdot\partial_l r \\ &+ G^{(2)}\left(\partial_j r\cdot\partial_{kl}r+\partial_k r\cdot\partial_{jl}r+\partial_l r\partial_{jk}r\right) \\ &+ G^{(1)}\partial_{jkl}r\end{aligned} \tag{11.28}$$

Derivatives of G with respect to r

The successive derivatives G with respect to r are all of the form:

$$G^{(n)} = (-ik)^n\cdot G\cdot f_n \tag{11.29}$$

where the f_n functions are obtained by the recurrence relation:

$$f_1 = 1+\frac{1}{ikr} \tag{11.30}$$

$$f_n = f_1\cdot f_{n-1}-\frac{1}{ik}f'_{n-1} \tag{11.31}$$

We find, for $n=1$ to 3:

$$G^{(1)} = (-ik)\,G\left(1+\frac{1}{ikr}\right) \tag{11.32}$$

$$G^{(2)} = (-ik)^2\,G\left(1+\frac{2}{ikr}+\frac{2}{(ikr)^2}\right) \tag{11.33}$$

$$G^{(3)} = (-ik)^3\,G\left(1+\frac{3}{ikr}+\frac{6}{(ikr)^2}+\frac{6}{(ikr)^3}\right) \tag{11.34}$$

Partial derivatives of r

The successive partial derivatives of r are:

$$\partial_j r = \frac{x_j-X_j}{r} = \alpha_j \tag{11.35}$$

$$\partial_{jk}r = \frac{\delta_{jk}-\alpha_j\alpha_k}{r} \tag{11.36}$$

$$\begin{aligned} \partial_{jkl} r &= \frac{3\alpha_j\alpha_k\alpha_l - (\delta_{jk}\alpha_l + \delta_{jl}\alpha_k + \delta_{kl}\alpha_j)}{r^2} \\ &= \frac{3\alpha_j\alpha_k\alpha_l - A_{jkl}}{r^2} \end{aligned} \tag{11.37}$$

where we define:

$$A_{jkl} = \delta_{jk}\alpha_l + \delta_{jl}\alpha_k + \delta_{kl}\alpha_j \tag{11.38}$$

Compact form for the radiated field

Finally the complete sound field can be represented in a very compact form as the product of four factors:

$$p = \mathbf{a} \cdot \mathbf{D} \cdot \mathbf{g}^t \cdot G \tag{11.39}$$

The vector **a** contains the successive multipole moments multiplied by the appropriate powers of $-ikr$:

$$\begin{pmatrix} M & -ikD_j & (-ik)^2 Q_{jk} & (-ik)^3 O_{jkl} & \dots \end{pmatrix} \tag{11.40}$$

The matrix **D** contains the directivity components of the sound field:

$$\begin{vmatrix} 1 & 0 & 0 & 0 & \dots \\ \alpha_j & \alpha_j & 0 & 0 & \dots \\ \alpha_j\alpha_k & 3\alpha_j\alpha_k - \delta_{jk} & 3\alpha_j\alpha_k - \delta_{jk} & 0 & \dots \\ \alpha_j\alpha_k\alpha_l & 6\alpha_j\alpha_k\alpha_l - A_{jkl} & 15\alpha_j\alpha_k\alpha_l - 3A_{jkl} & 15\alpha_j\alpha_k\alpha_l - 3A_{jkl} & \dots \\ \dots & \dots & \dots & \dots & \dots \end{vmatrix} \tag{11.41}$$

Its elements are linear combinations of terms in $\alpha_1^p \alpha_2^q \alpha_3^r$ with $p + q + r \leq o$, where o is the order of the corresponding multipole ($o = 0$ for a monopole, $o = 1$ for one dipole, $o = 2$ for a quadrupole, ...). In two-dimensions, the elements of the matrix are linear combinations of terms in $\sin^p\theta \cos^q\theta$ (Figure 11.7) or in $\sin p\theta \cos q\theta$ (Figure 11.8).

The vector **g** contains successive powers of $\frac{1}{ikr}$:

$$\begin{pmatrix} 1 & \frac{1}{ikr} & \frac{1}{(ikr)^2} & \frac{1}{(ikr)^3} & \dots \end{pmatrix} \tag{11.42}$$

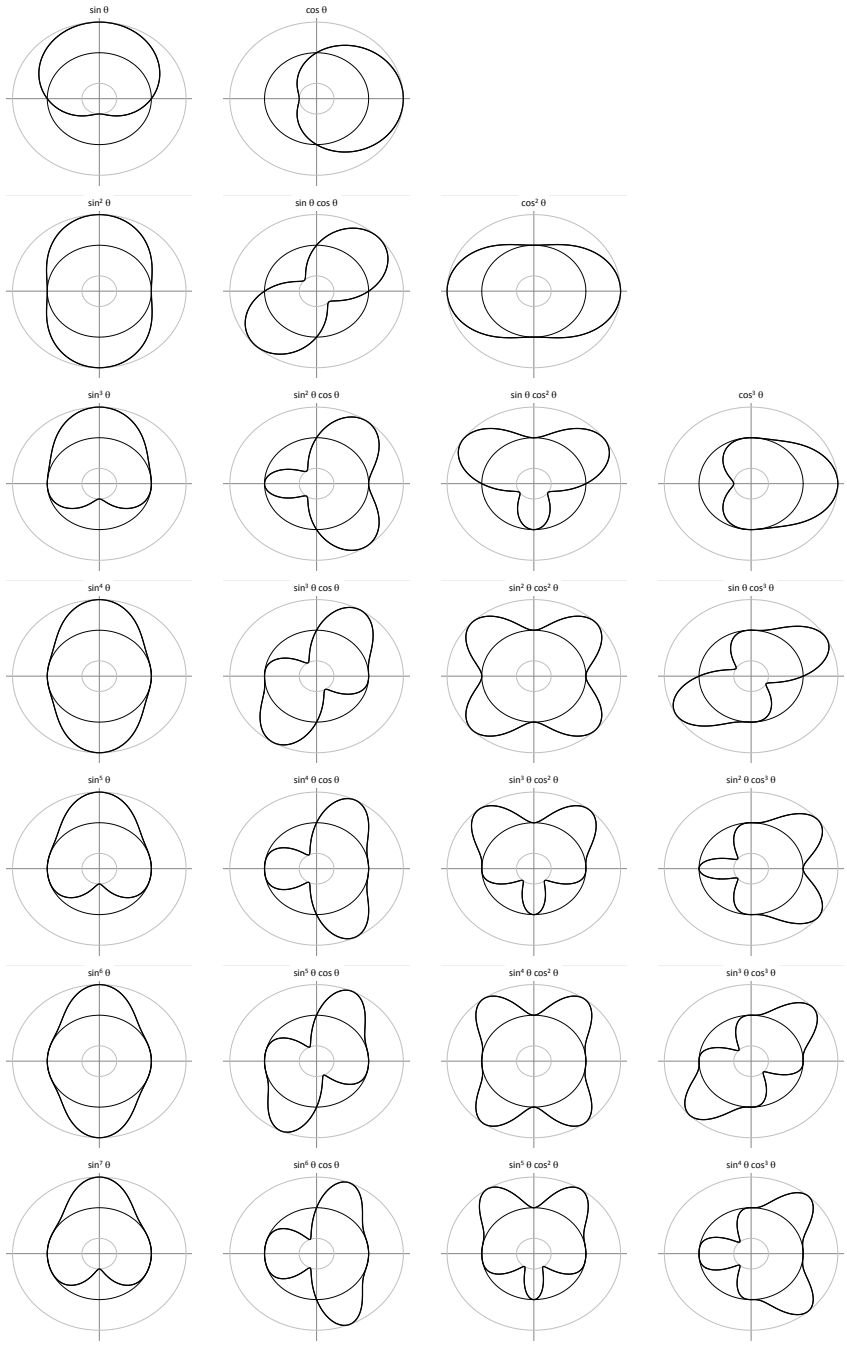

Figure 11.7: Elementary directivity diagrams ($\sin^p\theta\cos^q\theta$). Rows correspond to different values of $p+q$ (1 to 7). Columns correspond to different values of q (0 to 3).

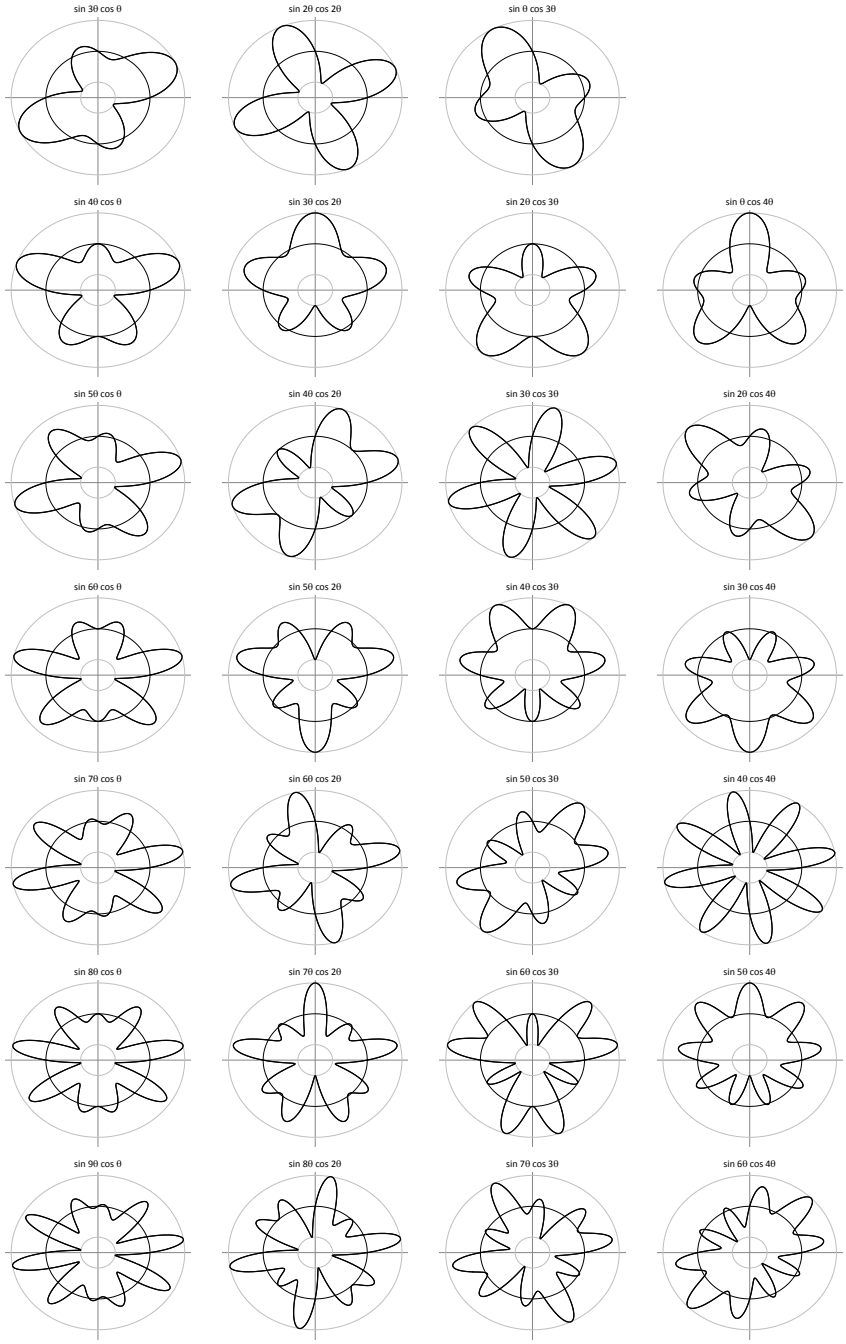

Figure 11.8: Elementary directivity diagrams ($\sin p\theta \cos q\theta$). Rows correspond to different values of $p + q$ (4 to 10). Columns correspond to different values of q (1 to 4).

This important result leads to numerous observations:

1. The acoustic field generated by a given set of sources (vector **a**) may be analysed in terms of its radial decay in a given direction (i.e. for a given **D** matrix) or by looking at its distribution on a sphere of given radius (given **g** vector).

2. In a given direction (i.e. for given α_j), the field contains different components with radial variation in $\frac{1}{(ikr)}$, $\frac{1}{(ikr)^2}$, $\frac{1}{(ikr)^3}$ $\cdots$

3. The decay rate does not involve the distance r, but an adimensional distance $kr = 2\pi\frac{r}{\lambda}$, where λ is the wavelength. kr is called the *Helmholtz number*.

4. The first term quickly dominates other terms which decay faster (-6 dB when doubling kr for the term of order 1, -12 dB for that of order 2, -18 dB for that of order 3, etc.).

5. The acoustic domain around a complex sound source is composed of two parts. The *near field* is the domain where the different components of the **g** vector are of equal importance. In the *far field*, the component in $\frac{1}{ikr}$ prevails. The boundary between near and far field is conventionally located five wavelengths away from the source ($kr \simeq 30$).

6. At a given distance r from the source, the directivity of the acoustic field is the linear combination (with complex coefficients) of elements of the matrix **D**.

7. Far away from the source, the terms of the first column dominate ($\alpha_1^p \alpha_2^q \alpha_3^r$). They define the directivity at infinity.

8. For a source distribution characterised by given multipole moments (vector **a**), the relative importance of the term of order n increases with k^n. We must therefore expect that the complexity of the directivity diagram of a source increases with frequency. This property is clearly demonstrated in Figure 11.9 which shows the sound field generated by a plane wave propagating in a duct opening onto a semi-infinite plane.

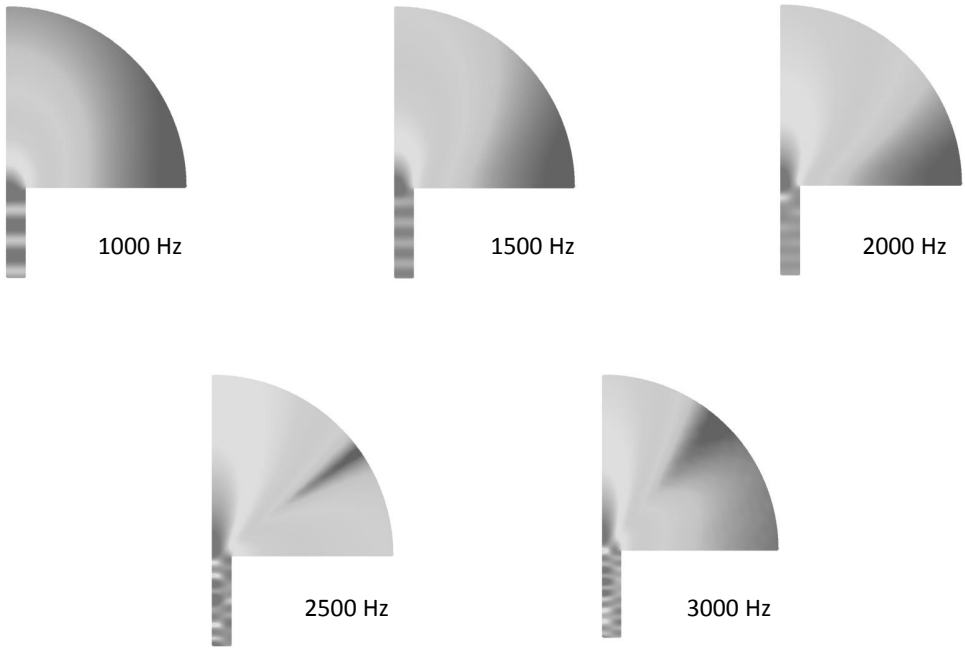

Figure 11.9: Effect of frequency on directivity: duct opening onto a semi-infinite plane. © ACTRAN by Free Field Technologies.

Relevance of multipole expansion

The relevance of the multipole analysis stems from the fact that *any noise source may be replaced by an equivalent distribution of monopoles*. Consider a vibrating surface S characterised by a distribution of normal velocity v_n. We define n point sources within the surface S and choose their amplitudes q_i to match the normal velocity profile v_n at n points of S (Figure 11.10). This cloud of point sources can then be replaced by a multipole expansion.

In this process, the amplitude of the individual sources depends on frequency. The associated multipole moments are then also frequency dependent. The importance of higher order terms tends to increase with frequency.[2] This strengthens the effect of the coefficients k^n.

[2] In vibro-acoustics this reflects the fact that higher frequency vibrations are more complex and involve higher order modes.

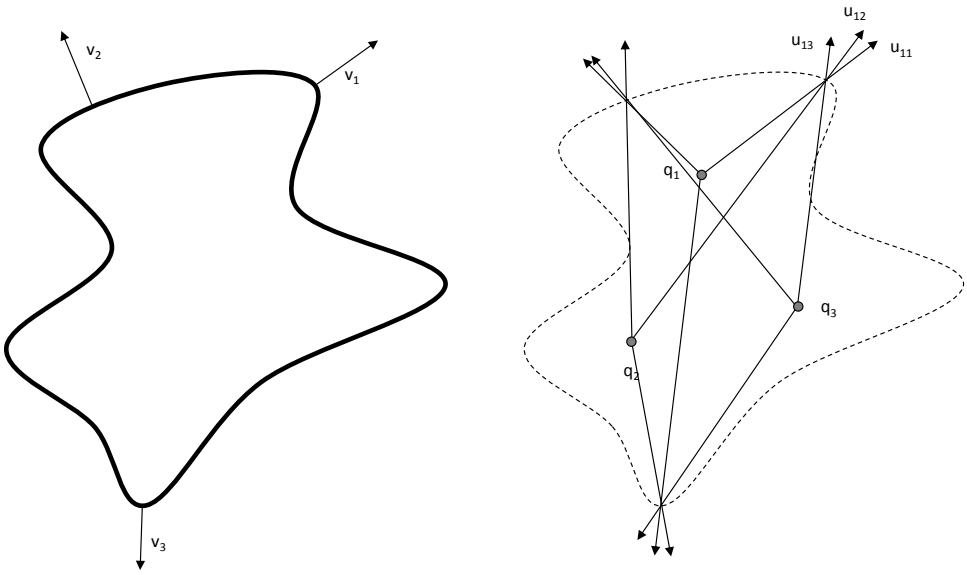

Figure 11.10: Any vibrating structure may be replaced by an equivalent set of point sources. The amplitudes q_1, q_2 and q_3 of the three sources on the right sketch may be set to match the normal velocity at three distinct points on the vibrating surface (left sketch). Only three sources are shown here, while hundreds of sources are usually required to match the velocity profile on the vibrating surface. The replacement of a vibrating surface by an equivalent set of point sources is asymptotically convergent; this will not be demonstrated here.

11.3 Helmholtz integral equation

11.3.1 Bounded domain

Consider a domain V, bounded by a surface S. The normal vector on S points away from V (Figure 11.11). The Helmholtz integral equation states that:

$$p(P) = -\oint_S [p(Q)\partial_n G(P,Q) + i\rho\omega v_n(Q)G(P,Q)]\, dS(Q) \tag{11.43}$$

where Q is a point of S, p the acoustic pressure, v_n the normal velocity and G the Green function associated with the Helmholtz equation:

$$G(P,Q) = \frac{e^{-ikr}}{4\pi r} \tag{11.44}$$

where r is the distance between P and Q. The Helmholtz integral relation will be demonstrated in the next sections.

Green's identity

Consider two functions u and v, *sufficiently continuous and differentiable* on both V and S. Green's identity relates the integrals of u and v on the volume V and the surface S:

$$\int_V [u\partial_{ii}v - v\partial_{ii}u]\, dV = \int_S [u\partial_n v - v\partial_n u]\, dS \tag{11.45}$$

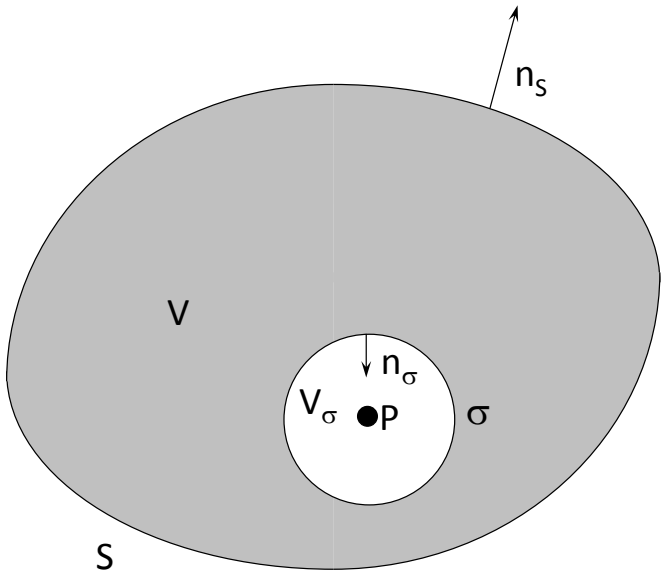

Figure 11.11: Helmholtz integral equation for an interior problem. Case 1: the point P is inside the domain V.

Green's identity can be demonstrated by integrating the volume integral by parts while applying the divergence theorem twice:

$$\begin{aligned}\int_V u\partial_{ii}v dV &= \int_V \left[\partial_i \left(u\partial_i v\right) - \partial_i u \partial_i v\right] dV \\ &= \int_S u\partial_n v dS - \int_V \partial_i u \partial_i v dV \\ &= \int_S u\partial_n v dS - \int_V \left[\partial_i \left(v\partial_i u\right) - v\partial_{ii}u\right] dV \\ &= \int_S \left[u\partial_n v - v\partial_n u\right] dS + \int_V v\partial_{ii}u dV \end{aligned} \tag{11.46}$$

Case 1: The point P is inside the domain V

Replace u by the pressure field p and v by the Green function G. As G is singular at P ($r = 0$), we cannot apply the identity to the entire domain V, but have to carve out a small spherical domain V_σ centered on P and bounded

by σ (Figure 11.11). We then have:

$$\begin{aligned}\int_{V-V_\sigma} [p\partial_{ii}G - G\partial_{ii}p]\, dV &= \int_S [p\partial_n G - G\partial_n p]\, dS \\ &+ \int_\sigma [p\partial_n G - G\partial_n p]\, d\sigma \end{aligned} \tag{11.47}$$

p and G being solutions of the homogeneous Helmholtz equation in $V - V_\sigma$, the volume integral vanishes:

$$\int_{V-V_\sigma} [p\partial_{ii}G - G\partial_{ii}p]\, dV = \int_{V-V_\sigma} \left[p(-k^2G) - G(-k^2p)\right] dV = 0 \tag{11.48}$$

The integral on σ can be calculated explicitly. If ε is the radius of the sphere σ, then the normal derivative on σ is equal and opposed to the derivative with respect to ε:

$$\int_\sigma [p\partial_n G - G\partial_n p]\, d\sigma \tag{11.49}$$

$$= -\int_0^{2\pi}\int_0^{\pi} \left[p\frac{\partial}{\partial\varepsilon}\left(\frac{e^{-ik\varepsilon}}{4\pi\varepsilon}\right) - \left(\frac{e^{-ik\varepsilon}}{4\pi\varepsilon}\right)\frac{\partial p}{\partial\varepsilon}\right]\varepsilon^2 \sin\theta d\theta d\phi \tag{11.50}$$

$$= -\frac{1}{4\pi}\int_0^{2\pi}\int_0^{\pi} \left[-p\,(ik\varepsilon + 1) - \varepsilon\frac{\partial p}{\partial\varepsilon}\right] e^{-ik\varepsilon} \sin\theta d\theta d\phi \tag{11.51}$$

If ε tends to zero, most terms disappear and we obtain:

$$\lim_{\varepsilon\to 0}\int_\sigma [p\partial_n G - G\partial_n p]\, d\sigma = \frac{p(P)}{4\pi}\lim_{\varepsilon\to 0}\int_0^{2\pi}\int_0^{\pi} \sin\theta d\theta d\phi = p(P) \tag{11.52}$$

The integral on σ therefore yields the value of pressure at P. Inserting this result in Equation 11.47 and taking Equation 11.48 into account, we find:

$$\int_S [p\partial_n G - G\partial_n p]\, dS + p(P) = 0 \tag{11.53}$$

And if we replace the pressure gradient by the normal velocity (Equation 6.5), we find the Helmholtz integral equation:

$$p(P) = -\oint_S [p(Q)\partial_n G(P,Q) + i\rho\omega v_n(Q)G(P,Q)]\, dS(Q) \tag{11.54}$$

Case 2: the point P is on the bounding surface S

If the point P is located on the boundary S of the domain V (Figure 11.12), σ is no longer a full sphere, but rather a portion of a sphere. The integral on σ is no longer equal to $p(P)$, but to:

$$\lim_{\varepsilon \to 0} \int_{\sigma} [p \partial_n G - G \partial_n p] \, d\sigma = \frac{\int_{\sigma} \sin\theta d\theta d\phi}{4\pi} p(P) = \frac{\alpha(P)}{4\pi} p(P) \tag{11.55}$$

where $\alpha(P)$ is the solid angle under which the point P sees the volume V. Some examples: if the surface is regular at P then $\alpha(P) = 2\pi$, if P is on the edge of a cube then $\alpha(P) = \pi$ and if P is at the apex of a cube then $\alpha(P) = \pi/2$. The Helmholtz equation for a point P belonging to S finally takes the form:

$$c(P)p(P) = -\oint_S [p(Q)\partial_n G(P,Q) + i\rho\omega v_n(Q) G(P,Q)] \, dS(Q) \tag{11.56}$$

where $c(P) = \alpha(P)/4\pi$ is a coefficient depending on the topology of S at P.

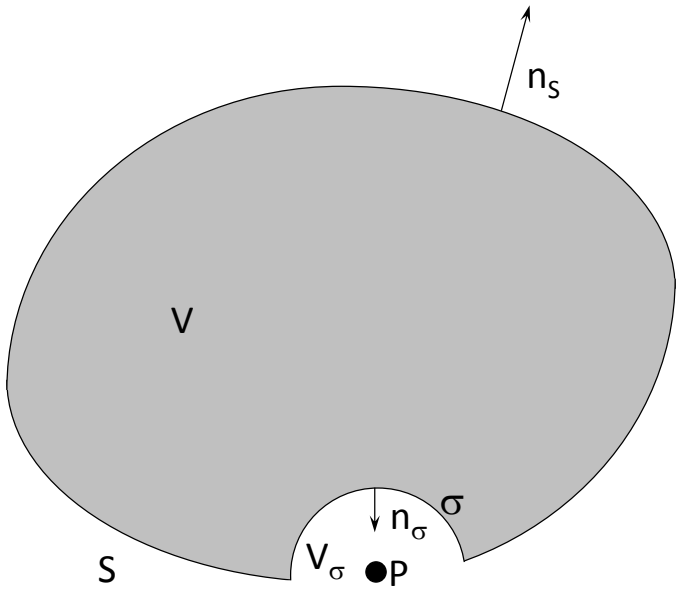

Figure 11.12: Helmholtz integral equation for an interior problem. Case 2: the point P is on the bounding surface S.

Case 3: the point P is outside the volume V

If the point P does not belong to V or S (Figure 11.13), there is no singularity to be excluded from the integration domain and we find:

$$\oint_S \left[p(Q)\partial_n G(P,Q) + i\rho\omega v_n(Q)G(P,Q)\right] dS(Q) = 0 \tag{11.57}$$

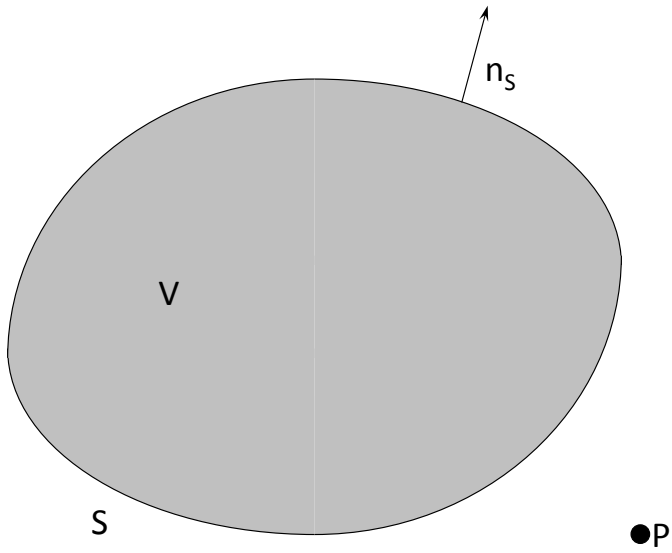

Figure 11.13: Helmholtz integral equation for an interior problem. Case 3: the point P is outside the volume V.

Comments

1. Equations 11.54 and 11.56 are different in nature. Equation 11.54 expresses that the pressure in domain V is entirely determined by the pressure and normal velocity distribution on S. If p and v_n are known on S, the sound field is known everywhere in V. Equation 11.56 is an *integral equation* relating the pressure and velocity distributions on S.

2. If the normal to S is defined as pointing into V, the sign of the integral

on S changes. The Helmholtz integral equation then becomes:

$$c(P)p(P) = \oint_S [p(Q)\partial_n G(P,Q) + i\rho\omega v_n(Q)G(P,Q)]\, dS(Q) \quad (11.58)$$

11.3.2 Unbounded domains

Consider an **unbounded domain** (Figure 11.14). The normal direction has changed as it has to point away from V. The integral on S and that on σ are calculated exactly as above. An additional integral appears on the surface at infinity Σ (sphere whose radius tends to infinity):

$$p(P) = -\oint_S [p(Q)\partial_n G(P,Q) + i\rho\omega v_n(Q)G(P,Q)]\, dS(Q) \quad (11.59)$$

$$-\frac{1}{4\pi}\lim_{\varepsilon\to\infty}\int_0^{2\pi}\int_0^{\pi} [-p\,(ik\varepsilon+1) + i\rho\omega\varepsilon v_\varepsilon]e^{-ik\varepsilon}\sin\theta d\theta d\phi \quad (11.60)$$

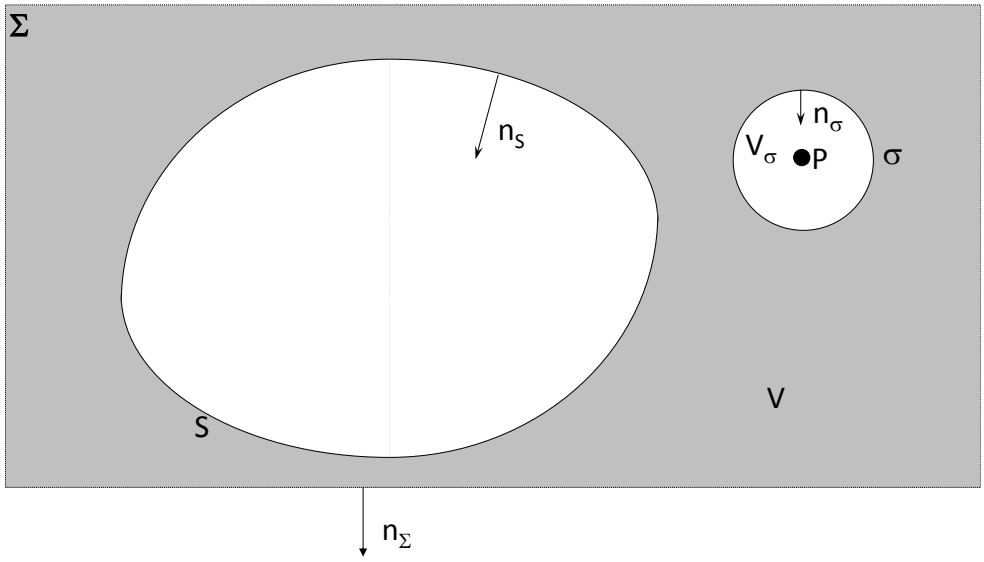

Figure 11.14: Helmholtz integral equation for an exterior problem. Case 1: P does not belong to S.

This integral is zero if the Sommerfeld condition is respected i.e. when:

$$\lim_{\varepsilon\to\infty}\left[-p\left(ik\varepsilon+1\right)+i\rho\omega\varepsilon v_\varepsilon\right]=0 \tag{11.61}$$

This condition imposes the following asymptotic behaviour to the *radial* acoustic impedance:

$$\lim_{\varepsilon\to\infty}\frac{p}{v_\varepsilon}=\lim_{\varepsilon\to\infty}\rho c\frac{ik\varepsilon}{1+ik\varepsilon}=\rho c \tag{11.62}$$

If P belongs to S, we find again Equation 11.56. The coefficient $c(P) = \alpha(P)/4\pi$ is the solid angle α under which P sees the *outside* S. Three examples: if S is regular at P then $c(P) = 1/2$, if P is on the edge of a cube then $c(P) = 3/4$ and if P is at the apex of a cube then $c(P) = 7/8$.

11.3.3 Indirect form of the integral equation

Consider a thin surface S and its normal vector n (Figure 11.15). To apply the Helmholtz integral equation to S, we must encircle it with a closed surface made of S^+ (on the side of n) and S^- (on the side opposite to n). We assume that the surface S_e representing the edges of the plate has no geometrical extension. All integrals on S_e are then equal to zero.

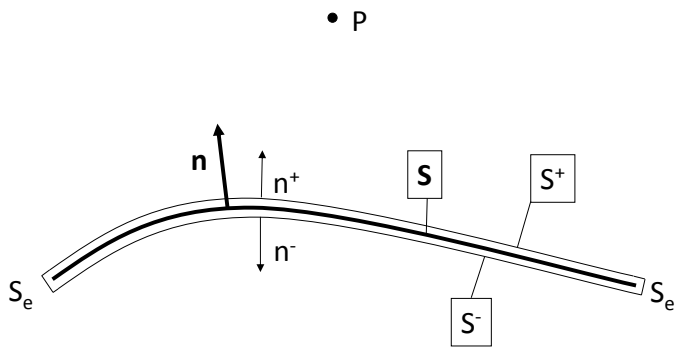

Figure 11.15: Notations for the indirect Helmholtz integral equation.

The pressure at a point P is then given by:

$$\begin{aligned} p(P) &= \int_{S^+} \left[p^+ \partial_{n^+} G + i\rho\omega G v^+_{n_+} \right] dS \\ &+ \int_{S^-} \left[p^- \partial_{n^-} G + i\rho\omega G v^-_{n_-} \right] dS \end{aligned} \tag{11.63}$$

but:

- integrating on S^- or S^+ is the same as integrating on S;
- $\partial_{n^+} G = \partial_n G$;
- $\partial_{n^-} G = -\partial_n G$;
- $v^+_{n^+} = v^+_n$;
- $v^-_{n^-} = -v^-_n$.

so that:

$$p(P) = \int_S \left[\left(p^+ - p^- \right) \partial_n G + i\rho\omega G \left(v^+_n - v^-_n \right) \right] dS \tag{11.64}$$

or, noting σ the difference of velocity and μ the difference of pressure on both sides of S:

$$p(P) = \int_S \left[\mu \partial_n G + i\rho\omega G \sigma \right] dS \tag{11.65}$$

By analogy to electromagnetic theory, σ is called the single layer potential and μ the double layer potential. If pressure and velocity are known on both sides of S then Equation 11.65 gives the pressure everywhere in the domain. This new integral equation is general and applies to any surface S, opened or closed, simply or multiply connected. If S is closed then Equation 11.65 holds whether P is located inside or outside S. When P belongs to S, the singular integral must be evaluated by specific techniques which will not be presented here[3].

[3]See for instance **Migeot J-L., Lecomte C., Meerbergen K.**. *Implementation and accuracy issues* in *Boundary element methods in Acoustics*, Editor: O. von Estorff, Computational Mechanics Publications Ltd (2000).

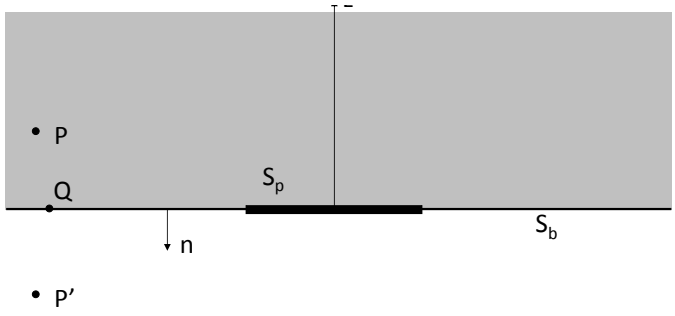

Figure 11.16: Baffled plate.

Note finally that if S represents the mid-surface of a thin plate, σ (velocity difference between both sides of the plate) is usually zero and we have:

$$p\,(P) = \int_S \mu \partial_n G dS \tag{11.66}$$

11.3.4 Sound radiation by a vibrating plate

Baffled plate

Consider a plate whose out-of-plane displacement is u_z (Figure 11.16). The plate is inserted in a rigid plane (called a *baffle*). S_p and S_b respectively denote the plate and baffle surface. We want to calculate the pressure at point P and define the symmetrical P' of P with respect to $S_p \bigcup S_b$. Q is a point of $S_p \bigcup S_b$. We now apply Equation 11.54 to the unbounded domain V located above the baffle:

$$\begin{aligned} p(P) &= -\int_{S_p} \left[p(Q)\partial_n G(P,Q) + i\rho\omega v_n(Q) G(P,Q)\right] dS(Q) \\ &\quad -\int_{S_b} \left[p(Q)\partial_n G(P,Q) + i\rho\omega v_n(Q) G(P,Q)\right] dS(Q) \end{aligned} \tag{11.67}$$

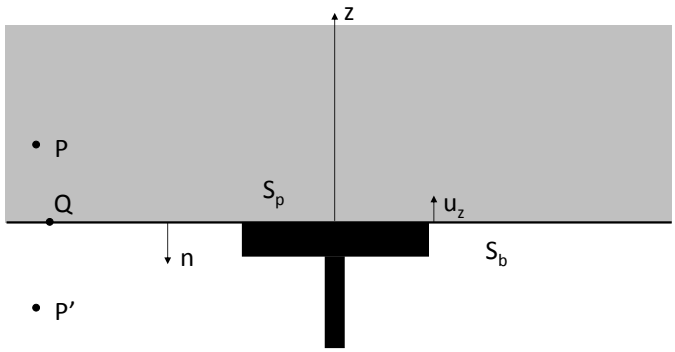

Figure 11.17: Baffled piston.

and apply Equation 11.57 to the same domain:

$$\begin{aligned} 0 &= -\int_{S_p} \left[p(Q)\partial_n G(P'.Q) + i\rho\omega v_n(Q)G(P'.Q)\right] dS(Q) \\ &\quad -\int_{S_b} \left[p(Q)\partial_n G(P'.Q) + i\rho\omega v_n(Q)G(P'.Q)\right] dS(Q) \end{aligned} \tag{11.68}$$

Adding the two equations and taking the following facts into account:

- $v_n = 0$ on S_b;
- $v_n = -i\omega u_z$ on S_p;
- $G(P,Q) = G(P'.Q)$ on S_b et S_p;
- $\partial_n G(P,Q) = -\partial_n G(P'.Q) = 0$ on S_b and S_p.

We obtain:

$$p(P) = -2\rho\omega^2 \int_{S_p} u_z(Q)G(P,Q)dS(Q) \tag{11.69}$$

Baffled piston

Consider now that u_z is constant. The noise radiated by a rigid baffled piston is:

$$p(P) = -2\rho\omega^2 u_z \int_{S_p} G(P,Q)dS(Q) \tag{11.70}$$

The integral can be calculated numerically or analytically. The pressure distribution is shown in Figure 11.18 for a circular piston of radius 10 cm vibrating with an acceleration of 1 m/s^2 ($u = -1/\omega^2$). If the diameter of the piston is small compared to the wavelength (i.e. if kr is small), we can consider the integrand as constant and obtain:

$$p(P) \simeq -2\rho\omega^2 S u_z \frac{e^{-ikr}}{r} \tag{11.71}$$

where r is the distance between P and the centre of the piston. The piston radiates, in this case, like a *monopole*.

Unbaffled plate

If the plate is not baffled, one can directly apply Equation 11.66:

$$p\,(P) = \int_S \mu \partial_n G dS \tag{11.72}$$

but we do not know the pressure difference μ between both faces. If the plate is small in comparison to the wavelength, we can nevertheless write:

$$p\,(P) \simeq \partial_n G\,(Q) \int_S \mu dS \tag{11.73}$$

where Q is at the centre of the plate. The **dipolar** character of the radiated sound field is quite visible and is in opposition to the **monopolar** behaviour observed in the baffled case.

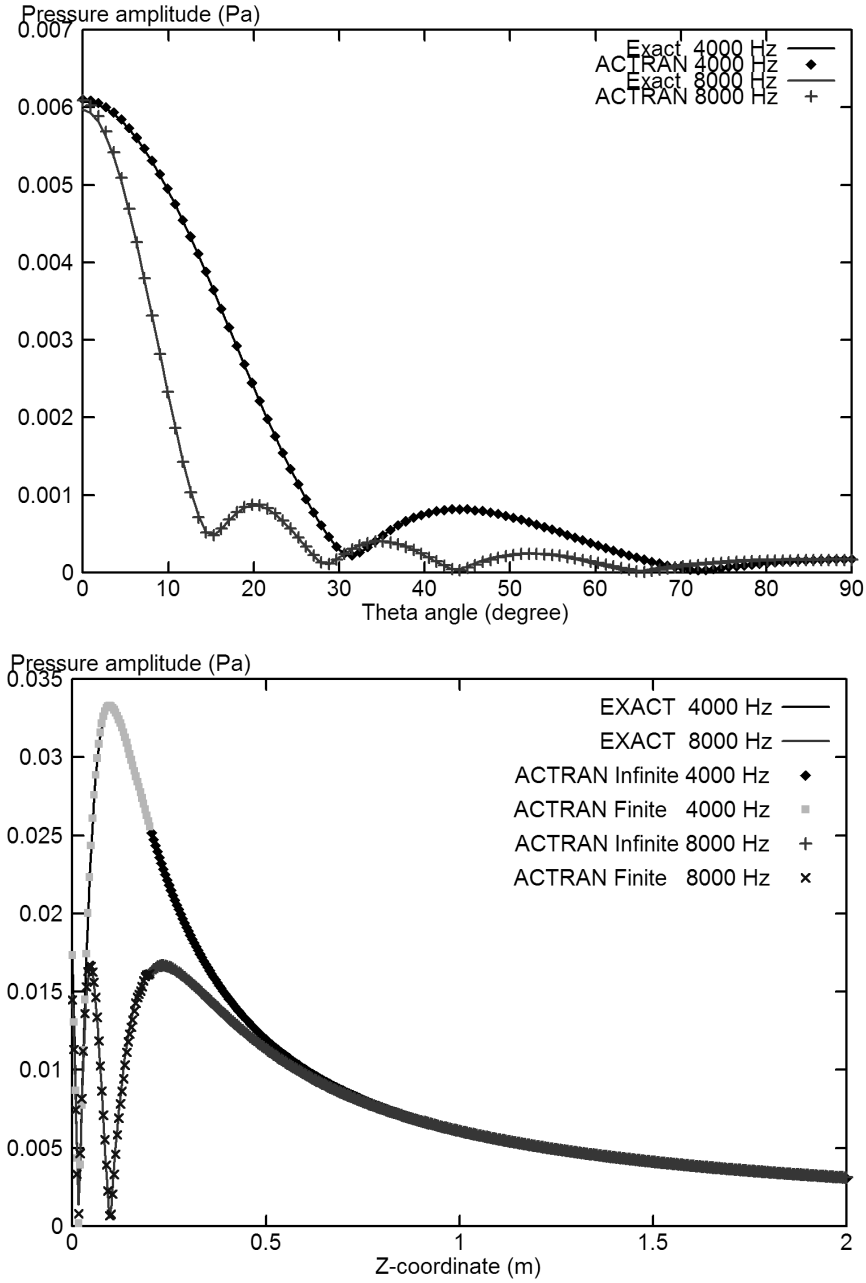

Figure 11.18: Radiation of a baffled piston at 4 and 8 kHz. Above: directivity diagram. Below: pressure distribution along the piston axis.

11.4 Power, efficiency and impedance

11.4.1 Radiated power

The radiated power is the integral of active intensity on the radiating surface or on a control surface encircling the radiating surface:

$$W_{rad} = \Re\left(\frac{1}{2}\int_S p v_n^* dS\right) \tag{11.74}$$

Note that S can be partitioned ($S = \cup_i S_i$). One can then associate a contribution W_i to each surface S_i. The total power is the sum of all contributions:

$$W_{rad} = \sum_i W_i \tag{11.75}$$

11.4.2 Radiation efficiency

Radiated power is sometimes compared to a conventional reference power calculated by considering that every point of S radiates independently and has a local acoustic impedance of ρc:

$$\begin{aligned} W_0 &= \Re\left(\frac{1}{2}\int_S \rho c v_n v_n^* dS\right) \\ &= \frac{1}{2}\int_S \rho c |v_n|^2 dS \end{aligned} \tag{11.76}$$

The ratio of both powers is called the *radiation efficiency*:

$$\sigma = \frac{W_{rad}}{W_0} \tag{11.77}$$

11.4.3 Radiation impedance

Consider a tube, or any acoustical component, connected by an opening S_o to a half space bounded by an infinite rigid baffle S_b (Figure 11.19). We can apply Equation 11.69 to S_o:

$$\frac{1}{2}p(P) = 2i\rho\omega \int_{S_o} v_z(Q)G(P,Q)dS(Q) \tag{11.78}$$

The relationship between pressure and velocity distribution on S_o is non-local. The operator R defined by:

$$R(u) = 4i\rho\omega \int_{S_p} u(Q)G(P,Q)dS(Q) \tag{11.79}$$

is called the radiation impedance of the semi-infinite half-space. The non-local relationship between pressure and velocity on S_o ($p = R(v_z)$) represents the effect of the semi-infinite half-space on the sound field in the acoustic component (Figure 11.19).

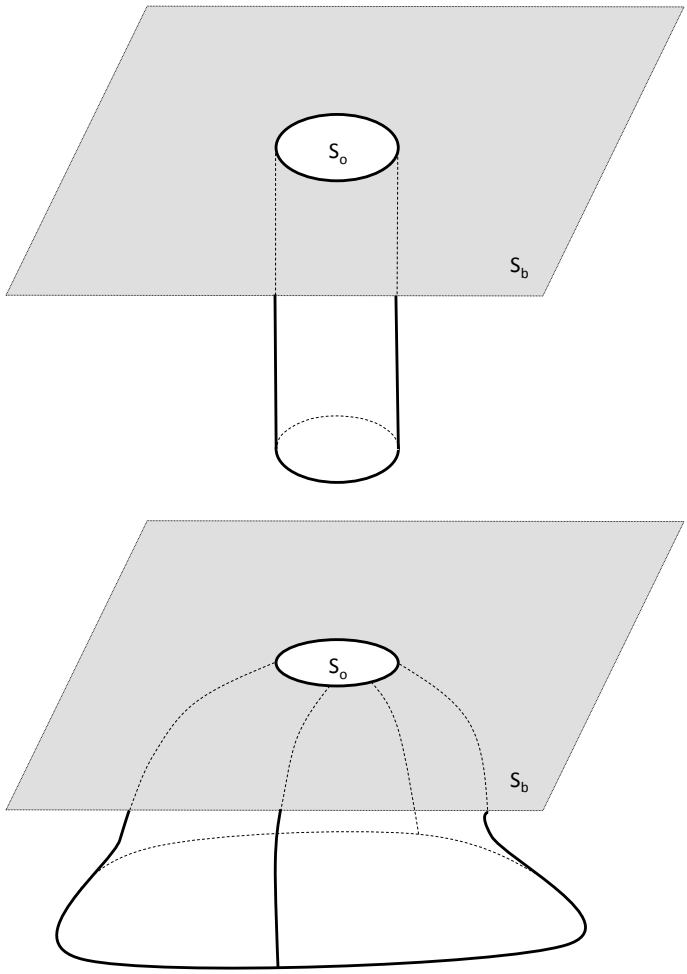

Figure 11.19: Non-local boundary condition on the surface S_o connecting an acoustic component to a semi-infinite (baffled) half-space.

12

Diffraction

In this brief chapter we show that a diffraction problem can be formulated as a radiation problem with modified boundary conditions. We do not discuss other classical diffraction theories (Fresnel, Kirchhoff, etc.).

Consider an exterior domain Ω bounded by a surface Γ. The unknown pressure field p obeys a non-homogeneous Helmholtz equation:

$$\Delta p + k^2 p = f \tag{12.1}$$

Three types of boundary conditions are defined on Γ :

$$\begin{aligned} p &= \bar{p} \quad on \quad \Gamma_p \\ \partial_n p &= -i\rho\omega\bar{v}_n \quad on \quad \Gamma_v \\ \partial_n p &= -i\rho\omega A_n p \quad on \quad \Gamma_Z \end{aligned} \tag{12.2}$$

where A_n is the normal admittance coefficient on surface Γ_Z and where Γ_p, Γ_v and Γ_Z define a partition of Γ. If we know the *free field* created by the distribution of source f, i.e. the field p_i solution of:

$$\Delta p_i + k^2 p_i = f \tag{12.3}$$

with no boundary conditions, we can define the *scattered field* $p_s = p - p_i$ and solve the following *homogeneous* problem for p_s:

$$\Delta p_s + k^2 p_s = O \tag{12.4}$$

with the modified boundary conditions:

$$\begin{aligned} p_s &= \bar{p} - p_i \quad on \quad \Gamma_p \\ \partial_n p_s &= -i\rho\omega\bar{v}_n - \partial_n p_i \quad on \quad \Gamma_v \\ \partial_n p_s &= -i\rho\omega A_n p - \partial_n p_i \quad on \quad \Gamma_Z \end{aligned} \tag{12.5}$$

Any diffraction problem can therefore be formally transformed into an equivalent radiation problem. The acoustic sources no longer appear at the right hand side of the partial differential equation, but are included in the boundary conditions. The methods seen in the previous chapter (multipole expansion, Helmholtz integral equation) can be used to calculate the scattered field. The total field is then obtained by adding the known incident field to the scattered field.

13

Refraction

The sounds reached him, as they would reach fish under water. Sounds not heard by ear, but by the whole body. Sounds absorbed and digested in such a way that sometimes their very meaning would change completely.
— **Georges Simenon** (1903-1989), Monsieur Monde Vanishes (1945).
Author's own translation from French to English.

Consider two media separated by a planar interface ($y = 0$) (Figure 13.1). The two media are characterised by their density (ρ_1, ρ_2) and speed of sound (c_1, c_2). Consider a plane wave of amplitude $I(\omega)$ propagating in medium 1 and characterised by the wave vector $(k_1 \sin\theta_1, -k_1 \cos\theta_1, 0)$. A part $R(\omega)$ of the wave is reflected with the wave vector:

$$\vec{k_1} : (k_1 \sin\theta_1, k_1 \cos\theta_1, 0) \tag{13.1}$$

while a part $T(\omega)$ is transmitted and propagates in medium 2 with the wave vector:

$$\vec{k_1} : (k_2 \sin\theta_2, -k_2 \cos\theta_2.0) \tag{13.2}$$

The acoustic field in medium 1 is given by:

$$p_1(\vec{r}, \omega) = I(\omega)\, e^{-ik_1 x \sin\theta_1 + ik_1 y \cos\theta_1} + R(\omega) e^{-ik_1 x \sin\theta_1 - ik_1 y \cos\theta_1} \tag{13.3}$$

whereas in medium 2 we have:

$$p_2(\vec{r}, \omega) = T(\omega) e^{-ik_2 x \sin\theta_2 + ik_2 y \cos\theta_2} \tag{13.4}$$

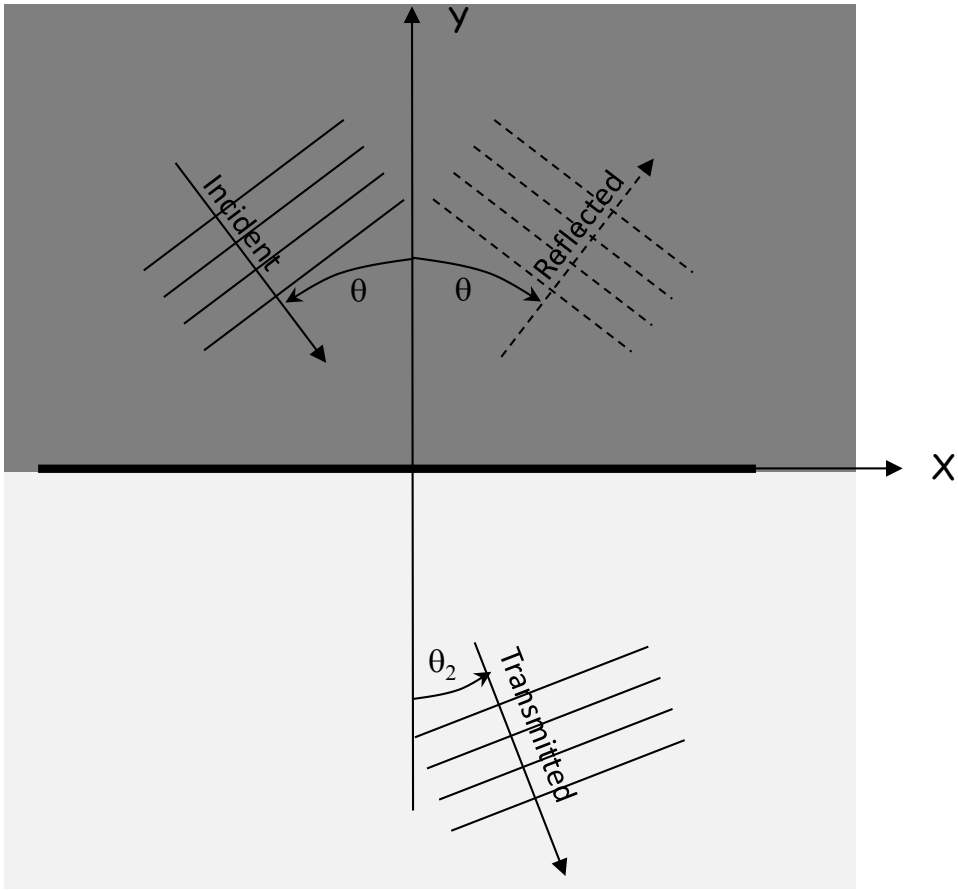

Figure 13.1: Refraction at the interface between two fluids.

Pressure must be continuous at the interface so that:

$$k_1 \sin\theta_1 = k_2 \sin\theta_2 \tag{13.5}$$

or:

$$\frac{\sin\theta_1}{c_1} = \frac{\sin\theta_2}{c_2} \tag{13.6}$$

This is the Snell[1]-Descartes law.

On the other hand we know that:

$$T(\omega) = I(\omega) + R(\omega) \tag{13.7}$$

The normal velocity continuity at the interface requires that:

$$\frac{I(\omega) - R(\omega)}{\rho_1 c_1}\cos\theta_1 = \frac{T(\omega)}{\rho_2 c_2}\cos\theta_2 \tag{13.8}$$

The two last equations jointly yield:

$$\frac{R(\omega)}{I(\omega)} = \frac{\frac{\cos\theta_1}{\rho_1 c_1} - \frac{\cos\theta_2}{\rho_2 c_2}}{\frac{\cos\theta_1}{\rho_1 c_1} + \frac{\cos\theta_2}{\rho_2 c_2}} = \frac{\frac{\rho_2 c_2}{\rho_1 c_1} - \frac{\cos\theta_2}{\cos\theta_1}}{\frac{\rho_2 c_2}{\rho_1 c_1} + \frac{\cos\theta_2}{\cos\theta_1}} \tag{13.9}$$

and:

$$\frac{T(\omega)}{I(\omega)} = \frac{\frac{2\cos\theta_1}{\rho_1 c_1}}{\frac{\cos\theta_1}{\rho_1 c_1} + \frac{\cos\theta_2}{\rho_2 c_2}} = \frac{2\frac{\rho_2 c_2}{\rho_1 c_1}}{\frac{\rho_2 c_2}{\rho_1 c_1} + \frac{\cos\theta_2}{\cos\theta_1}} \tag{13.10}$$

Observe that the ratio $\frac{R}{I}$ and $\frac{T}{I}$ are independent of ω. The incident intensity is given by:

$$I_{inc} = \frac{|I|^2}{\rho_1 c_1} \tag{13.11}$$

and the transmitted intensity:

$$I_{trans} = \frac{|T|^2}{\rho_2 c_2} \tag{13.12}$$

The transmission factor (ratio of transmitted to incident intensity) can be

[1] **Willebrord Snell van Royen**, born in 1580 in Leiden and died in 1626, was a Dutch humanist, mathematician and physicist. It is not clear whether Snell really was the first to state this refraction law, as it was the great Dutch astronomer Christiaan Huygens who, seventy years after the fact, proposed to associate Snell's name to that of Descartes.

calculated as follows:

$$\tau = \frac{|T(\omega)|^2 \rho_1 c_1}{|I(\omega)|^2 \rho_2 c_2} = \frac{4\frac{\rho_2 c_2}{\rho_1 c_1}}{(\frac{\rho_2 c_2}{\rho_1 c_1} + \frac{\cos\theta_2}{\cos\theta_1})^2} \tag{13.13}$$

Critical incidence angle

The Snell-Descartes law equates the projections of $\vec{k}_1$ and $\vec{k}_2$ on the interface. If $c_1 > c_2$ (emission in water and transmission in air), an angle θ_2 is found for any incident angle θ_1. If $c_1 < c_2$ (emission in air and transmission in water), there is a critical angle θ_c given by:

$$\sin\theta_c = \frac{c_1}{c_2} \tag{13.14}$$

θ_2 only exists if $\theta_1 < \theta_c$, $\theta_2 = 90°$ for $\theta_1 = \theta_c$ and there is no transmission for $\theta_1 > \theta_c$. For an air/water interface the critical angle is 13°.

Normal incidence

In the normal incidence case ($\theta_1 = \theta_2 = 0$), the transmission factor is given by:

$$\tau = \frac{4\frac{\rho_2 c_2}{\rho_1 c_1}}{(1 + \frac{\rho_2 c_2}{\rho_1 c_1})^2} \tag{13.15}$$

If $\rho_2 c_2 \gg \rho_1 c_1$, we find the approximation:

$$\tau \simeq \frac{4\rho_1 c_1}{\rho_2 c_2} \tag{13.16}$$

At an interface between air (1) and water (2) we have the following transmission coefficient:

$$\tau \simeq 10^{-3} \tag{13.17}$$

Sound transmission from middle to inner ear

The external and middle ear are filled with air, the inner ear is filled with a liquid called perilymph, whose acoustic properties are similar to those of

water. At the interface between the two media, assuming normal incidence, the loss factor is:

$$\begin{aligned} \rho_1 c_1 &= 1.225 \times 340 = 417 \\ \rho_2 c_2 &= 1000 \times 1500 = 1.5 \cdot 10^6 \\ \tau &\simeq \frac{4 \times 417}{1.5 \cdot 10^6} \end{aligned} \tag{13.18}$$

The loss is equal to $10 \log \tau$ or 29.5 dB. The middle ear balances this effect in two ways:

- the eardrum to oval window surface ratio is 20 and the pressure in the inner ear is amplified by the same factor;
- the ossicle chain of the middle ear provides an additional amplification factor of 1.3: the displacement at the base of the stirrup (first ossicle on the tympanic side) is indeed slightly lower than that of the hammer base (third ossicle on the oval window side).

Together these two effects ($10 \log (1.3 \cdot 20)^2 = 28.3 dB$) almost perfectly compensate for the loss from air to perilymph, the residual attenuation is only 28.3-29.5=-1.2 dB.

Lifeguard analogy

The lifeguard analogy (Figure 13.2) provides an intuitive insight into the Snell-Descartes law. Consider a swimmer N who needs help from a lifeguard M. Knowing that this lifeguard runs at a speed v_c and swims at a speed $v_n < v_c$, what is the MPN route that he should take to join the swimmer in the shortest possible time? The MBN route is clearly the shortest in distance while MCN and MAN respectively minimize swim and running time. To find the fastest route, let's calculate the time as a function of the coordinates (x, y) of point P:

$$T = \frac{\sqrt{(x - x_M)^2 + (y - y_M)^2}}{v_c} + \frac{\sqrt{(x_N - x)^2 + (y_N - y)^2}}{v_n} \tag{13.19}$$

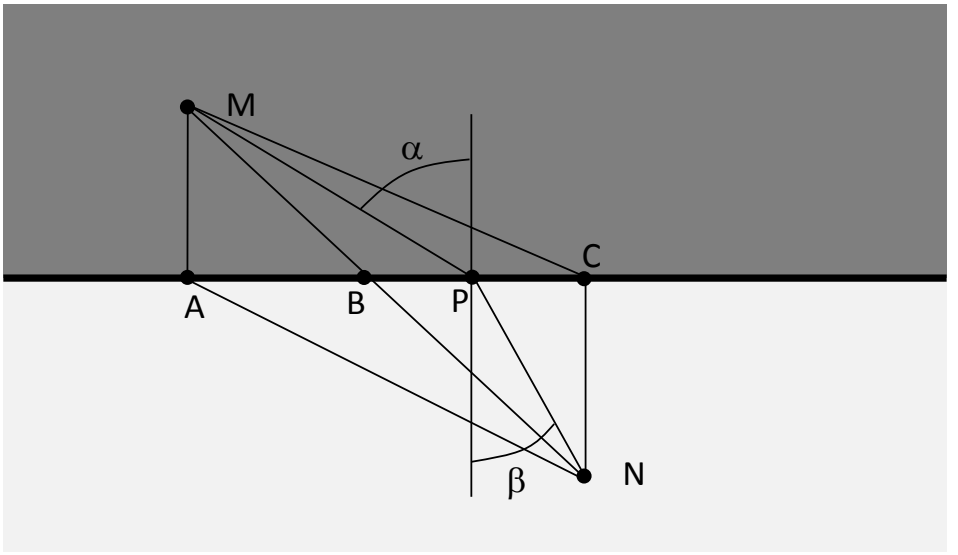

Figure 13.2: Refraction: the lifeguard analogy.

This time is minimum when:

$$\frac{x - x_M}{v_c\sqrt{(x - x_M)^2 + (y - y_M)^2}} - \frac{x_N - x}{v_n\sqrt{(x_N - x)^2 + (y_N - y)^2}} = 0 \qquad (13.20)$$

or, introducing the angles α and β, when:

$$\frac{\sin\alpha}{v_c} = \frac{\sin\beta}{v_n} \qquad (13.21)$$

which is exactly identical to the Snell-Descartes law. This analogy shows us that sound waves passing from one medium to another take a path minimizing their travel time.

14

Propagation in dissipative media

The least improbable explanation is that these things, UFOs, are artificial and controlled. My opinion for some time has been that they have an extraterrestrial origin.
— **Maurice A. Biot** (1905-1985), Life Magazine, April 7th, 1952.

Contents

14.1 Introduction 282
14.2 Equivalent fluid for a porous material 284
14.3 Biot theory 286
14.4 Practical use of poro-elastic materials 309

Acoustic waves lose energy while propagating. This is mainly due to two dissipative irreversible phenomena: viscous friction and non-isentropic heat exchange. These phenomena are always present during acoustic propagation because air is both viscous and not a perfect thermal insulator. However, as air viscosity and thermal conductivity are low, sound propagates over long distances without losing much energy. Dissipative phenomena can often be neglected or modelled very simply by giving an imaginary component to the speed of sound (Section 6.5.4).

Dissipation cannot be neglected when sound propagates in a porous material. Indeed, the fluctuations of acoustic pressure and velocities take place within cavities and ducts of very small dimensions. The velocity and temperature gradients which develop in this case are not inversely proportional to the wavelength, but to the size of those ducts and cavities. As viscous friction forces are proportional to the velocity gradient and thermal exchanges are proportional to the temperature gradient, these two effects become significant even if viscosity and thermal conductivity are low.

Propagation in porous media is characterised by important dissipation and acoustic energy is rapidly damped. This phenomenon is very useful to control the magnitude of stationary waves in cavities (interior of car, living room).

14.1 Introduction

Dissipation can be described in simple terms by reconsidering the derivation of the wave equation (Section 4.1):

- adding viscous dissipation in the porous medium via Darcy's law;
- introducing a linear hysteresis, related to non-isentropic thermal exchanges, in the equation of state linking pressure to density.

Starting from mass (Equation 4.1) and momentum (Equation 4.2) conservation equations, without the mass source term, and adding viscous friction forces f_i, we obtain:

$$\partial_t \rho_a + \rho_0 \partial_i v_{ia} = 0 \tag{14.1}$$

$$\rho_0 \partial_t v_{ia} + \partial_i p_a + f_i = 0 \tag{14.2}$$

According to Darcy's law, the frictional force per unit volume is opposed to the fluid flow in the porous material and proportional to the fluid velocity:

$$f_i = -R v_{ia} \tag{14.3}$$

The proportionality coefficient R, called *resistivity*, is defined precisely in Section 14.3.2 where the measurement procedure is described as well. Taking the Fourier transform of these equations, we obtain ($p_a(t) \Leftrightarrow p(\omega)$, $v_{ia}(t) \Leftrightarrow v_i(\omega)$, $\rho_a(t) \Leftrightarrow \rho(\omega)$):

$$i\omega\rho(\omega) + \rho_0 \partial_i v_i(\omega) = 0 \tag{14.4}$$

$$i\omega\rho_0 v_i(\omega) + \partial_i p(\omega) - R v_i(\omega) = 0 \tag{14.5}$$

Introducing hysteresis in the compression/expansion cycle modifies the proportional relationship between pressure (p_a) and bulk density (ρ_a) fluctuations (Equation 4.8). Hysteresis results from the non-reversible thermal exchange between the fluid and solid phases of the porous material. The easiest way to represent this phenomenon is to add a term, similar to volume viscosity, of the form:

$$p_a(t) = c_0^2 \rho_a(t) - K \frac{\partial \rho_a(t)}{\partial t} \tag{14.6}$$

where c_0 is the sound speed in the fluid and K is a coefficient characterising the loss of potential energy related to thermal exchanges. In the frequency domain (harmonic response) this relation becomes:

$$p(\omega) = c_0^2 \rho(\omega) - i\omega K \rho(\omega) \tag{14.7}$$

It is easy to eliminate ρ and v_i to obtain an equation involving only the pressure field $p(\omega)$:

$$\rho(\omega) = \frac{p(\omega)}{c_0^2 - i\omega K} \tag{14.8}$$

$$v_i(\omega) = \frac{\partial_i p(\omega)}{R - i\omega\rho_0} \tag{14.9}$$

$$i\omega \frac{p(\omega)}{c_0^2 - i\omega K} + \rho_0 \partial_i \left(\frac{\partial_i p(\omega)}{R - i\omega\rho_0} \right) = 0 \tag{14.10}$$

Rearranging terms and multiplying by $(R - i\omega\rho_0)/\rho_0$, we finally obtain:

$$\frac{i\omega R/\rho_0 + \omega^2}{c_0^2 - i\omega K} p(\omega) + \partial_{ii} p(\omega) = 0 \tag{14.11}$$

or:

$$\frac{1 + \frac{iR}{\omega\rho_0}}{1 - i\omega K/c_0^2} k^2 p(\omega) + \Delta p(\omega) = 0 \tag{14.12}$$

with $k = \omega/c_0$. Accounting for dissipative effects yields a *modified* Helmholtz equation involving a complex wave number:

$$\tilde{k} = k\sqrt{\frac{1 + \frac{iR}{\omega\rho_0}}{1 - i\omega K/c^2}} \tag{14.13}$$

The imaginary part of $\tilde{k}$ is positive.

14.2 Equivalent fluid for a porous material

14.2.1 Delany-Bazley model

The propagation of sound in porous materials with open pores is characterised by a complex, frequency dependent wavenumber. Such materials can be modelled by an equivalent fluid with complex and frequency dependent sound speed. One of the simplest models has been proposed by Delany and Bazley:[1]

$$\tilde{c} = \frac{c}{\beta - i\alpha} \tag{14.14}$$

with

$$\alpha = 1 + 0.0978 \left(\frac{R}{\rho_a f}\right)^{0.700} \tag{14.15}$$

[1] **Delany M.E., Bazley E.N.**, *Acoustical properties of fibrous absorbent materials*, Applied Acoustics 3, 1970, pp, 105-116.

and

$$\beta = 0.189 \left(\frac{R}{\rho_a f} \right)^{0.595} \tag{14.16}$$

In these expressions, f is the frequency in Hz, ρ_a is the bulk density of air, c is the speed of sound in air and R is the resistance of the porous medium (Section 14.3.2).

14.2.2 Miki model

Miki,[2] using measurements on many different materials with porosities close to one, proposed the following expressions for the characteristic impedance and the wave number:

$$Z_c = \rho_a c \left[1 + 5.50 \left(10^3 \frac{f}{R} \right)^{-0.632} - j8.43 \left(10^3 \frac{f}{R} \right)^{-0.632} \right] \tag{14.17}$$

$$\tilde{k} = \frac{\omega}{c} \left[1 + 7.81 \left(10^3 \frac{f}{R} \right)^{-0.618} - j11.41 \left(10^3 \frac{f}{R} \right)^{-0.618} \right] \tag{14.18}$$

where ρ_a is the bulk density of air, c the speed of sound and R the static resistivity in the direction of wave propagation. The expressions given below are valid for:

$$0.01 < \frac{f}{R} < 1.00 \tag{14.19}$$

From Z_c and $\tilde{k}$ we easily find the properties of the equivalent fluid ($\tilde{\rho_a}$, $\tilde{c}$):

$$\tilde{c} = \frac{\omega}{\tilde{k}} \tag{14.20}$$

$$\tilde{\rho_a} = \frac{\tilde{k} \cdot Z_c}{\omega} \tag{14.21}$$

[2] **Miki Y.**, *Acoustical properties of porous materials - modifications of Delany-Bazley models*, J. Ac. Soc. Japan, 11(1):19-24, 1990.

Figure 14.1: Maurice A. Biot (1905-1985).

14.3 Biot theory

The Biot[3] theory provides a general framework for the study of porous material in an acoustic field.

14.3.1 General assumptions

Biot's model is based on the following general assumptions:

[3]**Maurice Anthony Biot**, Belgian-American engineer (Figure 14.1), was born in Antwerp in 1905 and died in New York in 1985. He graduated from the Catholic University of Leuven and was then a student of Theodore von Kármán at Caltech. He published a series of pioneering articles on poro-elasticity and the mechanics of saturated porous media. The *Biot theory* is extensively used today in acoustics and soil mechanics.

- the heterogeneous medium is treated as an equivalent homogeneous medium made of a solid phase (skeleton) and a fluid phase (air in general);
- the volumic fraction is $(1-\Omega)$ for the skeleton and Ω for the air;
- the stress tensor and pressure are defined at each point of the medium;
- the wavelength λ is significatively longer than the characteristic dimensions of the material (pore and fibre diameter, skeleton feature size);
- displacements are small and linear elasticity applies;
- most pores are open;
- closed pores are considered as belonging to the skeleton and the effects related to fluid movement in closed pores are neglected;
- there is no mean flow and the fluid phase is at rest.

The state variables used are the displacements u of the skeleton and U of the fluid ($u-U$ model). In many cases the equations can be rewritten in terms of displacement u and acoustic pressure field p ($u-p$ model).

14.3.2 Biot parameters

The porous material is characterised by three sets of parameters:

1. Elastic parameters of the skeleton:
   - Young modulus E;
   - Poisson coefficient ν;
   - density of the bulk material forming the skeleton ρ_s;
   - instead of (E,ν) we can use the Lamé coefficients (λ,μ):

$$\lambda = \frac{\nu E}{(1+\nu)(1-2\nu)} \tag{14.22}$$

$$\mu = \frac{E}{2\,(1+\nu)} \tag{14.23}$$

or the shear and bulk moduli (G, K):

$$G = \mu = \frac{E}{2\,(1+\nu)} \tag{14.24}$$

$$K = \frac{E}{3\,(1-2\nu)} \tag{14.25}$$

2. Acoustic parameters of the fluid phase:
   - fluid density ρ_f.
   - fluid bulk modulus Q (as a first approximation, we use $Q = \rho_f c^2$, see Section 14.3.7 for a more detailed discussion).
3. Parameters specific to the porous medium and characterising the interaction between fluid and solid phases:
   - porosity Ω.
   - resistivity R.
   - Biot factor α.
   - tortuosity α_∞.

The physical meaning and measurement process of Ω, R and α_∞ are presented in the next sections. The Biot factor α, always close to 1 in air-saturated porous materials, is discussed in Section 14.3.4.

Porosity (Ω)

A sample of porous material with total volume V_t contains a volume V_f of fluid and V_s of solid. The porosity Ω is defined by:

$$\Omega = \frac{V_f}{V_t} = 1 - \frac{V_s}{V_t} \tag{14.26}$$

Porosity can be accurately measured by inserting a porous sample of volume V_e into the cavity of volume V_c of a steel cylinder (Figure 14.2). The cavity

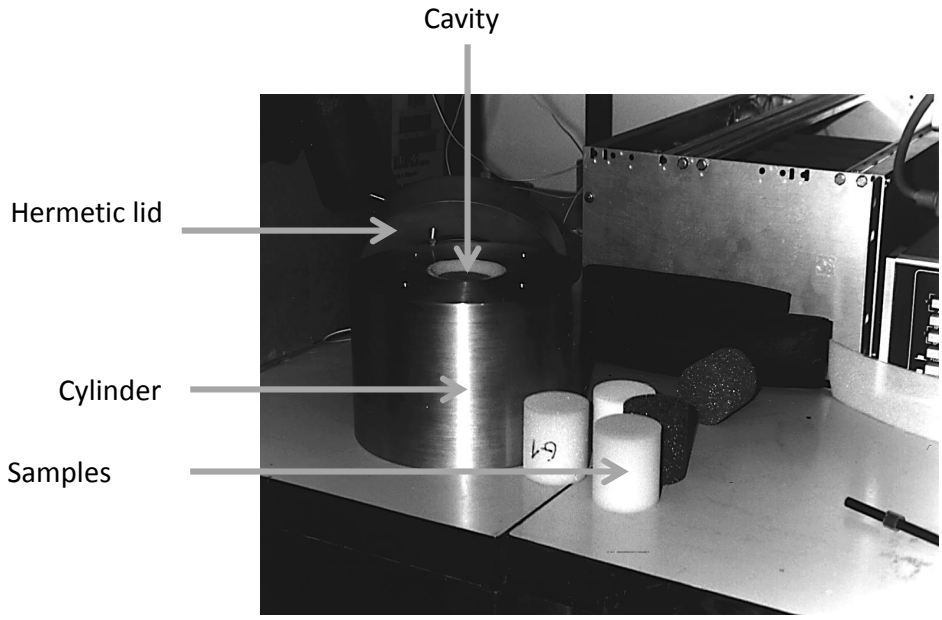

Picture taken by the author at the acoustics lab of Katholieke Universiteit Leuven.

Figure 14.2: Porosity measurement device.

containing the sample is sealed and a micrometric device is used to slightly change the volume. The pressure in the cavity increases from p_1 to p_2 due to the volume change ΔV. The thickness of the cylinder guarantees high thermal inertia and an isothermal process. If we neglect the compressibility of the skeleton, we can write:

$$p_1 \left(V_c - V_e \left(1 - \Omega\right)\right) = p_2 \left(V_c - V_e \left(1 - \Omega\right) - \Delta V\right) \tag{14.27}$$

The porosity is therefore equal to:

$$\Omega = \frac{p_2 \Delta V - \left(p_2 - p_1\right) \left(V_c - V_e\right)}{\left(p_2 - p_1\right) V_e} \tag{14.28}$$

Resistivity (R)

The flow of air through a porous material is limited by viscous interactions between the fluid and solid phase. Viscous forces are proportional to the relative velocity between the fluid and the skeleton:

$$F_R = R\left(\dot{u} - \dot{U}\right) \tag{14.29}$$

R is the resistivity of the porous medium. The *static* resistivity is measured by creating a flow of air $q = \Sigma v$ through a sample with thickness h placed in a test cell of cross section Σ (Figures 14.4 and 14.5). The pressure drop Δp between the upstream and downstream sides of the sample is measured with a differential manometer. Resistivity is given by:

$$R = \frac{\Delta p}{h\dot{U}} \tag{14.30}$$

but the velocity of air in the sample ($\dot{U}$) is greater than the velocity in the test cell (v) due to porosity which reduces the effective cross section:

$$\dot{U} = \frac{v}{\Omega} \tag{14.31}$$

The resistivity is finally given by:

$$R = \frac{\Omega \Delta p}{hv} \tag{14.32}$$

where R is measured in N.s/m^4 or Rayls/m (*Rayl* is a unit introduced in honour of Lord Rayleigh,[4] Figure 14.3). *Dynamic* resistivity depends on frequency as discussed in Section 14.3.7.

[4] **John William Strutt**, third **Lord Rayleigh**, was born on 12 November 1842 in Langford Grove, Maldon, Essex, and died on 30 June 1919 in Witham, Essex. He contributed to a wide area of topics: sound, wave, colour perception, electro-dynamics, electromagnetism, light diffraction, fluid mechanics and hydrodynamics, cavitation, viscosity, capillarity, elasticity and photography. *Theory of Sound*, published in two volumes in 1877-1878, is a cornerstone of acoustics. Rayleigh received the Nobel Prize in physics in 1904 for his discovery of argon.

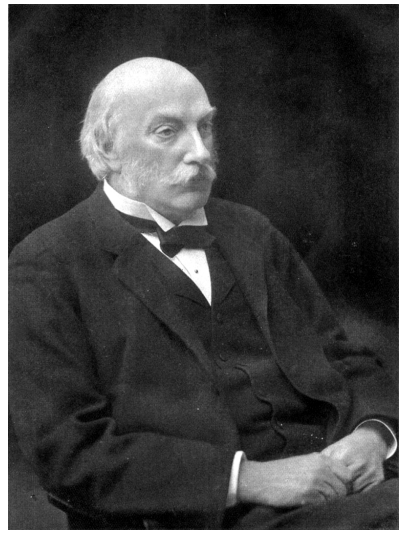

Figure 14.3: John William Strutt, third Lord Rayleigh.

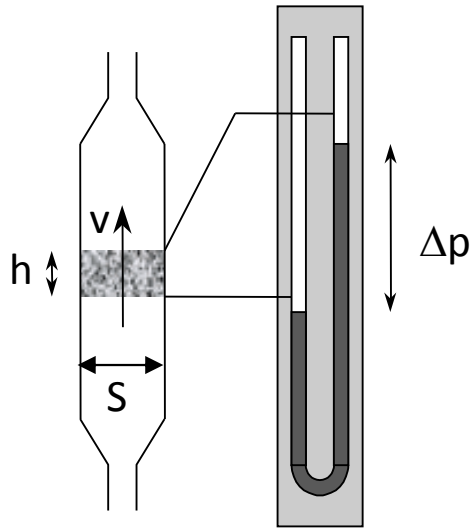

Figure 14.4: Schematic of the resistivity measurement set-up.

Picture taken by the author at the acoustics lab of Katholieke Universiteit Leuven.

Figure 14.5: Resistivity measurement device.

Tortuosity (α_∞)

Tortuosity measures the complexity of the trajectory of an air particle moving inside a porous medium. Biot defines tortuosity as the ratio of the kinematic energy of the microscopic molecular velocity of an inviscid fluid and the kinetic energy of the macroscopic wave.[5] Tortuosity can be measured by electric or ultrasonic methods.

In the **electrical method**, the sample is placed in a column of electrically conducting liquid of cross section S. The top and bottom sides of the sample are located at positions x_2 and x_3. A current I is generated by two electrodes above and below the sample (Figures 14.6 and 14.8). Potential differences are measured between positions x_4 and x_5 (V_1) and positions x_1 and x_4 (V_2). x_4 is usually very close to x_3 and x_2 close to x_1. If we assume that the sample is saturated in electrolyte, these potential differences may be expressed as functions of the fluid resistivity σ_f of the fluid and σ_e of the sample:

$$\begin{aligned} V_1 &= \frac{I}{S}\left(\sigma_f\left(x_4 - x_3\right) + \sigma_e\left(x_3 - x_2\right) + \sigma_f\left(x_2 - x_1\right)\right) \\ V_2 &= \frac{I}{S}\sigma_f\left(x_5 - x_4\right) \end{aligned} \tag{14.33}$$

From which we obtain:

$$\frac{\sigma_e}{\sigma_f} = \frac{V_2}{V_1}\frac{x_5 - x_4}{x_3 - x_2} - \frac{x_4 - x_3 + x_2 - x_1}{x_3 - x_2} \tag{14.34}$$

Tortuosity is defined by:

$$\alpha_\infty = \Omega\frac{\sigma_e}{\sigma_f} \tag{14.35}$$

The simpler and more accurate **ultrasonic method** is based on the fact that the propagation speed of an ultrasonic impulse through a porous material depends on tortuosity. The measuring device (Figure 14.7) comprises one ultrasound emitter and one receiver. An ultrasound impulse is emitted and the propagation time between the emitter and receiver is measured with and without the sample. Comparing reception delays provides the tortuosity value.

[5] **Lauriks W. and all.**, *Determination of the tortuosity of porous materials using new air-coupled ultrasonic transducers*, 11^{th} International FASE Symposium, Valencia, 1994.

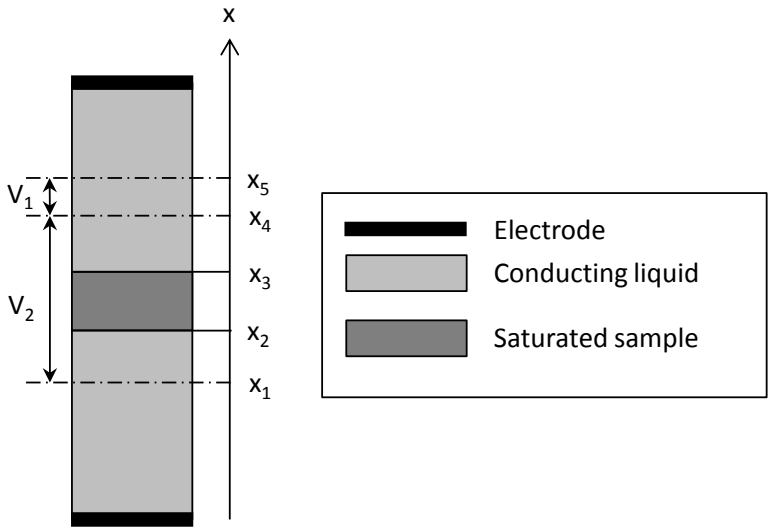

Figure 14.6: Electric measurement of tortuosity.

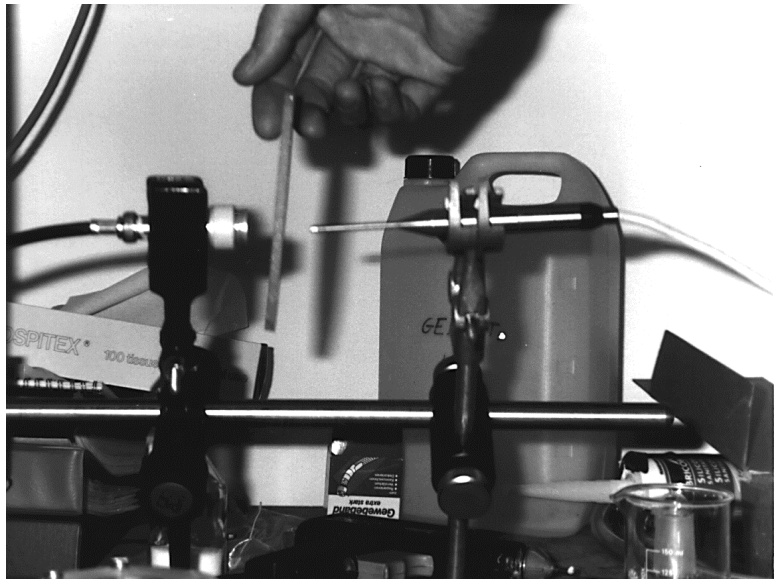

Picture taken by the author at the acoustics lab of Katholieke Universiteit Leuven.

Figure 14.7: Tortuosity measurement device: ultrasonic method.

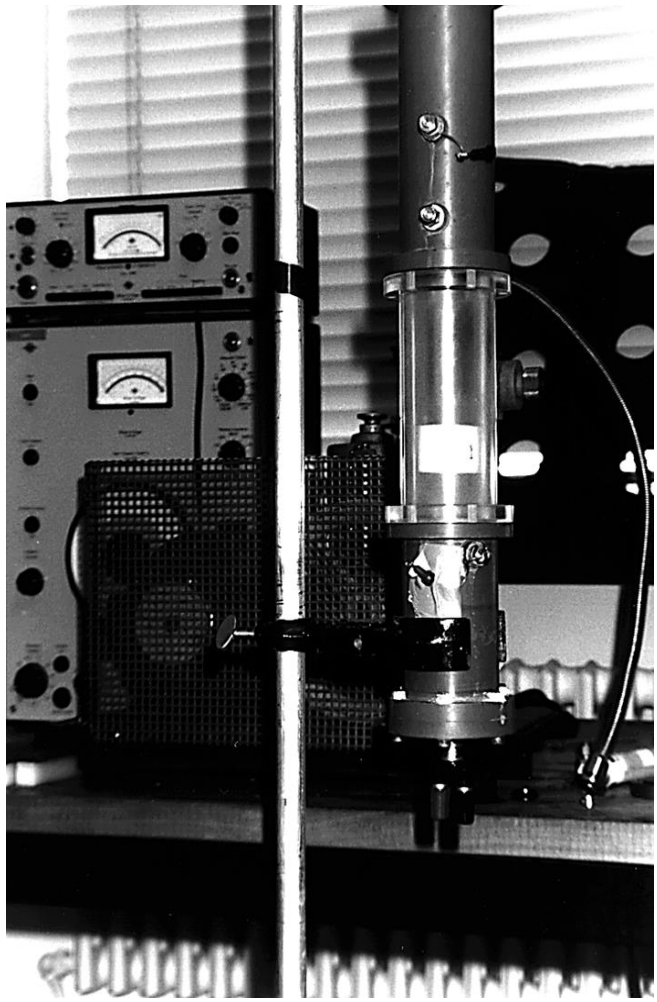

Picture taken by the author at the acoustics lab of Katholieke Universiteit Leuven.

Figure 14.8: Tortuosity measurement device: electrical method.

14.3.3 Equilibrium equations

The equilibrium equation for the skeleton is:

$$\partial_j \sigma_{ij}^S = (1-\Omega)\,\rho_s \ddot{u}_i + f_i^{FS} \tag{14.36}$$

where σ_{ij}^S is the elastic stress tensor in the skeleton and f_i^{FS} is an interaction term representing the force exerted by the fluid on the skeleton. The equilibrium equation of the fluid phase can be written as:

$$\partial_j \sigma_{ij}^F = \Omega \rho_f \ddot{U}_i + f_i^{SF} \tag{14.37}$$

where $\sigma_{ij}^F = -\Omega p \delta_{ij}$ is the isotropic stress tensor in the fluid and f_i^{SF} is an interaction term representing the force exercised by the skeleton on the fluid.

The fluid-skeleton interaction term $f_i^{FS} = -f_i^{SF}$ is the sum of two components. The first represents viscous forces and is proportional to the velocity difference between skeleton and fluid. The second term is inertial and proportional to the acceleration difference. The total interaction term is written as:

$$f_i^{SF} = -f_i^{FS} = \rho_{12}\left(\ddot{u}_i - \ddot{U}_i\right) - \tilde{b}\left(\dot{u}_i - \dot{U}_i\right) \tag{14.38}$$

The constants ρ_{12} and $\tilde{b}$ are linked to other Biot parameters:

$$\rho_{12} = \Omega \rho_f \left(1 - \alpha_\infty\right) \tag{14.39}$$

$$\tilde{b} = \Omega R \tag{14.40}$$

In harmonic conditions, the equilibrium equations become:

$$\partial_j \sigma_{ij}^S + \underbrace{\left[\underbrace{(1-\Omega)\,\rho_s - \rho_{12}}_{\rho_{11}} - \frac{i\omega\tilde{b}}{\omega^2}\right]}_{\tilde{\rho}_{11}} \omega^2 u_i + \underbrace{\left[\rho_{12} + \frac{i\omega\tilde{b}}{\omega^2}\right]}_{\tilde{\rho}_{12}} \omega^2 U_i = 0 \tag{14.41}$$

$$\partial_j \sigma_{ij}^F + \underbrace{\left[\underbrace{\Omega\rho_f - \rho_{12}}_{\rho_{22}} - \frac{i\omega\tilde{b}}{\omega^2}\right]}_{\tilde{\rho}_{22}} \omega^2 U_i + \underbrace{\left[\rho_{12} + \frac{i\omega\tilde{b}}{\omega^2}\right]}_{\tilde{\rho}_{12}} \omega^2 u_i = 0 \tag{14.42}$$

or:

$$\partial_j \sigma_{ij}^S + \tilde{\rho}_{11}\omega^2 u_i + \tilde{\rho}_{12}\omega^2 U_i = 0 \tag{14.43}$$

$$\partial_j \sigma_{ij}^F + \tilde{\rho}_{22}\omega^2 U_i + \tilde{\rho}_{12}\omega^2 u_i = 0 \tag{14.44}$$

Note that:

$$\tilde{\rho}_{12} + \tilde{\rho}_{22} = \Omega\rho_f \tag{14.45}$$

Replacing σ_{ij}^F by its definition in terms of pressure (p), the second equation becomes:

$$-\Omega\partial_i p + \tilde{\rho}_{22}\omega^2 U_i + \tilde{\rho}_{12}\omega^2\ u_i = 0 \tag{14.46}$$

or:

$$U_i = \frac{\Omega}{\tilde{\rho}_{22}\omega^2}\partial_i p - \frac{\tilde{\rho}_{12}}{\tilde{\rho}_{22}} u_i \tag{14.47}$$

We can then replace U by p in the first equilibrium equation:

$$\partial_j \sigma_{ij}^S + \omega^2 \underbrace{\left[\tilde{\rho}_{11} - \frac{\tilde{\rho}_{12}^2}{\tilde{\rho}_{22}}\right]}_{\tilde{\rho}} u_i + \frac{\Omega\tilde{\rho}_{12}}{\tilde{\rho}_{22}}\partial_i p = 0 \tag{14.48}$$

or:

$$\partial_j \sigma_{ij}^S + \omega^2 \tilde{\rho} u_i + \frac{\Omega\tilde{\rho}_{12}}{\tilde{\rho}_{22}}\partial_i p = 0 \tag{14.49}$$

14.3.4 Constitutive equations

Acoustic fluid

The constitutive relation of the acoustic fluid relates the pressure variation to the volumetric deformation of an infinitesimal sample and to the net flow of fluid through this sample. This is written as:

$$-p = Q\varepsilon_V + \alpha Q\varepsilon_S \tag{14.50}$$

where

- Q is the adiabatic bulk modulus of the fluid;
- $\varepsilon_V = \Omega \partial_j \left(U_j - u_j \right)$ is the net fluid flow through the sample;
- $\varepsilon_S = \partial_j u_j$ is the volumetric deformation of the sample;
- α is the Biot parameter, assumed to be equal to one.

This first constitutive equation is generally written as:

$$-\Omega p = \underbrace{Q\Omega^2}_{\tilde{R}} \partial_j U_j + \underbrace{\Omega Q \left(\alpha - \Omega \right)}_{\tilde{Q}} \partial_j u_j. \tag{14.51}$$

or:

$$-\Omega p = \tilde{R} \partial_j U_j + \tilde{Q} \partial_j u_j. \tag{14.52}$$

Elastic frame

The constitutive relation for the elastic frame decomposes the stress tensor into two components: fluid pressure and solid stress. It is written as:

$$\sigma_{ij}^S = \sigma_{ij} - \left(-\Omega p \right) \delta_{ij}. \tag{14.53}$$

with

$$\sigma_{ij} = \left(\lambda + \alpha^2 Q \right) \partial_k u_k \delta_{ij} + 2\mu \varepsilon ij + \alpha \Omega Q \partial_k \left(U_k - u_k \right) \delta_{ij} \tag{14.54}$$

where λ and μ and are the Lamé constants.

Combining constitutive relations

Equations 14.52, 14.53 and 14.54 can be combined to give:

$$\begin{aligned}
\sigma_{ij}^S &= \left(\lambda + \alpha^2 Q\right) \partial_k u_k \delta_{ij} + 2\mu\varepsilon_{ij} + \alpha\Omega Q \left(\partial_k \left(U_k - u_k\right)\right) \delta_{ij} \\
&- Q\Omega^2 \partial_k U_k \delta_{ij} - \Omega Q \left(\alpha - \Omega\right) \partial_k u_k \delta_{ij} \\
&= \left(\lambda + \alpha^2 Q\right) \partial_k u_k \delta_{ij} + 2\mu\varepsilon_{ij} + \left(\alpha\Omega Q - \Omega^2 Q\right) \partial_k U_k \delta_{ij} \\
&+ \left(\Omega^2 Q - 2\alpha\Omega Q\right) \partial_k u_k \delta_{ij} \\
&= \underbrace{\left(\lambda + Q\left(\alpha - \Omega\right)^2\right)}_{\tilde{A}} \partial_k u_k \delta_{ij} + 2\mu\varepsilon_{ij} + \underbrace{\Omega Q \left(\alpha - \Omega\right)}_{\tilde{Q}} \partial_k U_k \delta_{ij} \\
&= \tilde{A} \partial_k u_k \delta_{ij} + 2\mu\varepsilon_{ij} + \tilde{Q} \partial_k U_k \delta_{ij}
\end{aligned} \tag{14.55}$$

Eliminating U

U can be eliminated from the constitutive equations. Starting from the fluid equation, we can write:

$$\partial_k U_k = -\frac{\Omega}{\tilde{R}} p - \frac{\tilde{Q}}{\tilde{R}} \partial_k u_k \tag{14.56}$$

which, introduced in the equation of the solid phase, gives:

$$\begin{aligned}
\sigma_{ij}^S &= \tilde{A} \partial_k u_k \delta_{ij} + 2\mu\varepsilon_{ij} - \frac{\tilde{Q}^2}{\tilde{R}} \partial_k u_k \delta_{ij} - \frac{\tilde{Q}\Omega}{\tilde{R}} p \delta_{ij} \\
&= \left(\tilde{A} - \frac{\tilde{Q}^2}{\tilde{R}}\right) \partial_k u_k \delta_{ij} + 2\mu\varepsilon_{ij} - \frac{\tilde{Q}\Omega}{\tilde{R}} p \delta_{ij}.
\end{aligned} \tag{14.57}$$

but:

$$\frac{\tilde{Q}}{\tilde{R}} = \frac{\Omega Q \left(\alpha - \Omega\right)}{\Omega^2 Q} = \frac{\alpha - \Omega}{\Omega} \tag{14.58}$$

and:

$$\tilde{A} - \frac{\tilde{Q}^2}{\tilde{R}} = \left(\lambda + Q\left(\alpha - \Omega\right)^2\right) - \frac{\Omega^2 Q^2 \left(\alpha - \Omega\right)^2}{\Omega^2 Q} = \lambda \tag{14.59}$$

in such a way that:

$$\sigma_{ij}^S = \underbrace{\lambda \partial_k u_k \delta_{ij} + 2\mu \varepsilon_{ij}}_{\tilde{\sigma}_{ij}^S} - (\alpha - \Omega)\, p \delta_{ij} \tag{14.60}$$

$\tilde{\sigma}_{ij}^S$ is the stress tensor that would occur in a homogeneous solid made only of skeleton material subjected to the same strain tensor.

14.3.5 u-p model for poro-elastic materials

Solid phase

Introducing Equation 14.60 into Equation 14.49, we obtain:

$$\partial_j \tilde{\sigma}_{ij}^S + \omega^2 \tilde{\rho} u_i + \underbrace{\left(\frac{\Omega \tilde{\rho}_{12}}{\tilde{\rho}_{22}} - (\alpha - \Omega) \right)}_{\tilde{\gamma}} \partial_i p = 0 \tag{14.61}$$

or:

$$\partial_j \tilde{\sigma}_{ij}^S + \omega^2 \tilde{\rho} u_i + \tilde{\gamma} \partial_i p = 0 \tag{14.62}$$

which is the equilibrium equation of a flexible solid of density $\tilde{\rho}$ with an additional term coupling the skeleton strain to the fluid pressure in the pores. Note that:

$$\tilde{\gamma} = \frac{\Omega \tilde{\rho}_{12}}{\tilde{\rho}_{22}} - (\alpha - \Omega) = \Omega \left(\frac{\tilde{\rho}_{12}}{\tilde{\rho}_{22}} + 1 \right) - \alpha = \frac{\Omega^2 \rho_f}{\tilde{\rho}_{22}} - \alpha \tag{14.63}$$

Fluid phase

Take the divergence of Equation 14.47:

$$\partial_i U_i = \frac{\Omega}{\tilde{\rho}_{22} \omega^2} \partial_{ii} p - \frac{\tilde{\rho}_{12}}{\tilde{\rho}_{22}} \partial_i u_i \tag{14.64}$$

and solve Equation 14.52 for $\partial_i U_i$:

$$\partial_i U_i = -\frac{\Omega}{\tilde{R}} p - \frac{\tilde{Q}}{\tilde{R}} \partial_i u_i \tag{14.65}$$

The right hand side of both equations must be equal. After multiplying by $\omega^2\Omega$, we obtain:

$$\frac{\Omega^2}{\tilde{\rho}_{22}} \partial_{ii} p + \omega^2 \frac{\Omega^2}{\tilde{R}} p - \omega^2 \underbrace{\left(\frac{\Omega \tilde{\rho}_{12}}{\tilde{\rho}_{22}} - \frac{\Omega \tilde{Q}}{\tilde{R}} \right)}_{\tilde{\gamma}} \partial_i u_i = 0 \tag{14.66}$$

or

$$\frac{\Omega^2}{\tilde{\rho}_{22}} \partial_{ii} p + \omega^2 \frac{\Omega^2}{\tilde{R}} p - \omega^2 \tilde{\gamma} \partial_i u_i = 0 \tag{14.67}$$

14.3.6 Waves in a poro-elastic media

It is interesting to identify plane wave solutions associated to Biot's equations. Given the isotropic nature of Biot's equations, we can arbitrarily consider a plane wave propagating along the x_1 axis. All field variables are then independent of x_2 and x_3:

$$\begin{aligned}
p(x_1, x_2, x_3, t) &= \Re\left(p e^{i\omega t - ikx_1} \right) \\
u_1(x_1, x_2, x_3, t) &= \Re\left(u_1 e^{i\omega t - ikx_1} \right) \\
u_2(x_1, x_2, x_3, t) &= \Re\left(u_2 e^{i\omega t - ikx_1} \right) \\
u_3(x_1, x_2, x_3, t) &= \Re\left(u_3 e^{i\omega t - ikx_1} \right)
\end{aligned} \tag{14.68}$$

Introducing these expressions in Biot's equations, we obtain the following set of algebraic equations:

$$\begin{aligned}
-k^2(\lambda + 2\mu) u_1 + \omega^2 \tilde{\rho} u_1 - ik\tilde{\gamma} p &= 0 \\
-k^2 \mu u_2 + \omega^2 \tilde{\rho} u_2 &= 0 \\
-k^2 \mu u_3 + \omega^2 \tilde{\rho} u_3 &= 0 \\
-k^2 \frac{\Omega^2}{\tilde{\rho}_{22}} p + \omega^2 \frac{\Omega^2}{\tilde{R}} p + ik\omega^2 \tilde{\gamma} u_1 &= 0
\end{aligned} \tag{14.69}$$

Eight non trivial solutions can be found, each representing a plane wave propagating in the porous media along the x_1 axis. These eight solutions appear in pairs: if k, u_1, u_2, u_3, p is a solution then $-k, -u_1, u_2, u_3, p$ is also a solution. Four different plane wave types are therefore found, each propagating in both directions (towards the positive or negative x_1).

Shear waves

The first two non-zero solutions are obtained by setting u_1 and p to zero. The first and last equations are then satisfied. Looking at the second and third equations, we find:

- a shear wave u_2 that propagates along x_1 in both directions:

$$u_2 = \Re\Big(e^{i\omega(t\pm\frac{x_1}{c_\tau})}\Big) \tag{14.70}$$

  with a propagation speed $c_\tau = \sqrt{\frac{\mu}{\tilde{\rho}}}$;

- a shear wave u_3 that propagates along x_1 in both directions:

$$u_3 = \Re\Big(e^{i\omega(t\pm\frac{x_1}{c_\tau})}\Big) \tag{14.71}$$

  with the same propagation speed c_τ.

In a standard acoustic fluid, waves propagate without dissipation and with constant speed with respect to frequency or wavelength. Propagation is non-dispersive (Section 4.5). But porous media are dissipative and the magnitude of the wave progressively decreases (complex propagation speed) and is dispersive (the speed of the wave depends on its frequency or wavelength). Dissipation of shear waves is due to viscous dissipation. Indeed, Equation 14.47 shows that, even when the pressure fluctuation is zero, the fluid moves with respect to the skeleton:

$$U_i = -\frac{\tilde{\rho}_{12}}{\tilde{\rho}_{22}} u_i \tag{14.72}$$

Compression waves

The other two solutions represent compression waves. They are obtained by choosing $u_2 = u_3 = 0$ and by combining the first and last equations to eliminate p. We obtain:

$$\left(\left[-k^2(\lambda+2\mu)+\omega^2\tilde{\rho}\right]\left[\frac{-k^2}{\tilde{\rho}_{22}}+\frac{\omega^2}{\tilde{R}}\right]-\frac{k^2\omega^2}{\Omega^2}\tilde{\gamma}^2\right)u_1=0. \tag{14.73}$$

u_1 is non-zero only if k satisfies a second degree equation in k^2. This equation has two solutions

$$k^2=\omega^2\frac{\Gamma\pm\sqrt{\Delta}}{2\frac{\lambda+2\mu}{\tilde{\rho}_{22}}} \tag{14.74}$$

with

$$\Gamma = \frac{\tilde{\rho}}{\tilde{\rho}_{22}}+\frac{\lambda+2\mu}{\tilde{R}}+\frac{\tilde{\gamma}^2}{\Omega^2} \tag{14.75}$$

$$\Delta = \Gamma^2-4\frac{\tilde{\rho}}{\tilde{\rho}_{22}}\frac{\lambda+2\mu}{\tilde{R}} \tag{14.76}$$

We therefore find:

- A *slow* or *solid* compression wave that propagates along x_1 in both directions:

$$u_1 = \Re\left(e^{i\omega(t\pm\frac{x_1}{c_1})}\right) \tag{14.77}$$

$$p = \omega\frac{c_1\tilde{\rho}-\frac{\lambda+2\mu}{c_1}}{\tilde{\gamma}} \tag{14.78}$$

with a propagation speed:

$$c_1=\sqrt{\frac{2(\lambda+2\mu)}{\tilde{\rho}_{22}\left(\Gamma+\sqrt{\Delta}\right)}} \tag{14.79}$$

Indeed, for a porous material with light saturating fluid (air), this wave displays large solid displacements, and fluid displacements that are almost in opposition of phase with the solid displacements. To show this we have to evaluate U_1/u_1 using Equation 14.47, but calculations are fastidious and are therefore not detailed here. Damping due to viscous

forces is important and these waves decay rapidly. The propagation speed is slow because inertial effects are more important than the fluid and solid potential energies. Even if slow compression waves propagate only over short distances, they have to be considered in the boundary conditions, for example during reflection and refraction.

- A *fast* or *fluid* compression wave that propagates along x_1 in both directions:

$$u_1 = \Re\left(e^{i\omega(t\pm\frac{x_1}{c_2})}\right) \tag{14.80}$$

$$p = \omega\frac{c_2\tilde{\rho} - \frac{\lambda+2\mu}{c_2}}{\tilde{\gamma}} \tag{14.81}$$

with a propagation speed:

$$c_2 = \sqrt{\frac{2(\lambda+2\mu)}{\tilde{\rho}_{22}\left(\Gamma - \sqrt{\Delta}\right)}} \tag{14.82}$$

For typical materials with light fluid phase (air), this wave displays large fluid displacements that are usually in phase with the solid displacements. The demonstration requires the calculation of the ratio U_1/u_1 which will not be done here. Viscous damping is less important for fast compression waves. Inertial effects are moderate due to the low amplitude of solid displacements. This explains the higher propagation speed. These waves propagate over longer distances and are, together with shear waves, responsible for propagation at large distances from the source.

Numerical example

We illustrate the above results using a polyurethane foam. Properties are given in Table 14.9. Figure 14.10 shows the solid displacements for the three types of waves. Figure 14.11 shows how their propagation speeds vary with frequency. The real part controls the wavelength while the amplitude decay is defined by the imaginary part.

Parameter	Symbol	Value	Unit
Young Modulus	E	$2 \cdot 10^5$	[Pa]
Poisson ratio	ν	0.23	[-]
Solid density	ρ_S	830	$[kg/m^3]$
Average pressure*	p_0	101300	[Pa]
Fluid density*	ρ_F	1.225	$[kg/m^3]$
Specific heat* (constant p)	c_p	1004	$[J/(kg \cdot K)]$
Specific heat* (constant ρ_F)	c_v	716	$[J/(kg \cdot K)]$
Viscosity*	η	$1.82 \cdot 10^{-5}$	$[Ns/m^2]$
Thermal conductivity*	λ	0.0256	$[Wm^{-1}K^{-1}]$
Porosity	Ω	0.98	[-]
Static flow resistivity*	R_0	$22 \cdot 10^3$	$[Nm^{-4}s]$
Tortuosity	α_∞	1.2	[-]
Viscous length*	Λ_v	$1.7 \cdot 10^{-5}$	$[m]$
Thermal length*	Λ_t	$4 \cdot 10^{-5}$	$[m]$

Figure 14.9: Material properties of the polyurethane foam.

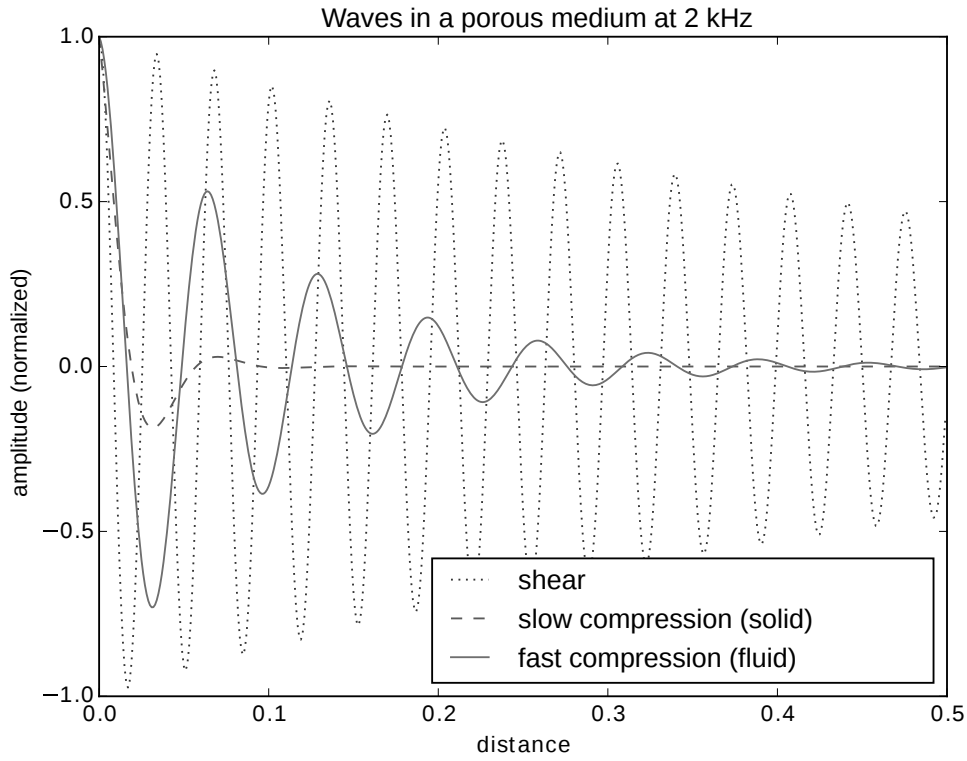

Figure 14.10: Displacement corresponding to the three types of plane wave observed in porous materials with elastic skeleton. The *slow* compression wave is quickly damped. The *fast* compression wave and the shear wave propagate over longer distances.

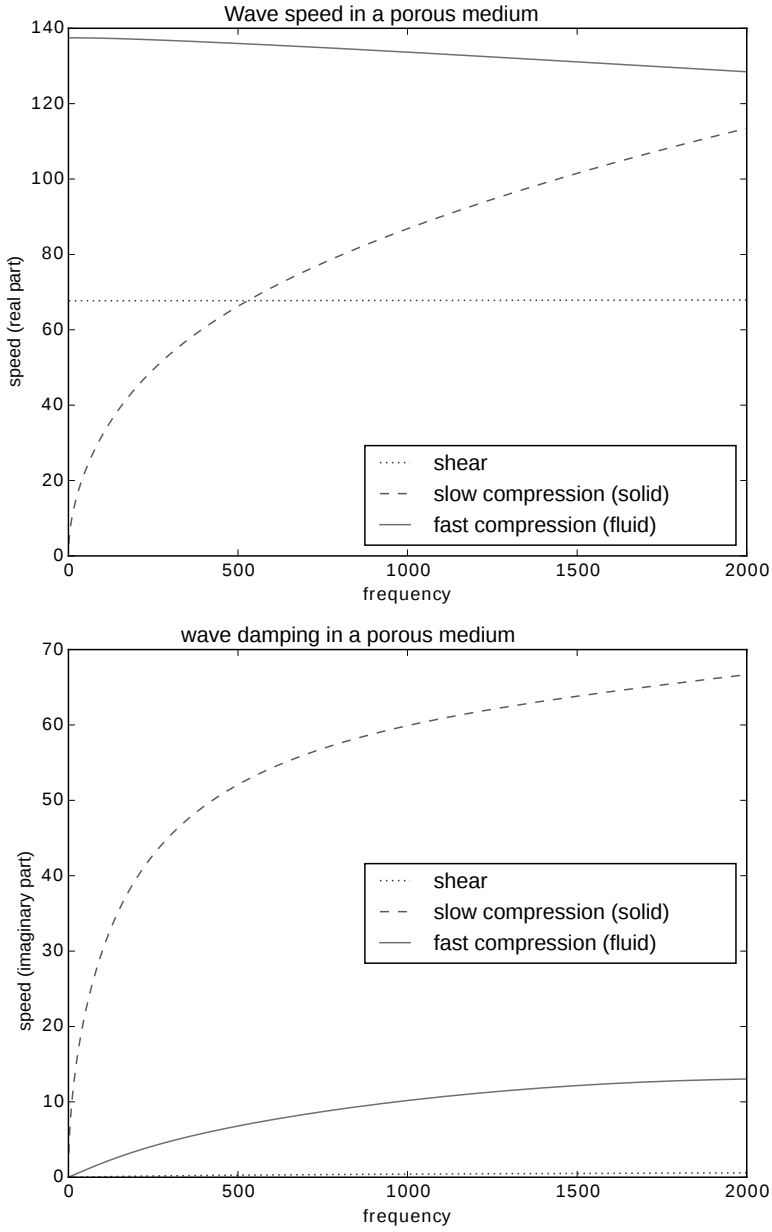

Figure 14.11: Complex speed of sound for different types of plane wave in a porous material with elastic skeleton.

14.3.7 Micro-models

At a microscopic level, porous materials are a complex network of small ducts connecting the pores. Viscous and thermal effects have a strong influence on the fluid bulk modulus Q and on the flow resistivity R. Their variation with frequency is defined by *micro-models*. We present here the classical Johnson-Champoux-Allard model.[6])

$$R = R_0 \sqrt{1 + i\omega \frac{4\alpha_\infty^2 \eta \rho_f}{(R_0 \Lambda_v)^2}} \tag{14.83}$$

$$Q = \gamma p_0 \left(\gamma - \frac{\gamma - 1}{1 + \frac{8\eta}{i\omega B^2 \rho_f \Lambda_t^2} \sqrt{1 + \frac{\omega B^2 \rho_f \Lambda_t^2}{16\eta}}} \right)^{-1} \tag{14.84}$$

where:

- $p_0 = Q_0$ is the atmospheric pressure (101,325 Pa);
- γ is the ratio of specific heat at constant pressure and volume (1.4 [-]);
- $B^2 = \frac{\eta c_p}{\lambda}$ is the Prandtl number (0.71 [-]);
- η is the dynamic viscosity of the fluid ($1.84 \cdot 10^{-5}\ Ns/m^2$);
- Λ_t is the thermal characteristic length ([m]);
- Λ_v is the viscous characteristic length ([m]);
- R_0 is the static resistivity ($[Nm^{-4}s]$).

Values are given for air in standard conditions. The characteristic lengths (Λ_t, Λ_v) are defined as follows:

[6] **Allard J.-F.**, *Propagation of sound in porous media*, Elsevier Applied Science, 1993. More elaborate models have since been proposed: Johnson-Champoux-Allard-Lafarge and Johnson-Champoux-Allard-Pride-Lafarge (JCAPL).

- The thermal characteristic length is twice the ratio of air volume to air surface in the open pore network:

$$\Lambda_t = \frac{2\int_{V_p} dV_p}{\int_{S_p} dS_p} \tag{14.85}$$

  Λ_t is the scale at which thermal exchange occurs between fluid and skeleton.

- The viscous characteristic length is given by:

$$\Lambda_v = \frac{2\int_{V_p} |v|^2 \, dV_p}{\int_{S_p} |v|^2 \, dS_p} \tag{14.86}$$

  where v is the macroscopic velocity field in the equivalent fluid. Λ_v is the scale at which viscous dissipation occurs.

At low frequency, the bulk modulus of the fluid Q_0 tends to its isothermal value p_0. At high frequency, it tends to its adiabatic value γp_0.

14.4 Practical use of poro-elastic materials

14.4.1 Limited impact of open porous layers

The dissipation of energy in porous materials is proportional to the local acoustic velocity. The normal velocity component vanishes on a rigid surface and dissipation is limited if the material thickness is small (Figure 14.12.a). Dissipation only becomes significant if the thickness of the absorbing layer is at least equal to a quarter-wavelength (Figure 14.12.b). Better attenuation may be obtained by placing the material a quarter-wavelength away from the wall where the velocity is maximum (Figure 14.12.c).

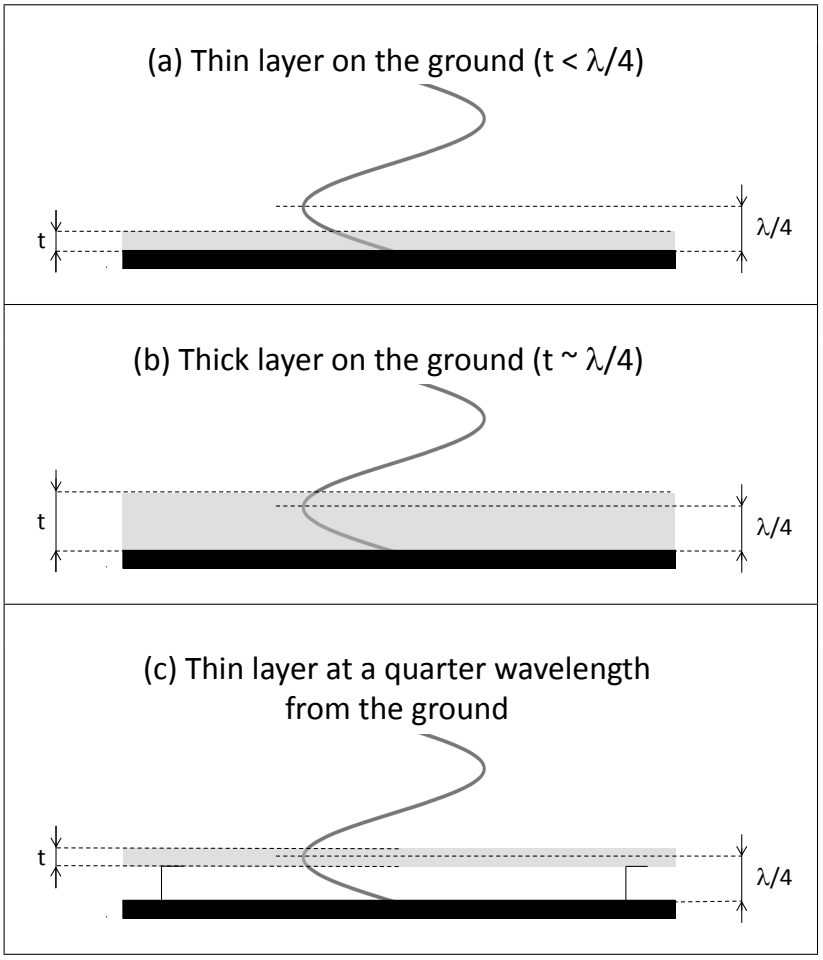

Figure 14.12: Rigid wall covered by a porous layer. Top: a thin layer ($< \frac{\lambda}{4}$) is glued to the wall. Middle: a thicker layer ($> \frac{\lambda}{4}$) is glued to the wall. Bottom: a thin layer ($< \frac{\lambda}{4}$) is located at a distance $\frac{\lambda}{4}$ from the wall. The wavy curve represents the acoustic velocity perpendicular to the wall (for a plane wave with normal incidence).

14.4.2 Qualitative analysis of poro-elastic sandwich

Porous materials are often used in multi-layer sandwich panels. In the transportation industry (aeronautics, automotive, railways), bare metallic walls (steel, aluminium) are covered by a layer of porous material then by a flexible impervious material called the *heavy layer* (Figure 14.13). The efficiency of these sandwich panels results from different mechanisms:

- As the porous layer is compressible, the three layers form a mass-spring-mass system which decouples the heavy layer from the base layer (Figure 14.14). The nature of the porous material (R, α_∞) and its thickness as well as the mass of the base and heavy layers determine the resonance frequency of the panel. At low frequency the heavy layer has larger displacements than the base layer (dynamic amplification). Above resonance, the heavy layer moves less than the base layer. At very high frequency, the heavy layer is nearly motionless (dynamic attenuation). A poro-elastic sandwich therefore produces, above a certain frequency, a vibration insulation effect: the vibrations of the heavy layer are weaker than that of the base layer.

- The heavy and base layers have different deformation patterns and the porous layer is locally compressed and depressed. This creates a complex oscillating flow in the porous layer, parallel to the panel Figure 14.15. This in-plane oscillatory flow creates an important viscous dissipation proportional to the material's resistivity.

- The heavy layer is usually made from a material that is more dissipative than the base layer. Consider a sandwich panel excited by a vertical motion imposed on its perimeter (Figure 14.16). The vibrations of the heavy layer are more damped than those of the base layer. The associated acoustic radiation is therefore weaker on the heavy layer side than on the base side. This delivers an additional insulation effect.

These three effects (dynamic isolation, viscous dissipation related to the oscillatory transverse fluid flow in the porous layer and reduced radiation efficiency of the heavy layer) collectively explain the performance and ubiquity of poro-elastic sandwich panels in many practical applications.

Figure 14.13: Cross section of a poro-elastic sandwich.

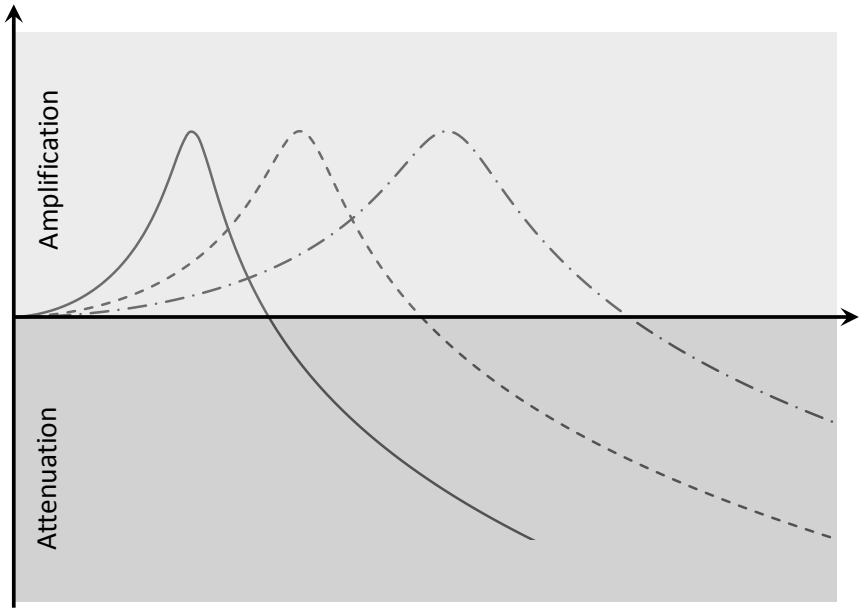

Figure 14.14: Vibration insulation effect in poro-elastic sandwich panels of increasing resonance frequency. Resonance frequency of the mass-spring-mass differs depending on the elastic properties of the porous layer and on the density of the heavy and base layers. Vibration insulation then starts at a different frequency.

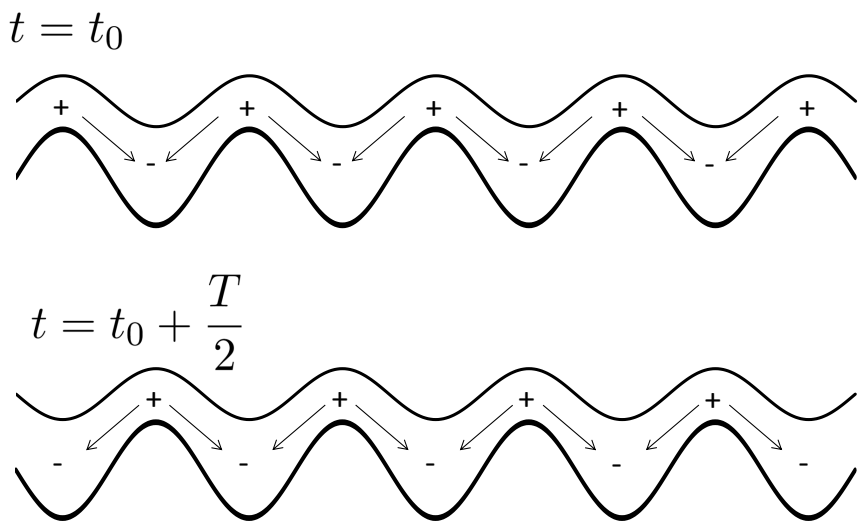

Figure 14.15: Oscillatory in-plane fluid flow within the porous layer.

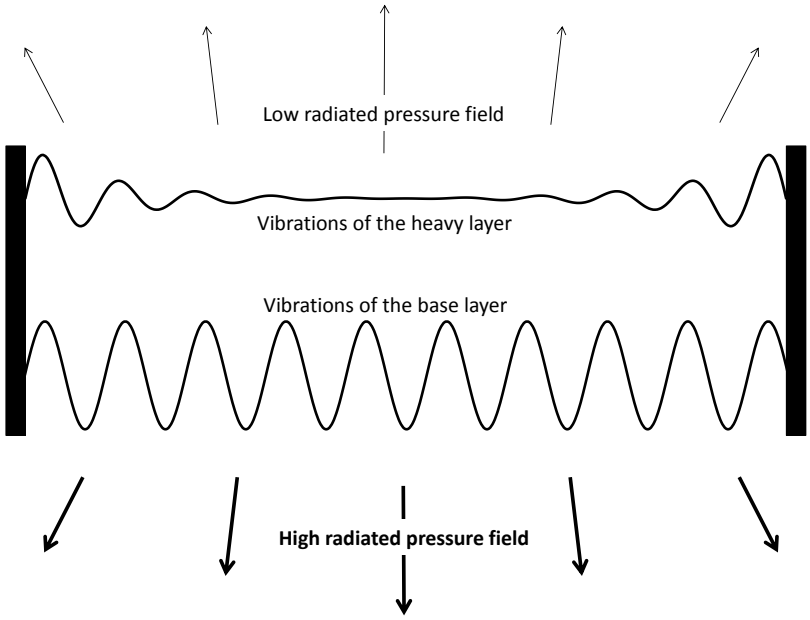

Figure 14.16: Comparison of the acoustic fields radiated by the sandwich panel on the heavy and base layer side.

15

Convected propagation

Contents

15.1 Constant flow 316
15.2 Potential flow 327
15.3 Arbitrary flow 333
15.4 Application to a turbo-engine 338

In Chapter 4, we progressively transformed the Navier-Stokes equations into a wave equation by making successive assumptions. One of those was that the acoustic fluid was globally at rest, the only movement being a local oscillation of the air particles caused by the sound waves. This assumption, classical in acoustics and relevant for a wide class of problems, is inadequate in applications where the sound field is *convected* by a background fluid flow. Sound convection for instance occurs in exhaust systems or air conditioning ducts and the noise radiated by an aircraft engine is clearly influenced by the aircraft speed.

This chapter studies the propagation of sound in a moving fluid. The key difficulty is to separate the field variables related to the background flow (hydrodynamic variables) from those associated to the acoustic field. Three models of increasing complexity will be presented: propagation of sound in a uniform flow, irrotational flow and finally, arbitrary flow.

15.1 Sound propagation in a constant mean flow

15.1.1 Convected wave equation

We first separate pressure, density and velocity in two components:

$$\begin{aligned} p &= p_0 + p_a \quad with \quad p_a \ll p_0 \\ \rho &= \rho_0 + \rho_a \quad with \quad \rho_a \ll \rho_0 \\ v_i &= v_{i0} + v_{ia} \quad with \quad v_{ia} \ll v_{i0} \end{aligned} \tag{15.1}$$

We then introduce this decomposition into the continuity (Equation 4.1) and Euler equations (Equation 4.2) with $q = 0$. Linearising the resulting equations, while taking into account the constant character of p_0, ρ_0 and v_{i0}, yields:

$$\partial_t \rho_a + \partial_i \left(\rho_0 v_{ia} + \rho_a v_{i0} \right) = 0 \tag{15.2}$$

$$\rho_0 \partial_t v_{ia} + \rho_0 v_{j0} \partial_j v_{ia} + \partial_i p_a = 0 \tag{15.3}$$

Using:

$$p_a = c_0^2 \rho_a \tag{15.4}$$

where c_0 is the speed of sound in the fluid at rest. We then find:

$$\frac{1}{c_0^2}\left(\partial_t p_a + v_{i0}\partial_i p_a\right) + \rho_0 \partial_i v_{ia} = 0 \tag{15.5}$$

$$\rho_0\left(\partial_t v_{ia} + v_{j0}\partial_j v_{ia}\right) + \partial_i p_a = 0 \tag{15.6}$$

The material derivative operator D_t is defined as follows:

$$D_t = \partial_t + v_{i0}\partial_i \tag{15.7}$$

It can be used to write both equations in the form:

$$\frac{1}{c_0^2} D_t p_a + \rho_0 \partial_i v_{ia} = 0 \tag{15.8}$$

$$\rho_0 D_t v_{ia} + \partial_i p_a = 0 \tag{15.9}$$

If we calculate the material derivative of the first equation and the divergence of the second, we obtain:

$$\frac{1}{c_0^2} D_{tt} p_a + \rho_0 D_t \partial_i v_{ia} = 0 \tag{15.10}$$

$$\rho_0 \partial_i D_t v_{ia} + \partial_{ii} p_a = 0 \tag{15.11}$$

Since the flow is constant, the operators D_t and ∂_i commute ($D_t\partial_i = \partial_i D_t$) and we can eliminate the acoustic velocity to find:

$$\frac{1}{c_0^2} D_{tt} p_a - \partial_{ii} p_a = 0 \tag{15.12}$$

If we note that:

$$D_{tt} = \left(\partial_t + v_{i0}\partial_i\right)^2 = \partial_{tt} + 2v_{i0}\partial_{it} + v_{i0}v_{j0}\partial_{ij} \tag{15.13}$$

the convected wave equation, assuming a uniform background flow, is written:

$$\left(\delta_{ij} - \frac{v_{0i}v_{0j}}{c_0^2}\right)\partial_{ij} p_a - \frac{2v_{i0}}{c_0^2}\partial_{it} p_a - \frac{1}{c_0^2}\partial_{tt} p_a = 0 \tag{15.14}$$

The Fourier transform of the preceding equation is the convected Helmholtz equation ($p_a(t) \Leftrightarrow P_a(\omega)$):

$$\left(\delta_{ij} - \frac{v_{0i}v_{0j}}{c_0^2}\right)\partial_{ij}P_a - \frac{2i\omega v_{j0}}{c_0^2}\partial_j P_a + \frac{\omega^2}{c_0^2}P_a = 0 \tag{15.15}$$

We find, in the case of background flow aligned on the x-axis:

$$\beta^2\frac{\partial^2 P_a}{\partial x^2} + \frac{\partial^2 P_a}{\partial y^2} + \frac{\partial^2 P_a}{\partial z^2} - \frac{2i\omega M}{c_0}\frac{\partial P_a}{\partial x} + \frac{\omega^2}{c_0^2}P_a = 0 \tag{15.16}$$

where $M = \frac{|v_0|}{c_0}$ is the Mach number[1] and where $\beta^2 = 1 - M^2$.

15.1.2 Acoustical resonances in a tyre

The air contained inside a tyre forms a toroidal cavity. From an acoustic standpoint, the cavity may be seen, at low frequency, as a cylindrical duct whose length ℓ is the circumference of the tyre measured halfway through its thickness. As an example, for a tyre of reference 195/65R15, the width of the tyre is 195 mm, the height of the side represents 65% of the width and the diameter of the rim is 15 inches; the length of the equivalent acoustic duct is then:

$$\ell = 2\pi \times \left(\frac{15}{2} \times \frac{2.54}{100} + \frac{1}{2} \times 65\% \times \frac{195}{1000}\right) = 1.59\ m \tag{15.17}$$

Pressure and velocity must be continuous at $x = 0$ and $x = \ell$: $p(0) = p(\ell)$ and $v(0) = v(\ell)$. The rotation of the tyre is modelled by considering that air inside the tube moves with a uniform velocity v_0 equal to the vehicle speed. The wave equation is then:

$$\left(1 - \frac{v_0^2}{c^2}\right)\frac{d^2p}{dx^2} - \frac{2i\omega v_0}{c^2}\frac{dp}{dx} + \frac{\omega^2}{c^2}p = 0 \tag{15.18}$$

[1] **Ernst Mach**, an Austrian physicist and philosopher, was born in Brno in 1838 and died in Münich in 1916.

which has a solution of the type:

$$p = Ae^{ik_1 x} + Be^{ik_2 x} \tag{15.19}$$

with:

$$k_1 = \frac{\omega}{c - v_0} \tag{15.20}$$

$$k_2 = \frac{-\omega}{c + v_0} \tag{15.21}$$

The solution is non-trivial only if:

$$e^{ik_1 \ell} = 1 \rightarrow k_1 = \frac{2n\pi}{\ell} \rightarrow f = \frac{n\,(c - v_0)}{\ell} \tag{15.22}$$

or if:

$$e^{ik_2 \ell} = 1 \rightarrow k_2 = \frac{2n\pi}{\ell} \rightarrow f = \frac{n\,(c + v_0)}{\ell} \tag{15.23}$$

We therefore have, as in the no-flow case, two waves propagating in opposite directions. But the apparent speed of the sound in the direction of the flow is $c + v_0$ while it is of $c - v_0$ in the opposite direction. The sound is *convected* by the background flow. The first two modes, which appear at the same frequency if $v_0 = 0$, are separated by $\Delta f = \frac{2v_0}{\ell}$. In the above example, we find the following values of Δf:

- 30 km/h (18.6 mph): $f_1 = 208.6$, $f_2 = 219.1$, $\Delta f = 10.5$ Hz.
- 60 km/h (37.3 mph): $f_1 = 203.3$, $f_2 = 224.3$, $\Delta f = 21.0$ Hz.
- 120 km/h (74.6 mph): $f_1 = 192.9$, $f_2 = 234.8$, $\Delta f = 41.9$ Hz.

The first two acoustic modes, and the increase of their frequency difference with velocity, are clearly visible in the low frequency rolling noise spectrum of a car. They are responsible for the distinctive noise heard when driving over road discontinuities. The broad band excitation on the tyre excites the two resonances, the pressure in the tyre becomes infinite and the suspension is considerably stiffened, causing the impact noise component heard inside the passenger compartment.

15.1.3 Prandtl-Glauert transformation

Time domain

Consider again Equation 15.16:

$$\beta^2 \frac{\partial^2 p_a}{\partial x^2} + \frac{\partial^2 p_a}{\partial y^2} + \frac{\partial^2 p_a}{\partial z^2} - \frac{2\,|v_0|}{c_0^2} \frac{\partial^2 p_a}{\partial x \partial t} - \frac{1}{c_0^2} \frac{\partial^2 p_a}{\partial t^2} = 0 \tag{15.24}$$

The *Prandtl-Glauert*[2] coordinates:

$$\begin{aligned} \xi &= \frac{x}{\beta} \\ \eta &= y \\ \zeta &= z \\ \tau &= \beta t + \frac{v_0 x}{\beta c_0^2} \end{aligned} \tag{15.25}$$

will be used to transform the convected wave equation into a standard non-convected wave equation. We find successively:

$$\frac{\partial p}{\partial x} = \frac{\partial p}{\partial \xi}\frac{\partial \xi}{\partial x} + \frac{\partial p}{\partial \tau}\frac{\partial \tau}{\partial x} = \frac{1}{\beta}\frac{\partial p}{\partial \xi} + \frac{v_0}{\beta c_0^2}\frac{\partial p}{\partial \tau} \tag{15.26}$$

$$\frac{\partial p}{\partial t} = \frac{\partial p}{\partial \tau}\frac{\partial \tau}{\partial t} = \beta \frac{\partial p}{\partial \tau} \tag{15.27}$$

$$\frac{\partial^2 p}{\partial x^2} = \frac{1}{\beta^2}\frac{\partial^2 p}{\partial \xi^2} + \frac{2v_0}{\beta^2 c_0^2}\frac{\partial^2 p}{\partial \xi \partial \tau} + \left(\frac{v_0}{\beta c_0^2}\right)^2 \frac{\partial^2 p}{\partial \tau^2} \tag{15.28}$$

$$\frac{\partial^2 p}{\partial t \partial x} = \frac{\partial^2 p}{\partial \tau \partial \xi} + \frac{v_0}{c_0^2}\frac{\partial^2 p}{\partial \tau^2} \tag{15.29}$$

$$\frac{\partial^2 p}{\partial t^2} = \beta^2 \frac{\partial^2 p}{\partial \tau^2} \tag{15.30}$$

[2] **Ludwig Prandtl**, a German engineer and physicist, was born in 1875 and died in 1953. He made several contributions to fluid and solid mechanics. **Hermann Glauert**, an English aerodynamics researcher, was born in 1892 and died in 1934. The transformation was taught by Prandtl several years before Glauert published it for the first time in 1928.

On the other hand we have:

$$\frac{\partial^2 p}{\partial y^2} = \frac{\partial^2 p}{\partial \eta^2} \quad and \quad \frac{\partial^2 p}{\partial z^2} = \frac{\partial^2 p}{\partial \zeta^2} \tag{15.31}$$

which, substituted in the original equation, gives:

$$\frac{\partial^2 p}{\partial \xi^2} + \frac{\partial^2 p}{\partial \eta^2} + \frac{\partial^2 p}{\partial \zeta^2} - \frac{1}{c_0^2}\frac{\partial^2 p}{\partial \tau^2} = 0 \tag{15.32}$$

The convected wave equation therefore becomes a standard wave equation when using the Prandtl-Glauert modified coordinates.

Frequency domain

The Prandtl-Glauert transformation can also be used in the frequency domain to transform the convected Helmholtz equation into a standard Helmholtz equation. The modified coordinates are:

$$\begin{aligned} \xi &= \frac{x}{\beta} \\ P_a &= P'_a e^{i\frac{\omega M x}{c_0 \beta^2}} \\ \omega' &= \frac{\omega}{\beta} \end{aligned} \tag{15.33}$$

and we find:

$$\frac{\partial P_a}{\partial x} = e^{i\frac{\omega M x}{c_0\beta^2}} \left(i\frac{\omega M}{c_0\beta^2} P'_a + \frac{\partial P'_a}{\partial x} \right) \tag{15.34}$$

$$\frac{\partial^2 P_a}{\partial x^2} = e^{i\frac{\omega M x}{c_0\beta^2}} \left(\frac{\partial^2 P'_a}{\partial x^2} + 2i\frac{\omega M}{c_0\beta^2}\frac{\partial P_a}{\partial x} - \frac{\omega^2 M^2}{c_0^2\beta^4} P'_a \right) \tag{15.35}$$

Introducing these expressions in the convected Helmholtz equation (Equation 15.16) and dividing by the exponential factor, we notice that the convective term containing $\frac{\partial P'_a}{\partial x}$ disappears. We obtain:

$$\beta^2 \left(\frac{\partial^2 P'_a}{\partial x^2} - \frac{\omega^2 M^2}{c_0^2\beta^4} P'_a \right) + \frac{\partial^2 P'_a}{\partial y^2} + \frac{\partial^2 P'_a}{\partial z^2} - \frac{2i\omega M}{c_0} i\frac{\omega M}{c_0\beta^2} P'_a + \frac{\omega^2}{c_0^2} P'_a = 0 \tag{15.36}$$

which simplifies into:

$$\beta^2 \frac{\partial^2 P'_a}{\partial x^2} + \frac{\partial^2 P'_a}{\partial y^2} + \frac{\partial^2 P'_a}{\partial z^2} + \frac{\omega^2}{c_0^2}\left(1 + \frac{M^2}{\beta^2}\right) P'_a = 0 \tag{15.37}$$

and finally, remembering the definition of β, we find the original Helmholtz equation without background flow:

$$\frac{\partial^2 P'_a}{\partial \xi^2} + \frac{\partial^2 P'_a}{\partial y^2} + \frac{\partial^2 P'_a}{\partial z^2} + k'2P'_a = 0 \tag{15.38}$$

with $k' = \frac{\omega'}{c_0} = \frac{k}{\beta}$.

15.1.4 Monopole source in a constant mean flow

We saw in Section 6.6.1 that an acoustic monopole located at the origin ($(0,0,0)$) produces a pressure field:

$$P_a = \frac{e^{-ikr}}{r} \tag{15.39}$$

with $k = \frac{\omega}{c_0}$ and $r = \sqrt{x^2 + y^2 + z^2}$.

The acoustic field induced by a monopole radiating in a uniformly moving fluid has the same expression in the Prandtl-Glauert space:

$$P'_a = \frac{e^{-ik'r'}}{r'} \tag{15.40}$$

with:

$$P'_a = P_a e^{-i\frac{\omega M x}{c_0 \beta^2}} \tag{15.41}$$

$$r' = \sqrt{\frac{x^2}{\beta^2} + y^2 + z^2} \tag{15.42}$$

$$k' = \frac{\omega'}{c_0} = \frac{\omega}{\beta c_0} \tag{15.43}$$

Transforming this expression back to the physical space, we obtain:

$$P_a = \frac{e^{\frac{-i\omega}{c_0\beta}\left(\sqrt{\frac{x^2}{\beta^2}+y^2+z^2}-M\frac{x}{\beta}\right)}}{\sqrt{\frac{x^2}{\beta^2}+y^2+z^2}} \tag{15.44}$$

It is easy to verify that this pressure field is the solution of Equation 15.16. We can compare this solution with the spherical wave emanating from a source in a fluid at rest. In the presence of flow, spherical symmetry disappears. The solution is no longer the same upstream, downstream or on the side of the source (Figure 15.1).

15.1.5 Doppler effect

The fundamental solution developed above can be used to study the Doppler[3] effect, which modifies the perceived sound frequency when the source and/or the observer are in motion. Consider a source moving at speed v_s (Figure 15.2) and an observer moving at a speed v_o. Both travel parallel to the x-axis and there is a distance d between their trajectories. In a coordinate system attached to the source, the fluid moves at speed $-v_s$ and the observer at speed $v_o - v_s$. The observer movement is described by:

$$\begin{aligned} x_o &= (v_o - v_s)\, t \\ y_o &= d \\ z_o &= 0 \end{aligned} \tag{15.45}$$

Transforming the solution (15.44) into the time domain and using the pressure at the (mobile) observer position, we obtain the time-dependent pressure seen by the observer. The two sources are at the same horizontal position at the

[3] **Christian Andreas Doppler**, an Austrian mathematician and physicist, was born in Salzburg in 1803 and died in Venice in 1853. The name Doppler-Fizeau is also often used to honour the French physicist **Hippolyte Fizeau** (Paris, 1819 - Jouarre 1896) who identified the red shift in light sources moving away from an observer).

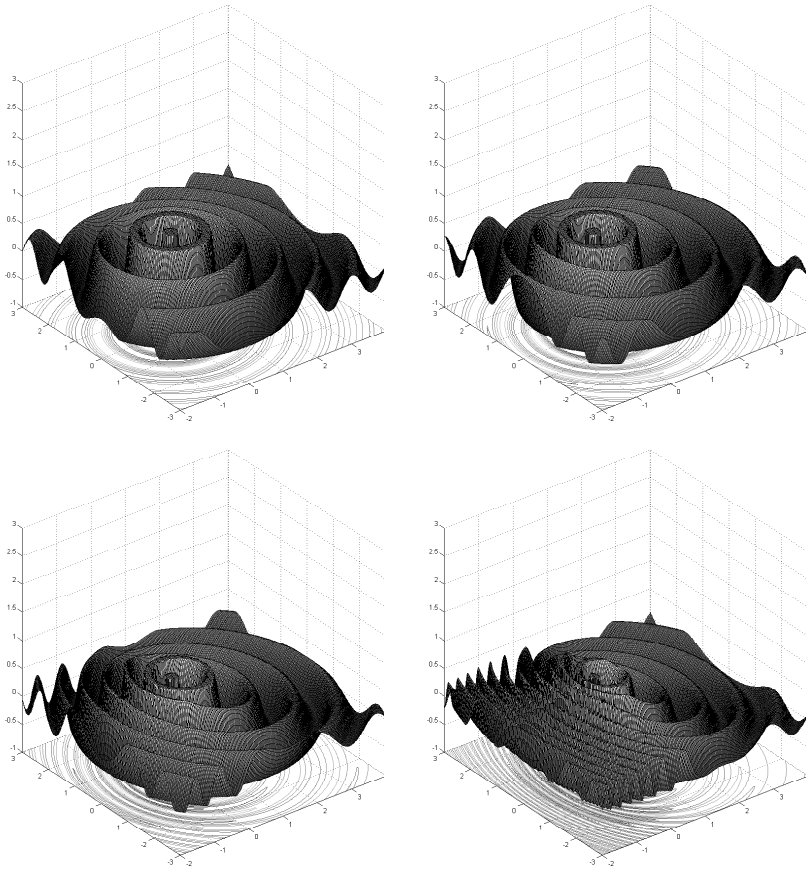

Figure 15.1: Real part of the acoustic pressure of a monopole radiating in a moving fluid (constant flow, M=0.0, M=0.2, M=0.4 and M=0.6).

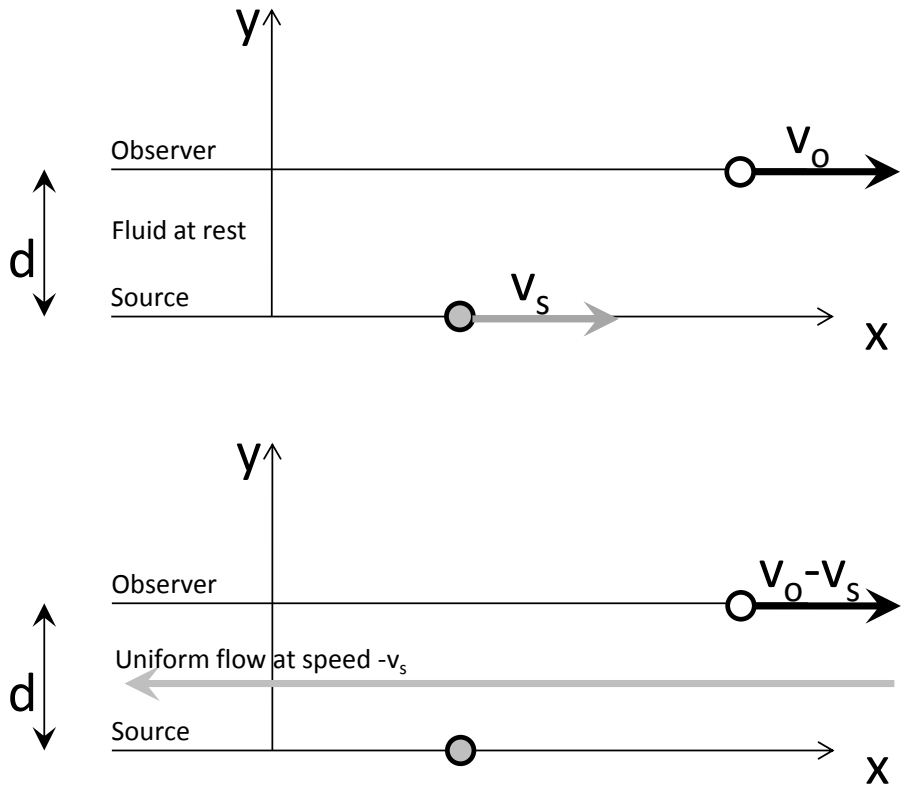

Figure 15.2: Two equivalent representations of the Doppler effect: moving source or moving fluid.

initial time $t = 0$:

$$\begin{aligned} P_a &= \Re\left(\frac{e^{\frac{-i\omega}{c_0\beta}\left(\sqrt{\frac{(v_o-v_s)^2t^2}{\beta^2}+d^2}+\frac{v_s}{c_0}\frac{(v_o-v_s)t}{\beta}\right)}}{\sqrt{\frac{(v_o-v_s)^2t^2}{\beta^2}+d^2}} \cdot e^{i\omega t} \right) \\ &= \beta\Re\left(\frac{e^{\frac{-i\omega}{c_0\beta^2}\left(\sqrt{(v_o-v_s)^2t^2+\beta^2d^2}+\frac{v_s(v_o-v_s)}{c_0}t-c_0\beta^2t\right)}}{\sqrt{(v_o-v_s)^2t^2+\beta^2d^2}} \right) \end{aligned} \tag{15.46}$$

It is interesting to compare the sound perceived by a fixed observer ($v_o = 0$) when the source is moving at speed $v_s = v$ ($\beta = \sqrt{1-\frac{v^2}{c_0^2}}$):

$$P_a = \beta\Re\left(\frac{e^{\frac{-i\omega}{c_0\beta^2}\left(\sqrt{v^2t^2+\beta^2d^2}-\frac{v^2}{c_0}t-c_0\beta^2t\right)}}{\sqrt{v^2t^2+\beta^2d^2}} \right) \tag{15.47}$$

to the sound perceived by an observer moving at speed $v_o = v$ relative to a fixed source ($v_s = 0$, $\beta = 1$):

$$P_a = \Re\left(\frac{e^{\frac{-i\omega}{c_0}\left(\sqrt{v^2t^2+d^2}-c_0t\right)}}{\sqrt{v^2t^2+d^2}} \right) \tag{15.48}$$

Figure 15.3 compares the signals perceived by the observer in both cases. It is also interesting to investigate the asymptotic behavior, far upstream or downstream, where frequencies stabilize. For that purpose let d tend to 0 in the solution obtained above for a mobile source and fixed observer:

$$P_a = \beta\Re\left(\frac{e^{\frac{-i\omega}{c_0\beta^2}\left(v|t|-\frac{v^2}{c_0}t-c_0\beta^2t\right)}}{v|t|} \right) = \beta\Re\left(\frac{e^{\frac{-i\omega}{c_0}\frac{v|t|-c_0t}{\beta^2}}}{v|t|} \right) \tag{15.49}$$

For a fixed source and mobile observer, we have:

$$P_a = \Re\left(\frac{e^{\frac{-i\omega}{c_0}(v|t|-c_0t)}}{v|t|} \right) \tag{15.50}$$

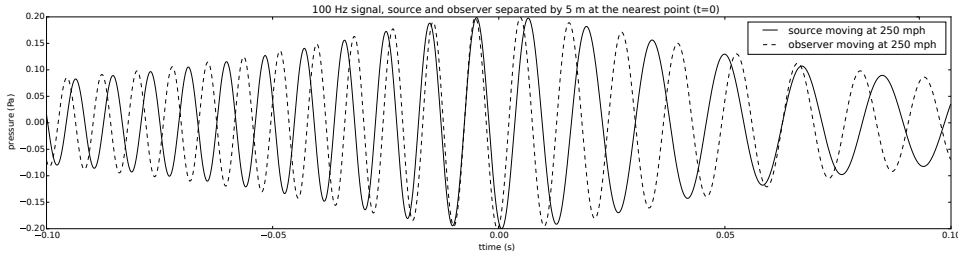

Figure 15.3: Asymmetry of the Doppler effect. The parameters (high speed: 400 km/h or 250 mph and low frequency) were chosen to make the frequency shift very visible. Frequency varies from 133 Hz to 67 Hz when the observer is in movement and from 149 Hz to 75 Hz when the source is in movement. The Doppler effect is more important when the source is moving than when the observer is moving.

The *asymptotic* frequencies in both cases are obtained from the time dependency in the complex exponential. We find:

- Moving Source:

$$f = \frac{f_0}{1 \mp \frac{v}{c_0}} \tag{15.51}$$

  the '$-$' sign corresponds to a source moving towards the observer ($t < 0$) and the '$+$' sign to a source moving away from the observer ($t > 0$).

- Moving Observer:

$$f = f_0 \left(1 \pm \frac{v}{c_0}\right) \tag{15.52}$$

  the '$+$' sign corresponds to an observer moving towards the source ($t < 0$) and the '$-$' sign to an observer moving away from the source ($t > 0$).

15.2 Propagation in a potential background flow

The propagation of sound waves over more general background flows can be analysed. If the flow is irrotational, an appropriate separation of the acoustic and hydrodynamic variables is still possible.

15.2.1 Velocity potential

Consider once again the continuity and Euler equations without distributed mass sources ($q = 0$):

$$\partial_t \rho + \partial_i (\rho v_i) = 0 \tag{15.53}$$

$$\rho (\partial_t v_i + v_j \partial_j v_i) + \partial_i p = 0 \tag{15.54}$$

and assume that the velocity field is irrotational:

$$\vec{\nabla} \times \vec{v} = 0 \Leftrightarrow \partial_i v_j = \partial_j v_i \tag{15.55}$$

In this case, a velocity potential ϕ can be defined:

$$\vec{v} = \vec{\nabla}\phi \Leftrightarrow v_i = \partial_i \phi \tag{15.56}$$

15.2.2 Continuity equation

We can develop the second term of the continuity equation and use the velocity potential as variable:

$$\begin{aligned} \partial_i (\rho v_i) &= v_i \partial_i \rho + \rho \partial_i v_i \\ &= v_i \partial_i \rho + \rho \partial_{ii} \phi \end{aligned} \tag{15.57}$$

The continuity equation, divided by density, becomes:

$$\frac{1}{\rho}\partial_t \rho + \frac{v_i}{\rho}\partial_i \rho + \partial_{ii}\phi = 0 \tag{15.58}$$

15.2.3 Euler equation

The irrotationality condition can be used to write:

$$v_j \partial_j v_i = \frac{1}{2} \partial_i \left(v_j v_j \right) \tag{15.59}$$

and the Euler equation, after division by ρ, becomes:

$$\partial_t v_i + \frac{1}{2} \partial_i \left(v_j v_j \right) + \frac{1}{\rho} \partial_i p = 0 \tag{15.60}$$

Introducing the potential ϕ, we obtain:

$$\partial_{ti} \phi + \frac{1}{2} \partial_i \left(v_j v_j \right) + \frac{1}{\rho} \partial_i p = 0 \tag{15.61}$$

The gradient operator can be factorised:

$$\partial_i \left[\partial_t \phi + \frac{v_j v_j}{2} + \int \frac{dp}{\rho} \right] = 0 \tag{15.62}$$

where the integral is taken along a stream line. The term between brackets depends only on time:

$$\partial_t \phi + \frac{v_j v_j}{2} + \int \frac{dp}{\rho} = F(t) \tag{15.63}$$

But if we assume that, far away from the sources, the conditions at the entrance of a stream line are constant, we can write:

$$\partial_t \phi + \frac{v_j v_j}{2} + \int \frac{dp}{\rho} = const. \tag{15.64}$$

This is a generalisation of the Bernoulli[4] theorem.

[4] **Daniel Bernoulli**, a Swiss physicist and mathematician, was born in Groningen in the Netherlands in 1700 and died in Basel in 1782. He is the son of **Jean Bernoulli**, who taught Leonhard Euler, and the nephew of **Jacques Bernoulli**, who gave his name to the eponymous differential equation. Daniel Bernoulli set the foundations of hydraulics and hydrodynamics in his book *Hydrodynamica, sive of Viribus and Motibus Fluidorum commentarii*, published in Strasbourg in 1738. In that book, Daniel Bernoulli also studied vibrating strings, but failed to obtain a valid solution. His work nevertheless put d'Alembert on the right track.

Calculating $\frac{1}{\rho}\partial_t\rho$

The time-derivative of the previous equation reads:

$$\partial_{tt}\phi + \frac{1}{2}\partial_t\left(v_j v_j\right) + \frac{1}{\rho}\partial_t p = 0 \tag{15.65}$$

but:

$$\partial_t p = \frac{dp}{d\rho}\partial_t\rho = a^2\partial_t\rho \tag{15.66}$$

Introducing the *local* sound velocity a defined by:

$$a^2 = \frac{dp}{d\rho} \tag{15.67}$$

we find:

$$\partial_{tt}\phi + \frac{1}{2}\partial_t\left(v_j v_j\right) + \frac{a^2}{\rho}\partial_t\rho = 0 \tag{15.68}$$

from which we obtain:

$$\frac{1}{\rho}\partial_t\rho = -\frac{1}{a^2}\left(\partial_{tt}\phi + \frac{1}{2}\partial_t\left(v_j v_j\right)\right) \tag{15.69}$$

Calculating $\frac{v_i}{\rho}\partial_i\rho$

Consider now the gradient of Equation 15.64:

$$\partial_{ti}\phi + \frac{1}{2}\partial_i\left(v_j v_j\right) + \frac{1}{\rho}\partial_i p = 0 \tag{15.70}$$

Introducing the local speed of sound a (Equation 15.67) and multiplying all terms by v_i:

$$v_i\partial_{ti}\phi + \frac{1}{2}v_i\partial_i\left(v_j v_j\right) + \frac{a^2 v_i}{\rho}\partial_i\rho = 0 \tag{15.71}$$

we get:

$$\frac{v_i}{\rho}\partial_i\rho = \frac{-1}{a^2}\left[v_i\partial_{ti}\phi + \frac{1}{2}v_i\partial_i\left(v_j v_j\right)\right] \tag{15.72}$$

but:

$$v_i\partial_{ti}\phi = v_i\partial_t v_i = \frac{1}{2}\partial_t\left(v_j v_j\right) \tag{15.73}$$

so that, finally:

$$\frac{v_i}{\rho}\partial_i\rho = \frac{-1}{2a^2}\left[\partial_t\left(v_j v_j\right) + v_i\partial_i\left(v_j v_j\right)\right] \tag{15.74}$$

15.2.4 Non-linear potential equation

Introduce now Equations 15.69 and 15.74 into Equation 15.58:

$$\partial_{ii}\phi - \frac{1}{a^2}\left[\partial_{tt}\phi + \partial_t\left(v_j v_j\right) + \frac{1}{2}v_i\partial_i\left(v_j v_j\right)\right] = 0 \tag{15.75}$$

or, using only the velocity potential:

$$\partial_{ii}\phi - \frac{1}{a^2}\left[\partial_{tt}\phi + \partial_t\left(\partial_j\cdot\phi\partial_j\phi\right) + \frac{1}{2}\partial_i\phi\cdot\partial_i\left(\partial_j\phi\cdot\partial_j\phi\right)\right] = 0 \tag{15.76}$$

or, using other notations:

$$\Delta\phi - \frac{1}{a^2}\left[\frac{\partial^2\phi}{\partial t^2} + \frac{\partial\left(\vec{\nabla}\phi\cdot\vec{\nabla}\phi\right)}{\partial t} + \frac{1}{2}\vec{\nabla}\phi\cdot\left(\vec{\nabla}\left(\vec{\nabla}\phi\cdot\vec{\nabla}\phi\right)\right)\right] = 0 \tag{15.77}$$

15.2.5 Acoustic decomposition

We will now separate the total velocity potential into its hydrodynamic and acoustic components. ϕ_0 corresponds to the background flow (hydrodynamic potential) and ϕ_a to the acoustic perturbation (acoustic potential):

$$\phi = \phi_0 + \phi_a \tag{15.78}$$

We make the following assumptions for ϕ_0:

- stationarity: ϕ_0 is independent of time;
- ϕ_0 is at least an order of magnitude larger than ϕ_a, but varies more slowly.

By introducing this decomposition into Equation 15.76 and by retaining only first order terms in ϕ_a, we obtain linear expressions for each term:

$$\partial_{ii}\phi = \partial_{ii}\phi_0 + \partial_{ii}\phi_a \tag{15.79}$$

$$\partial_{tt}\phi = \partial_{tt}\phi_a \tag{15.80}$$

$$\begin{aligned} \partial_t \left(\partial_i\phi \cdot \partial_i\phi\right) &= 2\partial_i\phi \cdot \partial_{it}\phi \\ &= 2\left(\partial_i\phi_0 + \partial_i\phi_a\right)\partial_{it}\phi_a \\ &\simeq 2\partial_i\phi_0 \cdot \partial_{it}\phi_a \end{aligned} \tag{15.81}$$

$$\begin{aligned} \frac{1}{2}\partial_i\phi \cdot \partial_i\left(\partial_j\phi \cdot \partial_j\phi\right) &= \partial_i\phi \cdot \partial_j\phi \cdot \partial_{ij}\phi \\ &= \partial_i\left(\phi_0 + \phi_a\right)\partial_j\left(\phi_0 + \phi_a\right)\partial_{ij}\left(\phi_0 + \phi_a\right) \\ &\simeq \partial_i\phi_0 \cdot \partial_j\phi_0 \cdot \partial_{ij}\phi_0 + \partial_i\phi_0 \cdot \partial_j\phi_0 \cdot \partial_{ij}\phi_a \end{aligned} \tag{15.82}$$

If we introduce the above expressions in Equation 15.76 and analyse separately the terms in ϕ_0 and ϕ_a, we find a non-linear potential equation for the mean flow:

$$\partial_{ii}\phi_0 - \frac{1}{a^2}\partial_i\phi_0 \cdot \partial_j\phi_0 \cdot \partial_{ij}\phi_0 = 0 \tag{15.83}$$

and an equation for the acoustic perturbation:

$$\partial_{ii}\phi_a - \frac{1}{a^2}\left[\partial_{tt}\phi_a + 2\partial_i\phi_0 \cdot \partial_{it}\phi_a + \partial_i\phi_0 \cdot \partial_j\phi_0 \cdot \partial_{ij}\phi_a\right] = 0 \tag{15.84}$$

Or, using the velocity components v_{0i}:

$$\partial_{ii}\phi_a - \frac{1}{a^2}\left[\partial_{tt}\phi_a + 2v_{0i}\partial_{it}\phi_a + v_{0i}v_{0j}\partial_{ij}\phi_a\right] = 0 \tag{15.85}$$

Finally, rewriting the term between brackets, we obtain:

$$\partial_{ii}\phi_a - \frac{1}{a^2}\left(\partial_t + v_{0i}\partial_i\right)^2\phi_a = 0 \tag{15.86}$$

For time-harmonic acoustic variables we find:

$$\partial_{ii}\phi_a - \frac{1}{a^2}\left(i\omega + v_{0i}\partial_i\right)^2\phi_a = 0 \tag{15.87}$$

15.3 Propagation in an arbitrary background flow

Perfection comes about little by little, through many calculations.
— **Polykleitos of Sicyon** (V^{th} century BC).
quoted by Philo of Byzantium (Philo Mechanicus) (III^{d} century BC), Works

15.3.1 Continuity equation

Introduce the decomposition in hydrodynamic and acoustic variables (Equation 15.1) into the mass conservation equation:

$$\partial_t \left(\rho_0 + \rho_a\right) + \partial_i \left[\left(\rho_0 + \rho_a\right)\left(v_{i0} + v_{ia}\right)\right] = 0 \tag{15.88}$$

and group terms of order 0, 1 and 2:

$$\begin{aligned} \partial_t \rho_0 + \partial_i \left(\rho_0 v_{i0}\right) &+ \\ \partial_t \rho_a + \partial_i \left(\rho_0 v_{ia} + \rho_a v_{i0}\right) &+ \\ \partial_i \left(\rho_a v_{ia}\right) &= 0 \end{aligned} \tag{15.89}$$

We neglect terms of order 2. Zero order terms yield a mass conservation equation for the background flow:

$$\partial_t \rho_0 + \partial_i \left(\rho_0 v_{i0}\right) = 0 \tag{15.90}$$

which, assuming a steady mean flow, gives:

$$\partial_i \left(\rho_0 v_{i0}\right) = 0 \tag{15.91}$$

Terms of order 1 yield a linear equation of mass conservation for the acoustic perturbations:

$$\partial_t \rho_a + \partial_i \left(\rho_0 v_{ia} + \rho_a v_{i0}\right) = 0 \tag{15.92}$$

15.3.2 Momentum equation

We apply the same process to the momentum conservation:

$$(\rho_0+\rho_a)\left[\underbrace{\partial_t v_{i0}}_{=0}+\partial_t v_{ia}+(v_{j0}+v_{ja})\,\partial_j\,(v_{i0}+v_{ia})\right]+\partial_i\,(p_0+p_a)=0 \quad (15.93)$$

At order 0 we obtain:

$$\rho_0 v_{j0}\partial_j v_{i0}+\partial_i p_0=0 \quad (15.94)$$

And at order 1:

$$\rho_0\left[\partial_t v_{ia}+v_{j0}\partial_j v_{ia}+v_{ja}\partial_j v_{i0}\right]+\rho_a v_{j0}\partial_j v_{i0}+\partial_i p_a=0 \quad (15.95)$$

15.3.3 Entropy and perfect gas

The entropy variation ds associated with a heat exchange δq at temperature T is defined as follows:

$$ds=\frac{\delta q}{T} \quad (15.96)$$

The first principle of thermodynamics expresses the total energy variation (de) of an elementary volume as the sum of the thermal (δq) and mechanical (δw) energy it exchanges with its environment:

$$de=\delta q+\delta w \quad (15.97)$$

or:

$$\delta q=de-\delta w \quad (15.98)$$

For a non-viscous fluid, pressure is the only external force:

$$\delta w=-pdv \quad (15.99)$$

The internal energy is a state function and we can develop the differential:

$$de = \frac{\partial e}{\partial T} dT + \frac{\partial e}{\partial v} dv \tag{15.100}$$

but by definition:

$$\frac{\partial e}{\partial T} = c_v \tag{15.101}$$

and, for an ideal gas where the only interactions between molecules are due to thermal agitation:

$$\frac{\partial e}{\partial v} = 0 \tag{15.102}$$

We successively find:

$$de = c_v dT \tag{15.103}$$

$$\delta q = c_v dT + p dv \tag{15.104}$$

$$ds = c_v \frac{dT}{T} + p \frac{dv}{T} \tag{15.105}$$

The ideal gas law ($pv = RT$ with $R = c_p - c_v$) allows us to replace variables (T, v) by (p, ρ):

$$ds = c_v \frac{dp}{p} - c_p \frac{d\rho}{\rho} \tag{15.106}$$

The entropy is a state function and therefore:

$$\frac{\partial s}{\partial p} = \frac{c_v}{p} \tag{15.107}$$

$$\frac{\partial s}{\partial \rho} = -\frac{c_p}{\rho} \tag{15.108}$$

so that:

$$\begin{aligned} \frac{\partial s}{\partial t} &= \frac{\partial s}{\partial p}\frac{\partial p}{\partial t} + \frac{\partial s}{\partial \rho}\frac{\partial \rho}{\partial t} \\ &= \frac{c_v}{p}\frac{\partial p}{\partial t} - \frac{c_v}{\rho}\frac{\partial \rho}{\partial t} \end{aligned} \tag{15.109}$$

and, in the same way:

$$\partial_i s = \frac{c_v}{p}\partial_i p - \frac{c_v}{\rho}\partial_i \rho \tag{15.110}$$

15.3.4 Energy equation

The material derivative of the entropy (also made of two contributions) is zero if we assume an isentropic flow:

$$\underbrace{\partial_t s_0}_{=0} + \partial_t s_a + (v_{j0} + v_{ja})\,\partial_j\,(s_0 + s_a) = 0 \tag{15.111}$$

but, according to Equation 15.106:

$$ds = c_v \frac{dp_0 + dp_a}{p_0 + p_a} - c_p \frac{d\rho_0 + d\rho_a}{\rho_0 + \rho_a} \tag{15.112}$$

We develop this expression to express the components s_0 and s_a:

$$ds = \frac{c_v}{p_0 + p_a}\left(dp_0 + dp_a - \frac{c_p}{c_v}\frac{p_0 + p_a}{\rho_0 + \rho_a}\,(d\rho_0 + d\rho_a)\right) \tag{15.113}$$

We now define:

$$\begin{aligned} c^2 &= \frac{c_p}{c_v}\frac{p_0 + p_a}{\rho_0 + \rho_a} = \gamma \frac{p_0\left(1 + \frac{p_a}{p_0}\right)}{\rho_0\left(1 + \frac{\rho_a}{\rho_0}\right)} \\ &\simeq \frac{\gamma p_0}{\rho_0}\left(1 + \frac{p_a}{p_0}\right)\left(1 - \frac{\rho_a}{\rho_0}\right) \simeq c_0^2\left(1 + \frac{p_a}{p_0} - \frac{\rho_a}{\rho_0}\right) \\ &\simeq c_0^2 + \underbrace{c_0^2\left(\frac{p_a}{p_0} - \frac{\rho_a}{\rho_0}\right)}_{=c_a^2} = c_0^2 + c_a^2 \end{aligned} \tag{15.114}$$

Keeping only terms of order 1, the variation of entropy can be written as:

$$\begin{aligned} ds &= \frac{c_v}{p_0 + p_a}\left(dp_0 + dp_a - \left(c_0^2 + c_a^2\right)(d\rho_0 + d\rho_a)\right) \\ &= \underbrace{\frac{c_v}{p_0}\left(dp_0 - c_0^2 d\rho_0\right)}_{=s_0} + \underbrace{\frac{c_v}{p_0}\left(dp_a - c_0^2 d\rho_a - c_a^2 d\rho_0\right)}_{=s_a} \end{aligned} \tag{15.115}$$

The equation of energy at order 0 is:

$$v_{j0}\partial_j s_0 = 0 \tag{15.116}$$

where

$$v_{j0}\frac{c_v}{p_0}\partial_j p_0 - v_{j0}\frac{c_p}{\rho_0}\partial_j \rho_0 = 0 \tag{15.117}$$

Remembering that $\frac{c_p p_0}{c_v \rho_0} = c_0^2$ (Section 4.6.1):

$$v_{j0}\partial_j p_0 = c_0^2 v_{j0}\partial_j \rho_0 \tag{15.118}$$

At order 1, replacing c_a by its value according to p_a and ρ_a, we find:

$$\begin{aligned} \partial_t p_a + v_{j0}\partial_j p_a + v_{ja}\partial_j p_0 &= c_0^2\left(\partial_t \rho_a + v_{j0}\partial_j \rho_a + v_{ja}\partial_j \rho_0\right) \\ &+ c_0^2 v_{0j}\partial_j \rho_0 \left(\frac{p_a}{p_0} - \frac{\rho_a}{\rho_0}\right) \end{aligned} \tag{15.119}$$

15.3.5 Linearised Euler equations

The sound propagation in arbitrary flow requires the resolution of two sets of equations. For the steady mean flow we have successively:

- the mass conservation equation (Equation 15.91):

$$\partial_i\left(\rho_0 v_{i0}\right) = 0 \tag{15.120}$$

- the momentum equation (Equation 15.94):

$$\rho_0 v_{j0}\partial_j v_{i0} + \partial_i p_0 = 0 \tag{15.121}$$

- and the energy equation (Equation 15.118):

$$v_{j0}\partial_j p_0 = c_0^2 v_{j0}\partial_j \rho_0 \tag{15.122}$$

Once the fields $(p_0, \rho_0, \vec{v}_0)$ are known, the linearised equations for the acoustic perturbations can be solved:

- mass conservation (Equation 15.92):

$$\partial_t \rho_a + \partial_i\left(\rho_0 v_{ia} + \rho_a v_{i0}\right) = 0 \tag{15.123}$$

- momentum equation (Equation 15.95):

$$\rho_0 \left[\partial_t v_{ia} + v_{j0}\partial_j v_{ia} + v_{ja}\partial_j v_{i0}\right] + \rho_a v_{j0}\partial_j v_{i0} + \partial_i p_a = 0 \qquad (15.124)$$

- and energy equation (Equation 15.119):

$$\begin{aligned} \partial_t p_a + v_{j0}\partial_j p_a + v_{ja}\partial_j p_0 &= c_0^2 \left(\partial_t \rho_a + v_{j0}\partial_j \rho_a + v_{ja}\partial_j \rho_0\right) \\ &+ c_0^2 v_{0j}\partial_j \rho_0 \left(\frac{p_a}{p_0} - \frac{\rho_a}{\rho_0}\right) \end{aligned} \qquad (15.125)$$

These equations cannot be reduced to a scalar wave equation as in the case of a potential background flow.

15.4 Application to a turbo-engine

Figure 15.4 represents an aircraft turbofan engine. The outside air enters the nacelle and is accelerated by the fan. Part of the flow passes through the engine itself (multi-stage compressor, combustion chamber, multi-stage turbine) while the rest goes through an annular *bypass* duct. At the rear of the engine, we observe a flow made of three concentric jets:

- hot and strongly accelerated gases coming out of the turbine;
- cold and accelerated gases coming out of the bypass;
- outside air.

At the interfaces between these three flow regions, we find strongly sheared transition flows.

Sound waves generated by the *fan* propagate upstream of the engine, within and then outside the nacelle, against the intake flow. These waves also propagate downstream, first guided by the bypass duct then freely through the shear layers.

We can model the wave propagation upstream assuming a potential flow (Section 15.2). Figure 15.5 shows the pressure field generated by the fan and

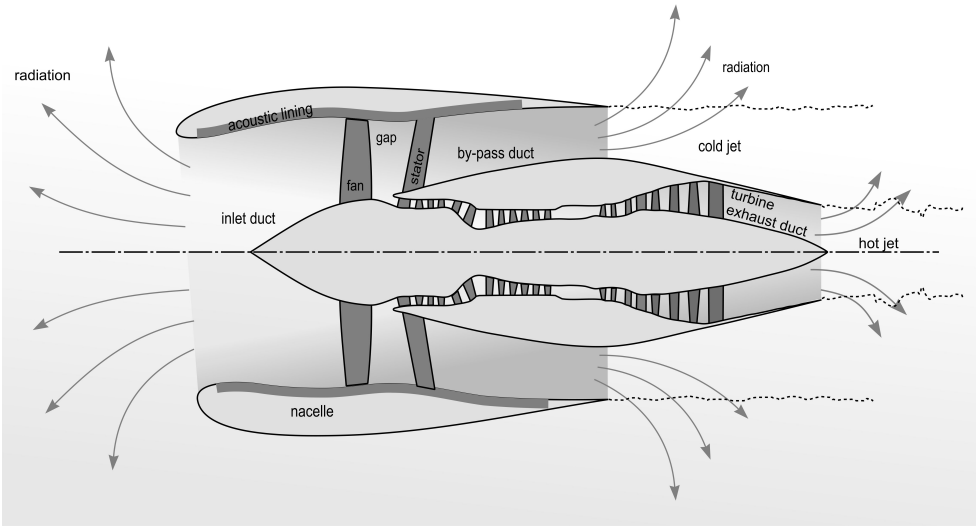

Figure 15.4: Dual flux turbofan aircraft engine.

radiating upstream of the engine. The fields calculated with and without background flow are compared. The effect of the flow on the wavelength and directivity appears clearly. This shows the importance of modelling the effects of sound convection for this type of application.

Downstream of the engine, on the other hand, the flow is not irrotational. The inhomogeneous temperature field and the shear layers are major features of the mean flow that must be taken into account. The solution of the linearised Euler equations (Section 15.3) are shown in Figure 15.6. The sound wave refraction through the shear layers is clearly visible.

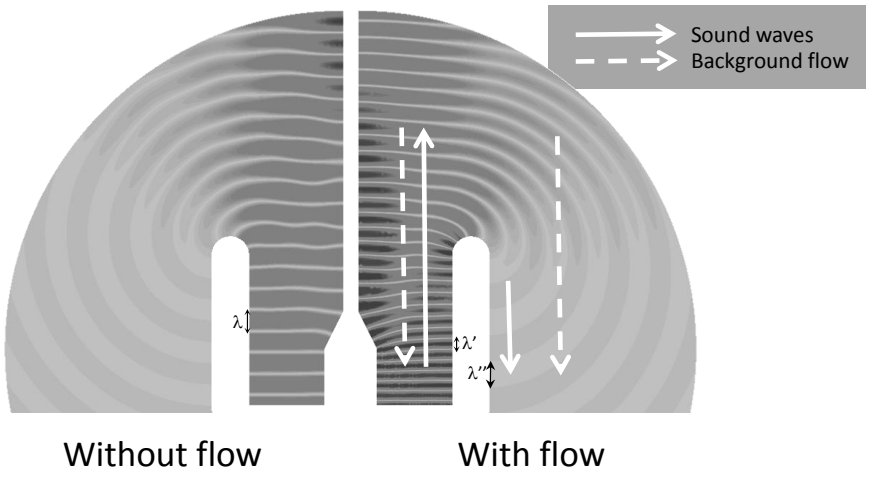

Figure 15.5: Upstream fan sound radiation through the engine nacelle. Left: sound field with no mean flow. Right: sound field with mean flow.

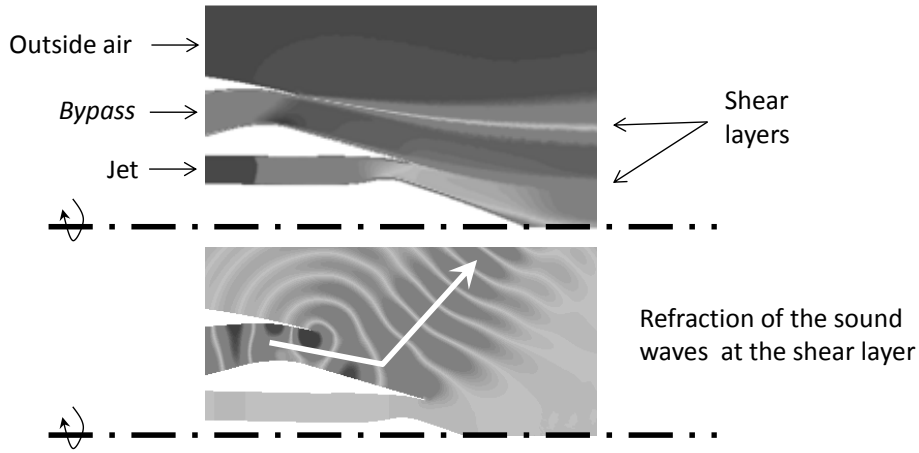

Figure 15.6: Fan radiation through the bypass showing refraction of the sound waves through the shear layers. Top: mean flow (three co-axial jets separated by two shear layers). Bottom: acoustic field generated by the fan.

16

Atmospheric propagation

Contents

16.1 Main phenomena 343
16.2 Axisymmetric formulation 347
16.3 Parabolic approximation 348
16.4 Finite difference solution 351
16.5 Evaluating Ψ at $r = 0$ 356
16.6 Numerical performances 359
16.7 Conclusions 367

Sound propagation in the atmosphere is usually studied in the context of environmental acoustic problems. Modeling such problems requires specific techniques adapted to particular propagation conditions. Propagation distances can range from a few meters to many kilometers with propagation occuring in a complex medium (the atmosphere) where wind and temperature effects can be highly significant. In addition, the modelling method should take into account the particular characteristics of the ground surface (absorbent or rigid) and the possible presence of obstacles (irregular ground surface, screens, etc.).

Conventional methods (finite element or boundary element methods) are inappropriate because they generate models of untractable size. Specialised methods are therefore necessary. The *parabolic* method is a simplified model for exterior acoustic problems. Simplification is achieved by neglecting some terms of the wave equation. A full derivation of the parabolic method is proposed in this chapter. The numerical techniques used to solve the parabolic equation are presented. The attractive features of the method are illustrated by an example.

The parabolic method is widely used in underwater acoustic and proves to be efficient for propagating acoustic disturbances over long distances. The method is therefore ideal for efficiently solving environmental problems in the atmosphere (propagation of sources along the ground surface for example). The reference book of Salomons[1] and the papers from West and Gilbert [2] provide further reading.

The approximations used in the derivation lead to certain limitations (the method is for instance only valid for receivers at *low* elevation angles, Figure 16.3). However, the method does exhibit other advantages (the transformation of the problem from elliptic to parabolic leads to higher computational efficiency).

[1] **Salomons E. M.**. *Computational atmospheric acoustics*, Kluwer Academic Publishers, 2001.

[2] **West M., Gilbert K.E., Sack R.A.**, *A tutorial on the parabolic equation model used for long range sound propagation in the atmosphere*, Applied Acoustics, 199-228 (1992) and **Gilbert K.E., While M.J.**, *Application of the parabolic equation to sound propagation in a refracting atmosphere*, J. Acoust. Soc. Amer., 630-637 (1989).

16.1 Main phenomena

Sound propagation in the atmosphere involves various mechanisms such as geometric attenuation, atmospheric absorption, turbulence and diffraction. Reflection and absorption on the ground surface deeply impact both magnitude and phase of the acoustic field. Additionally, wind and thermal gradients can generate refraction effects which change the noise level significantly. The ground profile can also strongly influence the observed levels. These different mechanisms are briefly described below.

16.1.1 Geometric attenuation

Geometric attenuation can be described by considering the radiation of a point source in a free field. At a distance r from the source, the radiated wave is described by a spherical surface ($4\pi r^2$). Without dissipative mechanisms, each doubling of the distance r leads to a reduction of the pressure by a factor 4 and of the sound pressure level by 6 dB. Geometric attenuation can be described by the following relation giving the sound pressure level L_p at a distance r from a source of power L_W :

$$L_p = L_W - 10\log(4\pi r^2) \tag{16.1}$$

16.1.2 Atmospheric absorption

Atmospheric absorption is characterised by a loss of sound energy resulting from the two following phenomenona:

- Thermal conduction and viscosity of the air: the temperature and velocity gradients present in the sound wave are respectively reduced by thermal conduction and momentum transfer. These two processes are

f_c	16	31.5	63	125	250	500	1,000	2,000	4,000
α	0.007	0.028	0.11	0.37	1.02	1.96	3.57	8.8	29.0

Table 16.1: Absorption coefficient α ([dB/km]) in the atmosphere (10°C, 1 atmosphere, 80% humidity) for central frequencies of one-third octave bands (f_c [Hz]) between 16 Hz and 4,000 Hz.

governed by thermal conduction and viscosity and lead to a loss of energy (heat release). They can be described by the equations of fluid mechanics. The attenuation associated to these effects becomes more important as frequency increases (gradients of field variables increase with the frequency).

- Energy loss by relaxation of oxygen and nitrogen molecules: the phenomenon of molecular relaxation results from the time delay in reaching equilibrium after applying external excitations. This delay is directly influenced by the concentration of the medium in poly-atomic molecules. The process leads to an additional loss of energy (heat release) and is strongly influenced by the presence of water molecules in the air (natural humidity).

The consideration of atmospheric absorption modifies Equation 16.1:

$$L_p = L_W - 10\log(4\pi r^2) - \alpha r \tag{16.2}$$

where α is the coefficient of atmospheric absorption (expressed in dB per unit length). The term $-\alpha r$ is significant for distances associated with environmental problems (hundreds of meters) and for high frequencies. Standard ISO 9613-1:1993[3] provides formulae for α as a function of frequency, temperature, atmospheric pressure and relative humidity. One should stress the fact that α is proportional to the square of the frequency. Table 16.1 gives values of α at the central frequencies of third-octave bands from 16 to 4,000 Hz. These values were calculated for a temperature of 10°C, an atmospheric pressure of 101325 Pa, and a humidity rate of 80%. This table clearly indicates that *high* frequencies are strongly attenuated in the atmosphere while *low* frequencies are only weakly attenuated.

[3] **ISO 9613-1:1993**, *Acoustics - Attenuation of sound during propagation outdoors - Part 1: Calculation of the absorption of sound by the atmosphere.*

16.1.3 Atmospheric refraction

In the atmosphere, temperature varies significantly according to altitude. Generally, temperature decreases with altitude during the day while it increases during the night. This results in corresponding variations in sound speed. A good approximation is that, between -20 and +40°C, a temperature increase of 1°C leads to an increase of the sound speed of 0.6 m/s (Equation 4.64). This variation of sound speed according to altitude is responsible for the acoustic refraction phenomena. A sound wave will be systematically refracted towards the region where the speed of sound is lower. This is illustrated in Figure 16.1 for two profiles of sound speed (day vs. night).

16.1.4 Turbulence

An atmosphere where temperature and wind speed profiles do not vary in time is an ideal case. In reality, these profiles fluctuate in time at different rates (time scale varies from seconds to hours). The rapid fluctuations of the velocity field in a fluid are due to turbulence and materialise as eddies of different sizes. Temperature fluctuations are also caused by eddies.

The atmospheric propagation model usually accounts for a turbulent atmosphere by adding a random component to the sound speed. The acoustic levels, averaged over several minutes, may then be evaluated using multiple realisations of the sound speed field.

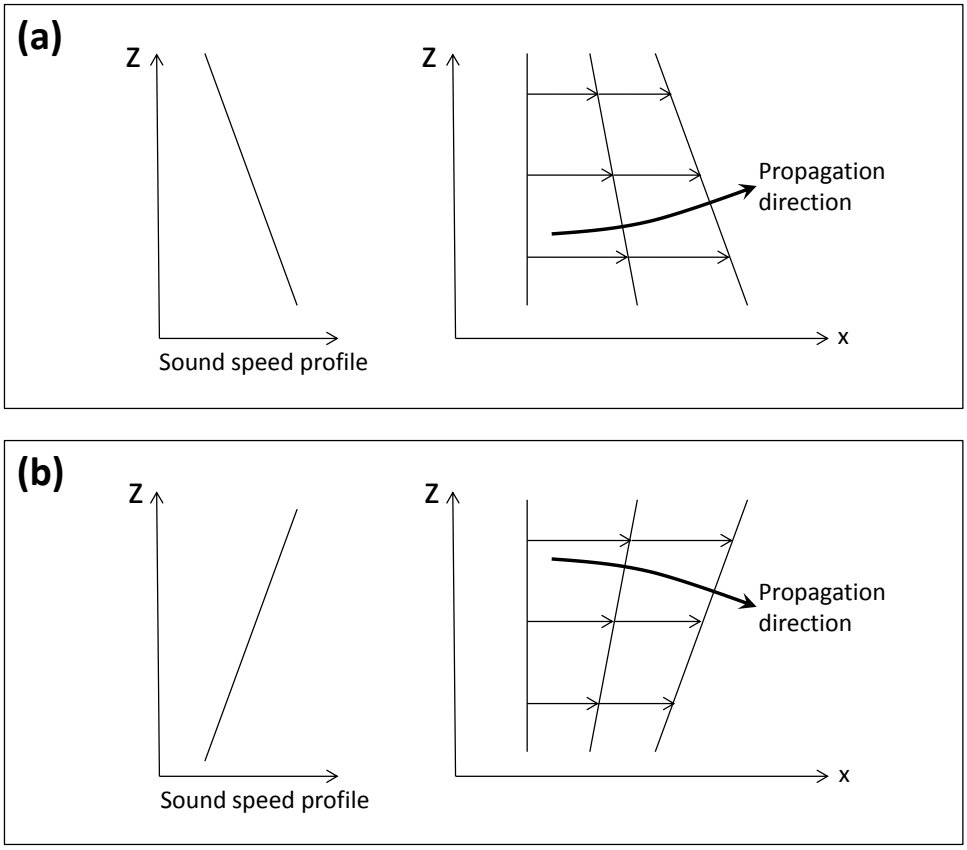

Figure 16.1: Atmospheric refraction for two sound speed profiles: (a) refraction towards ground resulting from decreasing sound speed with altitude z. (b) refraction away from ground resulting from increasing sound speed with altitude z.

16.2 Axisymmetric formulation

The presentation of the parabolic method in this section is based on the analysis of the radiation from a single source in a half-space domain (Figure 16.2). The Helmholtz equation in cylindrical coordinates is:

$$\frac{1}{r}\frac{\partial}{\partial r}\left(r\frac{\partial p}{\partial r}\right)+\frac{\partial}{\partial z}\left(\frac{\partial p}{\partial z}\right)+\frac{1}{r^2}\frac{\partial^2 p}{\partial \phi^2}+k_z^2 p=0 \tag{16.3}$$

where the wavenumber k_z may be dependent on z (case of a stratified atmosphere).

Since the problem is axisymmetric, the pressure field p does not depend on ϕ and Equation 16.3 becomes:

$$\frac{1}{r}\frac{\partial}{\partial r}\left(r\frac{\partial p}{\partial r}\right)+\frac{\partial}{\partial z}\left(\frac{\partial p}{\partial z}\right)+k_z^2 p=0 \tag{16.4}$$

The parabolic equation is obtained by successive approximations of Equation 16.4. Using the following factorised form of the solution $p(r,z)$:

$$p(r,z)=\frac{1}{\sqrt{r}}q(r,z) \tag{16.5}$$

an alternative to Equation 16.4 is obtained involving only the unknown $q(r,z)$:

$$\frac{\partial^2 q}{\partial r^2}+\frac{1}{4r^2}q+\frac{\partial^2 q}{\partial z^2}+k_z^2 q=0 \tag{16.6}$$

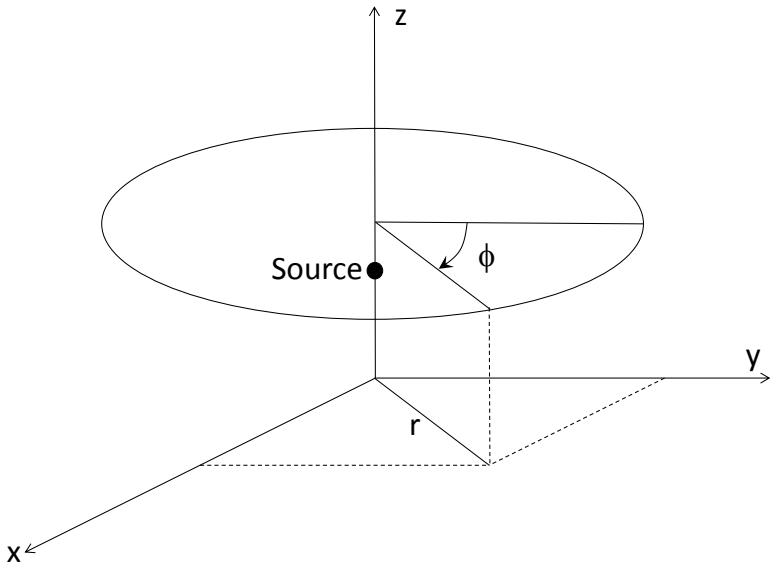

Figure 16.2: Source radiating in a half-space domain (cartesian and cylindrical coordinates).

16.3 Parabolic approximation

The parabolic equation can be obtained from Equation 16.6 by simplifiying the modelling of the far field, by assuming only outgoing waves and by the so-called *narrow angle* approximation.

16.3.1 Far field approximation

At radial distances $r \gg \lambda$ (λ is the wavelength), the second term of Equation 16.6 can be neglected. This equation reduces to the 2-D Helmholtz equation:

$$\frac{\partial^2 q}{\partial r^2} + \frac{\partial^2 q}{\partial z^2} + k_z^2 q = 0 \,. \tag{16.7}$$

16.3.2 Outgoing waves

Using a reference wavenumber k_a (corresponding to an average height if the medium is not homogeneous), Equation 16.7 can be expressed as:

$$\frac{\partial^2 q}{\partial r^2} + H_2(z)q = 0 \tag{16.8}$$

where H_2 is given by:

$$H_2(z) = k_a^2(1+s) \tag{16.9}$$

with s defined as:

$$s = \frac{1}{k_a^2}\left(\frac{\partial^2}{\partial z^2} + k_z^2 - k_a^2\right) \tag{16.10}$$

Equation 16.8 can be factorised according to:

$$\left(\frac{\partial}{\partial r} - iH_1(z)\right)\left(\frac{\partial}{\partial r} + iH_1(z)\right)q = 0 \tag{16.11}$$

where H_1 is given by:

$$H_1(z) = k_a\sqrt{1+s} \simeq k_a\left(1 + \frac{s}{2}\right) \tag{16.12}$$

If one consider only waves propagating along $r > 0$ direction, Equation 16.11 reduces to:

$$\left(\frac{\partial}{\partial r} + iH_1(z)\right)q = 0 \tag{16.13}$$

or as:

$$\frac{\partial q}{\partial r} + ik_a q + \frac{i}{2k_a}\left(\frac{\partial^2 q}{\partial z^2} + (k_z^2 - k_a^2)q\right) = 0 \tag{16.14}$$

16.3.3 *Narrow-angle* approximation

The solution $q(r, z)$ of Equation 16.14 can be expressed in the following factorised form:

$$q(r, z) = \psi(r, z) \exp(-ik_a r) \tag{16.15}$$

where the function ψ varies smoothly along the radial direction. Substituting this form into Equation 16.14 gives (after removing the multiplicative factor $\exp(-ik_a r)$):

$$2ik_a \frac{\partial \psi}{\partial r} - \frac{\partial^2 \psi}{\partial z^2} - (k_z^2 - k_a^2)\psi = 0 \tag{16.16}$$

or:

$$\frac{\partial \psi}{\partial r} = \alpha \frac{\partial^2 \psi}{\partial z^2} + \beta_z \psi \tag{16.17}$$

where α and β_z are given by:

$$\alpha = \frac{1}{2ik_a} \tag{16.18}$$

and:

$$\beta_z = \frac{k_z^2 - k_a^2}{2ik} \tag{16.19}$$

This is the *parabolic equation* that must be solved in the acoustic domain ($z \geq 0; r \geq 0$) with suitable boundary conditions. These conditions are usually expressed as:

- fixed impedance relating pressure p to normal velocity v_n at $z = 0$ (normal vector n points away from the fluid domain):

$$\left(\frac{p}{v_n}\right)_{z=0} = \left(\frac{p}{-v_z}\right)_{z=0} = Z\rho c \tag{16.20}$$

  where Z is the characteristic impedance along the ground surface.

- fixed impedance at $z = l_z$ (where l_z is the height of the fluid domain):

$$\left(\frac{p}{v_n}\right)_{z=l_z} = \left(\frac{p}{v_z}\right)_{z=l_z} = \rho c \tag{16.21}$$

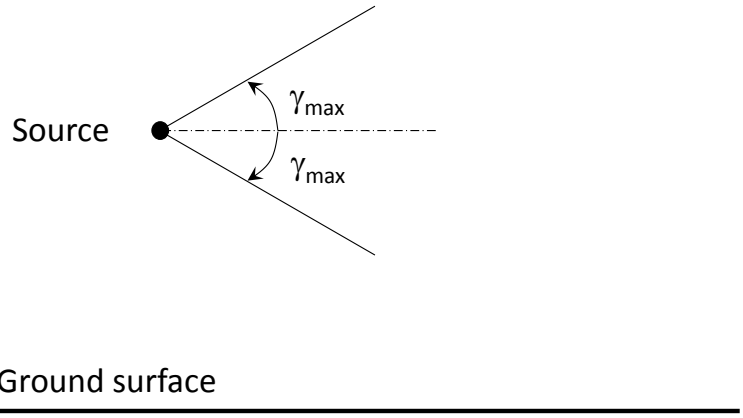

Figure 16.3: Restriction of elevation angles for parabolic method.

16.4 Finite difference solution

16.4.1 Discrete form

The form of Equation 16.17 is characteristic of an initial value problem. The solution of the equation with its boundary conditions (16.20) and (16.21) (reformulated in terms of ψ) can be obtained using a finite difference scheme. This numerical scheme is applied to a regular grid (radial step Δ_r, vertical step Δ_z) of the computing domain (radial length l_r, vertical length l_z). The values of ψ at the M points of coordinates $z_j = (j-1)\Delta z$ (where $j = 1, 2, \ldots, M$) are denoted $\psi_1, \psi_2, \ldots, \psi_M$. The discrete form of Equation 16.17 is obtained by replacing the second order derivative of ψ with respect to z by the following central finite difference approximation:

$$\left(\frac{\partial^2 \psi}{\partial z^2}\right)_{z=z_j} = \frac{\psi_{j+1} - 2\psi_j + \psi_{j-1}}{\Delta_z^2} \tag{16.22}$$

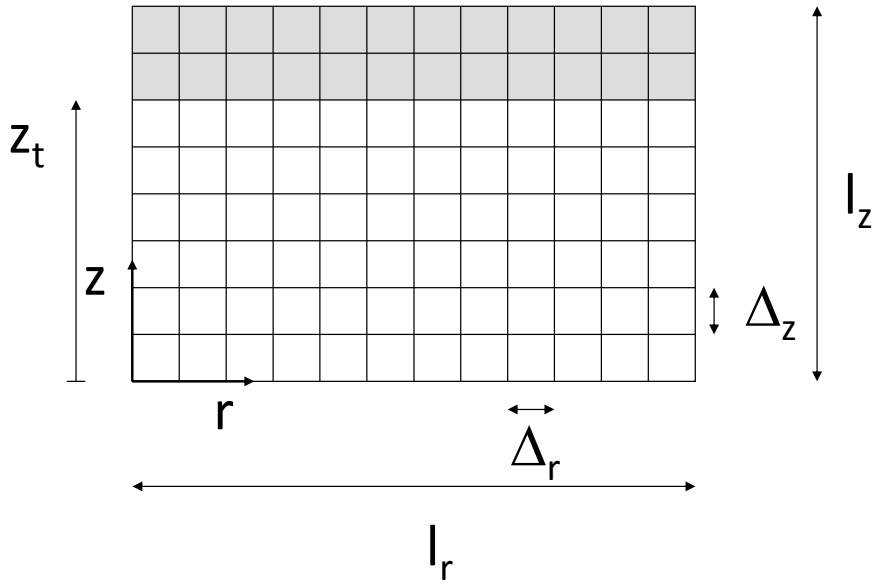

Figure 16.4: Finite difference grid of the $z \geq 0$ half-plane.

The discrete form of Equation 16.17 is therefore:

$$\frac{\partial}{\partial r}\begin{pmatrix} \psi_1 \\ \psi_2 \\ \psi_3 \\ \dots \\ \psi_{M-2} \\ \psi_{M-1} \\ \psi_M \end{pmatrix} = \frac{\alpha}{\Delta_z^2}\begin{bmatrix} -2 & 1 & 0 & \dots & 0 & 0 & 0 \\ 1 & -2 & 1 & \dots & 0 & 0 & 0 \\ \dots & \dots & \dots & \dots & \dots & \dots & \dots \\ \dots & \dots & \dots & \dots & \dots & \dots & \dots \\ \dots & \dots & \dots & \dots & \dots & \dots & \dots \\ 0 & 0 & 0 & \dots & 1 & -2 & 1 \\ 0 & 0 & 0 & \dots & 0 & 1 & -2 \end{bmatrix}\begin{pmatrix} \psi_1 \\ \psi_2 \\ \psi_3 \\ \dots \\ \psi_{M-2} \\ \psi_{M-1} \\ \psi_M \end{pmatrix}$$
$$+ \begin{pmatrix} \beta_1\psi_1 \\ \beta_2\psi_2 \\ \beta_3\psi_3 \\ \dots \\ \beta_{M-2}\psi_{M-2} \\ \beta_{M-1}\psi_{M-1} \\ \beta_M\psi_M \end{pmatrix} + \frac{\alpha}{\Delta_z^2}\begin{pmatrix} \psi_0 \\ 0 \\ 0 \\ \dots \\ 0 \\ 0 \\ \psi_{M+1} \end{pmatrix} \tag{16.23}$$

16.4.2 Discrete boundary conditions

The boundary condition (Equation 16.20) along the ground surface ($z = 0$) can be reformulated using the Euler equation:

$$\frac{\partial p}{\partial n} = -i\rho c k_z v_n \tag{16.24}$$

so that the boundary condition becomes:

$$\left(\frac{\partial p}{\partial z}\right)_{z=0} = +ik_z \frac{1}{Z}(p)_{z=0} \tag{16.25}$$

The first derivative of pressure p (at $z = \Delta_z/2$) is approximated by the finite difference:

$$\left(\frac{\partial p}{\partial z}\right)_{z=\frac{\Delta_z}{2}} \simeq \frac{p_1 - p_0}{\Delta_z} \tag{16.26}$$

The pressure derivative at $z = 0$ involves the second order derivative and is written as:

$$\left(\frac{\partial p}{\partial z}\right)_{z=0} \simeq \left(\frac{\partial p}{\partial z}\right)_{z=\frac{\Delta_z}{2}} - \frac{\Delta_z}{2}\left(\frac{\partial^2 p}{\partial z^2}\right)_{z=\Delta_z} \tag{16.27}$$

The use of this expression (with finite difference approximations for first and second order derivatives) in Equation 16.25 gives the following relation between pressure p_0, p_1 and p_2:

$$\left(2ik\frac{\Delta_z}{Z} + 3\right) p_0 = 4p_1 - p_2 \tag{16.28}$$

This condition can be reformulated in terms of ψ (since p is related to ψ through $p = \psi e^{-ik_a r}\sqrt{r}$):

$$\psi_0 = \sigma_1\psi_1 + \sigma_2\psi_2 \tag{16.29}$$

where σ_1 and σ_2 are given by:

$$\sigma_1 = \frac{4}{3 + 2ik\frac{\Delta_z}{Z}} \tag{16.30}$$

and:

$$\sigma_2 = \frac{-1}{3 + 2ik\frac{\Delta_z}{Z}} \tag{16.31}$$

In a similar way, the boundary condition Equation 16.21 along the upper surface ($z = l_z$) of the model can be formulated as:

$$\left(\frac{\partial p}{\partial z}\right)_{z=l_z} = -ik_z \left(p\right)_{z=l_z} \tag{16.32}$$

In a finite difference context, the first derivative of the pressure p (at $z = l_z - \Delta_z/2$) is given by:

$$\left(\frac{\partial p}{\partial z}\right)_{z=l_z-\frac{\Delta_z}{2}} \simeq \frac{p_{M+1} - p_M}{\Delta_z} \tag{16.33}$$

The evaluation of the pressure derivative at $z = l_z$ requires the use of the second order derivative according to:

$$\left(\frac{\partial p}{\partial z}\right)_{z=l_z} \simeq \left(\frac{\partial p}{\partial z}\right)_{z=l_z-\frac{\Delta_z}{2}} + \frac{\Delta_z}{2}\left(\frac{\partial^2 p}{\partial z^2}\right)_{z=l_z-\Delta_z} \tag{16.34}$$

The use of this expression (with finite difference approximations for first and second order derivatives) in Equation 16.32 gives the following relation between pressure p_M, p_{M-1} and p_{M-2}:

$$\left(2ik\frac{\Delta_z}{Z} + 3\right) p_{M+1} = 4p_M - p_{M-1} \tag{16.35}$$

This condition can be reformulated in terms of ψ as:

$$\psi_{M+1} = \tau_1 \psi_{M-1} + \tau_2 \psi_M \tag{16.36}$$

where τ_1 and τ_2 are given by:

$$\tau_1 = \frac{4}{3 + 2ik\frac{\Delta_z}{Z}} \tag{16.37}$$

and:

$$\tau_2 = \frac{-1}{3 + 2ik\frac{\Delta_z}{Z}} \tag{16.38}$$

16.4.3 System of algebraic equations

Substituting Equations 16.29 and 16.36 into Equation 16.23 leads to the following discrete system:

$$\frac{\partial \Psi}{\partial r} = (\gamma T + D)\,\Psi \tag{16.39}$$

using the following notation:

$$\gamma = \frac{\alpha}{\Delta_z^2} \tag{16.40}$$

$$\Psi = (\psi_1, \psi_2, \psi_3, \ldots, \psi_{M-1}, \psi_M)^T \tag{16.41}$$

$$T = \begin{bmatrix} -2+\sigma_1 & 1+\sigma_2 & 0 & \ldots & 0 & 0 & 0 \\ 1 & -2 & 1 & \ldots & 0 & 0 & 0 \\ \ldots & \ldots & \ldots & \ldots & \ldots & \ldots & \ldots \\ \ldots & \ldots & \ldots & \ldots & \ldots & \ldots & \ldots \\ \ldots & \ldots & \ldots & \ldots & \ldots & \ldots & \ldots \\ 0 & 0 & 0 & \ldots & 1 & -2 & 1 \\ 0 & 0 & 0 & \ldots & 0 & 1+\tau_1 & -2+\tau_2 \end{bmatrix} \tag{16.42}$$

$$D = (\beta_1\psi_1, \beta_2\psi_2, \beta_3\psi_3, \ldots, \beta_{M-1}\psi_{M-1}, \beta_M\psi_M)^T \tag{16.43}$$

The numerical treatment of Equation 16.43 relies on the preliminary integration of left and right hand sides along the radial direction between r and $r + \Delta_r$. The integrals of Ψ and its radial derivative can be expressed as:

$$\int_r^{r+\Delta_r} \Psi dr = \frac{1}{2}\left(\Psi(r+\Delta_r) + \Psi(r)\right)\Delta_r \tag{16.44}$$

$$\int_r^{r+\Delta_r} \frac{\partial \Psi}{\partial r} dr = \Psi(r+\Delta_r) - \Psi(r) \tag{16.45}$$

The integrated form of Equation 16.43 is therefore:

$$\Psi(r+\Delta_r) - \Psi(r) = \frac{1}{2}\left(\gamma T + D\right)\left(\Psi(r+\Delta_r) + \Psi(r)\right)\Delta_r \tag{16.46}$$

or:

$$M_2\Psi(r+\Delta_r) = M_1\Psi(r) \tag{16.47}$$

with:

$$M_1 = I - \frac{1}{2}(\gamma T + D)\,\Delta_r \tag{16.48}$$

$$M_2 = I + \frac{1}{2}(\gamma T + D)\,\Delta_r \tag{16.49}$$

Equation 16.47 is used for the evaluation of the vector Ψ at all successive radial positions. We first have to evaluate Ψ at $r = 0$ which is addressed in the next section.

The system Equation 16.47 involves a tri-diagonal matrix whose size is set by the number of points along the vertical direction. Matrix M_2 needs to be factorised only once. Each radial step requires a matrix-vector product for generating the RHS vector and then a resolution with the factorised matrix. This explains the numerical efficiency of the parabolic method.

16.5 Evaluating Ψ at $r = 0$

The initial field (Ψ at $r = 0$) is obtained by assuming that the wavenumber is constant along z. A particular procedure has to be devised for the evaluation of Ψ at $r = 0$ since the location of the source at $(r = 0, z = 0)$ prevents a direct use of the formal expression of the pressure radiated by a monopole source. An alternate solution scheme performs a plane wave expansion of q:

$$q(r, z) = \int_{-\infty}^{\infty} S(k_v) e^{-ik_v z - ik_r r} dk_v \tag{16.50}$$

q should verify Equation 16.14 with $k_z = k_a$:

$$\frac{\partial q}{\partial r} + ik_a q + \frac{i}{2k_a}\frac{\partial^2 q}{\partial z^2} = 0 \tag{16.51}$$

Substituting the plane wave expansion (Equation 16.50) into Equation 16.51 gives:

$$\int_{-\infty}^{\infty} \left(-ik_r + ik_a - \frac{ik_v^2}{2k_a} \right) S(k_v) e^{-ik_v z - ik_r r} dk_v = 0 \tag{16.52}$$

so that the following dispersion relation holds:

$$k_r = k_a - \frac{k_v^2}{2k_a} \tag{16.53}$$

The plane wave expansion can be rewritten as:

$$q(r,z) = \int_{-\infty}^{\infty} S(k_v) e^{iF(k_v)} dk_v \tag{16.54}$$

with:

$$F(k_v) = -k_v z - \left(k_a - \frac{k_v^2}{2k_a}\right) r \tag{16.55}$$

The evaluation of this integral relies on the method of stationary phase. The related stationary points are defined by:

$$F'(k_{v0}) = 0 \tag{16.56}$$

or

$$-z + \frac{2k_{v0}}{2k_a} r = 0 \tag{16.57}$$

which gives the location of the stationary point:

$$k_{v0} = \frac{z}{r} k_a \tag{16.58}$$

Since the second derivative $F'' = r/k_a$ is always positive, one can express the integral in Equation 16.54 in the form:

$$q(r,z) \simeq \sqrt{\frac{2\pi}{F''(k_{v0})}} S(k_{v0}) e^{iF(k_{v0})} e^{i\pi/4} \tag{16.59}$$

or

$$q(r,z) \simeq \sqrt{\frac{2\pi k_a}{r}} S(k_{v0}) e^{-ik_a r\left(1+\frac{z^2}{2r^2}\right)} e^{i\pi/4} \tag{16.60}$$

The distance R between the source (located in $(r = 0, z = 0)$) and the field point (r, z) is given by:

$$R = \sqrt{r^2 + z^2} = r\sqrt{1 + \frac{z^2}{r^2}} \simeq r\left(1 + \frac{z^2}{2r^2}\right) \tag{16.61}$$

so that Equation 16.60 can be rewritten as follows:

$$q(r,z) \simeq \sqrt{\frac{2\pi k_a}{r}} S(k_{v0}) e^{-ik_a R} e^{i\pi/4} \tag{16.62}$$

This expression should be compared to q field of a monopole source:

$$q(r,z) = \sqrt{r}\frac{e^{-ik_a R}}{R} \tag{16.63}$$

leading to the identification of $S(k_{v0})$:

$$S(k_{v0}) = \frac{r}{R}\frac{1}{\sqrt{2i\pi k_a}} \tag{16.64}$$

or using Equations 16.58 and 16.60:

$$S(k_{v0}) = \frac{1}{\sqrt{2i\pi k_a}}\left(1+\frac{k_{v0}^2}{2k_a^2}\right)^{-1} \simeq \frac{1}{\sqrt{2i\pi k_a}}\left(1+\frac{k_{v0}^2}{k_a^2}\right)^{-1/2} \tag{16.65}$$

This expression can be further simplified using:

$$\left(1+\frac{k_{v0}^2}{k_a^2}\right)^{-1/2} \simeq 1+\frac{k_{v0}^2}{2k_a^2} \simeq e^{-\frac{k_{v0}^2}{2k_a^2}} \tag{16.66}$$

so that the final expression of $S(k_{v0})$ is:

$$S(k_{v0}) = \frac{1}{\sqrt{2i\pi k_a}} e^{-\frac{k_{v0}^2}{2k_a^2}} \tag{16.67}$$

The related expression for $q(0,z)$ is obtained using Equation 16.54:

$$q(0,z) = \int_{-\infty}^{\infty} S(k_v) e^{iF(k_v)} dk_v = \int_{-\infty}^{\infty} \frac{1}{\sqrt{2i\pi k_a}} e^{-\frac{k_v^2}{2k_a^2}} e^{-ik_v z} dk_v \tag{16.68}$$

This integral can be evaluated analytically:

$$q(0,z) = \sqrt{\frac{k_a}{i}} e^{-\frac{k_a^2 z^2}{2}} \tag{16.69}$$

Since $q(0,z)$ is equal to $\psi(0,z)$, this expression gives the requested ψ values at $r=0$:

$$\psi(0,z) = \sqrt{\frac{k_a}{i}} e^{-\frac{k_a^2 z^2}{2}} \tag{16.70}$$

16.6 Numerical performances

The performance of the parabolic model, with the *narrow angle* approximation, is assessed below. Radiation from a point source over a rigid plane is taken as an example.

Problem statement

This basic case evaluates the pressure field radiated by a single source in a half-space bounded by a rigid plane surface (ground). The source is a monopole located 2 m above ground. It emits sound at frequencies between 30 and 1,000 Hz. The objective is to evaluate the pressure field in a domain of horizontal length L and height h. A reference cylindrical coordinate system (r,z) is selected (Figure 16.5). The total acoustic pressure field is the combination of the incident and scattered components. The incident field assumes free field propagation and can be expressed as:

$$p_{free} = S\frac{e^{(-ikR_1)}}{R_1} \tag{16.71}$$

where R_1 represents the distance between the source located at $(0,z_s)$ and the field point located at (r,z):

$$R_1 = \sqrt{r^2 + (z-z_s)^2} \tag{16.72}$$

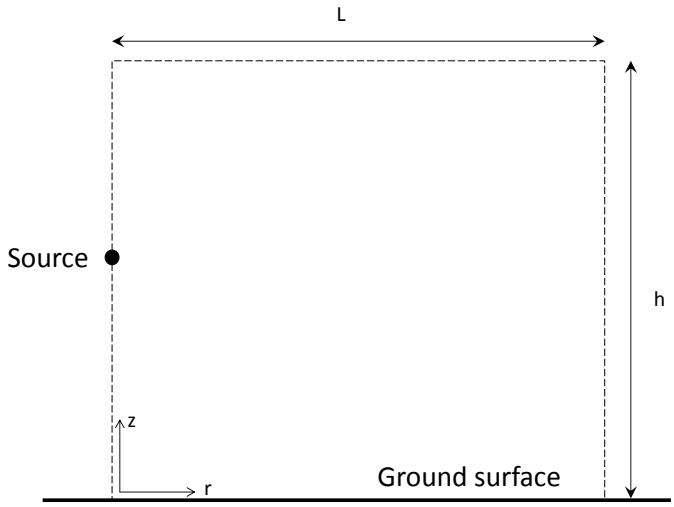

Figure 16.5: Single source radiating above a rigid plane surface.

while S is the source amplitude. The scattered (or reflected) pressure field (assuming a perfectly rigid ground) is given by:

$$p_{\text{reflected}} = QS\frac{e^{(-ikR_2)}}{R_2} \tag{16.73}$$

where R_2 is the distance between the image source located at $(0, -z_s)$ and the field point:

$$R_2 = \sqrt{r^2 + (z + z_s)^2} \tag{16.74}$$

while Q is the reflection coefficient which depends on the ground surface impedance. The total pressure at the field point located at (r, z) is therefore given by:

$$p_{\text{c}} = S\frac{e^{(-ikR_1)}}{R_1} + QS\frac{e^{(-ikR_2)}}{R_2} \tag{16.75}$$

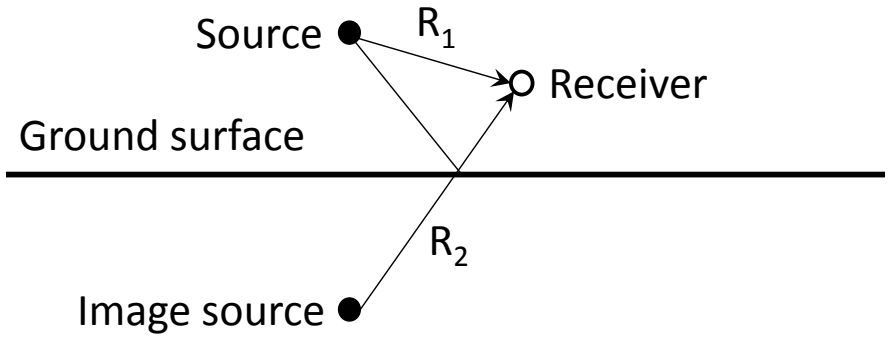

Figure 16.6: Decomposition of the total acoustic pressure into incident and scattered components.

Numerical results

The evaluation of the pressure field using the parabolic equation method requires the preliminary definition of a truncated domain. The upper part of this domain is covered by an absorbent layer. The discretisation process requires the selection of appropriate geometrical steps. In our example, the acoustic domain has length $L = 100$ m and height $h = 100$ m. Computations are made in the frequency range of 30 to 4,000 Hz. Discretisation along the vertical direction involves 1,000 points.[4]

The accuracy of the method can be highlighted by evaluating the response at four frequencies (100, 250, 500 and 1,000 Hz). Figures 16.7, 16.8 and 16.9 show the pressure field (logarithm of the magnitude of pressure) at these frequencies. These maps show the solution to be accurate at low elevation angles. However, for higher elevation angles, the solution is not accurate. This is confirmed by the comparison with exact pressure maps (Equation 16.75) shown in Figure 16.9 for a frequency of 500 Hz. The accuracy of the parabolic equation solution for points at low elevation angles with respect to the source is illustrated by Figures 16.10 and 16.11. The numerical solution (pressure) can be compared with the exact solution at 100, 250, 500 and 1,000 Hz for points located at the same height as the source. The parabolic equation

[4] **Salomons E. M.**, *Computational atmospheric acoustics*, Kluwer Academic Publishers, 2001.

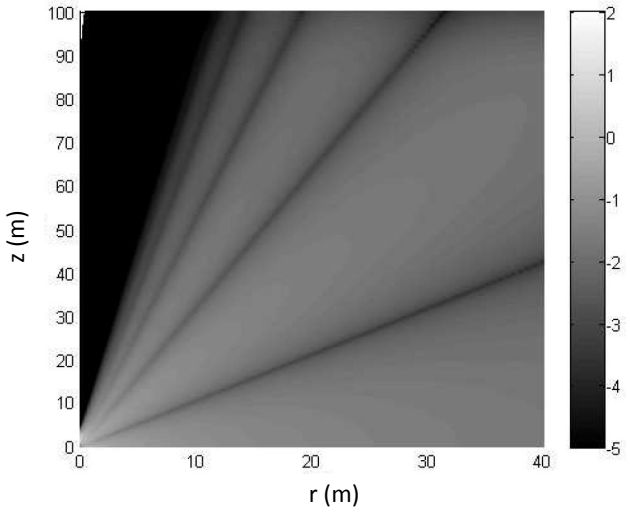

Figure 16.7: Map of pressure magnitude (log scale) at 100 Hz computed by the parabolic equation method for a source located at 2 m height above a rigid ground, domain size is [100 m $\times$ 100 m].

gives accurate results at these frequencies. The accuracy of the method is better at large radial distances from the source. This is consistent with the requirements of environmental applications where one is interested in the sound pressure at points far from the source and located at low elevation angles.

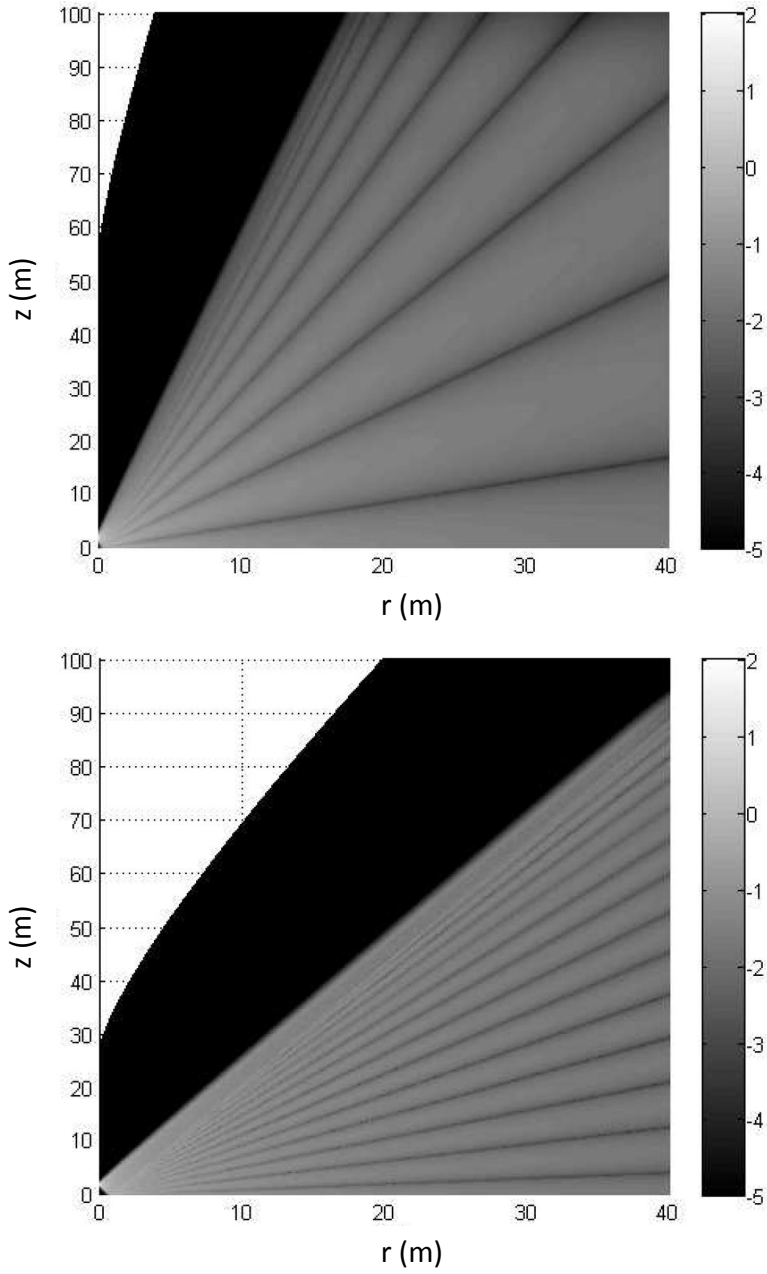

Figure 16.8: Pressure amplitude (log scale) at 250 Hz (top) and 1,000 Hz (bottom) computed by the parabolic method (radiation from a point source located 2 m above a rigid ground surface, acoustic domain = [100 m × 100 m]).

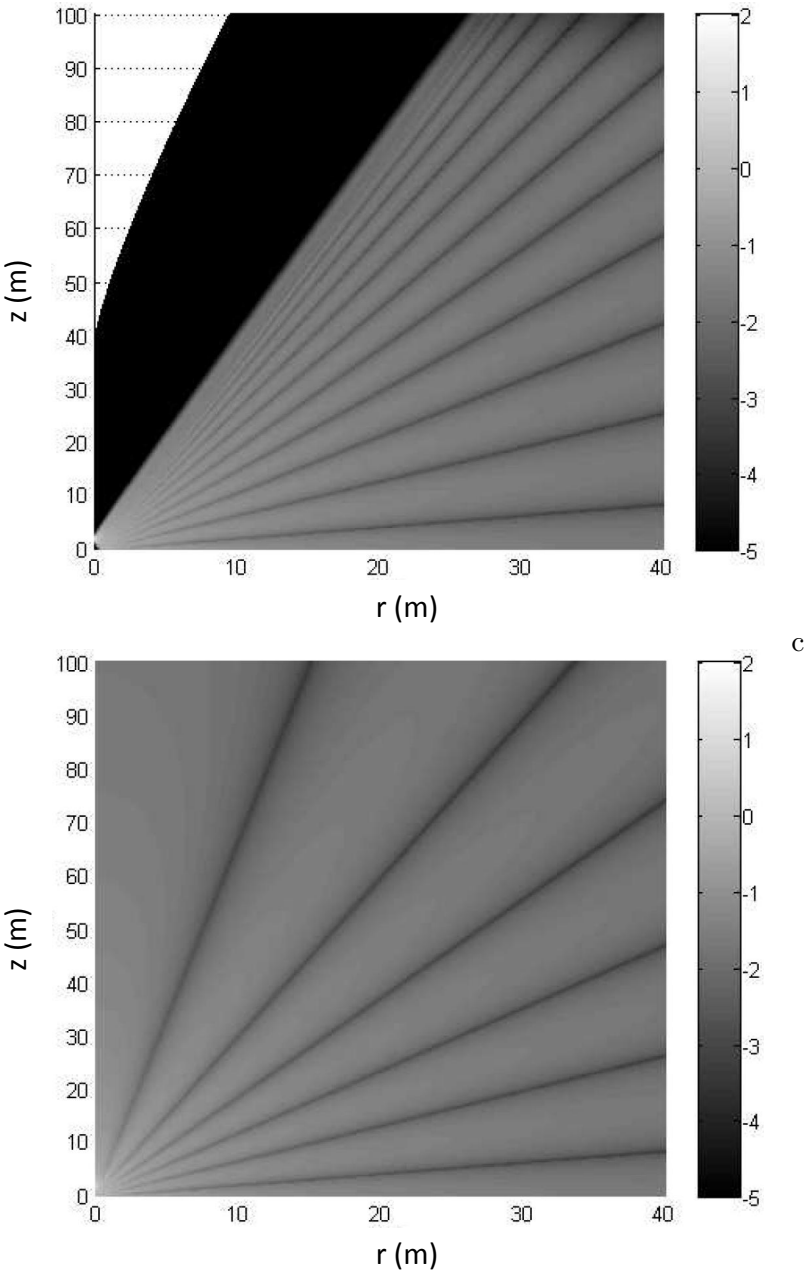

Figure 16.9: Pressure amplitude (log scale) at 500 Hz for the radiation from a point source located 2 m above a rigid ground surface (acoustic domain = [100 m × 100 m]): parabolic solution (top) and exact solution (bottom).

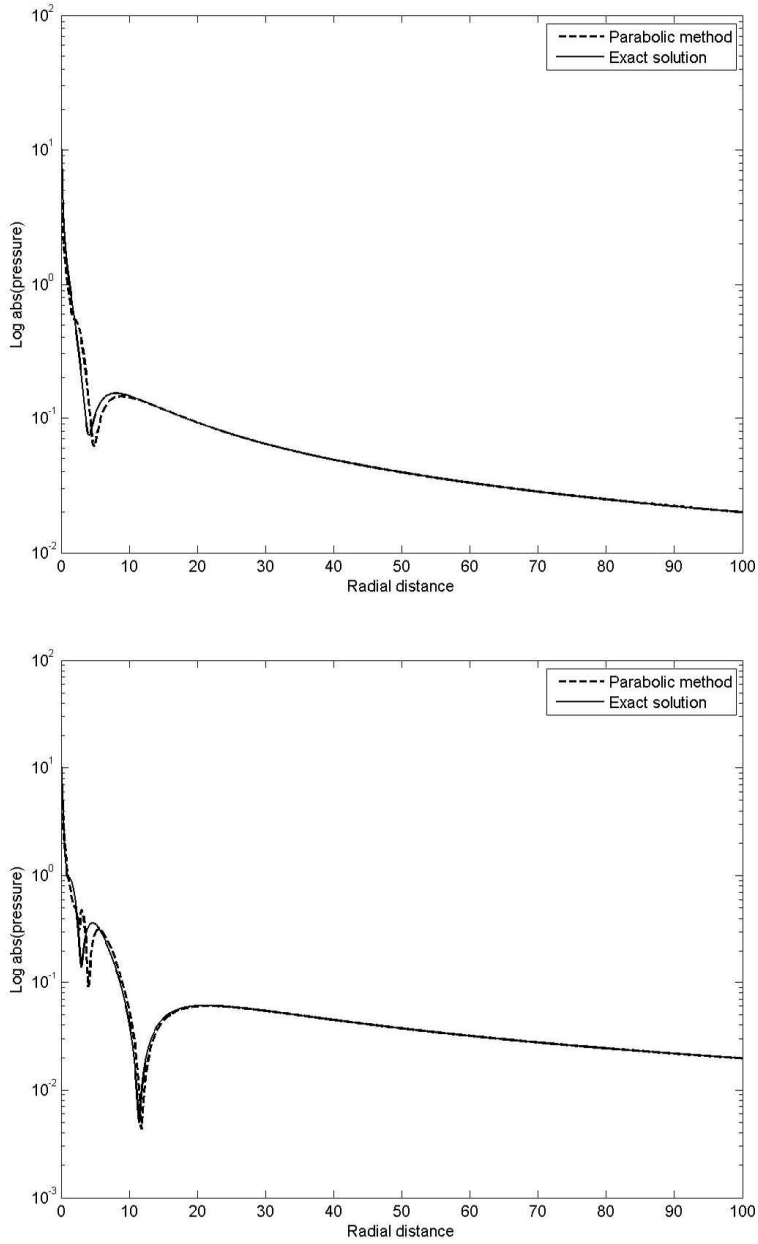

Figure 16.10: Comparison of pressures at $z = 2$ m computed by the parabolic method with the exact analytical solution at 100 Hz (top) and 250 Hz (bottom).

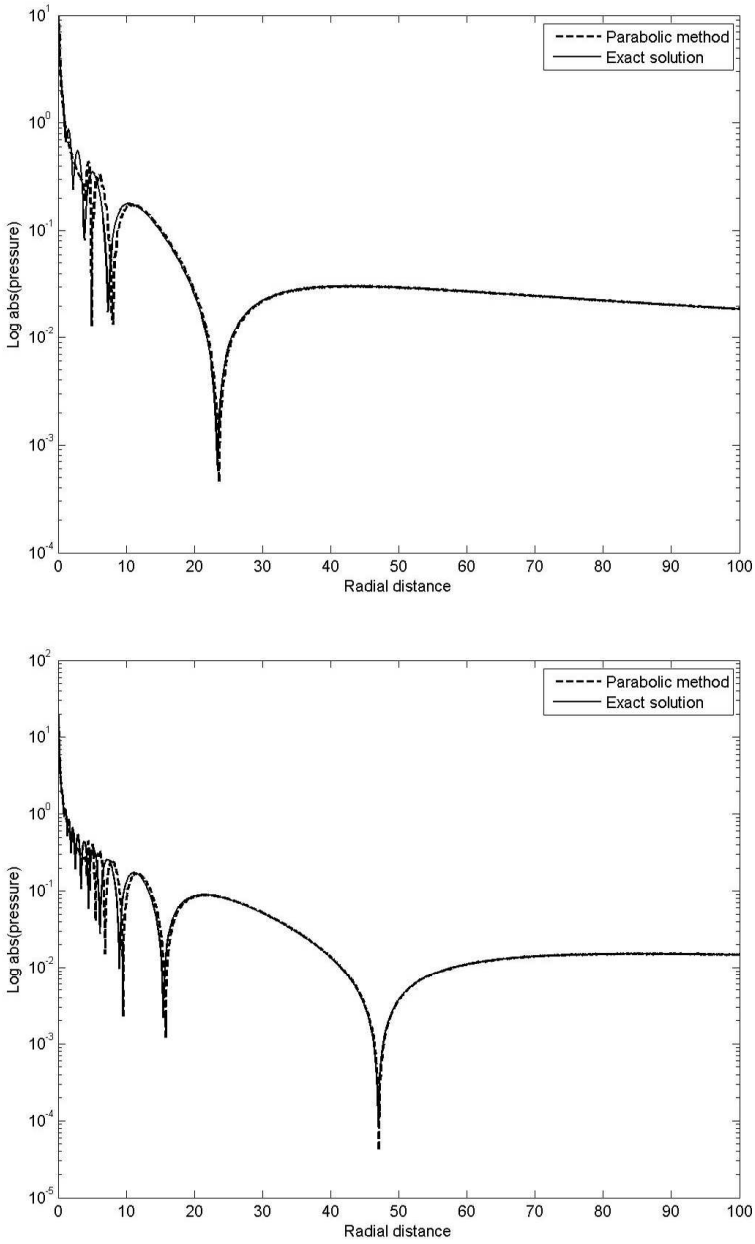

Figure 16.11: Comparison of pressures at $z = 2$ m computed by the parabolic method with the exact analytical solution at 500 Hz (top) and 1,000 Hz (bottom).

16.7 Conclusions

The propagation of acoustic perturbations in the atmosphere involves atmospheric absorption (very significant at high frequencies) as well as refraction induced by atmospheric heterogeneity (temperature gradients). The complexity of the velocity field (wind), the presence of turbulent structures, the absorption along the ground surface, the contours and the presence of obstacles (screens, buildings) impact the acoustic field radiated by the sources.

Since the acoustic waves propagate over large distances (ranging from a few meters to several kilometers), the use of conventional computational methods (finite elements, boundary elements) is inappropriate.

The parabolic method takes into account these physical specificities and proves more efficient than conventional models. This explains its widespread use in environmental acoustics.

17

Fluid-structure interaction

Contents

17.1 One-dimensional model 370
17.2 Matrix theory of fluid-structure interaction 379

A vibrating structure and the associated acoustic fluid form a coupled system. Both act and react on each other. In Chapter 11 we considered that vibrations were not influenced by the radiated sound field. A model where the reaction of the fluid on the structure can be neglected is called *weakly coupled* or assumes *one-way coupling*. In this chapter we now consider the case of *strong* or *two-way* coupling.

17.1 One-dimensional model

17.1.1 General case

Consider a piston connected to an acoustic component. The acoustic pressure on the piston is assumed to be uniform. The piston is characterised by its stiffness K, mass m, damping d and displacement u. An external force F is applied to the piston. The speed of the fluid particles in contact with the piston is $i\omega u$. If the acoustic component is characterised by an impedance Z_a, then the acoustic pressure on the piston is $i\omega Z_a u$. The dynamic equation of the mass spring system coupled to the acoustic component is:

$$Z_s u = F - Sp \tag{17.1}$$

with $Z_s = K + i\omega d - \omega^2 m$. Replacing p by its value and moving all terms involving the displacement u to the left hand side, we obtain the modified equation:

$$\left(Z_m + i\omega Z_a S\right) u = F \tag{17.2}$$

To ensure consistency of units (force over displacement) and sign convention (positive force has the opposite direction of positive pressure) we can define an impedance ζ_a which is the mechanical equivalent of Z_a:

$$\zeta_a = -i\omega Z_a S \tag{17.3}$$

With this notation, the dynamic equation of the piston becomes:

$$(Z_m - \zeta_a)\, u = F \tag{17.4}$$

If we define:

$$\mu = \frac{Z_m}{\zeta_a} \tag{17.5}$$

we find successively:

$$u = \frac{F}{Z_m - \zeta_a} = -\frac{F}{Z_m} \cdot \frac{\mu}{\mu - 1} \tag{17.6}$$

$$v = \frac{i\omega F}{Z_m - \zeta_a} = \frac{i\omega F}{Z_m} \cdot \frac{\mu}{\mu - 1} \tag{17.7}$$

$$p = -\frac{F}{S}\frac{\zeta_a}{Z_m - \zeta_a} = -\frac{F}{S} \cdot \frac{1}{1 - \mu} \tag{17.8}$$

The form involving the reduced impedance μ presents pressure, velocity and displacement of the coupled system as equal to their uncoupled counterparts multiplied by an amplification (or reduction) factor due to coupling. For pressure, this factor is:

$$\frac{p_c}{p_u} = \frac{1}{1 - \mu} \tag{17.9}$$

and for displacement and speed, it is:

$$\frac{u_c}{u_u} = \frac{v_c}{v_u} = \frac{\mu}{\mu - 1} \tag{17.10}$$

The indices u and c respectively refer to the uncoupled and coupled conditions. We can observe that:

- μ and the amplification factors are complex and frequency dependent;
- the coupled and uncoupled displacements (or velocities) are equal when $\mu = \infty$, that is when $\zeta_a = 0$;
- the coupled and uncoupled displacements (or velocities) have the same magnitude, but are opposite in phase when $\mu = \frac{1}{2}$ ($Z_m = 2\zeta_a$);
- the coupled and uncoupled pressures are equal when $\mu = 0$ ($Z_m = 0$). They have the same magnitude, but are opposite in phase when $\mu = 2$ ($Z_m = 2\zeta_a$).

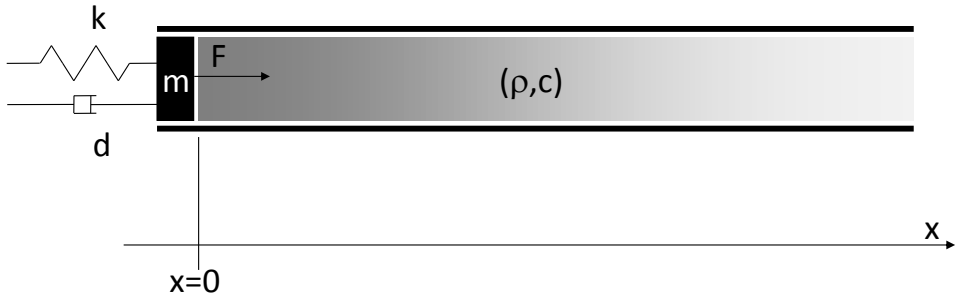

Figure 17.1: Mass-spring system coupled to an infinite fluid duct.

We also see that the coupled system is resonant when $Z_m = \zeta_a$ (impedance adaptation). The effect of the acoustic field on the dynamics of the piston results in an additional impedance (complex and frequency-dependent) $-\zeta_a$. The real part contributes to the piston stiffness ($\Re(\zeta_a) > 0$, added stiffness) or mass ($\Re(\zeta_a) < 0$, added mass) while the imaginary part contributes to its damping and represents the energy expended by the piston for generating and maintaining the acoustic field ($\Im(\zeta_a)$, added damping).

17.1.2 Tube of infinite length

Consider a mass-spring system coupled to an infinite duct filled with a fluid of density ρ and sound speed c. The acoustic impedance of the tube is:

$$Z_a = \rho c \rightarrow \zeta_a = -i\rho\omega cS \tag{17.11}$$

The dynamic equation is therefore:

$$(-\omega^2 m + i\omega(d + \rho cS) + K)U = F \tag{17.12}$$

The effect of the fluid column on the mass-spring system results in *added damping*. The energy dissipated in the equivalent damper is, quite logically,

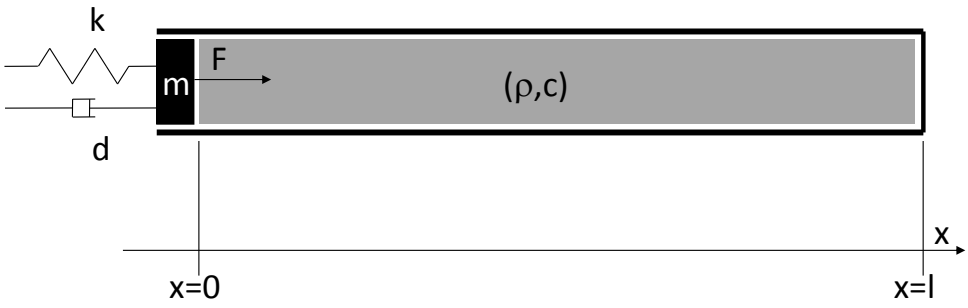

Figure 17.2: Mass-spring system coupled to a fluid duct of finite length.

equal to the energy propagated by the acoustic wave along the fluid column:

$$\begin{aligned} W_{damper} &= \frac{1}{2}\Re(F_{damper} \cdot v^*) \\ &= \frac{1}{2}\Re[(i\omega\rho cSU) \cdot (i\omega U)] = \frac{\rho cS\omega^2 U^2}{2} \end{aligned} \tag{17.13}$$

$$W_{rad} = I_a \cdot S = S \cdot \frac{|p|^2}{2\rho c} = \frac{\rho cS\omega^2 U^2}{2} \tag{17.14}$$

17.1.3 Tube of finite length

In the case of a duct of finite length ℓ, the impedance is (Equation 9.15):

$$Z(\omega, x=0) = -i\rho c\frac{\cos k\ell}{\sin k\ell} \rightarrow \zeta_a = -\rho c\omega S\frac{\cos k\ell}{\sin k\ell} \tag{17.15}$$

ζ_a is real and contributes to mass when it is negative, or to stiffness when it is positive. There is no added damping as the acoustic field in the tube is a standing wave: no active intensity is propagated and there is no loss by acoustic radiation. The energy transmitted by the mass to the fluid during a part of the cycle is transferred back from the fluid to the mass during another part of the cycle. The coupled system is resonant when $Z_m = \zeta_a$:

$$\left(K + i\omega d - \omega^2\right) = -\rho c\omega S\frac{\cos k\ell}{\sin k\ell} \tag{17.16}$$

or, successively:

$$K\left(1+2i\xi\frac{\omega}{\omega_0}-\left(\frac{\omega}{\omega_0}\right)^2\right)=-\frac{\rho c^2 S}{\ell}k\ell\cot k\ell \tag{17.17}$$

$$K\left(1+2i\xi\frac{\omega}{\omega_0}-\left(\frac{\omega}{\omega_0}\right)^2\right)=-\frac{\rho c^2 S}{\ell}k\ell\cot k\ell \tag{17.18}$$

$$\frac{K}{\frac{\rho c^2 S}{\ell}}\cdot\left(1+2i\xi\frac{\omega}{\omega_0}-\left(\frac{\omega}{\omega_0}\right)^2\right)=-k\ell\cot k\ell \tag{17.19}$$

where $\omega_0=\sqrt{\frac{k}{m}}$ is the uncoupled resonance frequency of the mass-spring system and $\xi=\frac{d}{2\sqrt{Km}}$ its damping factor. The first factor on the left hand side of Equation 17.19 is a measure of the relative stiffness of the spring and fluid column. The second term is the dynamic amplification of the uncoupled system. The resonances of the coupled mass-spring-tube system appear at the intersections of the curves representing the two sides of the above equation (Figure 17.3).

Consider the following set of parameters: $\rho = 1.225$ kg/m^3, $c = 340$ m/s, $\ell = 1$ m, $S = 1$ m^2, $d = 2\xi\sqrt{Km}$ with $\xi = 0.02$. K is chosen so that the resonance of the uncoupled mass spring system occurs at 300 Hz. A first case ($m = 1$) corresponds to a strong coupling because the mass of fluid in the tube (1.225 kg) is of the same order of magnitude as the mass connected to the spring. A second case ($m = 5$) corresponds to a weaker coupling. The dynamic response of the system can be analysed by looking at Figures 17.4 and 17.5. We can make the following observations:

1. The acoustic impedance is zero for $k\ell = \frac{\pi}{2} + n\pi$ when the tube is a quarter-wavelength resonator. At these frequencies, the mass spring system behaves as if there was no air, as the acoustic pressure acting on the piston (p_0) is zero. These points are indicated by the $\times$ mark in Figure 17.4.

2. There are two frequencies (black circles in Figure 17.4) where $Z_a = -2Z_m$ and $Z_a + Z_m = -Z_m$. At these frequencies, the dynamic response of the coupled and uncoupled systems have the same amplitude, but have a phase difference of 180°.

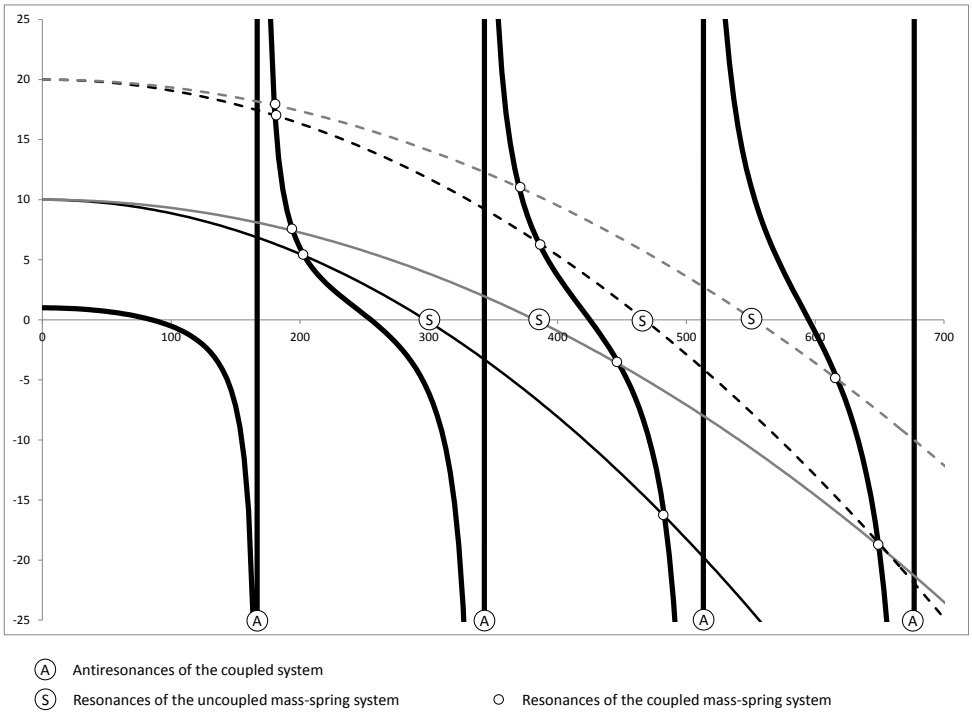

Figure 17.3: Analysis of the resonances of an undamped mass-spring system coupled to a tube. Different values of the relative stiffness $\frac{K\ell}{\rho c^2 S}$ and of the resonance frequency of the uncoupled system (ω_0) are considered. The resonances of the coupled system ($Z_m = \zeta_a$) are always preceded ($\omega < \omega_0$) or followed ($\omega > \omega_0$) by an anti-resonance ($\zeta_a = \infty$) where the fluid imposes an infinite resistance to the piston.

3. The system presents anti-resonances when $k\ell = n\pi$ (170, 340, 510, etc.). At these frequencies the acoustic impedance (and therefore the total impedance) becomes infinite: the faintest movement of the mass generates an infinite counter pressure. There is therefore neither movement ($U = 0$), nor pressure ($p = 0$). These points are represented by black diamonds in Figure 17.4.

4. The coupled system is resonant when the total impedance $Z_a + Z_m$ is zero. These points are represented by black squares in Figure 17.4. The second resonance (282Hz, grey square) corresponds to the resonance of the mass spring system, but appears at a lower frequency than that of the uncoupled case. The acoustic impedance is indeed negative around 300 Hz and acts as an *added mass* lowering the resonance frequency. This frequency shift is more important in the case of strong coupling ($m = 1$) than in weak coupling ($m = 5$).

5. The other resonances of the coupled system are of acoustic nature, but they do not occur when $Z_a = 0$, but rather when $Z_a = -Z_m$. At low frequency, Z_m is positive. Resonance occurs for large negative values of Z_a and is immediately *followed* by an anti-resonance ($Z_a = \infty$). At high frequency, Z_m is negative. Resonance occurs for large positive values of Z_a, immediately *preceded* by an anti-resonance ($Z_a = \infty$). The *acoustic* resonances of the coupled system therefore occur at frequencies which are close to the *anti-resonance* frequencies of the uncoupled acoustic system.

6. The resonance associated to the uncoupled resonance of the mass-spring system displays a single peak. Resonance-antiresonance pairs are observed for all other resonances.

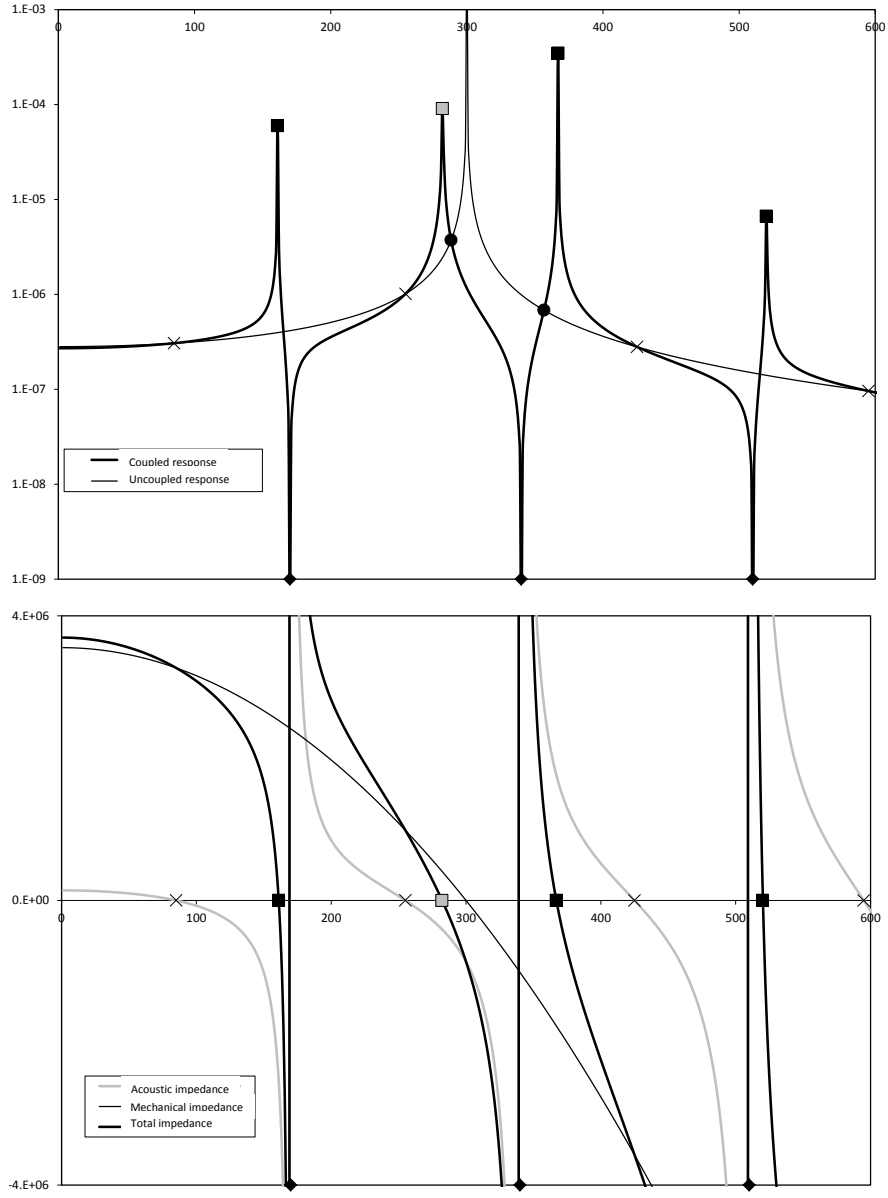

Figure 17.4: Upper graph: Dynamic response of a mass-spring system coupled to an air tube: strong coupling ($m = 1$ kg). The coupled response is a thick line, the uncoupled response a thin line. **Lower graph:** Impedances of the air duct (grey line), mechanical impedance (thin line) and total impedance (thick line).

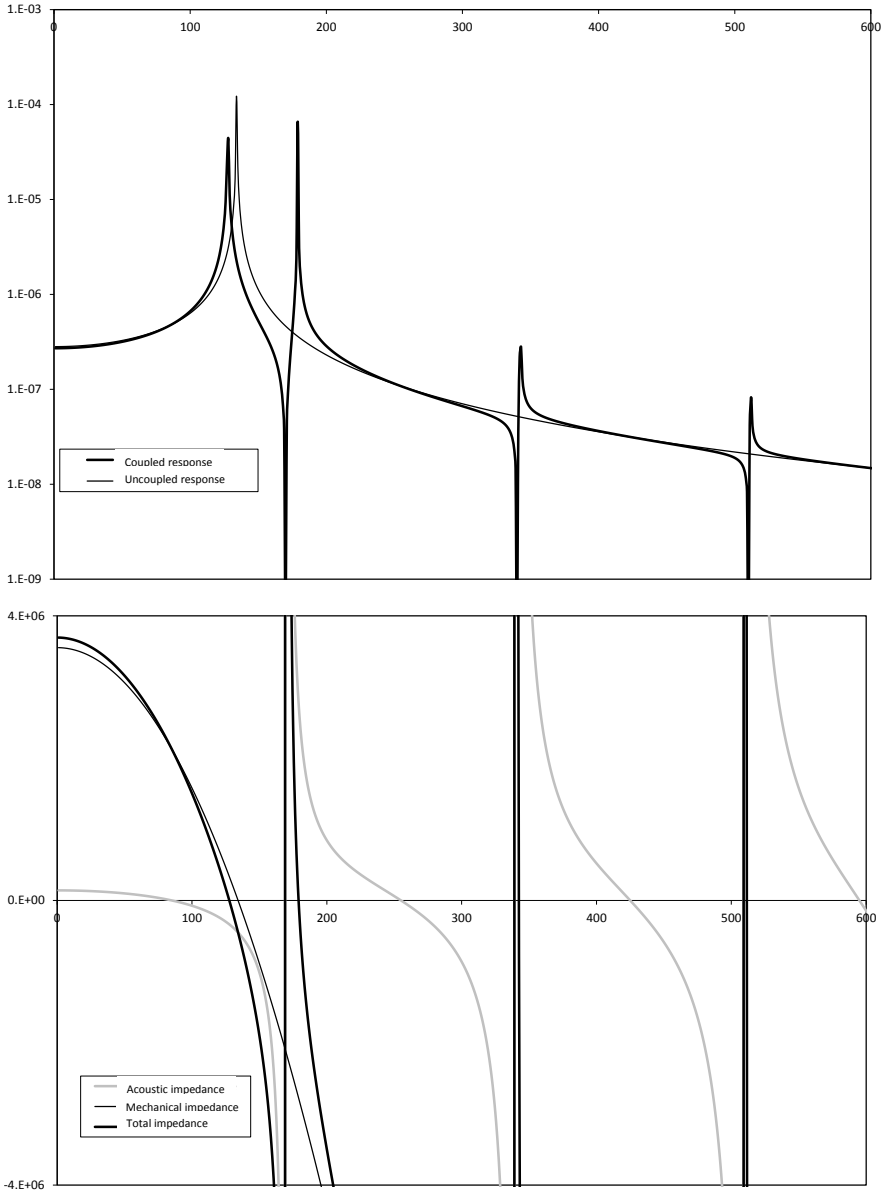

Figure 17.5: Upper graph: Dynamic response of a mass-spring system coupled to an air tube: weak coupling ($m = 5$ kg). The coupled response is a thick line, the uncoupled response a thin line. **Lower graph:** Impedances of the air duct (grey line), mechanical impedance (thin line) and total impedance (thick line).

17.2 Matrix theory of fluid-structure interaction

We now present a more general theory of fluid-structure interaction using the framework of finite element analysis. Consider the vibro-acoustic behaviour of a fluid domain F interacting with a structure S. The structure is modelled with finite elements and its harmonic dynamic behaviour is described by the system of equations:

$$\left[K_s + i\omega C_s - \omega^2 M_s\right](u) = (F_s) \tag{17.20}$$

where K_s is the stiffness matrix of the structure, M_s its mass matrix, C_s the damping matrix, u the vector of nodal displacements and F the force vector applied on the structure.

The acoustic domain is also modelled with finite elements and the pressure distribution is obtained by solving the following system of equations:

$$\left[K_f + i\omega C_f - \omega^2 M_f\right](p) = (F_f) \tag{17.21}$$

The vibrations of the structure and the acoustic pressure fields are interdependent. Indeed:

- The acoustic pressure excites the vibrations of the structure and a term F_s^p, proportional to p, must be added to the vector F_s:

$$(F_s^p) = -[C](p) \tag{17.22}$$

  The system of equations for the nodal displacements, taking into account the acoustic pressure loading, is therefore:

$$\left[K_s + i\omega C_s - \omega^2 M_s\right](u) = (F_s) - [C](p) \tag{17.23}$$

- The vibrations of the structure are the source of the acoustic field and the term F_f is proportional to vibration velocity:

$$(F_f^u) = -\rho\omega^2 [C]^t (u) \tag{17.24}$$

We therefore have the following system of equations for the acoustic field induced by a vibrating structure (assuming $F_f = 0$):

$$\left[K_f + i\omega C_f - \omega^2 M_f\right](p) = -\rho\omega^2 [C]^t (u) \tag{17.25}$$

In both expressions, C is a coupling matrix relating structural and acoustic variables.

The equations obtained for the structure and the fluid can be combined into a single system of equations:

$$\begin{bmatrix} K_s + i\omega C_s - \omega^2 M_s & C \\ \rho\omega^2 C^t & K_f + i\omega C_f - \omega^2 M_f \end{bmatrix} \begin{pmatrix} u \\ p \end{pmatrix} = \begin{pmatrix} F_s \\ 0 \end{pmatrix} \tag{17.26}$$

17.2.1 Weak and strong coupling

All vibro-acoustic systems are coupled. The structural vibrations create the sound field and the sound field excites the vibrations of the structure. When both effects are of equal importance, the coupling is said to be *strong*. In many cases (*weak coupling*) the effect of the acoustic field on the structure can be neglected. The weakly coupled system of equation is written as:

$$\begin{bmatrix} K_s + i\omega C_s - \omega^2 M_s & 0 \\ \rho\omega^2 C^t & K_f + i\omega C_f - \omega^2 M_f \end{bmatrix} \cdot \begin{pmatrix} u \\ p \end{pmatrix} = \begin{pmatrix} F_s \\ 0 \end{pmatrix} \tag{17.27}$$

and can be solved in two steps:

1. elimination of displacements by solving the first group of equations involving the structural degrees of freedom;
2. calculation of nodal pressures by inserting those displacements into the second group of equations.

The weak coupling approach applies when the structure is rigid and/or the fluid light. As an example, the vibrations of an engine block *are not* affected by the air surrounding the engine (rigid structure and light fluid). On the other hand, the vibrations of a ship hull *are* affected by the pressure field

in the surrounding water (flexible structure and heavy fluid). Similarly, a loudspeaker membrane is influenced by the mass of air that it moves (light fluid and light structure). In these two cases, coupling is *strong* and the coupled system of equations must be solved in a single step.

17.2.2 Modal approaches

The structural equations can be projected in the appropriate modal basis Φ_s:

$$\begin{bmatrix} [\Phi_s]^t [K_s + i\omega C_s - \omega^2 M_s] [\Phi_s] & [\Phi_s]^t [C] \\ \rho\omega^2 [C]^t [\Phi_s] & [K_f + i\omega C_f - \omega^2 M_f] \end{bmatrix} \cdot \begin{pmatrix} a_s \\ p \end{pmatrix} = \begin{pmatrix} [\Phi_s]^t F_s \\ 0 \end{pmatrix} \tag{17.28}$$

where a_s are the modal participation factors ($u = \Phi_s \cdot a_s$). If the fluid domain is bounded, the acoustic part can also be projected on its own modal basis Φ_f:

$$\begin{bmatrix} [\Phi_s]^t [K_s + i\omega C_s - \omega^2 M_s] [\Phi_s] & [\Phi_s]^t [C] [\Phi_f] \\ \rho\omega^2 [\Phi_f]^t [C]^t [\Phi_s] & [\Phi_f]^t [K_f + i\omega C_f - \omega^2 M_f] [\Phi_f] \end{bmatrix} \cdot \begin{pmatrix} a_s \\ a_f \end{pmatrix} = \begin{pmatrix} [\Phi_s]^t F_s \\ 0 \end{pmatrix} \tag{17.29}$$

where a_f are the acoustic modal participation factors ($p = \Phi_f \cdot a_f$).

17.2.3 Radiation impedance

Introducing the impedance matrices of the structure (Z_s) and fluid (Z_f), the coupled system of equations may be rewritten:

$$\begin{bmatrix} Z_s & C \\ \rho\omega^2 C^t & Z_f \end{bmatrix} \cdot \begin{pmatrix} u \\ p \end{pmatrix} = \begin{pmatrix} F_s \\ 0 \end{pmatrix} \tag{17.30}$$

The pressure can be eliminated by writing:

$$p = -\rho\omega^2 Z_f^{-1} C^t u \tag{17.31}$$

$$(Z_s - \rho\omega^2 C Z_f^{-1} C^t)u = F_s \tag{17.32}$$

or, defining $\zeta_f = \rho\omega^2 C Z_f^{-1} C^t$:

$$(Z_s - \zeta_f)u = F_s \tag{17.33}$$

ζ_f is called the radiation impedance matrix. It generalises the coefficient ζ_a used above (Equation 17.3). Its real part contributes to the mass and stiffness matrix ($K_s - \omega^2 M_s$). Note that the two effects (added mass and added stiffness) cannot be separated because a matrix is neither *positive* nor *negative*. The imaginary part of ζ_f contributes additional damping (radiative loss).

18

Transmission and insulation

Contents

18.1 Rigid plate on elastic mounts 386
18.2 Infinite flexible wall 390
18.3 Double walls 397
18.4 TL of finite plates 401
18.5 Transmission Loss measurement 403

This chapter describes how sound can be transmitted from one acoustic medium to another through an elastic partition and how sound is attenuated in the process. Attenuation is a measure of the acoustic insulation provided by the partition. It can be measured using various indicators:

- difference of sound level between two points situated on both sides of the partition;
- difference of sound energy in both media;
- *Transmission Loss*, which is the ratio of incident and transmitted power expressed in decibels.

Figure 18.1 shows how transmission loss varies with frequency. Different behaviors are observed in different frequency ranges:

1. At low frequency (zone 1) the insulation level mainly depends on wall stiffness. The transmission loss decreases with frequency until the first resonance frequency of the wall.
2. We then observe a zone (2) in which insulation is controlled by the successive resonances of the partition, the insulation is minimum at resonance and mainly varies with the amount of damping in the wall.
3. The *mass law* applies in the third zone: the insulation increases almost linearly with a slope of 6 dB/octave. The mass of the panel defines the insulation level.
4. Attenuation suddenly falls at the *coincidence frequency* (zone 4).
5. After coincidence (zone 5), insulation increases at a rate of 9 to 18 dB per octave, depending on the type of excitation.

The variation of transmission loss observed in zones 1 is well captured by the very simple model presented in Section 18.1 which assimilates the wall to a rigid plate mounted on elastic supports. A more advanced model is required to model the TL in zones 3, 4 and 5 where the compliance of the plate must be taken into account (a model involving a plate of infinite dimensions is presented in Section 18.2). Finally, a model accounting for the finite dimension of the plate is required to account for the complex variation of TL observed in zone 2 (Section 18.4).

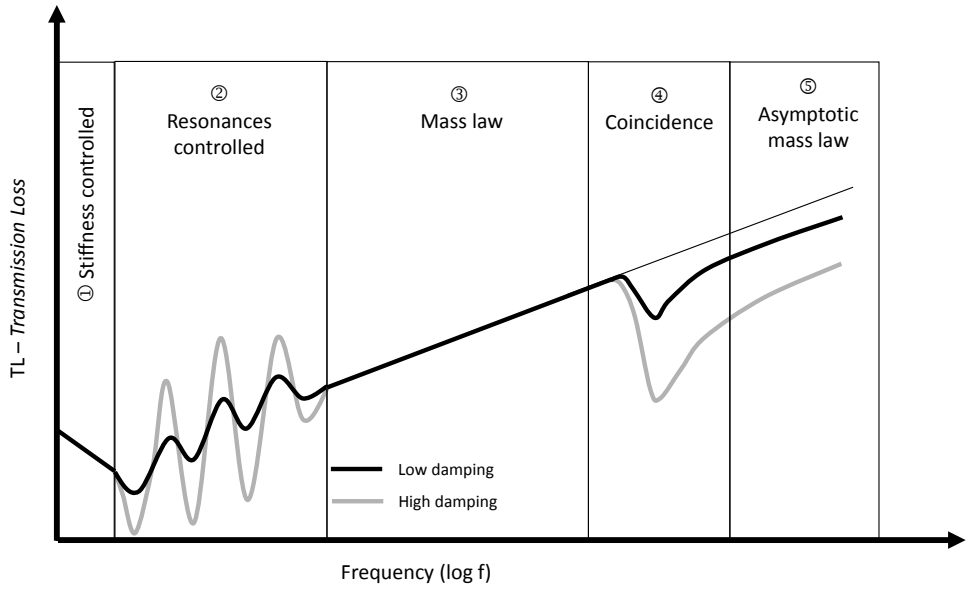

Figure 18.1: Typical acoustic insulation curves showing the different behaviors.

18.1 Rigid plate on elastic supports

Consider a stiff plate ($x = 0$) of mass m mounted on visco-elastic supports of stiffness k and damping d (Figure 18.2). The plate separates two media having respective impedances $Z_1 = \rho_1 c_1$ and $Z_2 = \rho_2 c_2$. An incident wave propagates in medium 1 along the x axis. The acoustic fields in media 1 and 2 are respectively:

$$p_1(x) = I(\omega)e^{-ik_1 x} + R(\omega)e^{ik_1 x} \tag{18.1}$$

$$p_2(x) = T(\omega)e^{-ik_2 x} \tag{18.2}$$

We call u_x the normal displacement of the plate. Velocity continuity at the wall imposes that:

$$\frac{I - R}{Z_1} = \frac{T}{Z_2} = i\omega u_x \tag{18.3}$$

from which we obtain:

$$R = I - i\omega Z_1 u_x \tag{18.4}$$

and

$$T = i\omega Z_2 u_x \tag{18.5}$$

The dynamic equation of the plate is:

$$(-\omega^2 m + i\omega d + k) \cdot u_x = F \tag{18.6}$$

where F is the force acting on the plate (net pressure exerted by the fluids multiplied by the area S of the plate):

$$F = (I + R - T) \cdot S = (I + (I - i\omega Z_1 u_x) - i\omega Z_2 u_x) \cdot S \tag{18.7}$$

The dynamic equation of the plate can therefore be written as:

$$(-\omega^2 m + i\omega(d + SZ_1 + SZ_2) + k) \cdot u_x = 2IS \tag{18.8}$$

As in Chapter 17, the dynamic equation of the coupled system is obtained by adding the acoustic impedance of the surrounding media to the mechanical impedance of the system. The structure is then loaded by the *blocked pressure* which is the pressure that would act on the plate if it was perfectly rigid and

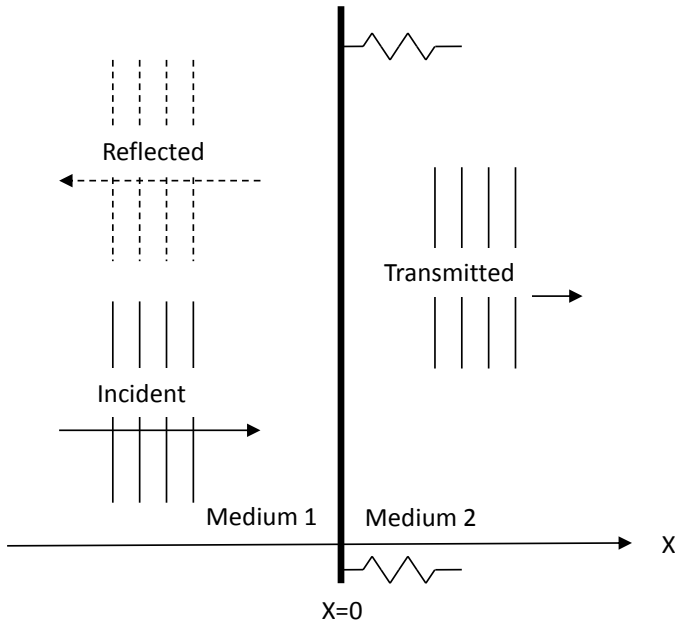

Figure 18.2: Rigid plate on elastic supports.

motionless. We obtain:

$$u_x = \frac{2IS}{-\omega^2 m + i\omega(d + SZ_1 + SZ_2) + k} \tag{18.9}$$

and

$$T = \frac{2i\omega ISZ_2}{-\omega^2 m + i\omega(d + SZ_1 + SZ_2) + k} \tag{18.10}$$

The transmission factor is defined as the ratio of transmitted to incident intensity:

$$\tau = \frac{\frac{|T(\omega)|^2}{2\rho_2 c_2}}{\frac{|I(\omega)|^2}{2\rho_1 c_1}} = \frac{4\omega^2 S^2 Z_1 Z_2}{k^2(1-\omega_r^2)^2 + \omega^2(d + SZ_1 + SZ_2)^2} \tag{18.11}$$

with:

$$\omega_r = \frac{\omega}{\omega_0} \tag{18.12}$$

and:

$$\omega_0 = \sqrt{\frac{k}{m}} \tag{18.13}$$

The transmission loss is defined as:

$$R = 10log\frac{1}{\tau} \tag{18.14}$$

Its variation with frequency is presented in Figure 18.3. At **low frequency**, where $\omega_r \ll 1$, we have $(1 - \omega_r^2) \simeq 1$ and $k \gg \omega(d + SZ_1 + SZ_2)$. We can then approximate the transmission factor in the following way:

$$\tau \simeq \frac{4\omega^2 S^2 Z_1 Z_2}{k^2} \tag{18.15}$$

At low frequency, the transmission loss is essentially determined by the stiffness coefficient k. It decreases at a rate of 6 dB/octave ($10 \log 2^2$).

At **high frequency**, the following approximations:

- $\omega_r >> 1$ and $(1 - \omega_r^2)^2 \simeq \omega_r^4$;
- $k^2\omega_r^4 = m^2\omega^4$

lead to a simplified expression for the transmission factor:

$$\tau \simeq \frac{4S^2 Z_1 Z_2}{m^2\omega^2} \tag{18.16}$$

At high frequency, the transmission loss is essentially defined by its mass and grows by 6 dB/octave.

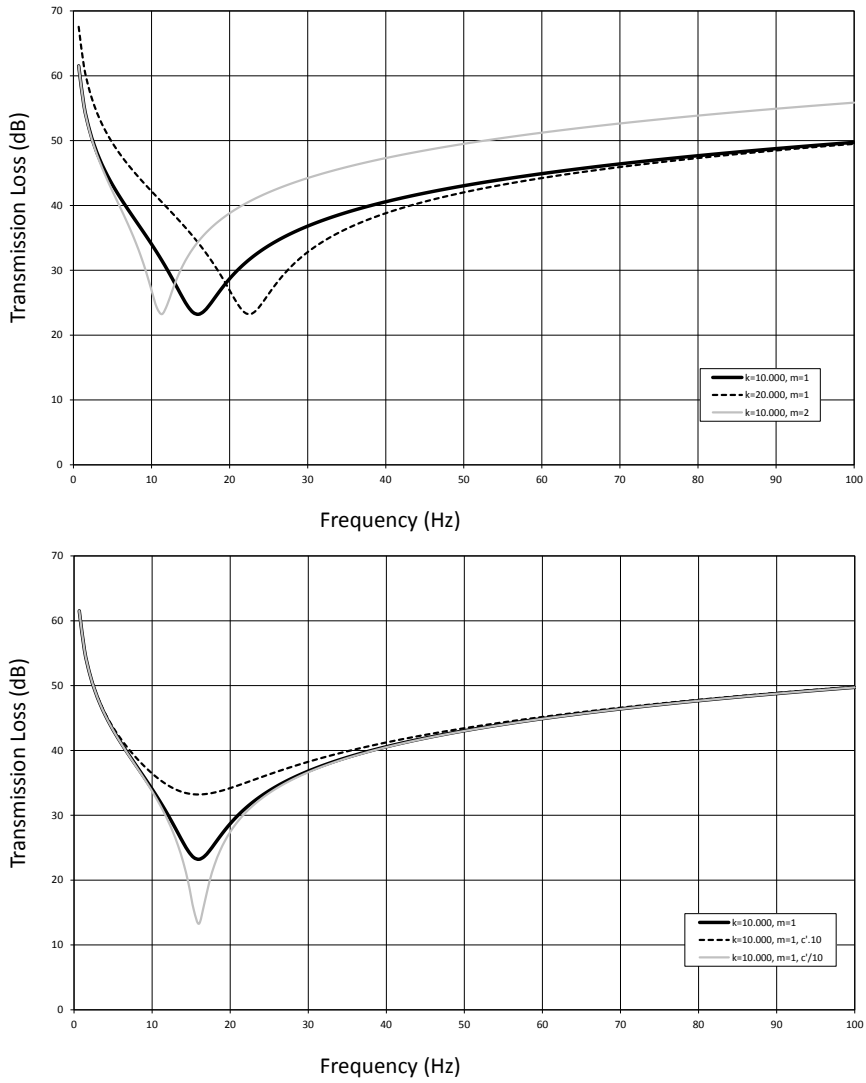

Figure 18.3: Transmission across a rigid plate mounted on elastic support. The **upper plot** shows the variation of the transmission loss with the stiffness of the supports and the mass of the wall. The two solid line curves use the same value for k and converge at low frequency. The two black curves have the same m value and converge at high frequency. The **lower plot** shows the effect of damping (very high and low damping values are used to highlight the effect).

18.2 Transmission across an infinite flexible wall

18.2.1 Attenuation evaluation

Consider a plane wave with incident angle of θ_1 exciting a thin plate ($y = 0$) of infinite extension separating two media (densities: ρ_1 and ρ_2; sound speeds: c_1 and c_2). The mechanical behavior of the plate is characterised by its bending stiffness D and its mass per unit area M defined by:

$$D = \frac{Eh^3}{12(1-\nu^2)} \tag{18.17}$$

$$M = \rho_s h \tag{18.18}$$

where E is the plate's Young modulus, ν its Poisson coefficient, ρ_s its density and h its thickness. The acoustic field in the emission medium is given by:

$$p_1 = I(\omega)e^{-ik_1(x\sin\theta_1 - y\cos\theta_1)} + R(\omega)e^{-ik_1(x\sin\theta_1 + y\cos\theta_1)} \tag{18.19}$$

while in the reception medium we find:

$$p_2 = T(\omega)e^{-ik_2(x\sin\theta_2 - y\cos\theta_2)} \tag{18.20}$$

This pressure load induces a vertical displacement u in the plate:

$$u(\omega, x) = U(\omega)e^{-i\kappa x} \tag{18.21}$$

where κ is the bending wave number in the plate. The projection of the different wave vectors on the $y = 0$ plane must be equal:

$$k_1 \sin\theta_1 = k_2 \sin\theta_2 = \kappa \tag{18.22}$$

The same condition can be expressed in terms of propagation speed:

$$\frac{c_1}{\sin\theta_1} = \frac{c_2}{\sin\theta_2} = c_b \tag{18.23}$$

where c_b is the speed at which the bending waves propagate in the plate. c_b is always equal or greater to the speed of sound in both media. The continuity of the normal velocities on the $y = 0$ plane provides the condition:

$$\frac{(I(\omega) - R(\omega))\cos\theta_1}{\rho_1 c_1} = \frac{T(\omega)\cos\theta_2}{\rho_2 c_2} = i\omega U(\omega) \tag{18.24}$$

from which we obtain:

$$R(\omega) = I(\omega) - \frac{i\rho_1 c_1 \omega U(\omega)}{\cos\theta_1} \tag{18.25}$$

$$T(\omega) = \frac{i\rho_2 c_2 \omega U(\omega)}{\cos\theta_2} \tag{18.26}$$

The dynamic equation of the plate is:

$$D\nabla^4 u - \omega^2 M u = (I(\omega) + R(\omega) - T(\omega))e^{-i\kappa x} \tag{18.27}$$

or, substituting u, $R(\omega)$ and $T(\omega)$ by their values:

$$(D\kappa^4 - \omega^2 M + \frac{i\rho_2 c_2 \omega}{\cos\theta_2} + \frac{i\rho_1 c_1 \omega}{\cos\theta_1}) \cdot U(\omega) = 2I(\omega) \tag{18.28}$$

which gives:

$$U(\omega) = \frac{2I(\omega)}{D\kappa^4 - \omega^2 M + \frac{i\rho_2 c_2 \omega}{\cos\theta_2} + \frac{i\rho_1 c_1 \omega}{\cos\theta_1}} \tag{18.29}$$

and

$$T(\omega) = \frac{i\rho_2 c_2 \omega}{\cos\theta_2} \frac{2I(\omega)}{D\kappa^4 - \omega^2 M + \frac{i\rho_2 c_2 \omega}{\cos\theta_2} + \frac{i\rho_1 c_1 \omega}{\cos\theta_1}} \tag{18.30}$$

The transmission factor is given by:

$$\tau = \frac{|T(\omega)|^2 \rho_1 c_1}{|I(\omega)|^2 \rho_2 c_2} \tag{18.31}$$

and the transmission loss by:

$$R = 10 \log \frac{1}{\tau} \tag{18.32}$$

If we consider the most common case, where the same fluid is found on both sides of the plate, we find:

$$\frac{T(\omega)}{I(\omega)} = \frac{1}{1 + \frac{\cos\theta}{2i\rho c\omega}(D\kappa^4 - \omega^2 M)} \tag{18.33}$$

or, in decibels:

$$R = 10\log\left[1 + \left[\frac{\cos\theta}{2\rho c\omega}\left(D\kappa^4 - \omega^2 M\right)\right]^2\right] \tag{18.34}$$

The attenuation is given in Figure 18.4 for various angles of incidence. We observe:

1. The attenuation is zero at the coincidence frequency.

2. At low frequency (before coincidence), the mass term $\omega^2 M$ dominates and the attenuation can be approximated by:

$$R \simeq 20\log\frac{\omega M\cos\theta}{2\rho c} \tag{18.35}$$

   The attenuation grows almost linearly at a rate of 6 dB/octave.

3. At high frequency (after coincidence) the impedance of the plate is dominated by the stiffness term $D\kappa^4$ and we find:

$$R \simeq 20\log\frac{D\omega^3\sin^4\theta\cos\theta}{2\rho c^5} \tag{18.36}$$

   The post-coincidence attenuation grows at a rate of 18 dB/octave (Figure 18.4).

18.2.2 Coincidence frequency

We also observe that the attenuation coefficient is zero (in the absence of damping i.e. for D real) when the mechanical impedance of the plate is zero:

$$D\kappa^4 - \omega^2 M = 0 \tag{18.37}$$

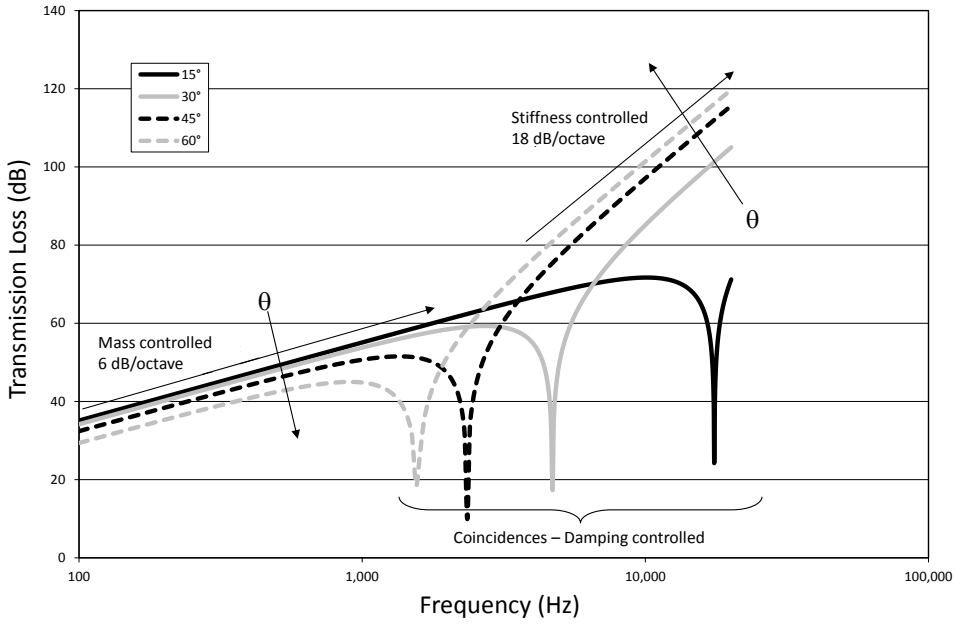

Figure 18.4: Variation of the transmission loss with the angle of incidence.

which happens when:

$$c_b = \sqrt{\omega \sqrt{\frac{D}{M}}} \tag{18.38}$$

that is when the bending waves in the plate propagate at their free propagation speed. Since:

$$c_b = \frac{c}{\sin\theta} \tag{18.39}$$

this is only possible, at a given pulsation ω, for an angle of incidence θ_c called the *coincidence angle* and given by:

$$\sin\theta_c = \frac{c}{\sqrt{\omega \sqrt{\frac{D}{M}}}} \tag{18.40}$$

Conversely, for any angle of incidence θ there is a *coincidence frequency* f_c given by:

$$f_c = \frac{1}{2\pi} \frac{c^2}{\sin^2\theta} \sqrt{\frac{M}{D}} \tag{18.41}$$

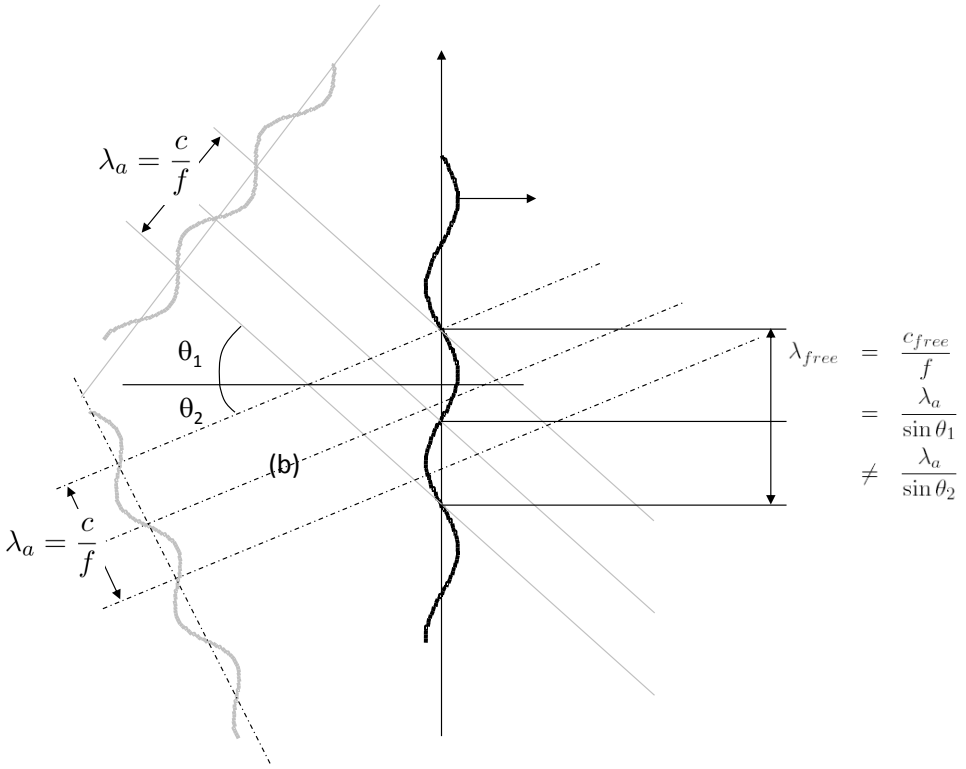

Figure 18.5: Coincidence phenomenon.

or:

$$f_c = \frac{1}{2\pi h}\frac{c^2}{\sin^2\theta}\sqrt{\frac{12\rho_s(1-\nu^2)}{E}} \tag{18.42}$$

Two remarks:

- In practice, damping prevents the attenuation from reaching zero at the coincidence frequency.
- The smallest coincidence frequency is called the critical frequency. It corresponds to an angle of incidence of 90° (grazing incidence):

$$f_c = \frac{c^2}{2\pi h}\sqrt{\frac{12\rho_s(1-\nu^2)}{E}} \tag{18.43}$$

We can present coincidence in the following way:

1. The acoustic field is the source of the vibrations of the plate.
2. The bending wavelength is equal to the distance between two successive acoustic wave fronts on the plate:

$$\lambda_{acousticprojected} = \frac{c}{f\sin\theta} = \lambda_{bending} = \frac{c_{flexion}}{f} \tag{18.44}$$

3. The bending wave speed is also set by the acoustic field:

$$c_{bending} = \frac{c}{\sin\theta} \tag{18.45}$$

4. But bending waves have a privileged propagation speed called free propagation speed. When we hit a plate with a hammer, bending waves are set in motion, starting from the impact point. These waves propagate at their free speed:

$$c_{free\ bending} = \sqrt{\omega\sqrt{\frac{D}{M}}} \tag{18.46}$$

   The propagation of free bending waves does not require energy.

5. If the propagation velocity imposed by the acoustic field is equal to the free speed, **the plate opposes no resistance**. The acoustic field does

not spend energy to vibrate the plate. There is no attenuation and transmission is complete.

18.2.3 Diffuse attenuation

A panel is seldom excited by a single plane wave of fixed incidence. The incident field usually contains a multitude of plane waves of different incidence. Consider a diffuse sound field where all incidence angles have the same likelihood. The transmission coefficient τ_d under diffuse excitation is obtained by summing the contributions of all directions to the incident and transmitted power:

$$\tau_d = \frac{\int_0^{2\pi}\int_0^{\frac{\pi}{2}} \tau(\theta) I \cos\theta \sin\theta d\theta d\phi}{\int_0^{2\pi}\int_0^{\pi} I \cos\theta \sin\theta d\theta d\phi} = \int_0^{\frac{\pi}{2}} \tau(\theta) \sin 2\theta d\theta \tag{18.47}$$

The $\cos\theta$ factor converts intensity into normal intensity while the $\sin\theta$ factor results from the expression of the surface element in spherical coordinates. The variation of τ_d with θ is shown in Figure 18.6. We observe:

1. Attenuation is lower for diffuse excitation than for fixed incidence (except around the coincidence frequency).

2. All but the lowest coincidence frequencies disappear under diffuse excitation. The critical frequency is the coincidence frequency at grazing incidence ($\theta = 90°$).

3. After the critical frequency, the transmission loss grows by 9 dB/octave vs. 18 dB/octave for fixed incidence sources.

Two asymptotic approximations can be obtained. At low frequency we have:

$$R_d = R_0 - 10\log\left[0.23 R_0\right] \tag{18.48}$$

where R_d is the diffuse attenuation and R_0 the normal incidence attenuation. Beyond the critical frequency, we have:

$$R_d = R_0 + 10\log\frac{\omega}{\omega_c} + 10\log\frac{2\eta}{\pi} \tag{18.49}$$

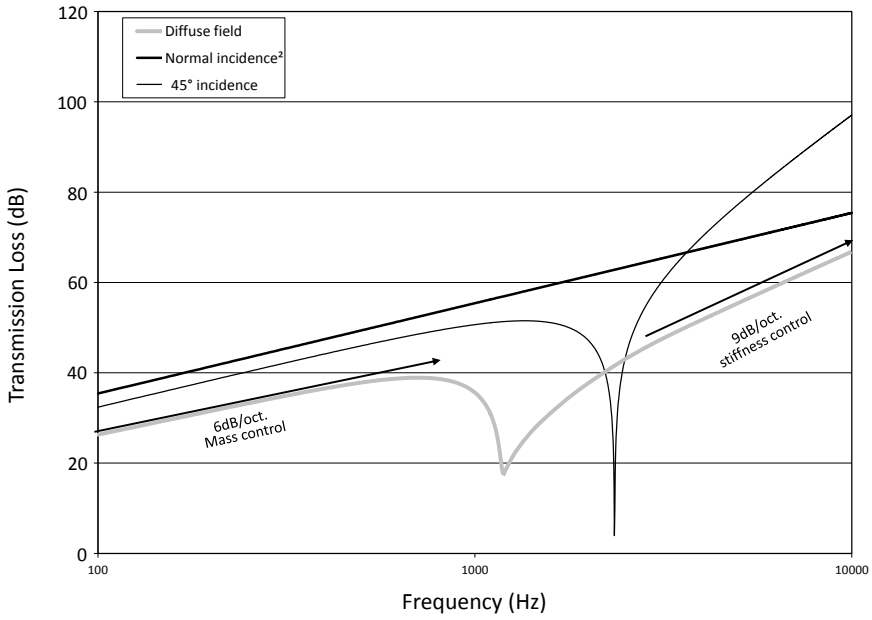

Figure 18.6: Variation of the transmission loss with frequency: diffuse excitation case. The TL for 0° and 45° incidence angles are given as reference.

where η is the loss factor of the plate bending stiffness D. This expression is consistent with the 9 dB/octave growth ($20\log 2 + 10\log 2$) seen above the critical frequency.

18.3 Double walls

18.3.1 Mass-air-mass resonance

We can analyse a double wall as a system of two masses (the walls) connected by a spring (the air layer). The stiffness associated to the air is:

$$k = \frac{\rho_a c^2}{h} \tag{18.50}$$

where ρ_a is the air density, c the speed of sound and h the thickness of the air layer. In the absence of any excitation, the movement of both masses is described by the system:

$$\begin{aligned} -\omega^2 m_1 u_1 + k\,(u_1 - u_2) &= 0 \\ -\omega^2 m_2 u_2 + k\,(u_2 - u_1) &= 0 \end{aligned} \tag{18.51}$$

The determinant of this system is:

$$\Delta = \omega^4 - \omega^2 k\,(m_1 + m_2) \tag{18.52}$$

The dynamic equations have non trivial solutions only when $\Delta = 0$ i.e. when:

$$\omega = \omega_r = \sqrt{k\left(\frac{1}{m_1} + \frac{1}{m_2}\right)} = c\sqrt{\frac{\rho_a}{\rho_v h}\left(\frac{1}{h_1} + \frac{1}{h_2}\right)} \tag{18.53}$$

In the last expression ρ_v, h_1 and h_2 are respectively the density and thicknesses of the walls.

18.3.2 Transmission Loss of double walls

Consider two infinite flexible plates located at $y = 0$ and $y = -\delta$ (Figure 18.7). The plates have bending stiffness and mass per unit area D_a, M_a, D_b and M_b. The same fluid ($Z_1 = \rho_1 c_1$) fills domains 1 ($y > 0$) and 3 ($y < -\delta$). Domain 2 ($0 > y > -\delta$) contains a different fluid ($Z_2 = \rho_2 c_2$). Knowing that the projection of all wave vectors (acoustic and dynamic) on the x axis are equal to κ, the acoustic fields in the three domains and the vertical displacements of both plates can be written as follows:

$$p_1 = Ie^{-i\kappa x + ik_{y1}y} + Re^{-i\kappa x - ik_{y1}y} \tag{18.54}$$

$$v_1 = -\frac{I}{\tilde{Z}_1}e^{-i\kappa x + ik_{y1}y} + \frac{R}{\tilde{Z}_1}e^{-i\kappa x - ik_{y1}y} \tag{18.55}$$

$$p_2 = Ae^{-i\kappa x + ik_{y1}y} + Be^{-i\kappa x - ik_{y1}y} \tag{18.56}$$

$$v_2 = -\frac{A}{\tilde{Z}_2}e^{-i\kappa x + ik_{y2}y} + \frac{B}{\tilde{Z}_2}e^{-i\kappa x - ik_{y2}y} \tag{18.57}$$

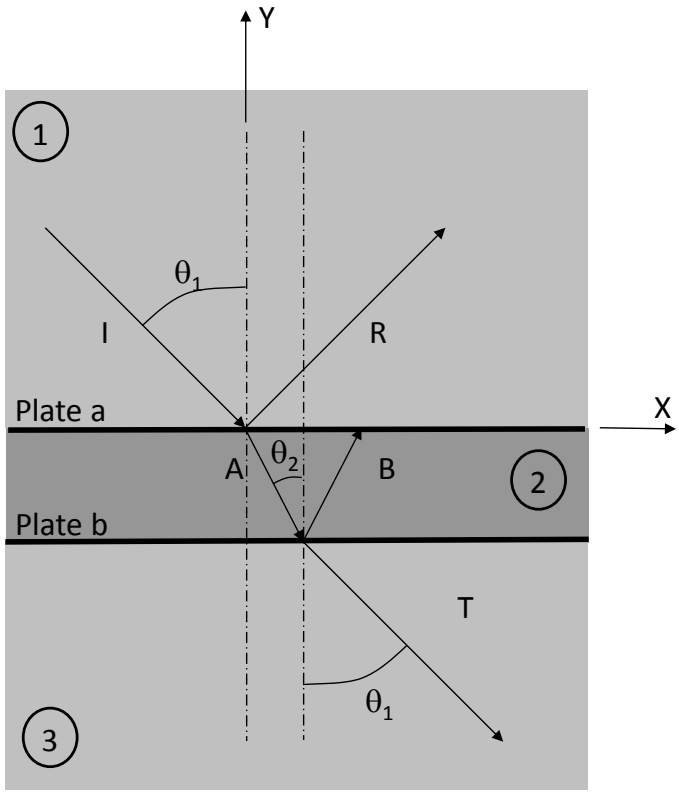

Figure 18.7: Transmission across a double wall.

$$p_3 = Te^{-i\kappa x + ik_{y1}y} \tag{18.58}$$

$$v_3 = -\frac{T}{\tilde{Z}_1}e^{-i\kappa x + ik_{y1}y} \tag{18.59}$$

$$u_a = U_a e^{-i\kappa x} \tag{18.60}$$

$$u_b = U_b e^{-i\kappa x} \tag{18.61}$$

with:

$$\kappa = k_1 \sin\theta_1 = k_2 \sin\theta_2 \tag{18.62}$$

$$k_{y1} = k_1 \cos\theta_1 \tag{18.63}$$

$$k_{y2} = k_2 \cos\theta_2 \tag{18.64}$$

$$\tilde{Z}_1 = \frac{Z_1}{\cos\theta_1} \tag{18.65}$$

$$\tilde{Z}_2 = \frac{Z_1}{\cos\theta_2} \tag{18.66}$$

Six equations relate the six variables:

- the speed continuity condition at $y = 0$:

$$\frac{(R-I)\cos\theta_1}{Z_1} = \frac{(B-A)\cos\theta_2}{Z_2} = i\omega U_a \tag{18.67}$$

  which provides two conditions:

$$R - i\omega\tilde{Z}_1 U_a = I \tag{18.68}$$

$$-A + B - i\omega\tilde{Z}_2 U_a = 0 \tag{18.69}$$

- the speed continuity condition at $y = -\delta$:

$$\frac{-Ae^{-ik_{y2}\delta} + Be^{ik_{y2}\delta}}{\tilde{Z}_2} = -\frac{Te^{-ik_{y1}\delta}}{\tilde{Z}_1} = i\omega U_b \tag{18.70}$$

  which provides two additional conditions:

$$-e^{-ik_{y2}\delta}A + e^{ik_{y2}\delta}B - i\omega\tilde{Z}_2 U_b = 0 \tag{18.71}$$

$$e^{-ik_{y1}\delta}T - i\omega\tilde{Z}_1 U_b = 0 \tag{18.72}$$

- the dynamic equation of the first plate (a):

$$\left(D_a\kappa^4 - \omega^2 M_a\right) U_a = (I + R - A - B) \tag{18.73}$$

  or:

$$-R + A + B + \left(D_a\kappa^4 - \omega^2 M_a\right) U_a = I \tag{18.74}$$

- the dynamic equation of the second plate (b):

$$\left(D_b\kappa^4 - \omega^2 M_b\right) U_b = Ae^{-ik_{y2}\delta} + Be^{ik_{y2}\delta} - Te^{-ik_{y1}\delta} \tag{18.75}$$

  or:

$$-Ae^{-ik_{y2}\delta} - Be^{ik_{y2}\delta} + Te^{-ik_{y1}\delta} + \left(D_b\kappa^4 - \omega^2 M_b\right) U_b = 0 \tag{18.76}$$

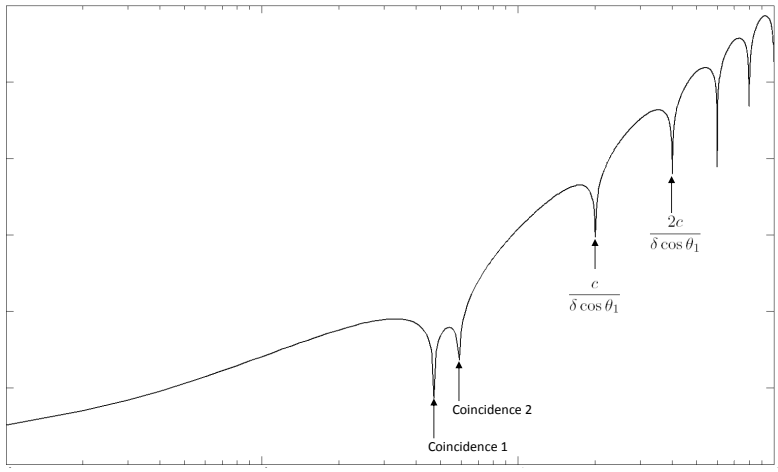

Figure 18.8: Typical variation of transmission loss through a double wall.

Solving this system gives R, A, B, T, U_a and U_b, from which the transmission factor τ and transmission loss R can be obtained (Figure 18.8):

$$\tau = \frac{|T(\omega)|^2}{|I(\omega)|^2} \Rightarrow R = 10 \log \frac{1}{\tau} \tag{18.77}$$

18.4 Transmission across a plate of finite extension

Consider a flat plate of thickness t inserted into a rigid infinite baffle (Figure 18.9). The baffle-plate system separates two fluid domains (1 and 2) which may have different properties. The plate is excited by an incident acoustic field. The dynamics of the plate follow the Kirchhoff plate model (rotational inertia and shear stresses are neglected). The dynamic equation of the plate is:

$$\left(-\rho_s t\omega^2 + D\omega^4\right) w(x,y) = p_2(x,y.0) - p_1(x,y.0) \tag{18.78}$$

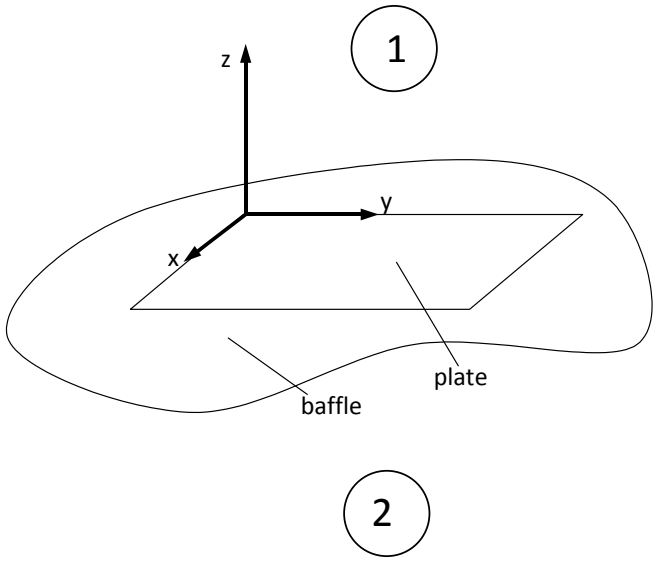

Figure 18.9: Acoustic transparency of plates of finite dimension.

where D is the bending stiffness of the plate:

$$D = \frac{Eh^3}{12(1-\nu^2)} \tag{18.79}$$

where E is its Young modulus, ν its Poisson coefficient, ρ_s its density and h its thickness. The excitation acting on the plate is the difference in sound pressure between both sides. In medium 1, the pressure is the sum of three terms: the incident pressure, the reflected pressure and the pressure radiated by the vibrations of the plate. The latter is obtained by a Rayleigh integral (Section 11.3.4):

$$p_1(x,y,z) = -p_i - p_r - 2\rho_{f1}\omega^2 \int_0^a \int_0^b w(x',y')G(x,y,z,x',y'.0)dx'dy' \tag{18.80}$$

In medium 2, the acoustic field only results from the plate vibration:

$$p_2(x,y,z) = 2\rho_{f2}\omega^2 \int_0^a \int_0^b w(x',y')G(x,y,z,x',y'.0)dx'dy' \tag{18.81}$$

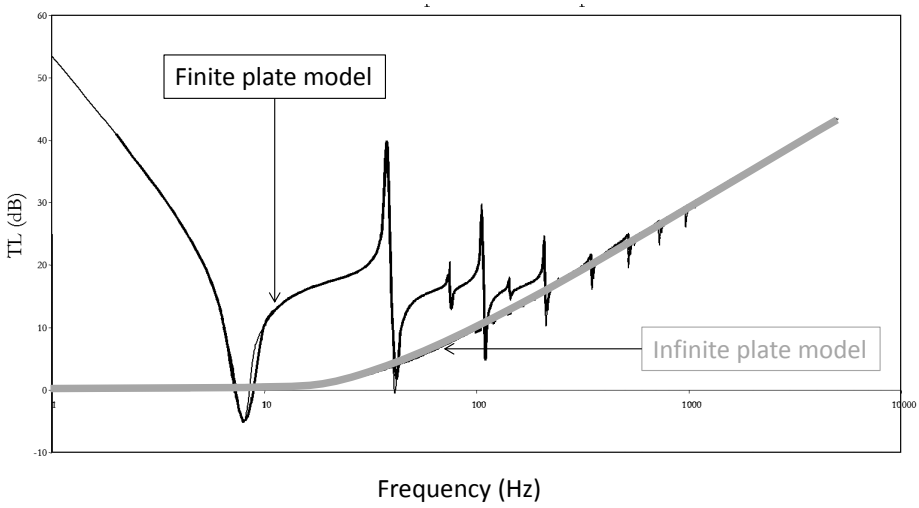

Figure 18.10: Attenuation calculated with the finite and infinite plate model.

The dynamic equation of the coupled system is therefore:

$$\begin{aligned} &\left(-\rho_s t\omega^2 + D\omega^4\right) w(x,y) \\ +2\left(\rho_{f1} - \rho_{f2}\right)\omega^2 &\int_0^a \int_0^b w(x',y') G(x,y,z,x',y'.0) dx' dy' \\ &= p_i(x,y.0) + p_r(x,y.0) \end{aligned} \tag{18.82}$$

This model may be used to accurately calculate the sound attenuation across a finite plate (Figure 18.10).

18.5 Transmission Loss measurement

18.5.1 Overview of the measurement methodology

The measurement of transmission loss is seldom made by actually measuring the incident and transmitted powers (Figure 18.11), but rather by compar-

ing the average sound levels measured in two acoustic rooms separated by the panel (Figure 18.12 and Figure 18.13). A source emits pink noise (Section 7.3.2) in one of the rooms and the average sound levels are measured in both rooms. The attenuation index R is the level difference between the rooms. A correction term that depends on the surface S of the tested element as well as on the volume V and reverberation time T_R of the reception room is added:

$$R = L_{emission} - L_{reception} + 10 \log \frac{S \cdot T_R}{0.16 \cdot V} \tag{18.83}$$

In many cases small samples are studied using *small cabins* (Figure 18.14).

18.5.2 Transmission Loss of realistic partitions

Figure 18.15 shows the transmission loss curve of a double wall typically used in construction. The mass-air-mass resonance, the mass law, coincidence frequency and post-coincidence growth are clearly seen. The individual resonances at low frequency do not appear because measurements are presented in octave bands.

Figure 18.11: Measurement of the intensity transmitted through a window.

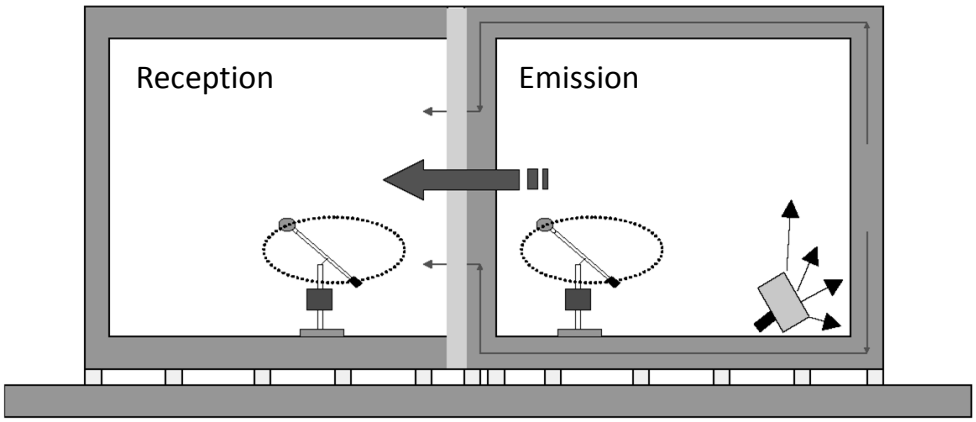

Figure 18.12: Schematic set-up for the measurement of transmission loss.

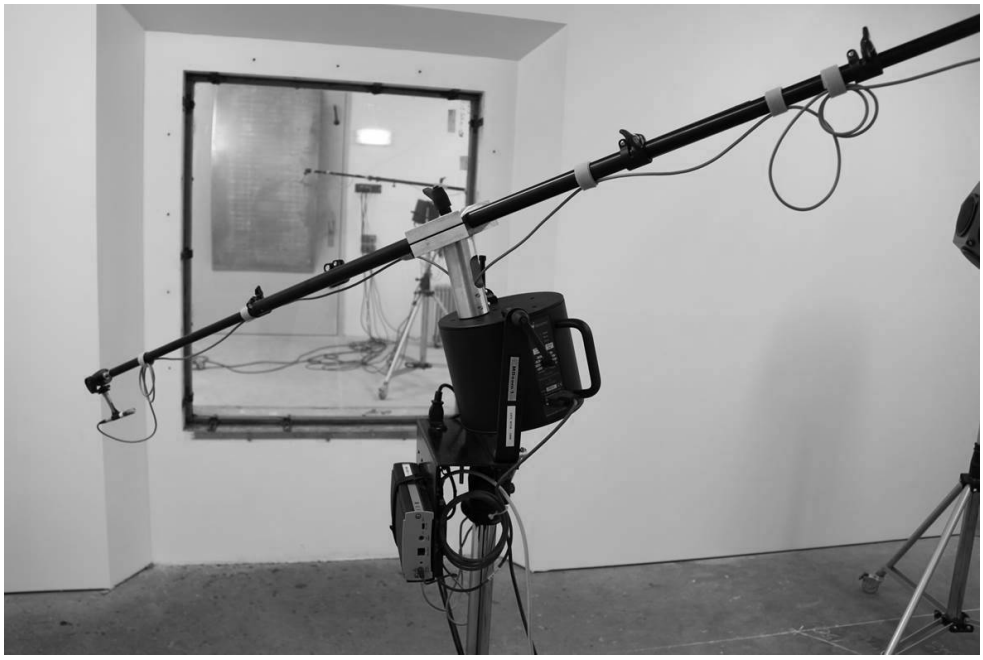

Figure 18.13: Measurement of the Transmission Loss through a window pane inserted between two reverberant chambers.

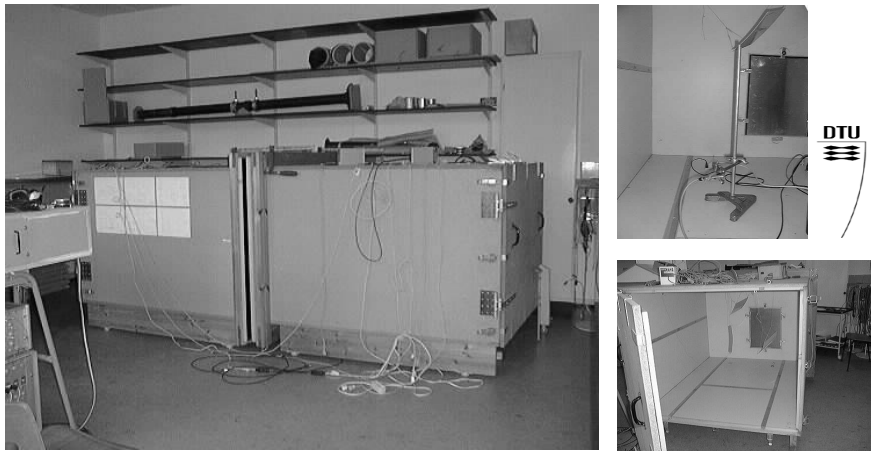

Photographs: Thomas Leclercq.

Figure 18.14: Measurement of TL in small cabins (Danish Technical University Lyngby).

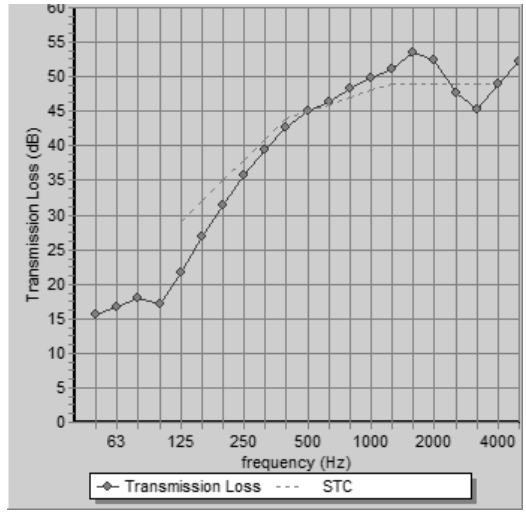

Image produced with the Insul software ©Marshall Day Acoustics.

Figure 18.15: Transmission Loss curves for typical double wall structures used in construction.

List of Figures

1 Introduction **1**

2 Definition and scope **3**

2.1 Emission, propagation, perception and effects of sound waves. . 5
2.2 Lindsay's Wheel of Acoustics. 7
2.3 Snapping shrimp. 9
2.4 Spectral range of sounds. 13
2.5 Spectral range of a piano. 13
2.6 An expensive honk! 16

3 Continuum Mechanics **19**

3.1 Continuity equation. 21
3.2 Forces acting on the volume (viscous fluid). 27
3.3 Forces acting on the volume (inviscid fluid). 28
3.4 Net flow of momentum in elementary volume. 29

4 The Wave Equation **33**

4.1 Linearisation of the pressure-density relationship. 36
4.2 The two terms of d'Alembert's solution (1). 42
4.3 The two terms of d'Alembert's solution (2). 42
4.4 Movement of air particles in a tube. 44
4.5 Period and phase shift. 45
4.6 Wavelength. 45
4.7 Speed of sound and speed of light in Dilbert's world. 50
4.8 Variation of sound speed with temperature. 52
4.9 Colladon-Sturm experiment. 53

5 Fourier Analysis **55**

5.1 Portrait of Joseph Fourier. 56
5.2 Combination of two signals of identical frequencies. 59
5.3 Active noise control according to Dilbert. 59
5.4 Constructive and destructive interferences. 60
5.5 Active control headset. 61
5.6 Active noise control in a car. 61

5.7 Combining signals whose frequency ratio is rational or irrational. 63
5.8 Combination of signals whose frequencies are all integer multiples of the same fundamental frequency. 64
5.9 Combination of signals whose frequencies are all integer multiples of the same fundamental frequency (2). 65
5.10 Combination of signals whose frequencies are all integer multiples of the same fundamental frequency (3). 66
5.11 Square wave. 70
5.12 Gibbs phenomenon: the Fourier series does not converge at the points of discontinuity of the square wave. 70
5.13 Amplitudes of the spectral components of the signal represented in Figure 5.14. 71
5.14 Periodic signal and its spectral components. 72
5.15 (A,B) spectrum of the signal of Figure 5.14. 73
5.16 (C,ϕ) spectrum of the signal of Figure 5.14. 74
5.17 ($\Re(E)$, $\Im(E)$) spectrum of the signal of Figure 5.14. 75
5.18 Rectangular window and its Fourier transform. 80
5.19 Echo effect. 82
5.20 Tyre and suspension passing over an obstacle on the road. . . . 84
5.21 Relationship between signal and spectrum width. 86
5.22 Impulsive signal and its Fourier transform. 86

6 Equations of Acoustics in Harmonic Regime 89
6.1 Sound intensity: general case. 93
6.2 Sound intensity: pressure and velocity in phase. 93
6.3 Sound intensity: pressure and velocity have a phase difference of 90°. 94
6.4 Wave vector of a plane wave with arbitrary incidence. 99
6.5 Acoustic pressure distribution associated to a monopole. 103
6.6 Radial impedance of a monopole. 104

7 Sound Levels 107
7.1 Reference values for the calculation of dB levels. 110
7.2 Relationship between sound pressure and sound pressure level. 110
7.3 Brüel and Kjaer *sound thermometer*. 111
7.4 Ernst Heinrich Weber and Gustav Fechner. 113
7.5 Weber-Fechner law. 113

7.6 Composition of two sound pressure levels. 115
7.7 The 3 dB rule. 115
7.8 Band-pass filter. 118
7.9 Normalised definition of octave bands. 118
7.10 Normalised definition of third-octave bands. 119
7.11 Definition of white and pink noise. 120
7.12 Narrow-band spectrum of white noise. 121
7.13 Narrow-band spectrum of pink noise. 121
7.14 Narrow-band spectrum of brown noise. 122
7.15 Curves of equal loudness. 124
7.16 dBA, dBB, dBC and dBD corrections. 126
7.17 Correction factors associated with A, C and U filters. 127
7.18 Equivalent and statistical levels. 129
7.19 NR curves. 130

8 Reflection and absorption 133
8.1 Reflection of a plane wave on a rigid wall. 136
8.2 Reflection on a rigid surface (normal incidence). 137
8.3 Reflection on a zero-pressure surface. 139
8.4 Reflection on a rigid wall under oblique incidence. 144
8.5 Variation of α with the angle of incidence. 146
8.6 Reflection and image source (normal incidence). 148
8.7 Reflection and image source (oblique incidence). 148
8.8 Reflection of a monopole on a rigid surface. 149
8.9 Reflection of a monopole: wave fronts. 150
8.10 Reflectogram for the single wall case. 151
8.11 Image sources in the case of two perpendicular planes. 152
8.12 The sound at point Q is contributed by four distinct sources. . 153
8.13 The reflectogram shows four successive impulses. 153
8.14 Reflection on two perpendicular surfaces: wave fronts. 154
8.15 Image sources in the case of a rectangular cavity. 155
8.16 Spherical wavefronts and Descartes law. 158
8.17 The method of image source may be analysed in terms of rays. 159
8.18 Ray path in an L-shaped cavity. 159
8.19 Ray path in a concert hall. 160
8.20 Map of sound pressure level (SPL) in a concert hall. 160
8.21 Reflectogram of a concert hall. 161

8.22 Cone tracing method. 162
8.23 Sign of the impedance coefficient and orientation of the normal vector. 163
8.24 Locally and non-locally reacting materials. 167
8.25 Example of a locally reacting acoustic treatment. 168
8.26 Impedance measurement with a Kundt tube. 168
8.27 Power emitted by dV and intercepted by dS. 173
8.28 Build-up and extinction of sound in a room. 175
8.29 Wallace Sabine (1868-1919). 177
8.30 Sound extinction. 178
8.31 Absorption in Dilbert's cubicle: a matter of area. 178
8.32 Anechoic room. 180
8.33 Reverberant chamber. 181
8.34 Semi-anechoic room. 181
8.35 Reverberation time according to Eyring and Sabine formulas. . 183

9 Resonances 185
9.1 Closed tubes excited by a velocity or a pressure source. 187
9.2 Frequency response in the closed duct. 189
9.3 Acoustic modes in a tube. 193
9.4 Pressure distribution approximated by modal superposition. . . 195
9.5 Velocity distribution approximated by modal superposition. . . 196
9.6 Three modes of a box-shaped cavity. 198
9.7 Acoustic mode of an air-conditioning unit. 200

10 Guided Propagation 201
10.1 Cutoff frequency: evanescent and propagating modes. 204
10.2 Three connected ducts. 206
10.3 Thévenin's theorem in duct acoustics. 208
10.4 T-connections. 209
10.5 Principles of the quarter-wavelength resonator. 211
10.6 Quarter-wavelength resonator in a car engine. 212
10.7 Helmholtz resonator. 212
10.8 Helmholtz resonator in the air intake circuit of a car engine. . . 213
10.9 Principles of the four microphone measurement technique. . . . 217
10.10 Four microphone technique: experimental set-up. 217
10.11 TL of an expansion chamber. 220

10.12Effect of non-plane wave modes on the transmission loss. 220
10.13Comparison of the TL of a duct connected to three different resonators. 221
10.14Comparison of Insertion Loss and Transmission Loss. 225
10.15Graphs of Bessel functions of the first kind. 229
10.16First zeros of derivatives of the Bessel functions. 229
10.17Schematic of cross section change. 230
10.18Pressure distribution near a cross section change. 236
10.19Horizontal velocity distribution near a cross section change. . . 237

11 Sound Radiation **239**
11.1 Dipole. 241
11.2 Conventions for directivity diagrams. 243
11.3 Directivity diagrams of monopoles and dipoles. 244
11.4 Lateral quadrupole. 246
11.5 Directivity diagram of the two quadrupole types. 248
11.6 Notation used while deriving the multipole expansion. 249
11.7 Elementary directivity diagrams ($\sin^p\theta\cos^q\theta$). 253
11.8 Elementary directivity diagrams ($\sin p\theta\cos q\theta$). 254
11.9 Effect of frequency on directivity. 256
11.10Vibrating structure and equivalent set of point sources. 257
11.11Helmholtz integral equation (1). 259
11.12Helmholtz integral equation (2). 261
11.13Helmholtz integral equation (3). 262
11.14Helmholtz integral equation (4). 263
11.15Indirect Helmholtz integral equation. 264
11.16Baffled plate. 266
11.17Baffled piston. 267
11.18Directivity of a baffled piston. 269
11.19Radiation impedance. 272

12 Diffraction **273**

13 Refraction **275**
13.1 Refraction at the interface between two fluids. 276
13.2 Refraction: the lifeguard analogy. 280

14 Propagation in Dissipative Media 281
14.1 Maurice A. Biot (1905-1985). 286
14.2 Porosity measurement device. 289
14.3 John William Strutt, third Lord Rayleigh. 291
14.4 Schematic of the resistivity measurement set-up. 291
14.5 Resistivity measurement device. 292
14.6 Electric measurement of tortuosity. 294
14.7 Tortuosity measurement device: ultrasonic method. 294
14.8 Tortuosity measurement device: electrical method. 295
14.9 Material properties of the polyurethane foam. 305
14.10 Three types of wave propagating in a porous material. 306
14.11 Propagation velocity of different waves in a porous material. . . 307
14.12 Efficiency of an open-pore porous material covering a rigid wall. 310
14.13 Cross section of a poro-elastic sandwich. 312
14.14 Vibration insulation effect in poro-elastic sandwich panels. . . . 312
14.15 Oscillatory in-plane fluid flow within the porous layer. 313
14.16 Acoustic radiation on the heavy and base layer side. 313

15 Convected Propagation 315
15.1 Monopole in a constant background flow. 324
15.2 Two equivalent representations of the Doppler effect. 325
15.3 Asymmetry of the Doppler effect. 327
15.4 Dual flux turbofan aircraft engine. 339
15.5 Upstream fan sound radiation through the engine nacelle. . . . 340
15.6 Sound radiation through the bypass: refraction effect. 340

16 Atmospheric Propagation 341
16.1 Atmospheric refraction for two sound speed profiles. 346
16.2 Source radiating in a half-space domain. 348
16.3 Restriction of elevation angles. 351
16.4 Finite difference grid. 352
16.5 Single source radiating above a rigid plane surface. 360
16.6 Decomposition of the total acoustic pressure into incident and scattered components. 361
16.7 Pressure at 100 Hz computed with the parabolic method. . . . 362
16.8 Pressure at 250 and 1,000 Hz computed by the parabolic method. 363
16.9 Parabolic and exact solutions at 500 Hz. 364

16.10Parabolic and exact solutions at 100 and 250 Hz. 365
16.11Parabolic and exact solutions at 500 and 1,000 Hz. 366

17 Fluid-Structure Interaction 369
17.1 Mass-spring system coupled to an infinite fluid duct. 372
17.2 Mass-spring system coupled to a fluid duct of finite length. . . 373
17.3 Resonances of a mass-spring system coupled to a tube. 375
17.4 Dynamic response of a mass-spring system coupled to an air tube: strong coupling. 377
17.5 Dynamic response of a mass-spring system coupled to an air tube: weak coupling. 378

18 Transmission and Insulation 383
18.1 Typical acoustic insulation curves. 385
18.2 Rigid plate on elastic supports. 387
18.3 TL of a rigid plate: effect of mass, stiffness and damping. . . . 389
18.4 Variation of the transmission loss with the angle of incidence. . 393
18.5 Coincidence phenomenon. 394
18.6 Variation of the transmission loss with frequency: diffuse excitation case. 397
18.7 Transmission across a double wall. 399
18.8 Typical variation of transmission loss through a double wall. . . 401
18.9 Acoustic transparency of plates of finite dimension. 402
18.10Attenuation calculated with the finite and infinite plate model. 403
18.11Measurement of the intensity transmitted through a window. . 405
18.12TL measurement principles. 406
18.13Transmission Loss measurement of a window pane. 406
18.14Measurement of TL in small cabins. 407
18.15Transmission Loss curves for typical double wall structures. . . 407

Index

Absorption
  Absorption coefficient, 141
  Absorption measurement in a reverberant room, 182
  Atmospheric absorption, 343
Acoustics, 4
  Definition, 4
  Etymology, 6
  Fields of acoustics, 6
  Linear acoustics, 40
  Non-linear acoustics, 40
Added mass, 373
Admittance, *see* Impedance
Attenuation, 98
  Complex sound velocity, 99

Bessel
  Bessel equation, 226
  Bessel functions, 226
  Friedrich Wilhelm Bessel, 226
Biot
  Biot theory, 286
  Maurice Anthony Biot, 286

Convolution product, 79
Cutoff frequency, 202, 226

d'Alembert
  d'Alembert equation, 33
  Jean le Rond d'Alembert, 39
Damping
  Added damping, 372
Decibel, *see* Sound levels
Delany-Bazley model, 284
Descartes law, 143
Diffraction, 273
Dipole, 240
Doppler effect, 323

Evanescent wave, 203, 230
Eyring, *see* Reverberation time

Filtering, 81
Fletcher-Munson curves, *see* Sound levels
Fluid-structure interaction, 370
Fourier
  Fourier series, 67
  Fourier transform, 76
  Joseph Fourier, 56
Frequency bands
  Brown noise, 120
  Octaves, 117
  Pink noise, 120
  Third octaves, 117
  White noise, 120

Gibbs phenomenon, 69, 235

Helmholtz
  Helmholtz equation, 90
  Helmholtz integral equation, 258
  Helmholtz resonator, 211
  Hermann Ludwig Ferdinand von Helmholtz, 90

Impedance, 91
  Adapted Impedance, 222
  Characteristic impedance, 97, 142
  Frequency dependency, 163
  Locally reacting material, 165
  Non-locally reacting material, 165
  Radiation impedance, 271

Reduced impedance, 142
Sign of impedance coefficient, 162
Source impedance, 222
Index notation, 22
Implicit summation, 23
Kronecker symbol, 24
Levi-Civita symbol, 24
Insertion Loss (IL), 202, 222
Insulation, *see* Transmission
Intensity, 92
Active intensity, 92
Intensity carried by a plane wave, 98
Intensity levels, 108
Reactive intensity, 92

Miki model, 285
Monopole, 101
Multipole analysis, 249

Noise
Definition, 4
Etymology, 5
White. pink and brown noise, *see* Frequency bands

Octave, *see* Frequency bands

Porosity, 288
Power, 108
Radiated power, 270
Radiation efficiency, 270
Prandtl-Glauert transformation, 320
Propagation
Atmospheric propagation, 342
Convected propagation, 316
Dispersive propagation, 46
Guided propagation, 201
Mecanics of propagation, 43
Non-dispersive propagation, 46
Propagation in a dissipative media, 282
Propagation with attenuation, 98

Quadrupole, 243, 245

Radiation, 240
Radiated power, 270
Radiation efficiency, 270
Ray Tracing Method, 156
Rayleigh
John William Strutt, third Lord Rayleigh, 290
Rayleigh integral, 266
Rayls (unit), 290
Reflection
on a free surface, 138
on a rigid surface, 134, 143
on an absorbing surface, 140, 144, 147
Reflection coefficient, 141
Reflectogram, 150
Spherical source, 147
Reflectogram, *see* Reflection
Refraction, 275
Atmospheric refraction, 345
Resistivity, 290
Resonance, 186
of a box-shaped cavity, 197
of a closed tube, 186, 191
of an arbitrary cavity, 199
of an open tube, 192
Resonator
Helmholtz resonator, 211
Quarter wavelength, 210
Reverberation time, 172

Eyring law, 179
Sabine law, 176

Sabine, *see* Reverberation time
Sound
Definition, 4
Etymology, 5
Spectral range, 12
Sound levels
L_{den}, 128
Power levels, 108
Pressure levels, 108
Addition, 114
dBA, dBB, dBC and dBD, 125
Decibel scale, 108
EPNdB, 130
Equivalent levels, 128
Fletcher-Munson curves, 123
Intensity levels, 108
Noise Rating (NR), 130
Statistical levels, 128
Sound speed, 50
Colladon-Sturm experiment, 53
Complex sound speed, 284, 285
Group velocity, 49
Local sound speed in a background flow, 330
Sound velocity
Complex sound velocity, 99
Source
Image source, 147
Plane waves, 97
Source of mass q, 22
Spherical waves, 101
Volume flow of a source, 104

Thévenin's theorem, 208
Third octave, *see* Frequency bands
Tortuosity, 293
Transfer matrix, 204
Cross section change, 207
Different forms of a transfer matrix, 214
Duct with constant cross section, 204
Measurement with four microphones, 216
T connection, 208
Transmission Loss (TL), 202
Transmission, 384
Bounded flexible partition, 401
Double wall, 397
Infinite flexible partition, 390
Rigid partition on elastic supports, 386
TL measurement, 403
Transmission Loss (TL)
TL of ducts, *see* Transfer matrix
TL of partitions, *see* Transmission

Weber-Fechner laws, 112
Windowing, 80

Nomenclature

Roman letters

A	Absorption area of a room: $A = \sum \alpha_i S_i$.
A	Admittance: admittance is the reciprocal of impedance.
$a, a_i, \vec{a}$	Acceleration.
$[C]$	Damping matrix.
c	Sound speed or celerity.
c or d	Damping constant of a spring.
c_p	Heat capacity at constant pressure.
c_v	Heat capacity at constant volume.
D	Bending stiffness.
D	Dipolar moment.
d or c	Damping constant of a spring.
E	Energy.
E	Young modulus.
f	Frequency (Hz).
$F, F_i, \vec{F}$	Force vector.
f_0	Fundamental frequency of a periodic signal.
f_{mn}	Cutoff frequency of a mode of orders (m, n).

G	Green's function associated to the Helmholtz equation. Depending on the context it may have two definitions: $G = \frac{e^{-ikr}}{r}$ or $G = \frac{e^{-ikr}}{4\pi r}$.
G	Shear modulus.
h	Height or thickness.
I	Amplitude of an incident wave.
I	Intensity.
i	Imaginary number defined by $i = \sqrt{-1}$.
$i(t)$	Instantaneous intensity.
IL	Insertion loss.
$[K]$	Stiffness matrix.
K	Bulk elastic modulus.
k	Stiffness.
k, $\vec{k}$	Wave number $k = \frac{\omega}{c}$. Wave vector $\vec{k}$.
l, ℓ	Length.
L_I	Intensity level ([dB]).
L_p	Pressure level ([dB]).
L_w	Power level ([dB]).
L_{Amax}	Maximum level over a period of reference ([dB]).
L_{den}	Weighted level *day-evening-night* ([dB]).
L_{eq}, L_{Aeq}	Equivalent level ([dB]).

$[M]$ Mass matrix.

M Mass per unit area.

m Mass.

N_i Shape function associated to node i of a finite element.

P See p.

p Pressure. p usually designates the acoustic pressure, but, if necessary, a subscript is used to differentiate between the acoustic pressure (p_a), the reference (p_0) or atmospheric (p_{atm}) pressure and the total pressure (p_{tot}). In the first few chapters, lower case p is used to represent the pressure signal $p(t)$ while upper case P is used for the spectrum $P(\omega)$. In later chapters, where there is no ambiguity, a lower case p is used for both spectrum $p(\omega)$ and signal $p(t)$.

p^+ Amplitude (real or complex) of a plane wave travelling along the x axis in the direction of the positive x.

p^- Amplitude (real or complex) of a plane wave travelling along the x axis in the direction of the negative x.

p_i Incident field.

p_s Scattered field.

Q Compressibility modulus.

Q Quadrupolar moment.

q Distributed source of mass in a volume.

$\Im$ Imaginary part of a complex number.

$\Re$ Real part of a complex number.

R	Amplitude of the reflected wave or ratio of the amplitude of the reflected wave to the amplitude of the corresponding incident wave.
R	Ideal gas constant: $R = c_p - c_v$.
R	Resistivity of a porous media.
R	Transmission loss coefficient (insulation).
r	Reflection coefficient.
r, θ, ϕ	Spherical coordinates.
r, θ, z	Cylindrical coordinates.
RPM	Rotations per minute.
S	Area.
T	Absolute temperature [K].
T	Amplitude of a transmitted wave.
T	Period.
t	Temperature [°C].
t	Time.
T_0	Period of the fundamental of a periodic signal.
T_R	Reverberation time.
TL	Transmission loss.
$\ddot{u}$	Acceleration.
$\dot{u}$	Speed.

u, U	Displacement. In poro-elastic media, u designates the displacement of the skeleton and U the displacement of the fluid phase.
V	Volume.
$v, v_i, \vec{v}$	Velocity.
v_g	Group velocity.
W	Power.
x, y, z	Cartesian or rectangular coordinates.
x_{RMS}	RMS value of quantity x.
z^*	Conjugate of the complex number z.
Z	Impedance: ratio between the pressure spectrum and the velocity spectrum.
$z(\omega)$	Reduced impedance: ratio between the impedance and the characteristic impedance of the media: $z = \frac{Z}{\rho c}$.
$z(\tau)$	Impulse response associated to impedance $Z(\omega)$.
Z_n	Normal impedance.

Sets

$\mathbb{C}$	Set of complex numbers.
$\mathbb{N}$	Set of natural numbers.
$\mathbb{Q}$	Set of rational numbers.
$\mathbb{R}$	Set of real numbers.

$\mathbb{Z}$	Set of integer numbers.

Greek letters

α	Absorption coefficient.
α	Biot coefficient.
α_∞	Tortuosity of a porous material.
$\delta()$	Dirac distribution.
δ_{ijk}	Levi-Civita symbol.
δ_{ij}	Kronecker symbol.
ϵ_{ij}	Strain tensor.
γ	Ratio of specific heat at constant pressure and constant volume: $\gamma = \frac{c_p}{c_v}$.
κ	Compressibility.
λ	First Lamé coefficient.
λ	Kinematic viscosity
λ	Wavelength.
Λ_t	Thermal characteristic length.
Λ_v	Viscous characteristic length.
μ	Double layer potential.
μ	Dynamic viscosity.
μ	Second Lamé coefficient or shear modulus.

ν	Poisson's ratio.
Ω	Porosity.
ω	Pulsation $\omega = 2\pi f$.
ϕ	Eigenvector.
ϕ	Phase angle.
ρ	Specific weight $[kg/m^3]$. ρ_0 is the constant part of the specific weight of an acoustic fluid and ρ_a is the fluctuating part caused by the propagation of the sound wave.
σ	Radiation efficiency.
σ	Resistivity of a porous media.
σ	Single layer potential.
$\sigma_x, \sigma_y, \sigma_z$	Diagonal components of the stress tensor.
τ	Transmission coefficient.
τ_{ij}	Stress tensor.
θ	Angle of incidence.

Operators and special characters

$< \bullet >$	Mean value of quantity $\bullet$.
$\bar{\bullet}$	A dash placed above a quantity $\bullet$ usually denotes the boundary value of that quantity.
$\bigcap$	Boolean set intersection.
$\bigcup$	Boolean set union.

$\oplus$ Addition of sound levels.

$\otimes$ Convolution product or convolution integral.

Δ Laplace operator or Laplacian.

$\doteq$ Equal per definition

$\exists$ Existential quantifier (there exists).

$\forall$ Universal quantifier (for all).

$\gg$ Is much larger than.

$\Im$ Imaginary part of a complex number.

$\in$ Belongs to.

∞ Infinity.

$\Leftrightarrow$ Is equivalent to.

$\Leftrightarrow$ The term on the right side of the double arrow is the Fourier transform of the term on the left side. Example: $p(t) \Leftrightarrow P(\omega)$: $P(\omega)$ is the Fourier transform of $p(t)$.

$\ll$ Is much smaller than.

∂_i Partial derivative with respect to coordinate x_i.

∂_t Partial derivative with respect to time.

$\prod$ Product.

$\propto$ Is proportional to.

$\Re$ Real part of a complex number.

$\rightarrow$ Implies.

$\sim$	Is of the same order of magnitude as.
$\simeq$	Is approximately equal to.
$\subset$	Is a subset of.
$\sum$	Sum.
$\vec{\nabla}$	Vector of components $\left(\frac{\partial}{\partial x}, \frac{\partial}{\partial y}, \frac{\partial}{\partial z}\right)$.